A study of proteins involved in Ca^{2+}-regulated exocytosis in AtT-20 cells

Jan Karen Mackintosh

Thesis submitted for the degree of Doctor of Philosophy

University of Edinburgh

October 1997

I dedicate this thesis to Steven, Mum, Dad and Eoin
For love, support and friendship

In memory of my best friends - Pepper and Dill

Contents

Declaration

This study was carried out under the supervision of Dr. David Apps and Dr. Jeff Haywood, Department of Biochemistry, University of Edinburgh between October 1994 and October 1997.

This thesis was composed by myself and the work presented herein was carried out by myself, unless otherwise stated.

Jan Mackintosh

Department of Biochemistry

University of Edinburgh

Hugh Robson Building

George Square

Edinburgh EH8 9XD

October 1997

Abstract

Regulated exocytosis has been studied mostly in neuronal or chromaffin cells, and several proteins that are thought to be involved have been identified. In this project proteins involved in vesicle docking and fusion in the AtT-20 (transformed mouse anterior pituitary) cell line were studied, as a comparison to these other cell types.

Immunoblotting and immunofluorescence were used to detect and localize SNARE's (soluble NSF attachment protein receptors) and also cytosolic and cytoskeletal proteins. These results showed that the proteins present were similar to those in chromaffin and neuronal cells, with a similar intracellular distribution.

Since AtT-20 cells secrete ACTH (adrenocorticotrophic hormone) in a Ca^{2+}-regulated manner, secretion could be measured using a radioimmunoassay for ACTH. This was used with a permeabilised cell system, allowing the introduction of recombinant proteins, drugs, antibodies and neurotoxins. Little effect was seen on introduction of some components, such as the synaptotagmin cytoplasmic domain and αSNAP, however a dramatic reduction in secretion was seen on introduction of the light chains of the neurotoxins Botulinum D and Tetanus toxin. These toxin subunits specifically cleave the v-SNARE synaptobrevin demonstrating its importance in regulated secretion in AtT-20 cells as has been demonstrated in chromaffin and neuronal cells.

The role of actin in exocytosis has also undergone much scrutiny, particularly in chromaffin cells. This was studied in AtT-20 cells using phalloidin, cytochalasin and a combination of the permeabilised cell assay and immunofluorescence. In contrast to chromaffin cells, the actin did not appear to form a distinct exocytotic barrier in AtT-20 cells. The introduction of actin-stabilizing and de-stabilizing factors also had no effect on the rate of exocytosis in AtT-20 cells. We conclude from this that actin may not have an essential role to play in Ca^{2+}-regulated exocytosis from AtT-20 cells.

Throughout this project ACTH secretion was measured using a rather laborious radioimmunoassay. It was decided to look at an alternative method of measuring regulated secretion, by stably transfecting the cells with a vector expressing a secreted alkaline phosphatase (SEAP) reporter gene, fused to human growth

hormone (hGH). The logic behind this was that the hGH would direct the SEAP into the regulated secretory pathway, allowing its release to be measured using photometric or chemiluminescent methods of detection. The vector was found to be very efficient in a traditional reporter gene role, but not sensitive enough to measure the relatively small amounts of ACTH released on stimulation of secretion.

The logical continuation of this project would be to use a molecular approach and transfect the AtT-20 cells with mutant forms of the proteins thought to be involved in exocytosis. It would naturally focus on those producing dominant negative phenotypes, leading to cells deficient in exocytosis.

Abbreviations

A_{405}	absorbance at 405nm
ACTH	adrenocorticotrophic hormone
ATP	adenosine-5'-triphosphate
ATPase	adenosine-5'-triphosphatase
bp	base pairs
BSA	bovine serum albumin
CRF	corticotrophin releasing factor
DNA	deoxyribonucleic acid
DTT	dithiothreitol
ECL	enhanced chemiluminescence
E. coli	*Escherichia coli*
EDTA	ethylenediamine tetraacetic acid
EGTA	1,2, di(2-aminoethoxy)ethane-N,N,N',N'-tetraacetic acid
g	relative centrifugal force
GTP	guanosine-5'-triphosphate
GTPase	guanosine-5'-triphosphatase
HEPES	N-(2-hydroxyethyl)piperizine-N'-2-ethanesulphonic acid
HGH	human growth hormone
HRP	horse radish peroxidase
Ig	immunoglobulin
IPTG	isopropylthiogalactosidase
kbp	kilobase pairs
kDa	kilodalton
μCi	microcurie

min	minute(s)
Mg	magnesium
NEM	N-ethylmaleimide
nm	nanometers
NSF	NEM sensitive factor
PBS	phosphate buffered saline
PCR	polymerase chain raction
pNPP	p-nitrophenyl phosphate
PMSF	phenylmethylsulphonyl fluoride
RIA	radioimmunoassay
RNA	ribonucleic acid
rpm	revolutions per minute
SDS	sodium dodecyl sulphate
SDS-PAGE	sodium dodecyl sulphate polyacrylamide gel electrophoresis
SEAP	secreted alkaline phosphatase
sec	second(s)
SNAP	soluble NSF attachment protein
SNARE	SNAP receptor
TBS	tris buffered saline
TCA	trichloroacetic acid
TEMED	N,N,N'N'-tetramethylethylenediamine
Tris	tris(hydroxymethyl)aminomethane

Acknowlegements

I would like to thank Dr. David Apps and Dr. Jeff Haywood for their supervision of this project. Many thanks particularly to David for a lot of hard work put in during his meticulous reading of this thesis (as well as for removal of simply, basically, probably, thus and however – the words media and antisera will forever haunt him)!

Thank you to Steven for giving me endless support and love, putting up with me and supplying constant on the spot computer maintenance (until he never wanted to see another Excel graph ever)! Thanks to Mum, Dad and Eoin for lots of supportive phone calls, games of croquet (you'll never win) and just for being there – sorry about the phone bills Dad!

Thanks to fellow shopaholics Leo and Shahida for constant friendship and advice over the three years, and for making working in the lab a good laugh! Thanks to Harry, Kate and Sharon for being good friends and for just *forcing* me to go down the pub, get drunk and fall over – Planet Earth lives on! Also thanks to Elaine and Susan from Hamilton, and my friends from Strathclyde for keeping in touch and not minding my not phoning for months on end.

Many thanks to Dr. James Pryde, Dr. Alan Boyd and Dr. Sutherland Maciver for taking a general interest in my work and giving me valued and perceptive advice, also thanks (I think) to Suds for the really crap jokes!

Throughout this project I have received materials, protocols and advice from various people, whom I have listed below. Thanks for giving up time or materials and hope I haven't missed anyone out: John Bennie, Dr. Susan Smith, Forbes Howie, Professor. R. Burgoyne, Daphne Glenn, Richard Barnard, Dr. Tim Levine, Dr. Thomas Martin, Dr. Lorna Webster, Dr. Frances Darchen, Dr. Cliff Shone, Dr. Timothy Whalley, Dr. Simon Guild, Dr. Robert Chow and Castle Computers (without whom this would have never got printed!).

Finally I wish to recognize the excellent support and level of funding (which all Ph.D. students should be entitled to) supplied by the Wellcome Trust throughout my Ph.D.

Chapter 1

Introduction

1.1 Ca^{2+}-regulated exocytosis in neuronal and neuroendocrine cells.

Exocytosis is defined as the fusion of the membrane of an intracellular vesicle with the plasma membrane (*Darnell et al., 1990*). This project studies the proteins involved in Ca^{2+}-regulated exocytosis using the transformed mouse anterior pituitary cell line AtT-20/D16-16 as a model.

1.1.1 Protein Synthesis, secretion and sorting.

(*Darnell, et al., 1990; Stryer, 1988; Fox, 1990; Nicholls, 1994*)

It has long been known that genes are transcribed into mRNA (messenger ribonucleic acid), and this is then translated into amino acid sequences by ribosomes. There are two classes of ribosomes, membrane-attached, thus creating the RER (rough endoplasmic reticulum) and unattached (cytosolic). Whilst these are functionally equivalent to one another, they translate different types of proteins, and this occurs as a result of the amino acid sequence of the protein itself. Most mitochondrial, chloroplastic, peroxisomal, glyoxisomal, soluble cytosolic and extrinsic membrane proteins are synthesised on unattached ribosomes. They enter the cytosol immediately and remain free or attach to other proteins, such as chaperones. Organelle proteins synthesised in this way undergo active uptake into the correct organelle by recognition of their signal sequences, which may later be proteolytically cleaved.

Secretory, integral, ER, Golgi, plasma membrane and lysosomal proteins (any of which may be glycoproteins) are all synthesised by the attached ribosomes in the RER. These proteins enter the Golgi at the *cis* face (directed by their signal sequences). They are transported through the Golgi stacks by transport vesicles budding and fusing, and during this time, they can undergo various modifications. These include modification of amino acid side chains, addition/modification of oligosaccharide side chains, proteolytic cleavages, disulphide bond formation, acetylation sulphation and phosphorylation. ER proteins simply stop within the ER, Golgi within the Golgi and lysosomal proteins travel to the *trans* Golgi stacks and are sorted into lysosomes. However secretory proteins enter a complex network of vesicles called the trans-Golgi reticulum, where they are sorted into continuously-secreted vesicles or those that undergo regulated secretion. The sorting of the

proteins at the reticulum stage is now understood to be due to the amino acid signal sequences of the proteins themselves, which are later cleaved. As the vesicles mature the proteins are often proteolytically processed into active peptides. Figure 1.1.1 summarises the process of protein synthesis and sorting. Until recent years much less has been known about the mechanism occurring after this i.e. how the vesicles are directed to the correct membrane and what physical attributes differentiate constitutive secretion from regulated secretion. Section 1.1 summarises the most recent data on exocytosis in neuronal and neuroendocrine cells. First, the main differences between neuronal and neuroendocrine cell protein synthesis, sorting and secretion will be summarised.

Neuronal cell synapses can be separated into two types: NMJ (neuromuscular junctions) and CNS (central nervous system) terminals. One of the main differences between these is that the NMJ can release several hundred synaptic vesicles on stimulation with only one action potential, whereas the CNS synapses can require several action potentials to release one vesicle. The morphology of these synapses also differ somewhat but the basic principle is the same in that both have a synaptic cleft, where the presynaptic membrane is juxtapositioned to the post-synaptic membrane. This means that the action of neurotransmitters tends to be very localised and there is the possibility of reuptake of neurotransmitters for recycling and further use. The time gap between stimulation and release of vesicles is often less than 1ms and in NMJs in particular can often be faster. Exocytosis occurs by the action potential ultimately causing a Ca^{2+} influx, which causes vesicle release. CNS terminals actually contain two types of vesicles: small synaptic vesicles (SSVs, containing neurotransmitters) and large dense core vesicles (LDCVs, containing neuropeptides). The main differences between these are that LDCV contents tend not to be released into a synaptic cleft, meaning their effects are less localised and there is no reuptake. LDCV exocytosis is perhaps more similar to the release of hormones by endocrine cells. The overall mechanism of release is still very similar, in that a stimulus causes a rise in $[Ca^{2+}]$ and this causes exocytosis, however the overall cytosolic increase in $[Ca^{2+}]$ tends to be larger. The lag time between stimulus and exocytosis is also longer and often between 50ms to 1s. Chromaffin cells from the adrenal medulla represent an ideal model for this kind of exocytosis, and for

neuroendocrine cells in general. It is important however, even with this degree of similarity, to bear in mind certain anatomical and physiological differences within the classification "neuroendocrine". The ACTH-secreting cell line AtT-20/D16-16, which is being studied in this project, originates in the anterior pituitary and is a "neuroendocrine cell line". ACTH secretion is stimulated by hormones from the hypothalamus and its role is to stimulate the adrenal cortex to release the glucocorticoids that stimulate gluconeogenesis in the liver. Chromaffin cells are in the adrenal medulla and are actually innervated by sympathetic neurones. Amongst other components, they release catecholamines that complement the sympathetic nervous system in the fear and flight reaction. This is a much faster-acting and less regulatory role than that seen for ACTH and it requires a completely different method of stimulation. Differences between systems must be kept in mind when data from many studies are being correlated to produce a single theory, and one should never presume that mechanisms will be identical.

1.1.2 The SNARE hypothesis

Protein traffic throughout the cell has long been studied, and many important findings were obtained using yeast mutants. Proteins were identified using temperature-sensitive mutants and also the ability of a protein/gene to compensate for a membrane traffic defect, which otherwise resulted in cell death *(Pryer et al., 1992)*. In terms of mammalian systems, there was no collection of mutants available for similar studies, other than the *unc*-mutants in the nematode *Caenorhabditis elegans (Clark et al., 1988)*. The main method of biochemical analysis in mammalian systems was the characterisation of the synaptic vesicle proteins, which were found to be abundant in synapses and specific to neuronal and neuroendocrine *cells (Jessell & Kandel, 1993)*. It was then realised that these proteins were isoforms of the proteins involved in yeast protein trafficking. The soluble proteins NSF (N-ethylmaleimide-sensitive factor) and SNAPs (soluble NSF attachment proteins) were isolated through their ability to restore activity to a mammalian inter-Golgi vesicular transport assay. Their yeast homologues SEC18 (NSF) and SEC17 (αSNAP) could replace them in this assay *(Wilson et al., 1989)*. Thus it was postulated that protein trafficking and vesicle fusion is actually fairly conserved between yeast and man. It appeared that throughout intracellular protein trafficking in the mammalian cell,

there were specific sets of vesicle proteins that docked with the complementary target membrane proteins. These were termed SNAREs (SNAP-receptors) and two types were recognised: t-SNAREs (target SNAREs on the plasma membrane) and v-SNAREs (vesicular SNAREs on the vesicle). The process also required SNAPs and NSF, and allowed efficient and accurate targeting of vesicles to the correct membranes in the cell *(Rothman, 1994)*. More specific studies of the process of regulated exocytosis were then undertaken.

Two approaches were used to show the involvement of SNAREs in synaptic vesicle release and regulated exocytosis:

- **Binding analysis:** Detergent solubilisation of synaptic vesicle membranes and analysis of their interactions with αSNAP and *NSF (Sollner et al., 1993; Wilson et al., 1992)*

- **Clostridial neurotoxins:** Inhibition of SV fusion and specific cleavage of syntaxin, synaptobrevin and SNAP-25 by neurotoxins. *(Schiavo et al., 1992; Blasi et al., 1993a; Blasi et al., 1993b)*.

With regards to the binding/complex studies various detergents were used to solubilise complexes from rat brain membranes *(Bennet et al., 1992)*. Using CHAPS to solubilise the membranes they found a large complex, which contained SV2, synaptotagmin, syntaxin, synaptobrevin, rab 3A and the vacuolar H^+-ATPase (proton pump). On solubilisation with octylglucoside SV2, syntaxin and rab3A were found to be present; and with TX100 there were two predominant interactions seen, between synaptotagmin and SV2 and between syntaxin and synaptobrevin. This was taken a step further when the soluble proteins αSNAP and NSF were introduced and stepwise binding assays were studied *(Sollner et al., 1993)*. One of these studies used a recombinant NSF protein with a myc tag attached to it. A TX-100 extract of bovine brain was also used along with recombinant αSNAP and protein-G beads, with a monoclonal antibody to myc attached. The membrane extract, protein-G beads and recombinant αSNAP were mixed together in the presence of a non-hydrolysable ATP analogue (ATPγS) and EDTA. The beads were then packed into a column and following washing to remove non-specific binding, specific eluates were examined. The wash with MgATP, which caused the elution of proteins due to ATP hydrolysis,

contained αSNAP, syntaxin, synaptobrevin and SNAP-25. A later study *(McMahon & Sudhof, 1995)* resolved this even further by looking at αSNAP binding to these various proteins, using a similar affinity-dependent method. It was already known that syntaxin and SNAP-25 were present as a tight complex on the plasma membrane *(Hayashi et al., 1994). Pevsner et al., 1994* had also shown that synaptobrevin binds weakly to syntaxin or SNAP-25 but tightly to the syntaxin/SNAP-25 complex. They showed αSNAP to bind weakly to syntaxin, SNAP-25 or the syntaxin/SNAP-25 complex and not at all to synaptobrevin. However binding was much enhanced when synaptobrevin was complexed with syntaxin or the syntaxin/SNAP-25 complex. This lead to a theory of SNAREs and targeted membrane fusion *(Sollner,1995)* which is shown diagrammatically in figure 1.1.2. Syntaxin and SNAP-25 were postulated to be the t-SNAREs and synaptobrevin the major v-SNARE. αSNAP and NSF were thought to be have a role similar to that in the Golgi, in that αSNAP acts as an adaptor protein for NSF, which has the ATPase activity to assist vesicle docking/fusion. Other proteins mentioned will be discussed later.

Tetanus and botulinum toxins are produced by anaerobic bacteria, whose spores can be found in soil. There is a single type of tetanus toxin (TeTx) and seven serologically distinct types of botulinum toxins (BoNT/A to BoNT/G). These toxins are released from bacteria as single chain polypeptides of 150kDa, and are activated by bacterial or host proteases, which cleave the molecule into two pieces. A 50kDa light chain peptide (L) remains attached to a 100kDa heavy chain peptide (H) by a disulphide bond. The H-chains allow the entry of the toxin into the cell, where the L-chain acts specifically to proteolytically cleave the SNAREs *(Niemann et al., 1994)*. Synaptobrevin is proteolysed by TeTx, BoNT/B, BoNT/D, BoNT/F and BoNT/G, syntaxin by BoNT/C and SNAP-25 by BoNT/A and BoNT/E *(Eisel et al., 1986; Whelan et al., 1992; Binz et al., 1990; East et al., 1992; Campbell et al., 1993; Hauser et al., 1990; Poulet et al., 1992)*. These toxins have now been tested in a number of different cell types other than strictly neuronal systems. *Glenn & Burgoyne, 1996* showed that the botulinum D light chain could substantially inhibit exocytosis in permeabilised chromaffin cells, and that C and E light chains showed partial inhibition. *Boyd et al.*, 1995 showed various botulinum toxins to cause an

inhibition of insulin secretion from an insulinoma cell line. The above data offered real proof of the involvement of the t and v-SNAREs in exocytosis.

1.1.3 The alternative SNARE hypothesis

Roth and Burgoyne, 1994 showed SNAP-25 to be enriched in the microsomal fraction of the adrenal medulla (although less than in brain microsomes). Immunocytochemistry showed it to be localised to the plasma membrane of chromaffin cells. Using immunoprecipitation it was demonstrated that SNAP-25 was in a complex with syntaxin, synaptobrevin, synaptotagmin, NSF, αSNAP and other unidentified proteins. This, together with the fact that neurotoxins cause inhibition of exocytosis in chromaffin cells showed that similar mechanisms are occurring in these cells as in the brain *(Glenn & Burgoyne, 1996; Bartels et al., 1994). Morgan and Burgoyne, 1995a and 1995b* used an entirely different approach to the co-precipitation assays mentioned so far. They showed that chromaffin cells permeabilised with digitonin would secrete catecholamines in response to micromolar levels of Ca^{2+}. However as time increased, their response to Ca^{2+} lessened, as soluble proteins necessary for exocytosis were lost through the digitonin-produced pores. This "cytosolic rundown" could be retarded through the addition of cytosol, and could thus be used as an assay for specific proteins important in exocytosis. They used this assay initially to assess the roles of NSF and αSNAP in a more functional way than previously mentioned. It was found that recombinant αSNAP could stimulate Ca^{2+}-dependent exocytosis in these rundown cells, however NSF could not. Both were shown to leak out of chromaffin cells with a similar time course, however as much of the NSF appeared to be membrane-bound, this may have provided a plentiful reservoir for the cell. The αSNAP-stimulated secretion was dependent on Ca^{2+} and Mg-ATP; and Botulinum neurotoxin A inhibited it, thus confirms it as "real" exocytosis.

Further studies in this laboratory and others separated exocytosis into two stages: ATP-dependent priming (requiring αSNAP and NSF) and ATP-independent triggering by Ca^{2+} *(Chamberlain et al., 1995; Morgan & Burgoyne, 1995a; Morgan & Burgoyne, 1995b). Banerjee et al., 1996* did similar experiments on permeabilised PC12 cells with similar results. Their priming assay involved a straightforward

incubation of the cell with or without ATP, and stimulation with Ca^{2+} showed norepinephrine to be released only in the presence of ATP. The triggering assay involved extensive washing of ATP pre-primed cells to remove any free ATP, unlike some of the previously mentioned studies. In this case, a combination of αSNAP and NSF increased Ca^{2+}-stimulated exocytosis in the presence of ATP, suggesting ATP hydrolysis to be necessary only in the priming stage. They also showed that both αSNAP and NSF were necessary to rescue rundown cells and allow exocytosis to occur. *Barnard et al., 1996* showed the C terminus of αSNAP to be the important feature in recruitment of NSF, as deletion of the first 120 N-terminal amino acids caused no change in its stimulatory activity.

An additional role for ATP in the priming of exocytosis may be through the lipid kinases. It has been found that ATP-dependent priming requires the cytosolic proteins phosphatidylinositol transfer protein (PEP3) and phosphatidylinositol-4-phosphate-5-kinase (PEP1) *(Hay et al., 1995)*. These act along with the vesicular membrane phosphatidylinositol-4-kinase to synthesise phosphatidylinositol (4,5) bisphosphate ($PtdIns(4,5)P_2$), this being necessary for Ca^{2+}-stimulated exocytosis *(Wiedemann et al., 1996)*. Thus, ATP appears to act as a substrate in the priming reaction for NSF and the lipid kinases. CAPS (Ca^{2+}-dependent activator protein for secretion) is a 145kDa soluble protein which has an essential role in Ca^{2+} triggering. It was shown, using the permeabilised/rundown PC12 cell system, that CAPS was needed in the ATP-dependent Ca^{2+} triggering part of exocytosis *(Walent et al., 1996)*. It binds to phospholipids, particularly $PtdIns(4,5)P_2$, but dissociates and binds to other phospholipids on binding Ca^{2+} *(Lovett et al., 1997)*. Antibodies to $PtIns(4,5)P_2$ or phospholipase C (both of which perturb $PtIns(4,5)P_2$) inhibit secretion, thus suggesting a role for phospholipids and CAPS.

So far SNAREs, SNAPs and NSF have been discussed, all of which have homologues in the constitutive yeast trafficking systems. This project studies Ca^{2+}-regulated exocytosis, and it follows that some other factor is needed to confer regulation on the system. This is likely to be a Ca^{2+}-sensitive fusion clamp(s) that prevents the fusion of vesicle with plasma membrane, until the influx of Ca^{2+} occurs. This may cause a conformational change in the clamp, and would allow fusion to

proceed. The other alternative is that Ca^{2+} acts in a positive sense by producing a conformational change in a protein that then actively causes fusion.

1.1.4 The fusion clamp

The putative fusion clamp has proved highly elusive although the main candidate has always been synaptotagmin. Synaptotagmin is a 65kDa integral vesicular membrane protein, and it is now known that at least nine isoforms exist. It has two large, highly conserved repeats in its cytoplasmic domain that are homologous to the C_2 domain of protein kinase C *(Perin et al., 1990)*. These C_2 domains appear to give synaptotagmin its Ca^{2+}- and phospholipid-binding properties, and purified synaptotagmin binds 4 moles Ca^{2+} per mole protein *(Brose et al., 1992)*. It demonstrates Ca^{2+}-dependent PtdIns(4,5)P_2 binding and inositol hexakisphosphate (an inhibitor of neurosecretion) will compete with its binding to the synaptotagmin C_2 domain *(Schiavo et al., 1996; Ohara-Imaizumi et al., 1997)*. This may suggest that PtdIns(4,5)P_2 is part of a clamp, restraining fusion, and that synaptotagmin acts as a Ca^{2+} sensor that binds the former thus allowing fusion to proceed. Eaton Myasthenic Syndrome (EMS) is an autoimmune disease of the NMJ. IgG fractions from EMS patients co-precipitate ω-conotoxin sensitive Ca^{2+} channels and synaptotagmin, suggesting synaptotagmin forms complexes with these channels *(Leveque et al., 1992)*. Synaptotagmin also binds to syntaxin and a putative α–latrotoxin receptor (neurexin) which will be discussed later *(Petrenko et al., 1991)*.

Again it is important to remember that many of these studies on synaptotagmin used *in-vitro* precipitation methods rather than functional assays. Other studies of synaptotagmin, in particular genetic experiments, have yielded sometimes contradictory results. Microinjection of a peptide from the cytoplasmic domain of synaptotagmin inhibited exocytosis in PC12 cells *(Elferink et al.,1993)*. However the stable transfection of AtT-20 cells with a truncated cytoplasmic domain of synaptotagmin had no effect on Ca^{2+}-regulated secretion *(Wendland & Scheller, 1994)*. Synaptotagmin gene knockouts in *Drosophila* can be fatal *(Littleton et al., 1993)* or may still allow synaptic transmission to occur *(Diantonio et al., 1993)*. Gene knockouts in mice have been shown to be fatal *(Geppert et al.,1994b)* but in *C. elegans* resulted only in an impairment of synaptic function *(Nonet et al., 1993)*.

Much conflicting data now exists and the explanation may be variations in the experimental systems used, or multiple pathways within the cell allowing bypassing of the fault. There is also a possibility with genetic knockouts that functional isoforms still exist. The most recent results postulate that synaptotagmin is a v-SNARE which interacts with the t-SNARE SNAP-25, bringing the core complex in close proximity with itself (i.e. the Ca^{2+} sensor) *(Schiavo et al., 1997)*. This result was used to explain why the docking of synaptic vesicles still occurred after neurotoxin proteolysis *(Sweeney et al., 1995)*.

Although much research has concentrated on synaptotagmin, other fusion-clamp or fusion-activator candidates have been put forward, the main one being the α-latrotoxin receptor. α-latrotoxin is the active component of black widow spider venom, which causes massive Ca^{2+}-independent exocytosis at the NMJ *(Rosenthal & Meldolesi., 1989)*. The concept of a Ca^{2+}-sensitive fusion clamp would mean that on its becoming non-functional exocytosis would occur in the absence of Ca^{2+}, thus the mechanism of the toxin was of great interest.

The first proteins to be isolated through their binding to α-latrotoxin were the neurexins, which are a family of polymorphic neuron-specific cell surface receptors. Neurexin I was thought to bind both α-latrotoxin and synaptotagmin *(Ushkaryov et al., 1992; Hata et al., 1993)*. More recent experiments have identified a new protein which binds α-latrotoxin, perhaps more convincing as it does so in the absence of Ca^{2+}, unlike neurexin I. This protein, termed α-latrophilin, is a single N-glycosylated polypeptide chain which is enriched in synaptosomes *(Davletov et al., 1996; Krasnoperov et al., 1997)*. The area of interest now is the action of α-latrotoxin, of which it appears to have two: Ca^{2+}-dependent and Ca^{2+}-independent. On binding to a presynaptic receptor α-latrotoxin appears to form large non-selective cation channels that allow Ca^{2+} entry, hence triggering exocytosis *(Rosenthal & Meldolesi, 1989)*. Other studies show massive exocytosis occurring in the absence of Ca^{2+} *(Ceccarelli et al., 1979)*, thus it may be that there are two receptors: Ca^{2+} independent and dependent.

Figure 1.1.3 summarises the alternative SNARE hypothesis and fusion-clamp mechanism. This section has reviewed the findings on the two main fusion clamp

candidates, but as with the SNARE hypothesis, nothing is clear-cut and the real answer has not yet been obtained. The sheer complexity of the pathway, and the involvement of a number of different proteins, are what continue to cloud the issue. The following section will briefly discuss other proteins that may also have a role in exocytosis, in order to complete and summarise a very complex story.

1.1.5 Other proteins involved in exocytosis

Cytoskeletal proteins are one of the most important new groups of proteins to emerge as having a role in exocytosis. There is substantial evidence that in some cells the bulk of secretory vesicles are inhibited from fusion with the plasma membrane by interactions with the cytoskeleton. The fact that certain synaptic vesicle proteins, such as synapsin I, interact with the cytoskeleton seem to back up this theory. Synapsin I is a synaptic vesicle protein that is phosphorylated on cell depolarisation *(Browning et al., 1985)*, and interacts with various elements of the cytoskeleton including F-actin *(Bahler & Greengard, 1987)*. It is possible that vesicles interact with an actin network and are localised at the plasma membrane, but prevented from fusion. The role of actin in secretory cells may also be connected with the two distinct time phases of vesicle release. Superfusion of the dendritic areas from rat hippocampal neurons, with solutions containing increased K^+ and Ca^{2+} concentrations, produced a distinct trend in post-synaptic excitatory events *(Stevens & Tsujimoto, 1995)*. It was shown that the initial release rate was approximately 20 quanta per sec per synapse, however this rapidly declined to a much lower rate. This readily-releasable pool, as it is described, could be replenished with a time constant of approximately 10s. Morphological studies on chromaffin cells shows around 30,000 vesicles that lie well below the area of cortical actin. There are however 500 vesicles which appear to lie outside this cortical actin, and are docked at the plasma membrane *(Morgan, 1995)*. Permeabilised chromaffin cells appear to release 4% of their total vesicle content, on stimulation with Ca^{2+}, and in the absence of ATP. A much larger percentage is released in the presence of ATP (*Holz et al., 1989)*. Patch clamp capacitance studies showed that Ca^{2+}-regulated exocytosis in chromaffin cells which had been washed to remove ATP, corresponded to approximately 800 'docked' vesicles. The readily-releasable pool of vesicles appear to be those vesicles docked in close proximity to the plasma membrane, which are available for

immediate Ca^{2+}-triggered ATP-independent release. Functional studies have shown that inhibitors of myosin light chain kinase will inhibit ATP-dependent secretion in permeabilised adrenal cells *(Kumakura et al., 1994)*. The reverse can also be shown in that F-actin depolymerising agents increase Ca^{2+}-regulated exocytosis by causing an increase in the readily-releasable pool of vesicles *(Roth & Burgoyne 1995; Vitale et al., 1995a)*. The former study also implicated the 14-3-3 proteins in having a role, as they increased the secretion of catecholamines in permeabilised chromaffin cells. This property was abolished on addition of the F-actin stabilising drug phalloidin. Recombinant scinderin (an F-actin severing protein) has been shown to increase the Ca^{2+}-stimulated release of seretonin from platelets *(Zhang et al., 1996)* and many studies have shown actin-stabilising factors increase Ca^{2+}- regulated exocytosis in chromaffin cells *(Sakurai, et al., 1997)*.

These studies all suggest an additional role for ATP, other than in αSNAP/NSF-dependent priming of vesicles already discussed. ATP may also be required in the recruitment of vesicles to the plasma membrane, by assisting with cortical actin rearrangement, perhaps by being utilised by an ATP-dependent motor such as Myosin II.

A second major category of proteins implicated in exocytosis are the **rab proteins.** These are small GTP-binding proteins which are active in their GTP-bound form and inactive in their GDP-bound form. They have been found to be required in various stages of intracellular membrane trafficking *(Pfeffer, 1992)* and rab3A is abundant in synaptic vesicles. It is anchored to membranes by two geranyl moieties *(Ngsee et al., 1990)* when it is in its GTP-bound form. Upon GTP hydrolysis it dissociates and is maintained in the cytoplasm by a regulatory protein called GDI (GDP dissociation inhibitor) *(Araki et al., 1990)*. Rabphilin is an 86 kDa protein which appears to maintain rab3A in its active form by promoting exchange of GDP for GTP *(Kishida et al., 1993)*. Studies have shown rab3A to play a role in exocytosis in chromaffin cells *(Holz et al., 1994)* and in neurones *(Geppert et al., 1994a)*. The fact that clostridial neurotoxins inhibit exocytosis stimulated by non-hydrolysable analogues of GTP (GTP-γ-S) indicates a definite convergence of the GTPase and SNAP/SNARE pathways *(Glenn & Burgoyne, 1996)*. It has also been suggested that rabphilin3A is a Ca^{2+} sensor in exocytosis. The most commonly expressed

synaptotagmin isoform, synaptotagmin I, binds syntaxin at Ca^{2+} concentrations of 200-500μM *(Geppert et al., 1994b)*. In neurones localised Ca^{2+} concentrations of this level are thought to occur, however in neuroendocrine cells often only 10μM is required. Rabphilin 3A has the required Ca^{2+}- and phospholipid-binding domains and has a Ca^{2+} dissociation constant of 1-10μM *(Yamaguchi et al.,1993)*. It is possible that synaptotagmin is a low-affinity Ca^{2+} receptor for fast neurotransmission, whilst rabphilin (and its interaction with rab 3) acts as a high-affinity Ca^{2+} receptor in the slower release of LDCVs. Certainly the overexpression of rabphilin 3A in chromaffin cells enhances Ca^{2+}-regulated exocytosis *(Chung et al., 1995)*.

There are many other proteins put forward as having roles in exocytosis, too many to review fully, but a very brief summary can be offered, in the form of table 1.1. Diagram 1.1.4 shows the various proteins which may be involved in Ca^{2+}-regulated exocytosis.

As shown in the table and discussed above, there are now a vast number of proteins which may be involved in exocytosis. Taking all of these studies into consideration, do we assume that the synaptic vesicle contains a huge fusion complex (secretosome), with many different binding reactions occurring, and would this in fact be spatially possible? It seems unlikely that all of these proteins play such a similar role and care should be taken on the interpretation of *in vitro* binding studies. Whilst they offer a good method for the identification of proteins which bind the synaptic vesicle and therefore may be involved, it should not be automatically assumed that they are all involved in exocytosis. Cell assays and genetic manipulations are the ways by which we will be able to fully elucidate actual roles for these proteins and the mechanism for Ca^{2+}-regulated exocytosis, and this promises to be a lengthy and complex process. The next section will be a review of the AtT-20 cell line that was studied in this project.

Figure 1.1.1 Protein processing and sorting

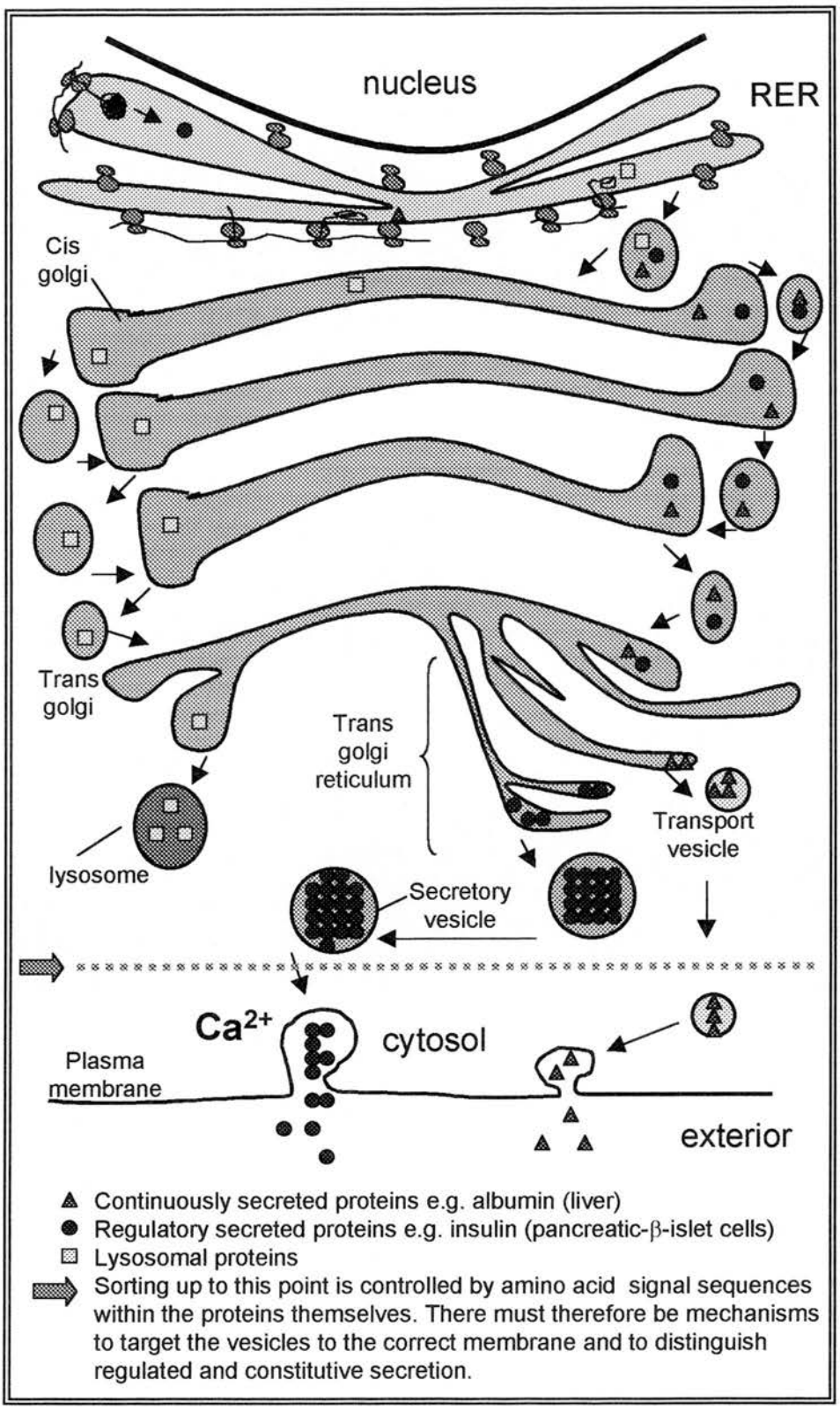

Figure 1.1.2 The SNARE hypothesis

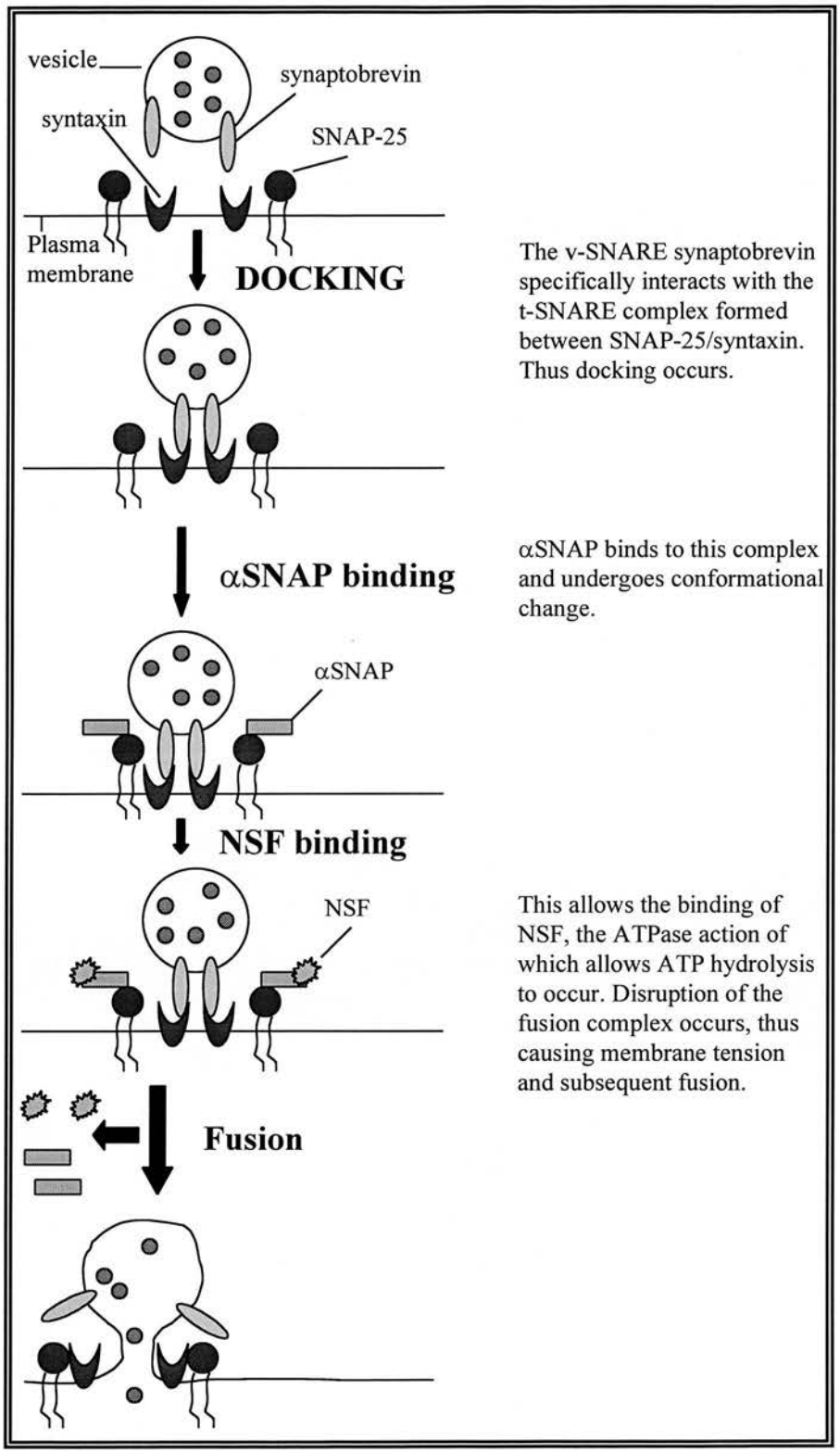

Figure 1.1.3 The alternative SNARE hypothesis

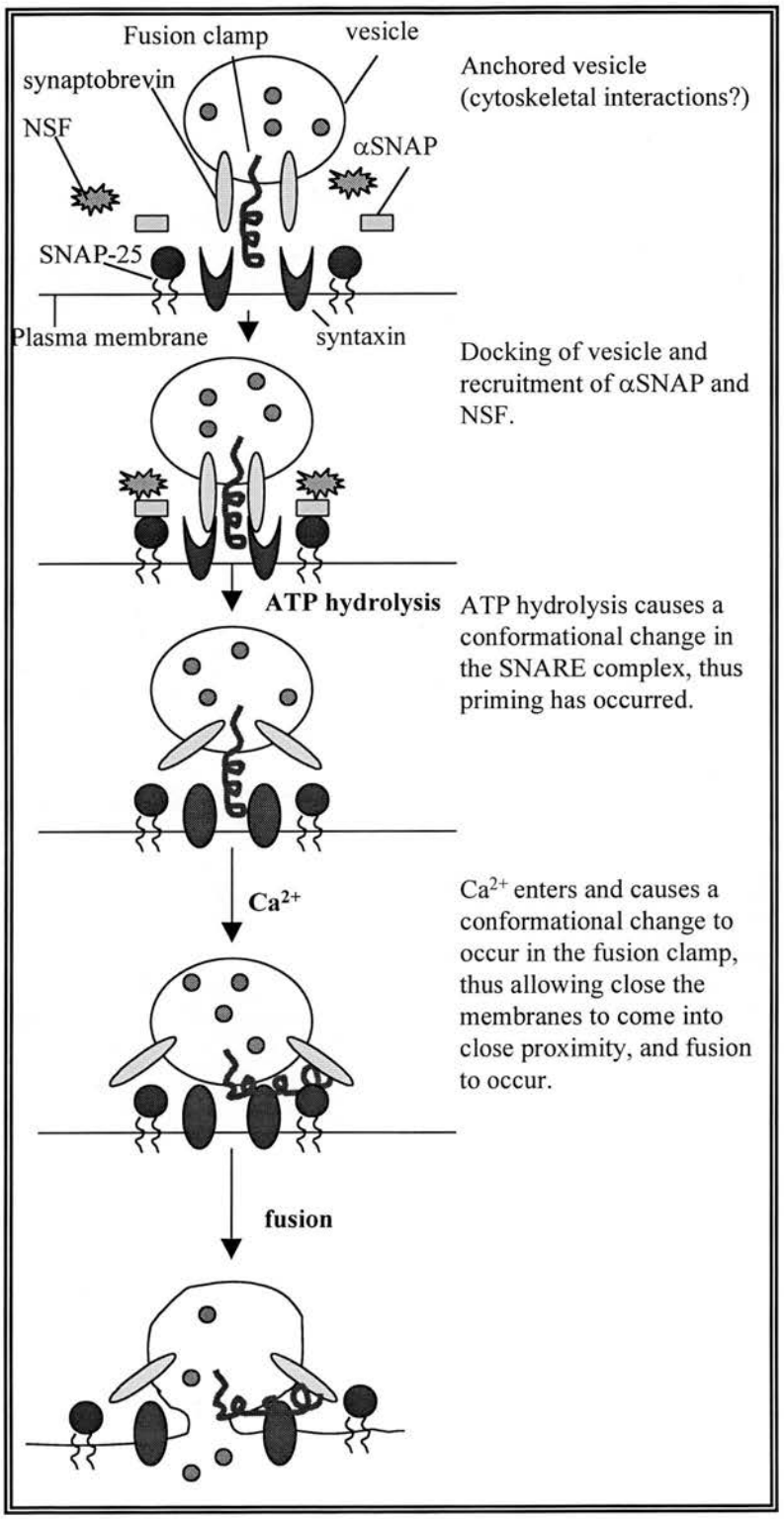

Figure 1.1.4 Proteins involved in exocytosis

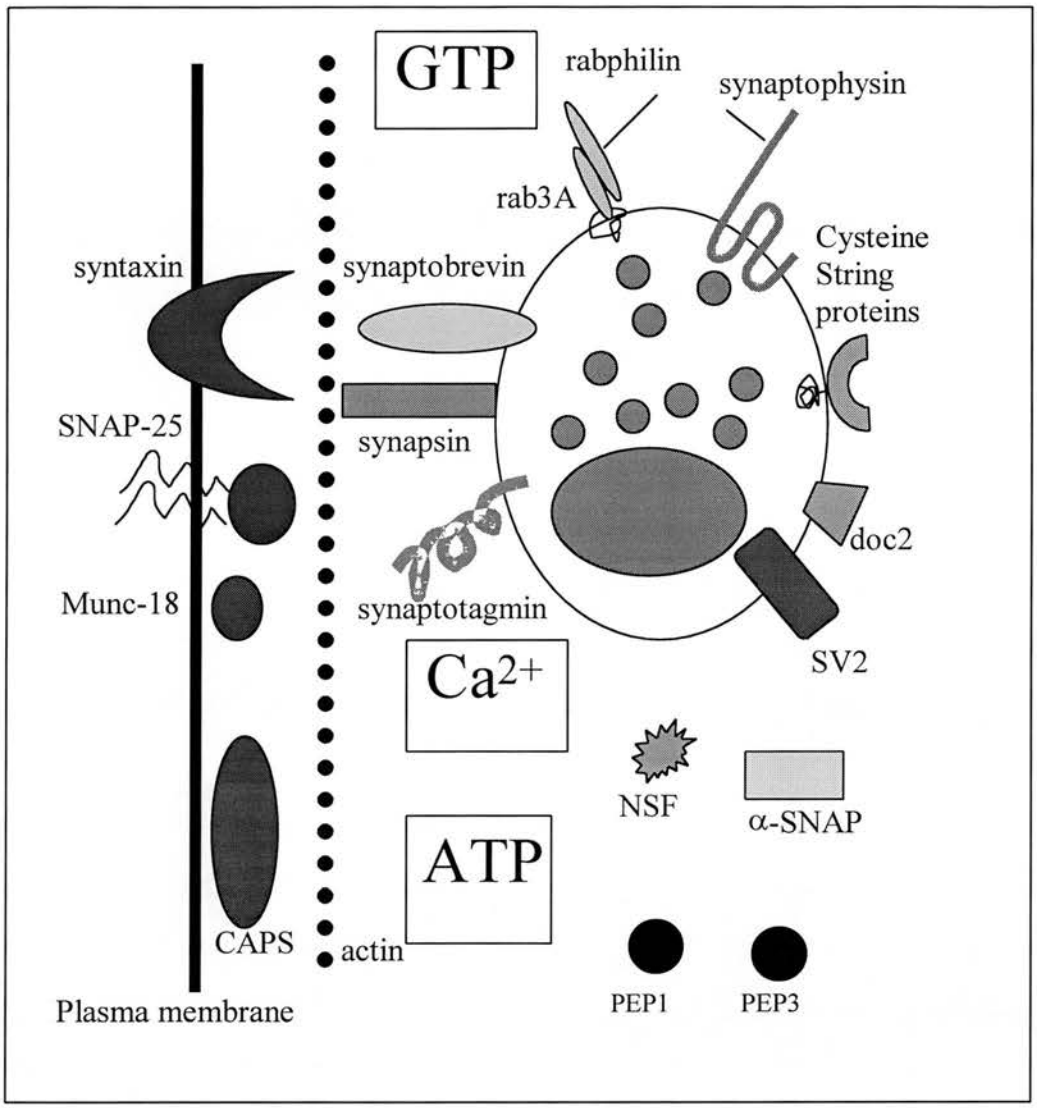

Table 1.1 PROTEIN	SIZE, TYPE & LOCALISATION	POSSIBLE FUNCTION(S)
Synaptotagmin	65kDa; vesicle (integral)	Calcium sensor.
Synaptobrevin/ VAMP	18kDa; vesicle (integral)	v-SNARE.
Syntaxin	36kDa; plasma membrane (integral)	t-SNARE.
SNAP-25	25kDa; plasma membrane (associated)	t-SNARE.
αSNAP	36kDa; cytosolic	adaptor to NSF.
NSF	76kDa; cytosolic (trimer)	ATPase activity; priming of the SNARE complex.
Actin	43kDa; plasma membrane & throughout cell	Barrier to vesicle fusion.
Rab3	25kDa; vesicle (associated)	GTPase activity. Vesicle release and recycling. Ca^{2+} sensor.
Rabphilin	86kDa; vesicle (associated – not necessarily by rab3)	Binding partner of rab3. Promotes its GTP/membrane bound. state
Synapsin	74kDa; vesicle (associated)	Anchorage of vesicle to cytoskeleton.
Synaptophysin	38kDa; vesicle (integral) 4 membrane spanning domains	SNARE interactions, binds to synaptobrevin and prevents synaptobrevin binding to other SNAREs. A major component of SVs, with unknown function *(Sudhof et al., 1987; Edelmann et al., 1995).*
Doc-2	44kDa; vesicle (integral)	A SV protein with two C_2 domains, which bind Ca^{2+} and phospholipids. Co-localises with synaptophysin and is another candidate for the Ca^{2+} sensor *(Orita et al., 1995).*

CAPS	145kDa; vesicle and plasma membrane (associated)	Vesicle and plasma membrane aggregation (Ca^{2+} triggered stage).
Munc-18	67kDa; vesicle (associated)	SNARE interactions: interacts with syntaxin and interferes with its binding to synaptobrevin. On phosphorylation of munc-18, its binding to syntaxin is inhibited *(Fujita et al., 1996)*.
14-3-3 proteins	30kDa; cytosolic/ interactions with cytoskeleton	Actin depolymerisation.
Cysteine string proteins	34kDa; vesicle (associated)	Peripheral membrane proteins of SVs, function unknown. Shown to interact with Ca^{2+} channels *(Braun & Scheller, 1995)*.
α-latrophilin	120kDa; plasma membrane (integral, extracellular)	Ca^{2+}-dependent receptor for αlatrotoxin. Cellular function unknown.
Neurexins	29-220kDa; plasma membrane (integral, extracellular)	Original αlatrotoxin receptor Ca^{2+}-independent αlatrotoxin receptor?
Annexins	36kDa; plasma membrane (associated)	A family of Ca^{2+}- and phospholipid binding proteins, enriched in SVs and bind synapsin I *(Inui et al., 1994)*.
Complexins	18kDa, cytosolic	Enriched in neurons and compete with aSNAP for binding to the SNARE complex *(McMahon et al., 1995)*.
PEP1	cytosolic	PtIns4P5kinase. PtdIns(4,5)P_2 production. Priming role.
PEP3	cytosolic	PtdIns transfer protein. PtdIns(4,5)P_2 production. Priming role.

SV2	82kDa; vesicle (integral)	A SV trans-membrane protein which resembles other plasma membrane proteins involved in protein transport across the membrane. Possible role in concentration of neurotransmitters within the vesicle. Also reported to bind synaptotagmin *(Jahn & Sudhof, 1994)*.

1.2 The AtT-20 cell line

The AtT-20 cell line is derived from the mouse anterior pituitary, and these cells synthesise and secrete adrenocorticotrophic hormone (ACTH), β lipotropin and related opioid peptides (endorphins). They represent a useful model for a number of studies as they are a homogeneous population of cells, unlike their *in vivo* counterparts which represent only a small fraction (2-5%) of the total cells within the anterior pituitary *(Sabol, 1980)*.

In vivo the hypothalamus releases corticotrophin-releasing hormone (CRH) which stimulates the anterior pituitary to release ACTH. This travels to the adrenal cortex and releases glucocorticoids that go on to stimulate gluconeogenesis in the liver *(Fox, 1990)*. Glucocorticoids are steroid hormones and therefore exert their effect through modulating mRNA synthesis. Their role is to increase blood glucose concentrations by increasing the rate of glucose production by the liver. One of the major glucocorticoid hormones is cortisol and it is ACTH that controls the rate of its synthesis and secretion, mainly by binding to adrenal cortex plasma membrane receptors and increasing adenylate cyclase activity. The anterior pituitary gland is therefore under the indirect control of the central nervous system (CNS) through the negative control of blood cortisol and the positive control of hypothalamic CRH. The physiological role of cortisol is to prepare the body for physical and metabolic activity thus it produces an increase in blood glucose concentration along with fatty acid mobilisation and an increased sensitivity to thyroxine and adrenaline. It is thought that this mainly occurs by cortisol changing the response of tissues to other hormones and regulators. This role means that every individual has a unique daily rhythm of cortisol with the most important peak being just prior to waking. It also guarantees this pathway a role during times of physical and emotional stress (*Newsholme & Leech, 1992*).

Figure 1.2.1 shows the hypothalamic-pituitary-adrenal axis

At present AtT-20 cells have been used in the study of two main areas:

- **Intracellular signalling events**

AtT-20 cells have been used extensively to study the signalling pathways that are activated on stimulation with CRH.

- **Prohormone processing and sorting**

Much of the information available on these cells represents the slightly earlier stages of the pathway than those involved in this study. This project is more concerned with the events closer to the plasma membrane and the proteins involved i.e. the actual docking and fusion of the vesicle with the plasma membrane.

This study will compare Ca^{2+}-regulated exocytosis in AtT-20 cells with the data already available for other cell types, predominantly neuronal and chromaffin cells. It will then correlate this data with the information already known about the signalling pathways.

Current findings in AtT-20 cells will now be reviewed under the following headings:

- **Basal/ constitutive secretion and pro-hormone processing**
- **Intracellular signalling**
- **Molecular mechanisms of Ca^{2+}-regulated exocytosis**

1.2.1 Basal/constitutive secretion and pro-hormone processing

AtT-20 cells have been extensively used in the study of the constitutive and regulated secretory pathway, and particularly in the analysis of the signals which direct proteins into the regulated pathway *(Stahl et al., 1996; Castle et al., 1995)*. They have also frequently been used in the study of intracellular trafficking and pro-hormone processing, often using methods of transfection to insert exogenous pro-hormones into the cell line *(Brakch et al., 1994; Eskeland et al., 1996)*. POMC itself (see figure 1.2.2), the peptide precursor from which ACTH, α-MSH, β-endorphin and other related peptides are produced, has also been studied in great detail. The maturation of the pro-hormone begins by the signal sequence being cleaved in the ER *(Walter et al., 1984)*. The identity of this signal sequence has been investigated by *Cool & Loh, 1994*. The first 10, 26, 50 and 101 N terminal amino acids of

POMC were fused to a reporter gene, and the localisation of the fusion protein studied. Immunofluorescence and subcellular fractionation showed that all the sequences, except for the first 10 amino acids, were able to direct the reporter gene into secretory granules, which forskolin (a secretagogue) could then go on to release. Binding studies with the first 76 amino acids of POMC also showed it to bind to the luminal side of granules in a pH-dependent manner. Similar binding was not obtained when CLIP and β-lipotropin were used. Thus it appears that the first 26 amino acids are necessary to target POMC to the regulatory pathway, and that this occurs via a pH-dependent binding mechanism. POMC is then transported through the Golgi complex where further maturation takes place including glycosylation, sulphation and phosphorylation *(Huttner, 1988; Eipper & Mains, 1982)*. Proteolytic processing i.e. POMC cleavage, begins in the trans-Golgi network (TGN) and continues as the secretory granules mature *(Tanaka & Kurosumi, 1992; Tooze et al., 1987)*. AtT-20 cells express the pro-hormone convertase PC1 at 20% of the molar levels of POMC *(Zhou & Mains, 1994)* and PC1 has been shown to be involved in POMC cleavage at paired basic sites *(Seidah et al., 1991). Tanaka et al., 1996* confirmed this co-localisation of PC1 with POMC in secretory granules. They also concluded that, whilst an acidic pH is favourable for proteolytic POMC processing, it is not a necessity, and more important is the efficient sorting of the POMC into secretory granules.

The AtT-20 cell line exhibits a high basal level of secretion that is often as much as 40% of stimulated secretion. There has been speculation as to the nature of this basal secretion, and in particular whether it occurs by the same pathway as constitutive. *Matsuuchi & Kelly, 1991* studied a variant AtT-20 cell line, deficient in regulated secretion, and postulated that basal secretion (i.e. a spontaneous release of regulated proteins occurring in the absence of stimulation) is not via the constitutive pathway. This is important when estimates are being made of the efficiency of sorting into the regulated pathway. It may also have an important physiological role, allowing the cells to respond to both positive and negative stimuli. Other data however appear to contradict this. *Surprenant, 1982* showed the direct link between increased electrical activity and secretory activity in AtT-20 cells. 82% of the cells showed spontaneous electrical activity that was increased on application of a depolarising current. On

removal of external calcium, the spontaneous action potentials were abolished and it was proposed that the mechanisms causing regulated secretion are different from those causing basal release. They postulated that basal secretion is due to release of ACTH from cellular components other than secretory granules. As yet, it appears that the real identity of basal secretion remains somewhat indistinct and it would be interesting to analyse it further.

1.2.2 Intracellular signalling in AtT-20 cells

ACTH secretion is stimulated by a 41-residue peptide called corticotrophin releasing hormone (CRH) *(Hook et al 1982)*. It has been established for many years that increasing intracellular Ca^{2+} concentration causes exocytosis in various cell types *(Douglas, 1968)*, and this has been shown to be true for AtT-20 cells *(Surprenant, 1982)*. However, the link between CRH stimulation and Ca^{2+} influx remains poorly defined. In the AtT-20 cell system, there is also the added complication of understanding how the negative inhibition of the glucocorticoids fits into this complex signalling pathway.

cAMP and cAMP-dependent Protein Kinase (PKA) have been shown to be involved in the control of ACTH release from anterior pituitary cells and AtT-20 cells *(Axelrod & Reisine, 1984)*. *Miyazaki et al., 1984* showed that whilst PKA will phosphorylate several macromolecules in AtT-20 cells, this does not appear to be directly linked to the ACTH secretion event. He suggested that cAMP-dependent PK was involved in the regulation of the intracellular Ca^{2+} concentration and this Ca^{2+} influx followed the PKA activation. AtT-20 cells have a type-1 CRH receptor that is linked to adenylate cyclase by the stimulatory G protein G_s, *(Pozzoli et al., 1996)* and CRH stimulates both ACTH secretion and biosynthesis of the ACTH precursor pro-opiomelanocortin (POMC) via this receptor *(Lundblad, 1988)*. *Litvin et al., 1984* used the cyclic nucleotide phosphodiesterase inhibitor MIX (3-methylisobutylxanthin) to increase intracellular cAMP levels to 10 times that seen during CRH stimulation, (which caused a two-fold increase). This caused no increase over the ACTH secretion seen with normal CRH-stimulated cAMP levels. This demonstrated the need for only small changes in intracellular cAMP concentrations in order to mediate ACTH secretion. This twofold cAMP rise was also accompanied

by activation of only a small fraction of the cAMP-dependent protein kinase within the cell. *Guild & Reisine, 1987* showed that CRH, forskolin (a direct adenylate cyclase activator; *Heisler & Reisine 1984*) and K^+-induced depolarisation stimulated ACTH secretion and a rise in intracellular Ca^{2+} concentrations. Protein kinase inhibitors have been introduced (via liposomes) into intact AtT-20 cells and shown to produce a subsequent large decrease in forskolin or CRH-stimulated, but not K^+-stimulated, ACTH release (*Reisine et al., 1986; Reisine & Guild 1985*). This directly demonstrated the essential role of adenylate cyclase (acting via the cAMP-dependent protein kinase, PKA) in increasing intracellular Ca^{2+} and causing ACTH release. It also enforced the idea that K^+ causes ACTH release by transiently opening voltage-gated Ca^{2+} channels and not by increasing cAMP levels. The same method was used to show the necessity of PKA in increased POMC gene expression (*Reisine et al., 1985*).

Permeabilised AtT-20 cells have been used extensively to study the later stages in the signalling cascade and have proved useful in resolving the Ca^{2+}-dependent and independent parts of the pathway. This is done mainly by the use of Ca^{2+}-EGTA buffers, which maintain a constant free Ca^{2+} concentration, which can effectively be zero. From such studies it appears that cAMP has a role in Ca^{2+}-evoked ACTH release (as well as in causing the initial Ca^{2+} influx) as it will increase the amount of ACTH released in response to varying Ca^{2+} concentrations (*Guild, 1991*). Ca^{2+}-EGTA buffers ensured that the cAMP-mediated rise in ACTH secretion could not be occurring via a further Ca^{2+} influx. Thus the cAMP appears to be playing an additional regulatory role at a site distal to that of Ca^{2+} entry.

Protein kinase C (PKC) may also play a role in ACTH secretion from AtT-20 cells (*Reisine & Guild, 1987*). Activators of PKC such as phorbol-12-myristate-13-acetate (PMA) increase cytosolic Ca^{2+} concentrations and stimulate ACTH release from intact cells in a dose-dependent manner thereby suggesting the involvement of PKC, possibly via the phospholipase C cascade. *Rane and Dunlop, 1986* first suggested a link between PKC activity and modulation of Ca^{2+} channel function. *Reisine and Guild, 1987* took this a step further by suggesting that this Ca^{2+} influx was mediated by K^+ channel blockage. Depolarisation of intact AtT-20 cells prevents PMA from

causing any further increase in Ca^{2+} levels whilst TEA (tetraethylammonium), which blocks K^+ channels, prevents PMA but not CRF from causing Ca^{2+} influx. Thus it appears that PMA-activated ACTH secretion may work via TEA-sensitive K^+ channels that depolarise the cells and cause a Ca^{2+} influx. PKC may directly phosphorylate either the K^+ channels or a protein that will interact with these, thus causing a blockage. A biphasic pattern of ACTH release is obtained on stimulation with PMA, the cells quickly becoming unresponsive to further stimulation with K^+, CRF or forskolin. It is possible that the phosphorylation events causing K^+ channel blockage could at a slightly later time cause a blockage of Ca^{2+} channels.

CRF stimulation of ACTH secretion via the adenylate cyclase/cAMP-dependent protein kinase system is unlike this as the response is maintained for as long as the stimulus is present and no biphasic pattern is seen. This, together with the fact that PKA inhibitors block [Ca^{2+}] increase and ACTH secretion mediated by forskolin or CRH but not by PMA, demonstrates the distinct pathways of PKC and *PKA (Reisine & Guild, 1987; Reisine et al., 1985*). It is also important to note that TEA has no effect on CRH-stimulated [Ca^{2+}] increase and ACTH secretion. Possibly, the Ca^{2+} channels are directly stimulated as the TEA-sensitive K^+ channels are obviously not involved. *Luini et al., 1985* have shown that 8-bromo-cyclic-AMP (a membrane permeant form of cAMP) can increase the frequency of Ca^{2+} channel opening in voltage-clamped patches of intact AtT-20 cells, therefore the cAMP appears to stimulate Ca^{2+} channels via PKA phosphorylation events. *Heisler and Reisine., 1984* supported this by showing that the Ca^{2+} channel blocker nifedipine inhibited forskolin and 8-bromo cAMP-mediated ACTH secretion. *Loechner et al., 1996* identified the presence of three different Ca^{2+} channel types in AtT-20 cells: dihydropyridine-sensitive (nimodipine, L-type channel), ω-Agatoxin-sensitive (PQ-type channel) and ω-conotoxin MVIIC-sensitive (N-type channel). They showed that only the nimodipine-sensitive channels were involved in KCl and CRH stimulation of ACTH secretion. Thus it appears that although the mechanisms of KCl and CRH evoked release vary, the Ca^{2+} channels involved are the same ones.

In permeabilised cells chelerythrine blocks PMA-mediated enhancement of Ca^{2+}-stimulated ACTH release but not the Ca^{2+} evoked secretion itself. Again Ca^{2+}-EGTA buffers were used to ensure no rise in the Ca^{2+} concentration therefore the PKC was

acting at a distal site and had a regulatory role. However unlike PKA, PKC has the ability to evoke ACTH secretion in the absence of Ca^{2+}, although at a lower level than that conferred by Ca^{2+}. Thus we see the regulatory roles of PKA and PKC to be distinct *(Mcferran & Guild, 1994)*. It has also been shown that PKC has a number of isoenzymes *(Hug & Sarre, 1993)* and that these are involved at different stages of the signalling pathway. *McFerran., et al 1995*, using the permeabilised AtT-20 cell system, showed that the α and ε isozymes of PKC act at a site distal to Ca^{2+} entry to regulate Ca^{2+}-mediated ACTH secretion. The β isozyme could act at a much earlier stage in the pathway to actually regulate the cytosolic Ca^{2+} concentration.

To summarise these findings: PKA activators will not cause ACTH secretion in the absence of Ca^{2+} whereas PKC activators will. The PKA pathway is the one by which CRH appears to mediate ACTH secretion. It also has a synergistic effect distal to Ca^{2+} entry where it appears to have a regulatory role. As yet, there is no direct link between CRH-mediated ACTH secretion and PKC. The effects of PKC and its activators on CRH and Ca^{2+}-mediated ACTH secretion are purely additive, thus suggesting that the two pathways are effectively independent and that the PKA pathway is the one involved in the Ca^{2+} messenger system (and CRH-mediated ACTH secretion). As yet the role of PKC remains unclear.

Events have been discussed which occur prior to the Ca^{2+} influx and which regulate at a point distal to Ca^{2+} entry in the pathway. As yet this section has not touched on the mechanisms after the Ca^{2+} influx, which are of course much closer to the topic of this thesis. While there are many proteins that are possible candidates for having roles in later events, only one has been shown to have a direct involvement in ACTH secretion at a site distal to Ca^{2+} entry. This effector appears to be a G protein.

Guanosine 5'-O-3-thiotriphosphate (GTP-γ-S) is a non-hydrolysable GTP analogue which stimulates AtT-20 cells to secrete ACTH in the absence of Ca^{2+} or ATP (*Guild, 1991*). This demonstrates a specific difference in the two levels of the pathway in that Ca^{2+}-stimulated ACTH secretion requires ATP whilst GTP-γ-S mediated secretion does not. In the absence of ATP, levels of secretion were slightly reduced at lower concentrations of GTP-γ-S, however at higher concentrations of GTP-γ-S the ATP had little effect. In fact the omission of ATP actually caused a

significant drop in basal ACTH secretion, which it has been suggested, is due to the added ATP generating GTP via nucleoside diphosphate kinase *(Gomperts, 1990)*. Obviously the effect of this GTP analogue points to the involvement of a guanosine 5'-triphosphate binding protein. It appears that G-proteins may have a role in mediating the effects of Ca^{2+} in various secretory cell systems *(for review see Gomperts 1990)* and at present the specific G protein involved has been given the term G_E. G_E may be a member of one of two families of G proteins: heterotrimeric G proteins, with three distinct sub units (α, β and γ) or small monomeric ras-like G proteins *(Gilman, 1987; Taylor, 1990; Hall, 1990)*. In AtT-20 cells rab3 (a monomeric G protein) seems to play a role in localisation, sequestration and storage of secretory vesicles *(Ngsee et al., 1993)*, and within this rab 3 family are isoforms which have different cellular distribution thus suggesting slightly varying roles *(Martelli et al., 1995)*. *Luini & Dematteis, 1988* identified an inhibitory form of G_E (G_{Ei}) which mediates somatostatin inhibition of ACTH secretion and may be heterotrimeric. Mastoparan is an amphiphilic tetradecapeptide that can form α helical structures in the phospholipid membrane. These appear to mimic the cytosolic loops of G protein- coupled receptors and therefore to activate heterotrimeric G proteins *(Higashijuma, 1988; Weingarten, 1990)*. However it should be noted that other diverse effects have also been seen with mastoparan (*Malenick and Anderson, 1983*). *McFerran & Guild, 1995* showed that mastoparan could stimulate ACTH secretion in permeabilised cells in a time- and dose-dependent manner, mirroring the stimulation obtained with GTP-γ-S and Ca^{2+}, and thus suggesting a specific effect on G_E. They postulated that mastoparan acts specifically on G_E in this system. Their use of the mastoparan analogues Mas-7 (which can stimulate heterotrimeric G proteins) and Mas-17 (which is unable to do so) points towards G_E being heterotrimeric, as the former stimulates ACTH secretion whilst the latter does not. They also show that the absence of ATP causes a large decrease in ACTH secretion (unlike the small decrease seen with GTP-γ-S mediated ACTH secretion). Again this may support the theory that the added ATP simply increases available GTP as opposed to having a direct role. The residual activity seen in the absence of ATP may then be due to the mastoparan activating nucleoside diphosphate kinase *(Kikkawa et al., 1992)*, or it could be due to a non-G_E mediated form of ACTH secretion.

At present this is the level of understanding that has been reached in ACTH secretion from AtT-20 cells. However there is also another important physiological aspect in the pathway that we must look at, that of inhibition of ACTH secretion. The main physiological inhibitors of ACTH secretion in AtT-20 cells are the glucocorticoids (such as cortisol) and these have a typical negative feedback role (see figure 1.2.1)

There are two distinct mechanisms by which glucocorticoids exert their inhibitory effect (*Shipston et al.,1995*):

- **EARLY (<3hours; within 10 minutes)**

This involves *de novo* protein synthesis and subsequent decrease in ACTH secretion *(Keller-Wood et al., 1988).*

- **LATE (>6 hours to days)**

This involves an actual suppression of cell function by inhibiting ACTH biosynthesis and down-regulating CRH signalling pathways *(Lundblad & Roberts, 1988).*

As this review covers the intracellular signalling pathways of AtT-20 cells the area focused on will be the early inhibition of ACTH secretion by glucocorticoids. *Phillips & Tashjian, 1982* showed dexamethasone to cause a decrease in ACTH secreted on stimulation by hypothalamic extract, by phorbol esters, or by 8-bromo-cAMP but not by high K^+. It also had no effect on the basal levels of ACTH secretion. They showed that there was no decrease in intracellular levels of ACTH and used cycloheximide (an inhibitor of protein synthesis) to conclude that the inhibition was due to the synthesis of new protein. The molecular mechanism of this glucocorticoid-induced protein (GIP) remains under scrutiny.

Clark & Kemppainen, 1994 showed dexamethasone to inhibit ACTH secretion but not that stimulated by K^+ or maitotoxin (which stimulates a Ca^{2+} influx by Ca^{2+}-dependent membrane depolarization). They used the Ca^{2+} indicator fura-2 to measure intracellular $[Ca^{2+}]$ and show that its increase was necessary for ACTH secretion. However on treatment with dexamethasone and stimulation of ACTH secretion there was no decrease in the intracellular Ca^{2+} rise, but a decrease was seen in the ACTH secretion. This led to the theory that the inhibitory effect of the GIP must occur distal to Ca^{2+} entry, although it is difficult to reconcile this with the fact that

glucocorticoids do not have an effect on high K^+-mediated ACTH secretion. *Link et al, 1993* reported a similar result in rat anterior pituitary cells stimulated to secrete by oxytocin.

There are however results which contradict this theory. Other groups have found that the inhibition of ACTH secretion by dexamethasone does in fact cause a decrease in the stimulated intracellular rise of calcium ions *(Antoni et al., 1992).* Such results suggest a role for the GIP in preventing or decreasing the *influx* of calcium ions. *Shipston et al., 1996* showed that PKA activation (by CRF or 8-bromo-cAMP) caused (in addition to Ca^{2+} influx via L-type Ca^{2+} channel activation) an inhibition of the Ca^{2+}-activated BK-type K^+ channel. Thus CRH stimulation usually prevents the Ca^{2+}-induced feedback hyperpolarization mediated by these channels, thereby allowing a greater Ca^{2+} influx. Iberiotoxin specifically blocks the BK channel, and abolishes glucocorticoid inhibition of CRF-stimulated ACTH secretion. They therefore postulate that glucocorticoids cause the synthesis of GIP, which in turn blocks PKA-activated inhibition of the BK channel, thus preventing the intracellular $[Ca^{2+}]$ rise.

Another theory *(Castellino et al., 1992)* suggests a role for glucocorticoids in inhibiting ACTH secretion by stabilisation of the actin barrier. It was shown that cytochalasin D destabilised plasma membrane actin and that dexamethasone partially protected the cells against these effects, and thickened the actin bundles. However electron microscopy showed the actin filaments not to intervene as a direct barrier between secretory droplets and the plasma membrane. They concluded that the role of actin in exocytosis in AtT-20 cells was to hold the granules away from, but close to their discharge sites, as opposed to acting as a direct barrier. A difficulty in interpreting these data is that the total increase of actin cross-linking proteins is actually very small and can only be reliably detected after 6 hours.

This brings to a conclusion the review of intracellular signalling in At-20 cells. Figure 1.2.3 summarises this very complex, if fairly well characterised pathway.

1.2.3 Molecular mechanisms of exocytosis in AtT-20 cells

As mentioned before, little work has been done in AtT-20 cells on the molecular mechanisms of exocytosis which occur slightly further down the pathway. The following section reviews the work that has been undertaken at this present time.

Rab proteins (ras-like GTP-binding proteins) have been the most extensively studied proteins in AtT-20 cells, in terms of their role in exocytosis. Many monomeric small G proteins (20-25 kDa) have been implicated in acting as molecular switches in regulated membrane trafficking (see section 1.1; *Bourne et al., 1991*). Of these rab proteins, rab3 is of particular interest due to its localisation to synaptic vesicles in neurons *(Fischer von Mollard et al., 1990). Ngsee et al., 1993* transfected AtT-20 cells with an elasmobranch homologue of endogenous rab3A (o-rab3) and showed it to be localised exclusively at the tips of the cell processes (where regulated secretory proteins accumulate). Two mutations, affecting GTP binding and hydrolysis, blocked the localisation of o-rab3 to the tips of the cell processes. These same mutations also caused less efficient targeting of ACTH-containing vesicles to the processes, but had no effect on ACTH secretion (basal or stimulated). These results suggest that the rab3 proteins are important in vesicle transport to the process tips, but do not have a role in the actual release of vesicles in a regulated manner. However without actually removing all functional rab-3, it is very difficult to have absolute confidence in this statement.

Martelli et al., 1995 identified rab3D in AtT-20 cells and showed it to have a diffuse vesicular distribution in the cytoplasm of the cell body, the processes and the tips, unlike rab3A. They put forward the possibility that it defines a regulatory secretory pathway which functions independently of cell polarity, however it is important to note that, as yet, there is no experimental evidence to back up this finding.

Wendland and Scheller, 1994 investigated the effects on secretion in AtT-20 cells of stable transfection with soluble fragments of synaptotagmin, a putative calcium sensor. If the synaptotagmin were acting in this manner, the soluble, non-functional synaptotagmin should create a dominant negative phenotype, by interfering with the secretory machinery. Subcellular fractionation analysis showed that the fragments were localised to both soluble and membrane fractions, possibly by protein-protein

interactions. Neither basal nor regulated secretion was affected in the stable mutants, suggesting either that another pathway is present which is able to bypass the synaptotagmin stage, or that synaptotagmin is simply not a requirement of regulated secretion in AtT-20 cells.

1.3 Project aims

This chapter has reviewed two main areas:

- The molecular mechanisms of exocytosis
- Secretion from AtT-20 cells

The purpose of this project is to bring these two areas together and to elucidate whether similar mechanisms of exocytosis are involved in these cells, as are present in other cell types.

Increasingly it becomes apparent that considerable variation can be seen between different cell types and particularly different experimental systems. It is important to remember the very different physiological roles which neuronal and chromaffin cells (the best studied exocytosis systems) have, in comparison to AtT-20 cells.

- The first aim was to completely characterise the AtT-20 cells using western blotting and immunofluorescence, to assess which of the many proteins thought to be involved in exocytosis, were actually present in this cell line.

- The second aim was to explore the role of these proteins in more detail by setting up a permeabilised cell system and RIA (to measure ACTH secretion). This would allow the entry into the cells of various recombinant proteins, antibodies, drugs and toxins and subsequent measurement of their effect on exocytosis.

- A third aim of this project was to look at a possible alternative to the complex and time-consuming RIA presently used for measurement of regulated secretion in AtT-20 cells.

Figure 1.2.1 Hypothalamus-Pituitary-Adrenal Axis

(Newsholme & Leech, 1992; Fox, 1990)

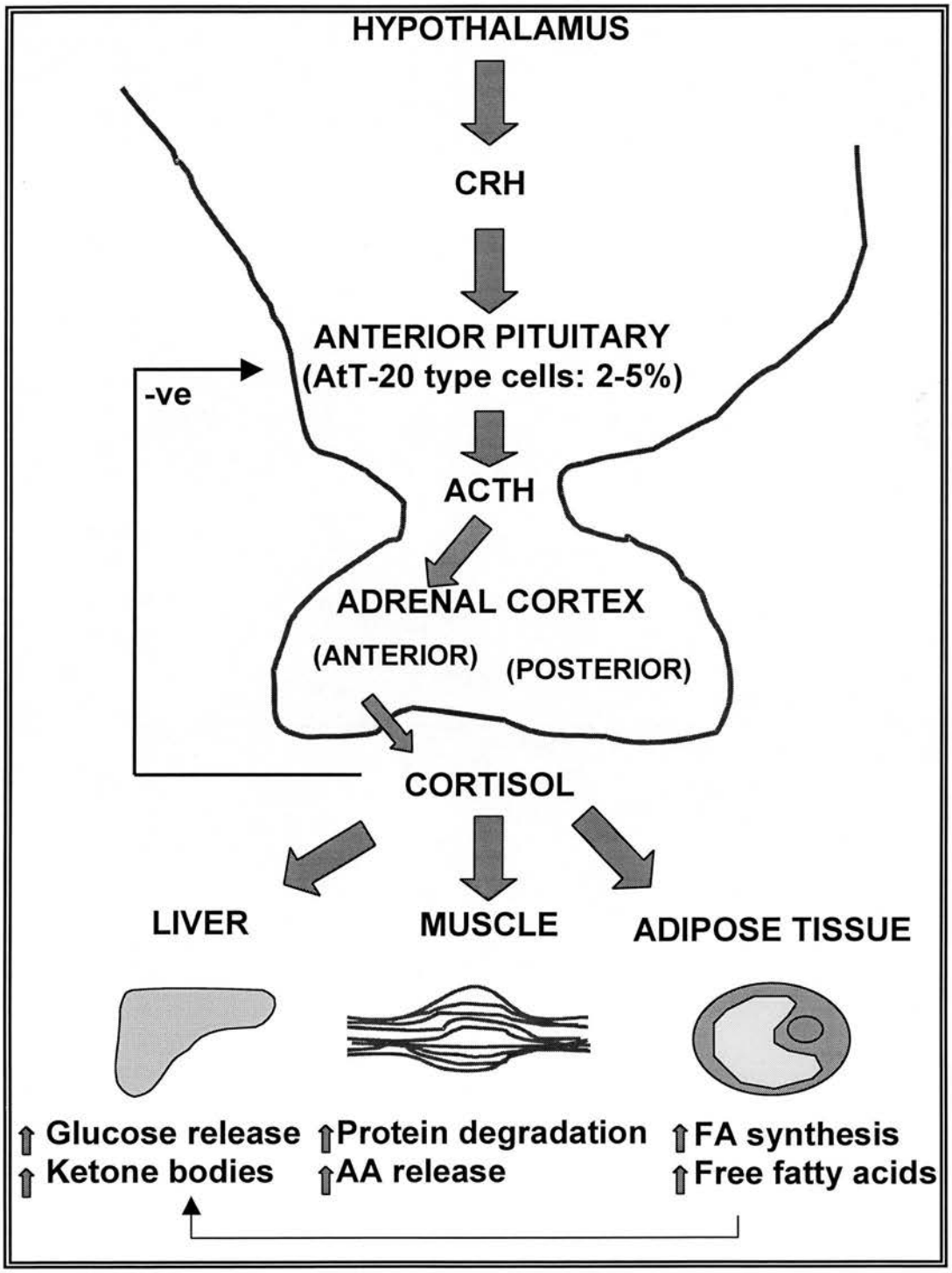

Figure 1.2.2 Structure of pro-opiomelanocortin

(Nakanashi et al., 1979)

Abbreviations: MSH, melanocyte-stimulating hormone; ACTH, adrenocorticotrophin; CLIP, corticotropin-like intermediate-lobe peptide; LPH, lipotropin.

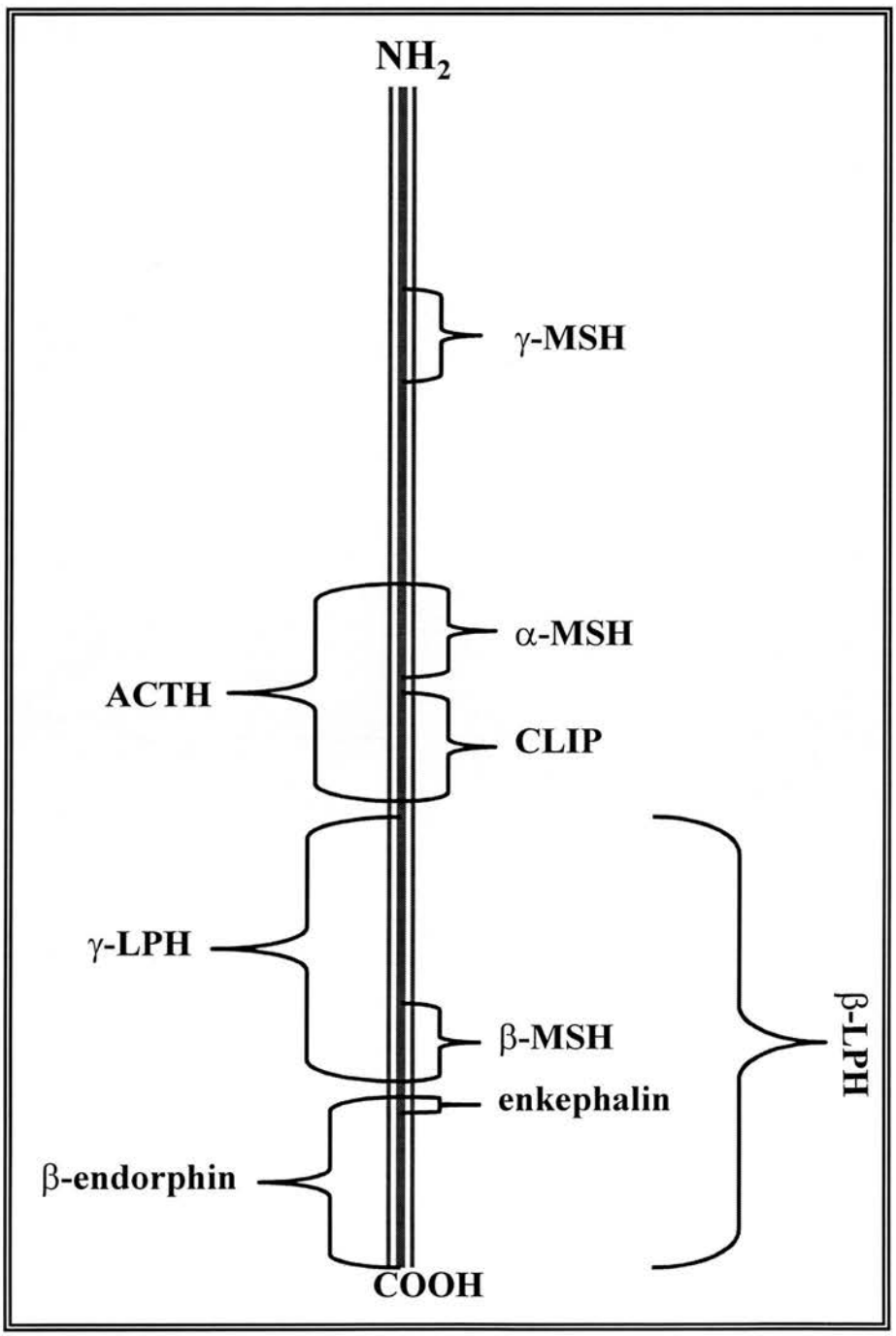

Figure 1.2.3 CRF cascade

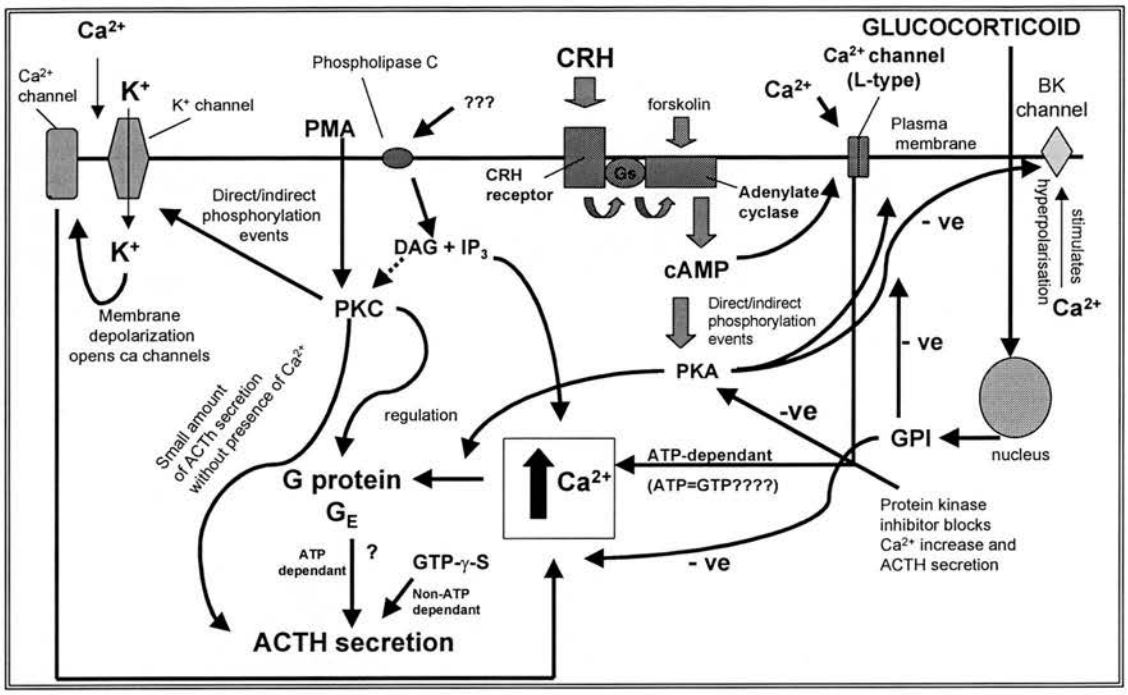

Chapter 2

Materials and Methods

MATERIALS

General Chemicals for biochemical techniques were obtained from BDH Chemicals and Sigma Chemical Co., as were all photographic reagents.

Radiochemicals were all obtained from Amersham International plc.

Molecular Biology reagents were generally from Promega, Qiagen, GibCo BRL or BioLabs. The plasmidmini-prep kit, Qiaex II Gel Extraction Kit, mRNA extraction kit and Ni^{2+}-agarose were all from Qiagen. The Great Escape Genetic Reporter kit, containing the SEAP plasmid and the chemiluminescent detection method, was from Clontech. All growth medium materials (yeast extract, tryptone and bact-agarose) were from DIFCO. Reverse transcriptase superscript II was from GibCo BRL. Taq polymerase, 1kb DNA ladder and dNTPs were all from Promega. Vent DNA polymerase and restriction enzymes were from BioLabs. IPTG was from BDH. All primers were from Oswell or Cruachem and nucleic acid sequencing was done by Oswell.

Cell Culture Reagents were from GibCO BRL, and plasticware was from Greiner. The Lipofectamine™ reagent was from GibCO BRL. The Alkaline Phosphatase Leukocyte Cytochemical stain Kit and the trypan blue stain were from Sigma. Normal AtT-20 cell culture used GibCO DMEM (4500 mg/ml glucose), containing 10% v/v FCS and 100 IU/ml penicillin/streptomycin. Cells were frozen in GibCO freezing medium. Transfections were made using GibCO Optimem™ medium, incomplete DMEM (i.e. DMEM with no FCS or antibiotics) or selective complete DMEM (with 2.5mg/ml G418). Incubations in the absence of 5% CO_2 (for KCl or CRF stimulation assays) used a powdered form of DMEM which was supplemented with Hepes/NaOH (pH 7.4) and BSA.

Radioimmunoassay materials were from NIDDK (National Institute of Diabetes and Digestive Kidney Diseases). Human ACTH (1-39 synthetic peptide, AFP6328031) and Human anti-ACTH rabbit antiserum (AFP2938C) were both obtained from NIDDK. Radioimmunoassay tubes were from Luckam. PEG (average molecular weight 8000) and BSA (high purity) were from Sigma Chemical Co. Donkey anti-rabbit antiserum and normal rabbit serum were from SAPU (Scottish

Antibody Production Unit). Digitonin was from Calbiochem. CRF, 8-bromo-cAMP, dexamethasone, cytochalasin D and phalloidin were all from Sigma Chemical Co.

Antibodies were from various different sources. Secondary antibodies used for the detection of immunofluorescence microscopy or western blots were from SAPU, except for anti-mouse and anti-rabbit antibodies conjugated to rhodamine, which were from Sigma Chemical Co. Anti-syntaxin HPC-1 antibody was also from Sigma Chemical Co. All other antibodies used in western blotting and immuofluorescence were kindly donated by various laboratories and are acknowledged in context, as are various recombinant proteins.

METHODS

2.1 Cell culture of AtT-20 cells

AtT-20 cells were grown in a similar way to that described by *Sabol, 1980.* AtT-20 cells (clone D16-16, obtained from F. Antoni, Dept. of Pharmacology, Edinburgh University) were grown in high glucose (4500mg/ml) DMEM medium with 10% v/v FCS and 100 IU/ml penicillin/streptomycin until a confluency of approximately 80% (approximately 5 X 10^5cells per 25cm^2 flask) was reached, at which point the cells were passaged at a 1:3 dilution. This was done by first washing the cell monolayer with 5ml of PBS and then adding 2ml of trypsin/EDTA. Having ensured complete coverage of the monolayer the majority of the trypsin/EDTA was decanted off. The cells were left in the residual trypsin/EDTA for 5min at room temperature and were then resuspended in 6ml medium. This 6ml medium was distributed between three 25cm^2 flasks and an additional 3ml fresh medium was added to each. These flasks were then passaged in 3-5 days time, when the cells reached approximately 80% confluency. This same protocol was carried out for 75cm^2 – 500cm^2 flasks/dishes and for 6-24 well plates with the appropriate scale up according to surface area. Cells were grown at 37°C with 5%CO_2.

2.1.1 Freezing AtT-20 cells

Cells were grown until they reached 80-90% confluency in a 75cm^2 flask at which point they were removed from the flask surface with 0.25% w/v trypsin/ 0.1% w/v EDTA as detailed above. They were then resuspended in approximately 10ml of medium and centrifuged at 1000rpm for 5min using a bench centrifuge. The medium was decanted from the tube and the cells were resuspended in 3ml of ice-cold freezing medium, 1ml of which was aliquoted per freezing vial. The vials were kept overnight at –70°C and transferred, after 24 hours, to liquid nitrogen where they were stored until needed. The cells were taken up from liquid nitrogen by thawing the vial quickly in a 37°C water bath and re-suspending in 10ml medium. They were then centrifuged at 1000rpm using a bench centrifuge for 5min (to remove them from toxic dimethylsulphoxides, in the freezing medium) then resuspended in 5ml fresh medium in a 25cm^2 flask.

2.1.2 Large scale harvesting of cells

This method was obtained from James Pryde (Raine Laboratory, Edinburgh University; unpublished work).

2.1.2.1 Materials

KHEM buffer:

50mM KCl, 10mM EGTA, 50mM Hepes, 1.92mM $MgCl_2$.

PIC (protease inhibitor cocktail) – used at 1:1000 (stored in DMSO)

Aprotinin 1mg/ml, Leupeptin 1mg/ml, Pepstatin 1mg/ml, Antipain 1mg/ml, Benzamidine 1M, PMSF 40mg/ml.

Complete KHEM buffer (KHEM plus the following added):

1mM DTT, 1µM cytochalasin B, 1µl/ml PIC (see above).

TEA/KCl

Triethanolamine (TEA) 10mM, KCl 150mM.

All solutions used were at pH 7.4.

2.1.2.2 Method

Cells were grown in 500cm^2 Petri dishes until 80% confluent, at which point the dishes were placed on ice, in the cold room. The plates were washed twice with 50ml KHEM buffer, and were then incubated for 45min with 20ml complete KHEM buffer. This was then removed and stored for later use, and the cells were swollen with 50ml TEA/KCl for 10min, after which time they were again incubated in complete KHEM buffer for 2-5min. This was decanted and the dishes placed on their sides to drain until no more buffer was collected, at which point the cells were scraped off using a sliced rubber bung. Approximately 0.8-1ml cells were collected per dish and these were then ruptured with approximately 30 down strokes in a small Dounce homogeniser (2ml at a time). Cell breakage was assessed using 0.4% w/v trypan blue solution and was found to be greater than 80-90%. To remove nuclear material the homogenate was centrifuged at 2000rpm for 5min using a microfuge, and the post-nuclear supernatant (PNS) was stored in liquid nitrogen (unless used immediately).

2.1.3 Fractionation of post-nuclear supernatant

This method was similar to that detailed *by Wendland & Scheller,1994* except that a continuous sucrose gradient was used and the fractions collected were not TCA precipitated. A 12ml continuous linear sucrose gradient was produced using a gradient maker and peristaltic pump. The sucrose solutions were made up in 10mM Hepes pH7.4 and 2mM EGTA, and were 0.4M and 1.925M. In later experiments slightly varying sucrose gradients were tested and these are detailed in Chapter 3. 1ml of PNS was carefully layered onto the top of each gradient and the tubes were centrifuged (in a Beckman SW41 rotor, on an L8-55 Beckman, 55,000g) for 2 hours at 4^{o}C. 1ml samples were then removed using a peristaltic pump and a needle placed at the bottom of the tube, and stored at -70^{o}C, until needed.

2.1.4 Estimations of sucrose concentrations

A refractometer and refractive index conversion tables were used to estimate the actual sucrose concentration in each fraction from the gradient.

2.1.5 Protein estimations

Protein estimations were made of each cell fraction using the methods detailed below. These methods were also used throughout the project.

2.1.5.1 Peterson's assay

A simplification of the method of *Lowry et al., 1977* was used here.

A standard curve was produced using duplicates of 0-60μg bovine serum albumin which were made up to 400μl with water, as were all samples. 40μl of 10% w/v sodium deoxycholate was added to each and they were left to stand for 10min at room temperature. 40μl of 72% v/v trichloroacetic acid (TCA) was then added to each tube. Samples were incubated at room temperature for 5min, and centrifuged at 6000rpm for 10min using a microfuge, and the supernatants were then discarded. This step allowed the removal of any substances that might interfere with the protein assay.

CTC: 10% sodium carbonate, 0.1% w/v copper sulphate (pentahydrate), 0.2% w/v potassium sodium tartrate. Sodium carbonate was made up first and then slowly added to a solution of the latter two compounds.

Reagent A: was made up using equal amounts of: CTC, 0.8N NaOH, 10% w/v SDS, water.

Reagent B: One volume of Folin-Ciocalteu phenol reagent was mixed with five volumes water.

The sample was brought to a volume of 400μl with water, and 400μl of reagent A was added, and incubated for 10min at room temperature. 200μl of reagent B was then added and the absorbance read at 750nm after 30min.

2.1.5.2 Bradford's assay

The following protocol is a modification of the protocol detailed below: *Bradford, 1976.*

25 mg of Coomassie Brilliant Blue G was dissolved in 25ml 96% v/v ethanol with stirring overnight, and 50ml of 85% v/v orthophosporic acid was then added. This was made up to 100ml with water to produce a 5 X stock solution of dye.

The standard curve was obtained using BSA samples of 0-100μg. All samples were made up to 100μl in 150mM NaCl and 1ml of 1 X Bradford reagent (diluted in 150mM NaCl) was added to each sample. Having vortexed well, these were incubated at room temperature for 30min, and the absorbance read at 595nm.

2.1.6 Galactosyl transferase assay

The transfer of galactose from [^{3}H]-UDP-galactose to the glycoprotein acceptor ovomucoid *(Bretz & Staubli, 1977)* was assayed, as a method of identifying the position of the Golgi apparatus in the sucrose gradient during cell fractionation.

Assay mix: 40mM sodium cacodylate pH6.6, 17.5mg/ml ovomucoid, 40mM mercaptoethanol, 0.2% v/v Triton X-100, 2mM ATP pH7.0, 40mM $MnCl_2$, 0.5μCi/ml [^{3}H]-UDP-gal (specific activity 10-25 Ci/mmol; 370-925 GBq/mmol). 20μl samples were incubated with 80μl of the above assay mix at 37°C for 30min. The reaction was stopped using 1ml of ice-cold 0.5M phosphotungstic acid/hydrochloric acid (PTA/HCl) and the samples centrifuged at 2000rpm for 4min in a microfuge. The supernatant was aspirated and the pellets washed 3 times with 1ml PTA/HCl as detailed above, and then given a last wash with 96% v/v ethanol before being solubilised with 50ml of 2M Tris base and 200ml of 1% w/v SDS. The samples were mixed on a shaker for 10min and 1ml of Beckman (cocktail T) scintillation fluid was added to each sample. These were then loaded into Beckman 5ml scintillation vials and counted.

2.1.7 Biotinylation of cell surface antigens

In order to detect plasma membrane proteins in the gradient fractions a large scale AtT-20 cell preparation was done in the presence of a biotinylating reagent (i.e. biotinylation of whole cells). The protocol is as in 2.1.3, except for the additional steps detailed below.

Biotinylation buffer pH7.5: 137mM NaCl, 5mM KCl, 5mM glucose, 1mM $MgCl_2$, 1mM $CaCl_2$, 6mM $NaHCO_3$.

500cm^2 dishes were placed on ice in the cold room and washed twice with 20ml PBS per dish. 35ml of biotinylation buffer, containing N-hydroxysuccinimidyl-biotin (NHS-biotin) at a concentration of 300μg/ml, was added to each dish and incubated

for 30min. 175µl lysine (0.1mg/ml stock solution) was added per dish and mixed, in order to remove unreacted NHS-biotin and so prevent biotinylation of intracellular proteins on homogenisation. The biotinylation buffer was then decanted and the cells then harvested exactly as detailed in 2.1.3.

After blotting, and blocking free protein sites, the biotinylated cell surface antigens were detected using streptavidin-peroxidase at a concentration of 1/4000 in the normal secondary antibody buffer.

2.1.8 Triton Fractionation of cell pellet

AtT-20 cells were grown until eight confluent 450cm^2 flasks were obtained, and the cells were then removed using trypsin/EDTA. The cells were centrifuged for 5min, at 1000rpm, on the bench centrifuge to obtain a pellet that was used in the protocol detailed below.

2.1.8.1 Pre-condensation of TX-114

This procedure is similar to that detailed by *Bordier, 1981* and its purpose was to remove any contaminants from the Triton X-114.

20g of Triton X-114, and 16mg of butylated hydroxytoluene (dissolved in 100µl ethanol) was added to 980ml of 10mM Tris-salt pH7.4/ 150mM NaCl. This mixture was left on ice for 8 hours, during which time the solution became clear. It was then transferred to a separating funnel and warmed overnight at 30°C, which caused separation into an aqueous phase and a detergent phase, the former of which was discarded. The discarded aqueous phase was then replaced with fresh buffer, and the process repeated twice more, finally recovering the detergent phase.

2.1.8.2 TX-114 phase separation of integral membrane proteins

The protocol used here was adapted from that described in *Pryde & Phillips, 1986* and *Pryde, 1986.* The AtT-20 cell pellet, described above, was resuspended in 4ml of Tris-salt buffer (10mM Tris pH7.6, 150mM NaCl). TX-114 was then added to a concentration of 2% at 4°C, and the solution left on ice for 2 minutes. This was then centrifuged at 100,000rpm (TL100.3 rotor, TL-100 centrifuge) for 10min, after which the supernatant was removed and kept on ice, whilst the pellet was

resuspended in Tris-salt buffer. This was centrifuged as before, and resuspended 400µl of Tris-salt buffer. This fraction was the phospholipid-rich fraction (P1).

1.6ml of the supernatant was then loaded on to a 1.4ml sucrose cushion mix (0.25M sucrose, 10mM Tris pH7.6, 0.15M NaCl, 0.06% TX-114), in a conical test tube and incubated at 30°C for 3 minutes. The samples were then centrifuged for 10 minutes at 4000rpm in a bench centrifuge, and the top aqueous layer removed and kept on ice. The sucrose cushion was removed, leaving behind a thick detergent-rich phase, which was diluted by adding a small volume of Tris-salt buffer. The process of phase separation was repeated and the final detergent phase diluted with an equal volume of Tris-salt buffer. This was the P2 fraction.

To the aqueous layer from the above phase separation had TX-114 was added to a concentration of 0.5%. This was overlayed on a sucrose cushion and the phase separation repeated, again keeping the aqueous layer. TX-114 was then added to a concentration of 2% and phase separation repeated, taking the final aqueous layer as the end product. This was the hydrophilic fraction (S2).

2.2 Gel electrophoresis and western blotting

Separation of proteins was achieved by electrophoresis through polyacrylamide gels following the basic procedure of *Lammili, 1970,* using the Hoeffer "Tall Mighty Small" apparatus.

2.2.1 SDS-PAGE

2.2.1.1 Solutions for SDS-PAGE

Separating gel: 0.1% w/v SDS, 330mM Tris HCl pH8.8,10-15% w/v acrylamide: bis-acrylamide, 0.1% w/v APS, 0.1% v/v TEMED.

Stacking gel: 0.11% w/v SDS, 0.14mM Tris HCl pH6.5, 4.5% w/v Acrylamide:Bis-acrylamide, 0.1% w/v APS, 0.1% v/v TEMED.

The acrylamide:bis-acrylamide was at a ratio of 30:0.8.

Electrophoresis buffer (5 X stock): 0.248M Tris-base, 1.92M Glycine, 0.5% w/v SDS, 1mM EDTA.

Sample buffer (4 X stock): 0.2M Tris-HCl pH6.5, 20% w/v SDS, 8mM EDTA, 40% v/v glycerol, 40mM DTT, 0.2mg/ml bromophenol blue. Samples were usually heated to 100°C although variations of this were used, and these are detailed in the results chapters.

Molecular weight markers: DaVII (14-66kDa) and High MW markers (29-205kDa), both of which were from Sigma Chemical Co.

2.2.1.2 Assembly of gel cassette and pouring of gels

The alumina backing plate, glass plate and plastic spacers were cleaned with methanol. The cassette was then assembled with the alumina plate first, spacers and glass plate; all flush with the back reservoir base. These were held in place with 4 clips and then the apparatus placed on a glass plate in some molten 1.5% agar to seal it. The appropriate volumes of 10% APS and TEMED were then added to the separating gel mix, this was mixed and then pipetted in between the alumina and glass plates up to a level that allowed room for the separating gel and comb. Until set, this gel mixture was overlayed with water-saturated butan-2-ol Once this was set the top was washed the stacking gel mix was pipetted on top of the separating gel, and a 10 or 15 well comb inserted. Once this had set, the gel cassette was inserted into a bottom tank and electrophoresis buffer added to the bottom and top tanks. Samples were loaded and the gel was run at 20mA (constant current) for approximately 1.5 hours.

2.2.1.3 Solutions for coomassie staining of gels:

Gel fix: 10% v/v acetic acid, 20% v/v methanol.

Gel stain: 0.125% w/v Coomassie blue R, 50% v/v methanol, 7.5% v/v acetic acid.

Destaining solution: 7% v/v acetic acid, 10% v/v methanol.

2.2.1.4 Fixing, staining and destaining of gels

Having run the gels, the apparatus was disassembled and the gels transferred to fix for 10-30min, where they were incubated with gentle shaking. They were then transferred into stain for 10min and then into destain overnight, again with gentle shaking. Finally they were then dried down or vacuum-sealed until they were scanned.

2.2.1.5 Densitometric scanning of gels

Quantitation of recombinant toxins was done using a combination of Bradford protein assays and a Densitometer Raster scan, using a Joyce-Loebl computer program for analysis.

2.2.2 Western blotting

2.2.2.1 Solutions for western blotting

Transfer Buffer: 20mM Na_2HPO_4, 20% v/v methanol, 0.02% w/v SDS.

TBS X 10: 200mM Tris HCl pH7.4, 1.5N NaCl.

Blocking buffer: 0.5% Tween20, 0.05% sodium azide, 5% Marvel (in TBS).

Washing buffer: 0.05% Tween-20 in TBS.

Primary antibody solution: 5% v/v normal horse serum, 5mg/ml BSA, 0.05% w/v sodium azide, 0.5% v/v Tween-20 (in TBS). The primary antibody was usually used at 1/1000 dilution (details of the antibody and concentrations are given in the appropriate chapter).

Secondary antibody solution: 0.05% v/v Tween-20 in TBS. Secondary antibody was either anti-rabbit conjugated to HRP or anti-mouse IgG conjugated to HRP. Both were used at a dilution of 1/4000 and were from SAPU.

Ponceau S (10 X stock): 2% w/v Ponceau S, 30% v/v TCA, 30% v/v sulphosalicylic acid.

2.2.2.2 Western blotting protocol

A cassette was set up in transfer buffer with a layer of sponge, and four pieces of filter paper at either side. The gel to be blotted was carefully lifted onto this and a piece of nitrocellulose was placed on top. The cassette was closed and placed into the blotting apparatus, which was already full of transfer buffer. The proteins were transferred onto the nitrocellulose for 3 hours at 1.5amp or overnight at 0.5amp.

The nitrocellulose was removed from the tank and stained with Ponceau S in order to assess the position of the marker bands. This was done by incubating the blot in Ponceau S for 10min and then washing with water until the bands appeared. These were marked on the nitrocellulose with pen and then the blot was transferred into

blocking solution for 3hours or overnight. The blocking solution was then removed and the primary antibody solution added and incubated for 3 hours or overnight. Having removed this the blot was washed 3 times for 15min with wash solution and the secondary antibody solution was added for 45-60min. This was removed and the blot was washed 3 times for 20min. All incubations were done with gentle rocking and washing with more vigorous shaking. The blot was then well covered with ECL solution for 2min, and having poured this off, the blot was wrapped in cling-film. This was then exposed to Amersham X-ray film, which was subsequently developed using an automatic developer.

2.2.2.3 Positive controls for Western Blotting

Various positive controls were used during the Western blotting section of this project. Chromaffin granule membranes (CGM) and mitochondria were obtained from Dr. David Apps (Dept. of Biochemistry, University of Edinburgh) and synapotsomes from Leonora Ciufo (Dept. of Biochemistry, University of Edinburgh). Golgi-apparatus and microsomal preparations were done as follows.

Golgi Preparation: Rat liver homogenate was made up to a sucrose concentration of 1.6M and then 1ml loaded at the bottom of a 0.5M-1.3M sucrose gradient (in 10mM Hepes pH 7.4). This was centrifuged at 41K in a swinging bucket rotor (SW41), in a Beckman L8-55 centrifuge at 41,000rpm, for 60min at 4°C. The middle band of membranes was removed and diluted to 0.25M sucrose, and centrifuged in a SW45 rotor/ Beckman L8-55 centrifuge, for 30min at 4°C/45K. The pellet was then removed and the sucrose concentration made up to 1.6M and 2.0M KCl and 1ml loaded at the bottom of a continuous 0.5-1.3M sucrose gradient. This was centrifuged for 30min at 41K in an SW41 rotor/Beckman L8-55 centrifuge at 4°C. The band in the centre was removed, and shown to have a sucrose concentration of 0.988M, which was around the expected level for Golgi-apparatus.

Microsomal preparation: The microsomal preparation was done using a discarded fraction from a chromaffin granule preparation. The first supernatant was removed and spun at 50,000rpm in the 50.2Ti rotor (L8-55 centrifuge), for 60 min at 4°C. The pellet was then resuspended in 10mM Hepes (pH7.4), 2mM EDTA.

2.3 Indirect immunofluorescence microscopy

2.3.1 Solutions for immunofluorescence microscopy

PBS (phosphate buffered saline) pH 7.4: 137mM NaCl, 2.7mM KCl, 4.3mM Na_2HPO_4, 1.47mM KH_2PO_4.

Fix solution: 3% v/v p-formaldehyde in PBS containing 1mM $CaCl_2$ and 1mM $MgCl_2$.

Quench solution: 50mM NH_4Cl in PBS.

Permeabilisation solution: 0.2% v/v Triton-X-100 in PBS.

Block solution: 0.2% v/v fish skin gelatin in PBS.

Moviol mounting medium: 25% v/v glycerol, 10% w/v Moviol 4-88, 100mM Tris HCl pH 8.5. If the secondary antibody being used was conjugated to FITC, anti-fade would also be added to this solution (this was n-propyl-gallate at 5mg/ml).

Hoescht dye: 2μg/ml Hoescht dye in PBS. This was only used periodically, as it stains DNA and therefore the nucleus. It was also used on a regular basis to check for mycoplasma contamination of the cells, of which there was none throughout this project.

2.3.2 Protocol for indirect immunofluorescence microscopy

AtT-20 cells were plated onto sterilised coverslips in 6-well plates, and grown for 3 days until approximately 60-70% confluent. The cells were then washed three times with 2ml PBS containing 1mM $CaCl_2$ and 1mM $MgCl_2$. 2ml of fix solution was then added for 10min, after which the cells were washed three times with 2ml PBS. 2ml quench solution was added for 10min, the cells were washed as in the last step, and 2ml permeabilisation solution was added for 4min. Washing from this point on consisted of the permeabilised cells being washed three times with 2ml blocking solution (over 5min), and a further three washes with 2ml PBS.

The primary antibodies are detailed in the results chapters but were usually at 1/100 dilution and were always made up in blocking solution. 100μl droplets were placed onto parafilm and the coverslips were inverted onto the drops and left there for 20min. They were then returned to the 6-well plate and washed, after which the same

procedure was used for the secondary antibody incubation. Secondary antibodies were generally anti-rabbit or anti-mouse IgG conjugated to rhodamine, although for double labelling the same antibodies were often used linked to FITC, as detailed in the Chapter 3. Following this incubation the cells were washed, rinsed in distilled water, dried and mounted on glass slides with a 20µl drop of Moviol mounting medium. They were stored at 4^0C overnight, to allow the Moviol to set, and then viewed on a fluorescence microscope using the appropriate filter. Before mounting with moviol the cells could also be stained with Hoescht stain, by incubation with 2ml for 10min and washing afterwards in the normal way. Other directly-conjugated fluorescent tags were used to stain the cells (e.g. phalloidin conjugated to coumarin to stain actin), and these simply required a single incubation stage, and were done as detailed above.

2.3.3 Immunofluorescence photography of cells

2.3.3.1 Developing films

Photographs were taken using a Leica camera system attached to a similar microscope. Kodak 400 T-max films were used and the speed was set at 1600 ASA instead of 400 ASA in order that minimal exposure times were obtained. This meant that the development times for the film were increased slightly (7min to 11min). When pictures of non-fluorescent cells were taken the same film was used, but the speed was set at 400 ASA and development times were as stated on the instructions (7min). Photographs were generally taken using a 63X oil-immersion lens.

The film was inserted into a developing tank in the dark room, in complete darkness. 400ml water was added per film, left for 2min, and on removal, 400ml of developing solution was added. This was agitated every 2min, up to the desired development time. The developer was replaced with 5% v/v acetic acid (stop solution), incubated for 2min, and then replaced by fix solution for a further 15min. On removal of this the film was rinsed in water for 5min, the final wash containing a drop of 10% v/v Triton-X-100. The film was then dried and stored until ready to print.

2.3.3.2 Printing negatives

The film was printed on Illford photographic paper (high resolution), and the stop solution and fix solution were as detailed in 2.3.3.1. Exposure times ranged from 10-30 seconds, after which the paper was placed into a tray of Sigma photographic paper developer and rocked gently for 1-2min. It was then transferred into stop solution for 30sec-1min, fix for 5-10min, and the photographs were then rinsed with water for at least 10min, before being dried.

2.3.4 Affinity purification of antibodies for use in immuonfluorescent staining of AtT-20 cells

This protocol was obtained from Alan Boyd (Department of Biochemistry, Edinburgh University; unpublished work)

SDS-PAGE was used as described in section 2.2.1 with a single lane comb, to obtain a band of the appropriate recombinant protein. This was transferred to nitrocellulose using the western blotting protocol detailed in section 2.2.2, and stained with Ponceau S to identify the band of interest. A strip was cut from the nitrocellulose, containing this band, and was washed with TBS to remove residual Ponceau S. The antigen-bearing face of the nitrocellulose was marked and incubated in blocking buffer for 90min. As much antiserum (against the recombinant protein) as would stay on by capillary action was loaded onto the strip, and incubated at room temperature for 2 hours. The depleted serum was removed, the strip washed 3 times with TBS, and 0.2M glycine/HCl pH2.8 added for 20min to elute specific antibodies. This eluate was neutralised using 0.2M Tris/HCl pH8.5, and the solution stored at 4°C with NaN_3.

2.4 ACTH radioimmunoassay

This protocol was obtained from John Bennie (Royal Edinburgh Hospital) and is based on that detailed by *Woods, et al., 1992.*

2.4.1 Iodination of ACTH

A 1ml SEP-PAK C18 (octodecasilica) column was attached to a 5ml syringe and was primed with two 1ml washes of 80% v/v acetonitrile, 0.1% v/v TFA, followed by three 1ml washes of 0.1% v/v TFA. 1 μg ACTH peptide, stored in 10μl 0.01N HCl at –70°C, was radio-iodinated using ^{125}I (specific activity 569.8MBq/μg of iodine; 15.4 mCi/μg of iodine). This was done by adding 40μl of 0.5M sodium phosphate buffer (pH8.0), 5μl of $Na^{125}I$ and 5μl of 2mg/ml chloramine T to the 1μg of ACTH. After 60 seconds the reaction was stopped by the addition of 1ml of 0.1% v/v TFA, and was also added to the column. The liquid was gently pushed through the column and the reaction vial washed out with another 1ml 0.1% TFA, which was also transferred onto and through the column. These eluates (E1 and E2) were collected in 3ml tubes and a stepwise elution of the radio-iodinated ACTH was begun. Steps of 10, 20, 30, 40, 50, 60, 70 and 80% v/v acetonitrile (in 0.1% v/v TFA) was used (1ml washes), and it was found that the ACTH was eluted at the 40 or 50% fraction. 0.8ml methanol was added to these tubes to prevent freezing (which would have damaged the iodinated ACTH), and they were stored at –20°C for 3-4 weeks with no loss of biological activity.

2.4.2 Measurement of ACTH by radioimmunoassay

2.4.2.1 Materials

Radioimmunoassay buffer: 8.94g Na_2HPO_4 (anhydrous), 4.84g $Na_2EDTA.2H_2O$, 0.2g NaN_3 was warmed to dissolve, in 800ml water. 400KIU/ml or 0.15 TIU/ml of aprotinin was added and the buffer was made up to 1000ml. All stages of assay used this buffer with various detailed additions, and it could be stored at 4°C and used as needed. The final pH was pH7.4

2.4.2.2 Method

All manipulations were done on ice or in the cold room. The standard curve was produced using 0 (B_0), 0.02, 0.04, 0.08, 0.156, 0.312, 0.625, 1.25, 2.5, 5, 10, 20, 40 and 80ng/ml ACTH samples, and all points were measured in triplicate. NSB (non-specific binding) samples had the appropriate buffer volume in place of ACTH antiserum. TC (total count) samples were 50μl untreated samples of iodinated

ACTH. Standards were made up in radioimmunoassay buffer containing 0.25% w/v high-purity BSA. 50µl of standard or unknown samples were added to 3ml tubes, along with 50µl of ^{125}I-ACTH diluted in radioimmunoassay buffer with 0.1% v/v TX-100 (the iodinated ACTH having been diluted to 10000 cpm per 50µl aliquot). Anti-ACTH was diluted 1/60,000, in radioimmunoassay buffer (containing 1% NRS and 0.1% TX-100), and added to the same 3ml tubes which were vortexed well and incubated in the cold room overnight. 250µl of a 1/25 dilution of donkey anti-rabbit antiserum (in radioimmunoassay buffer containing 0.01% v/v TX-100) was added and the tubes incubated on ice for a further 3 hours after vortexing well. 600µl of 8.7% w/v PEG (in radioimmunassay buffer with 0.25% BSA) was added, the tubes vortexed and then centrifuged for 1 hour at 4,200rpm in a J6B centrifuge (i.e. 4000g). The supernatants were carefully aspirated the ^{125}I content of the tubes measured for 3 minutes per sample, using a Nuclear Enterprises NE1612 turbo gamma counter.

2.5 Cell assays

2.5.1 Non-permeabilised cell assays

All incubation times and concentrations are typical; where variations were used these are detailed in the appropriate results chapter.

2.5.1.1 Ba^{2+} stimulation of cells

(Hurtley, 1993 Journal of Cell Science 106, 649-656)

All incubations were done at room temperature. Cells were grown in 24-well dishes to 80% confluency and washed with 1ml Locke's buffer (154mM NaCl, 5.6mM KCl, 5.6mM glucose, 1.2mM $MgCl_2$, 2.2mM $CaCl_2$, 5mM Hepes, pH 7.0). They were then allowed to equilibrate in 1ml Mg-Locke's buffer (154mM NaCl, 5.6mM KCl, 5.6mM glucose, 3.4mM $MgCl_2$, 5mM Hepes, pH 7.0) for 10min followed by a 10minute incubation with 1ml Ba-Locke's buffer (154mM NaCl, 5.6mM KCl, 5.6mM glucose, 5mM $BaCl_2$, 1.2mM $MgCl_2$, 5mM Hepes, pH 7.0). Control cells (giving non-stimulated basal rates of secretion) were at this last stage treated in parallel with Locke's buffer.

2.5.1.2 CRF stimulation of cells and inhibition with dexamethasone

Cells were grown in 24-well plates until 80% confluent and then washed with 1ml of serum-free (SF) DMEM (pH 7.4; obtained in powder form, supplemented with 0.6% w/v Hepes/NaOH and 0.25% BSA per 100ml made up). 250µl of this SF DMEM was added to each well and the plate was incubated at 37°C for 30min (without CO_2), after which any wells requiring incubation with dexamethasone were treated with 250µl of SF medium containing dexamethasone at twice the required concentration. This was added without removal of the 250µl SF medium, and control cells were treated in the same way with 250µl SF medium, minus the dexamethasone. The plates were then incubated for 90min at 37°C, however if no dexamethasone was being used this step was omitted, although the 30 minute incubation with SF medium was still included. The medium was then aspirated, the appropriate concentration of CRF added, and the plates incubated for 30min at 37°C.

2.5.1.3 Stimulation of cells with 8-bromo-cAMP

As before cells were grown to 80% confluency in 24-well plates, and then washed with 1ml of SF medium. They were then incubated for approximately 15min at 37°C/5% CO_2 with the appropriate concentration of 8-bromo-cAMP in 1ml SF medium.

2.5.1.4 Stimulation of cells with high potassium concentration

KCl solution: A solution (total volume 25ml) was made up containing 20.5ml of 1.15% w/v KCl, 0.6ml of 1.18% w/v $CaCl_2$, 0.2ml of 3.82% w/v $MgCl_2$, 0.2ml of 0.5M Hepes/NaOH pH 7.4, 50mg glucose. This was diluted with two parts SF DMEM to make a high K^+ (50mM) solution which would de-polarise AtT-20 cells.

Cells were grown to 80% confluency in 24-well plates and then washed with 1ml SF DMEM (normal liquid form without FCS or penicillin/streptomycin). They were then incubated with 1ml of a 50mM KCl solution at 37°C, for 30min.

2.5.1.5 Removal of samples in assays of non-permeabilised cells

Immediately after the final incubation, the plates were placed on ice and 300µl samples removed and centrifuged for 5min at 13.000rpm (4°C) using a microfuge.

Samples of the supernatant were then removed and stored at -70°C, until the ACTH concentrations were measured by radioimmunoassay.

2.5.2 Permeabilised AtT-20 cell assay

All incubations are done at room temperature. 24-well plates were incubated with 200µl 0.1% w/v poly-L-lysine per well for 5min, washed with 1ml sterilised distilled water and left to dry for 3-5 hours. Cells were plated and grown until 80% confluent as usual. They were then washed with 1ml permeabilisation buffer pH 6.6 (139mM potassium glutamate, 20mM PIPES, 5mM EGTA, 2mM $MgCl_2$, 2mM Na_2ATP) and then incubated with 1ml permeabilisation buffer containing 20µg/ml digitonin for 10min. The digitonin was aspirated off and a 15min pre-Ca^{2+} stimulation stage was used to allow the entry of recombinant proteins, antibodies or drugs into the cells. This involved the dilution of the various factors in the permeabilisation buffer and the addition of 500µl of this per well, control cells being treated in parallel with permeabilisation buffer only. Having done this 500µl of Ca^{2+} stimulation buffer (at double the required concentration of Ca^{2+}) was added directly to the wells, to the 500µl buffer already present. This was incubated for 10min at which point the plate was placed on ice, 300µl samples removed and centrifuged for 5min at 13,000rpm (4°C) using a microfuge, and the supernatants were kept at -70°C until the ACTH concentration was measured by radioimmunoassay. The Ca^{2+} stimulation buffer contained 20µM free Ca^{2+}, giving a final concentration of 10µM free Ca^{2+}, as calculated using the computer program "ca.calc" (kindly donated by Richard Ashley, Dept. of Biochemistry, Edinburgh University). In this buffer 20µM Ca^{2+} was given by adding $CaCl_2$ to a final concentration of 6.4mM. Control cells were treated in parallel with Ca^{2+}-free permeabilisation buffer.

2.5.3 Buffer replacement

Various toxins and recombinant proteins that were used were obtained in buffers other than the permeabilisation buffer. Because of the importance of maintaining the precise Ca^{2+} concentration it was often necessary to transfer these factors into the correct buffer. Biorad Biogel (P6-DG) was swollen in distilled water and approximately 1.5ml was added to an Eppendorf tube, with a small hole in the base and a plug of packed glass wool. The gel was allowed to settle and the resin then

equilibrated by slowly dripping 5ml permeabilisation buffer through the Eppendorf tube, which was then centrifuged for 2min at 1000rpm using a bench centrifuge. Up to 250µl of the protein/toxin solution was then placed on the top of the column, which was then incubated for 5min and centrifuged as before. The concentration of protein/toxin before and after ion exchange was assessed using gel electrophoresis or A_{280}.

2.5.4 Total lysis of AtT-20 cells

This protocol was taken from *Sambrook et al., 1989*. Total ACTH content was measured by lysing the cells with a triple detergent lysis buffer, containing 50mM Tris.HCl (pH 8.0), 150mM NaCl, 0.02% w/v NaN_3, 0.1% w/v SDS, 100µg/ml PMSF, 1µg/ml aprotinin, 1% v/v Nonidet P-40 and 0.5% w/v sodium deoxycholate. The cells were washed with 1ml of PBS, containing 1mM $CaCl_2$ and 1mM $MgCl_2$, and then 1ml of lysis buffer added, and the plate incubated on ice for 20min. The buffer was then removed and treated as with any other radioimmunoassay sample, however on assaying these samples a separate B_0 sample was used containing 50µl of lysis buffer in place of the 50µl RIA standard buffer usually used.

2.5.5 Lactate dehydrogenase (LDH) assay on permeabilised cells

AtT-20 cells were permeabilised as described in section 2.5.2, with variations being detailed in chapter 5. LDH concentrations were measured in the digitonin solution and in the permeabilisation buffer used in subsequent stages. Samples were assayed for LDH activity using a Roche Cobas Fara automated centrifugal analyser, and LDH assay kit (Sigma Chemical Co. 340-LD).

2.6 Production and purification of toxins

2.6.1 Production of toxins

The plasmids used were a kind gift from H. Niemann (Tubingen, Germany) and were based on the Quigen expression vector pQE with the light chain genes of botulinum D or tetanus toxin inserted. The toxins were expressed as His_6-tagged

fusion proteins which allowed purification using a Ni-agarose system. Maps and details of these plasmids can be found in the Appendix.

2.6.1.1 Competent NM522 cells

These were made using a method based on that described by *Sambrook et al., 1989.* This same reference also details the basic protocol for the transformation of the cells (section 2.6.1.2).

5ml of L broth (0.5% w/v NaCl, 0.5% w/v yeast extract, 1.0% w/v tryptone) was inoculated with NM522 *E. coli* cells and grown at 37°C overnight with shaking. 50ml of L broth was then inoculated with 1ml of this culture and grown under the same conditions until the A_{600} reached between 0.4 and 0.7. The cells were harvested by centrifugation at 5000rpm (4°C, 5min) and resuspended in 20ml of 0.1M $MgCl_2$, after which they were again harvested in the same way. This pellet was resuspended in 10ml cold $CaCl_2$ and the cells stored on ice for 1 hour, before being stored at -70°C until needed for transformation with the toxin and other plasmids.

2.6.1.2 Transformation of NM522 cells with toxin-expressing plasmids

2µl of plasmid was added to 200µl of competent NM522 cells and left on ice for 1 hour, before heat-shocking the cells at 42°C for 2-3min. 800µl of 2YT medium (0.5% w/v NaCl, 1.6% w/v tryptone, 1.25% w/v yeast extract) was then added and the cells incubated at 37°C for 1 hour. A 200µl aliquot was spread on to selective agar (2YT medium with 1.5 % w/v agarose and 100µg/ml ampicillin). The plates were incubated overnight at 37°C in order to obtain toxin-expressing clones, which were subsequently used to inoculate 5ml of selective 2YT medium containing 100µg/ml ampicillin. These cultures were grown overnight at 37°C with shaking and were used for the purposes of a large-scale toxin preparation.

2.6.1.3 Large scale production of crude toxin

500ml of 2YT medium containing 100µg/ml ampicillin was inoculated with a 5ml culture, prepared as detailed above. This was grown at 37°C until the A_{600} reached 0.6-0.7 at which point the cells were induced to produce protein by the addition of 0.5mM IPTG (for BoNTD) or 0.2mM IPTG (for TeTX). The culture was grown under the same conditions for a further 2.5 hours at which point the cells were

harvested by centrifugation at 4000g for 20min at 4°C. The bacterial pellet was then resuspended in 10ml sonication/elution buffer (SE buffer; 50mM NaH_2PO_4 pH8.0, 300mM NaCl) containing 5mM benzamidine, 0.5mM PMSF and 1μg/ml pepstatin A. The bacteria were disrupted by pulse sonication on ice for two 1min periods of sonication. The lysate was then cleared by centrifugation at 7000rpm for 20min using a 50Ti rotor, (L8-55 Beckman centrifuge) at 4°C, the supernatant removed and further purification of toxins carried out.

2.6.2 Purification of toxins

2.6.2.1 Purification of botulinum D light chain toxin (BoNTD-LC)

The final protocol used is detailed here, however before selecting this various washing stages were tried and these are detailed in Chapter 5. All washes were done on ice and involoved re-suspending the Ni-agarose gel and centrifuging briefly at 1000rpm on a bench centrifuge. 1ml Ni-NTA-agarose (50% slurry) was placed in a conical glass tube and washed 5 times with 4ml SE buffer (pH 8.0), after which 9ml of the lysate supernatant was added. The tube was incubated on a roller mixer in the cold room overnight to allow the his-tagged light chain toxin to bind to the Ni-agarose gel. The Ni-agarose gel was centrifuged as above and the supernatant removed by aspiration, followed by ten 4ml washes with SE buffer pH 8.0. The Ni-agarose was then washed ten times with 4ml washes of 10mM imidazole, in SE buffer pH 8.0, and then 10 times with 4ml washes in 30mM imidazole, in SE buffer pH 8.0. Elution of the toxin was brought about by washing with 0.5ml of 100mM imidazole in SE buffer pH 8.0, and the yield was slightly improved by incubating them together on the roller mixer at 4°C for 30min. This 0.5ml toxin preparation was then transferred into permeabilisation buffer after buffer exchange using the Biogel system already described. A control preparation was done with untransformed NM522 cells grown in non-selective medium, which was fractionated and eluted in parallel to the BoNTD-transformed NM522 cells.

2.6.2.2 Purification of tetanus toxin light chains (TeTX-LC)

The binding of the his-tagged TeTx to the Ni-agarose was done as described above for BoNTD, however the washing and elution steps differed as follows. Having removed the first supernatant the Ni-agarose was washed 5 times with 4ml of SE

buffer pH8.0, followed by 5 washes with 4ml of SE buffer pH6.5. Elution was achieved with 10 washes of 0.5ml SE buffer at pH5.0. The highest protein concentration was in fraction 10, and the yield was improved by a 30minute incubation at 4°C on the roller mixer. Again this 0.5ml toxin preparation was buffer exchanged using the Biogel system described above and a similar control cell preparation (using untransformed NM522 cells) was done in parallel.

2.7 Transfection of AtT-20 cells

2.7.1 Lac-Z assay

A lac-Z reporter assay was used to assess whether the lipofectamine method of transfecting AtT-20 cells with plasmids was suitable, and also for examination of varying transfection conditions. The plasmid used is detailed in the Appendix. Transient transfection of cells was examined by detecting expressed β-galactosidase in cells using histochemistry.

2.7.1.1 Transfection of AtT-20 cells with lac-Z expressing plasmid

Ratios of DNA:lipofectamine were varied and are as detailed in Chapter 6. Cells were plated in 6-well plates and grown until 60-70% confluent. The transfection mixture was prepared in polystyrene tubes by mixing varying amounts of DNA with 100µl of Optimem™ serum free (SF) medium, and then varying amounts of lipofectamine with 100µl Optimem™ SF medium. The two solutions were then combined, gently mixed and left at room temperature for 30min. The cells were rinsed with 2ml of Optimem™ SF medium, and a further 0.8ml of Optimem™ SF medium added to the transfection mixture. Having removed the wash, the transfection mixture was added to the cells (approximately 1ml per well), and left for 5 hours at 37°C in 5%CO_2. This was then replaced with complete DMEM (DMEM with penicillin/streptomycin and 10% FCS) for 24 hours, at which point the cells were tested for β-galactosidase activity using the method detailed below.

2.7.1.2 β-galactosidase staining of cells transfected with lac-Z plasmid

PEM buffer: 100mM potassium phosphate buffer (pH7.4), 5mM EDTA, 2mM $MgCl_2$.

Fix: 0.2% v/v glutaraldehyde, in PEM buffer.

Wash solution: 0.01% w/v Na deoxycholate, 0.02% v/v Nonidet P-40, in PEM buffer.

Stain: 0.5mg/ml X-gal, 10mM $K_3[Fe(CN)_6]$, 10mM $K_4[Fe(CN)_6]$, in wash solution.

The cells were washed twice in PBS containing 1mM$CaCl_2$ and 1mM $MgCl_2$, and then in 2ml fix solution for 5min. This was aspirated off and the cells washed another three times with wash solution. 2ml of stain was then added to the cells and they were incubated in the dark at room temperature for 3 hours, after which time the cells were again washed twice with wash solution, transfected cells stained blue and the plates were photographed.

2.7.2 Transfection of AtT-20 cells with SEAP or HGH-SEAP plasmid

Two types of vectors were used in these experiments, both based on the Clonetech (pSEAP-control) plasmid. The first is a simple reporter vector which causes the transfected cells to secrete alkaline phosphatase, which itself can be assayed in a number of ways. The second construct was made by Alan Colley (Department of Biochemistry, University of Edinburgh) and involved the attachment of the human growth hormone gene to the alkaline phosphatase gene. The idea was that the cells would secrete the fusion protein in a Ca^{2+}-regulated manner, as opposed to constitutively. This secreted alkaline phosphatase could then be assayed in a number of ways, and the system would offer an alternative method of measuring regulated exocytosis, that is much quicker and simpler than the ACTH-RIA currently used. The plasmid maps and details can be found in the Appendix. All DNA/lipofectamine concentrations are detailed in the Chapter 6, as different concentrations were tried.

2.7.2.1 Preparation of plasmid DNA

Plasmid DNA was made by transfecting competent NM522 cells (as detailed in section 2.6.1.2 but using L broth) with the original plasmid DNA (constructed and purified by Alan Colley. The cells were spread on selective L broth agar (containing

ampicillin) and placed at 37°C overnight, after which a colony was picked to inoculate a 5ml L broth culture, which was grown at 37°C overnight with shaking. This 5ml culture was then processed to pure plasmid DNA using the Qiagen mini-prep system. DNA concentration and purity was calculated using $A_{260/280}$ values and the plasmid obtained was checked by undertaking the appropriate restriction enzyme digests (see below and Chapter 6). $A_{260/280}$ ratios were always above 1.8 and the DNA was therefore deemed to be pure enough to use for transfection.

2.7.2.2 Gel electrophoresis of DNA

TBE buffer: 1.08% w/v Tris base, 0.55% w/v Boric acid, 2mM EDTA pH 8.0.

TE buffer: 10mM Tris HCl, 1mM EDTA (pH 8.0).

Blue Juice (6 X): 0.5mg/ml bromophenol blue, 40% v/v sucrose (made up in TE buffer).

Agarose gels were set up. The sides were taped and 1-1.5% molten agarose (in TBE) poured in to the correct level. The spacer was inserted and the gel left to set, after which the tape was removed and the gel placed in a tank, which was filled with enough TBE to cover the gel completely. 10-15µl samples in 'blue juice' were then loaded, and the gel was run at 120mV for 45min-1hour. It was then stained with 2-5mg/ml ethidium bromide (in TBE), viewed using UV light, and photographed.

2.7.2.3 Restriction enzyme digests

The precise restriction (RE) enzyme digests used are detailed in the Chapter 6. In general 1µg DNA was mixed with 40U of the restriction enzyme (2µl) in the corresponding RE buffer, in a total volume of 15µl. This was incubated for 1 hour at 37°C and then 10µl run on a 1-1.5% agarose gel, which was stained with ethidium bromide as above.

2.7.2.4 Transfection of AtT-20 cells with SEAP/HGH-SEAP plasmids and selection of stable transfectants

Cells were plated in 6-well plates and grown as described previously until 60-70% confluent. The method of transfection was as described for the lac-Z plasmid, in that after 5 hours the transfection mixture was removed and replaced with complete

DMEM medium. Again the DNA:lipofectamine ratios varied and are described in Chapter 6. After 24 hours of incubation with complete DMEM, this was aspirated off and replaced with selective medium, which was complete DMEM containing G418 (2.5mg/ml). The G418 caused acidification of the medium, which was titrated to pH7.4 using 20mM Hepes/NaOH. Transiently-transfected or non-transfected cells died and lost attachment to the plate after 2-5 days, leaving small foci of cells which displayed G418 resistance. The medium was changed every 3-6 days until the foci were deemed large enough to be cloned (visible by the naked eye). They were picked off using sterile 20µl tips, placed in 96-well plates and resuspended in 200µl selective complete DMEM. This process was repeated with foci within the 96 well plates being moved in the same way to new 96 well plates to ensure that clones had been obtained. At this stage, when 40-50% confluency was reached, 100µl trypsin-EDTA solution was added for 30sec and then the majority of it removed. The nearly -detached cells were then resuspended in 500µl of complete selective DMEM and placed in 24-well plates until 50-60% confluent, at which point the same process was used to dislodge them, with increased quantities of trypsin-EDTA. The cells were placed in 6-well plates, then the process repeated, and the cells plated in a 25cm^2 flask, after which cell passaging was as described before (section 2.1). The stable cell lines were grown up and frozen down as previously described (section 2.1), and could be plated and used for experiments. To ensure that there was no loss of DNA or gene expression, the cells were maintained in G418 containing selective complete DMEM.

Many of the experiments were done using transiently-transfected cells. This was done by plating the cells in 24-well plates and transfecting them with the appropriately scaled volume of transfection mixture (as described in this section). After 5 hours it was removed, replaced with complete DMEM, and the cells were assayed after 24-72 hours.

2.8 Assay of alkaline phosphatase (SEAP) activity

Stable or transiently-transfected cells were plated or left in 24 well plates and grown until 70-80% confluency or for a further 24-72 hours. The medium the cells were

grown in could then be assayed for constitutively-secreted HGH-SEAP or for SEAP (depending on which plasmid had been used). Cells transfected with the HGH-SEAP plasmid could also be stimulated to secrete in a regulated manner by any of the methods detailed in section 2.5.1, and the levels of alkaline phosphatase then measured. In all cases samples were removed and centrifuged at 13000rpm (4°C) for 5min,in a microfuge, then assayed immediately or stored at –70°C.

2.8.1 Chemiluminescence method for detection of SEAP or HGH-SEAP

This method used the Clontech Great Escape Detection Kit and was carried out as detailed in the instructions. A chemiluminescent substrate (CSPD™) was used, along with an enhancer to produce a light reaction detectable by exposure to X-Ray film and subsequent development.

2.8.2 Cytochemistry of alkaline phosphatase

The Sigma alkaline phosphatase cytochemistry kit was used and the protocol was as detailed in the instructions. In this case the cells were plated onto coverslips in 6-well plates, and then examined microscopically.

2.8.3 Spectrophotometric detection of SEAP or HGH-SEAP

The method used here was as reported by *Cullen & Malim, 1992*. The samples were processed in 96-well plates and absorbances read at 405nm using a Dynatech 700006 automated plate reader. The only variation was that the substrate was obtained in tablet form (pNPP; from Sigma Chemical Co.) and due to poor solubility, each tablet was dissolved in 1ml (instead of 633µl) of SEAP buffer.

2.9 Reverse-transcriptase polymerase chain reaction (RT-PCR)

This method was used as an alternative to Western blotting, in an attempt to identify the mRNAs for synaptobrevin and syntaxin in AtT-20 cells. The first method tried was the purification of mRNA from AtT-20 cells and subsequent RT-PCR. As difficulties were encountered using this method a total RNA preparation was then used, with subsequent RT-PCR. The nucleotide sequences for mouse synaptobrevin and syntaxin genes were not available, therefore the primers were designed using rat

syntaxin A and rat synaptobrevin 1. The gene sequences and primers are detailed in the Appendix. Western blotting had already been used successfully to identify the presence of synaptotagmin, therefore this was used as a positive RT-PCR control. Primers for this were designed and kindly donated by Leonora Ciufo (Department of Biochemistry, Edinburgh University)

2.9.1 mRNA preparation

This was done using a Qiagen kit and following the manufacturer's protocol. All apparatus and solutions were RNAase-free. However since only a very small fraction of the RNA in a cell is mRNA its detection was difficult. After an unsuccessful RT-PCR, it was impossible to assess whether this negative result was due to faliure of the RT-PCR or an initial lack of mRNA. Thus a total RNA preparation, which could be measured spectrophotometrically, was used.

2.9.2 Total RNA preparation

The method used here was that detailed in the RNAzol^{TM} B Tel-Test Bulletin no.2 (Biogenesis Ltd). 5ml of RNAzol was used per 75cm^2 flask, and all other steps The solution was stored at –20°C, or –70°C for long term storage.

2.9.3 RT-PCR reaction

Two methods were used for the initial production of the cDNA (i.e. the RT part of the reaction). The first used the syntaxin, synaptobrevin or synaptotagmin primers to specifically produce the corresponding cDNA only, and the second used random primers to produce total cell cDNA.

2.9.3.1 RT production of cDNA

The following components were added to a nuclease-free Eppendorf tube: 2µl random primers or specific 3' primer, 1.5µl total RNA or messenger RNA (i.e. 1µg total RNA or 60ng mRNA), 7.5µl water and 1µl RNAsin (Promega). The contents of the tube were mixed gently and then heated to 70°C for 10min, after which the tube was chilled on ice. The following additional components were then added: 4µl of 5 X RT buffer, 2 µl DTT (stock 0.1M) and 1µl dNTP mix (stock concentration of 10mM

each). The contents of the tube were gently mixed, 100µl of mineral oil layered on top, and then incubated at 25°C for 2min, after which 1µl of reverse transcriptase was added and the 25°C incubation continued for 10min. The tube was then immediumtely incubated at 42°C for 50min, followed by 70°C for 10min.

2.9.3.2 PCR amplification of specific cDNA product

The following components were added to a sterile Eppendorf tube: 10µl of 10 x PCR buffer, 6µl $MgCl_2$ (25mM stock), 2µl dNTP mix (stock concentration of 10mM each), 1µl 5'primer, 1µl 3'primer, 2µl Taq DNA polymerase, 74µl water and 2µl cDNA from RT reaction. These were gently mixed and 100µl mineral oil layered on top. They were then incubated at: 95°C for 1.5min, 45°C for 2min and 72°C for 1min. This was done for 30 cycles and then incubated at 10°C until the samples were removed and run on agarose gels as detailed above.

2.10 Site-directed mutagenesis of NSF

A vector containing the cloned CHO (chinese hamster ovary) cell line NSF gene, tagged with 6 histidine residues, was kindly donated by Professor R. Burgoyne (University of Liverpool). The aim was to use site-directed mutagenesis *(Ho et al., 1989)* to mutate a single amino acid residue (Thr_{373} to Pro_{373}), and the reasons behind this are explained in Chapter 6. The flanking and mutagenic primers were designed using the gene map provided, and both these and the plasmid maps, can be seen in the appendix, along with a brief description of the technique, which involves the production of two amplified pieces of cDNA at the 5` and 3` ends of the gene. At the 3` end of the former and the 5` end of the latter, is the mutated amino acid and an overhang of approximately 12 bases. The next step would therefore be to join the two mutated pieces of DNA together using another PCR step and the two flanking non-mutagenic primers. Plasmid mini-preps were done using the same technique described in section 2.7.1.1 and the plasmid was examined using restriction enzyme digests, as detailed in section 2.7.1.3. In this case all primers were obtained from Cruachem.

2.10.1 Site-directed mutagenesis by PCR

Both VENT polymerase and Taq polymerase were used in these experiments and are detailed in Chapter 6.

Taq polymerase PCR The following components were added to an Eppendorf tube: 10µl of 10 X PCR buffer, 8µl of $MgCl_2$ (25mm stock), 2µl dNTPs (stock of 10mM each), 2µl Taq polymerase, 74µl water and 2µl NSF template. For production of the 5'fragment the primers added were 5' and 3'M, and for the 3' fragment the primers 5'M and 3' were used. All were added at 1µl per PCR reaction. The tubes were then incubated at: 95°C for 1.5min, 50°C for 1.5min and 72°C for 1min. This was done for 30 cycles and then incubated at 10°C until the samples were removed and run on agarose gels as described above.

Vent PCR: The same reaction mixture was used except 1µl VENT was used, the $MgCl_2$ excluded, and the appropriate 10 x PCR buffer used. $MgSO_4$ was added to a concentration of 2mM or 4mM, as detailed in Chapter 6.

2.10.2 Purification of 5' and 3' fragments

To ensure that none of the original un-mutated template would be present in the next part of the reaction, 100µl of the reaction mixtures were run on a 1.5% agarose gel. The correctly sized fragments were then purified using a Qiagen gel extraction kit and the included protocol.

2.10.3 Production of mutated cDNA

The following components were added to a sterile Eppendorf tube: 2µl of 5' fragment, 2µl of 3' fragment, 2µl VENT, 10µl of 10 X PCR buffer, 81µl water, 2µl dNTP (stock of 10mM each), 1µl 5' primer and 1µl 3' primer. $MgSO_4$ was added to a concentration of 2mM or 4mM, as detailed in Chapter 6. The tubes were then incubated at: 95°C for 1.5min, 50°C for 1.5min and 72°C for 1min. This was done for 30 cycles and then incubated at 10°C until the samples were removed and run on agarose gels as detailed above.

Appendix to Chapter 2

(A) Botulinum D and tetanus toxin light chain expression vectors

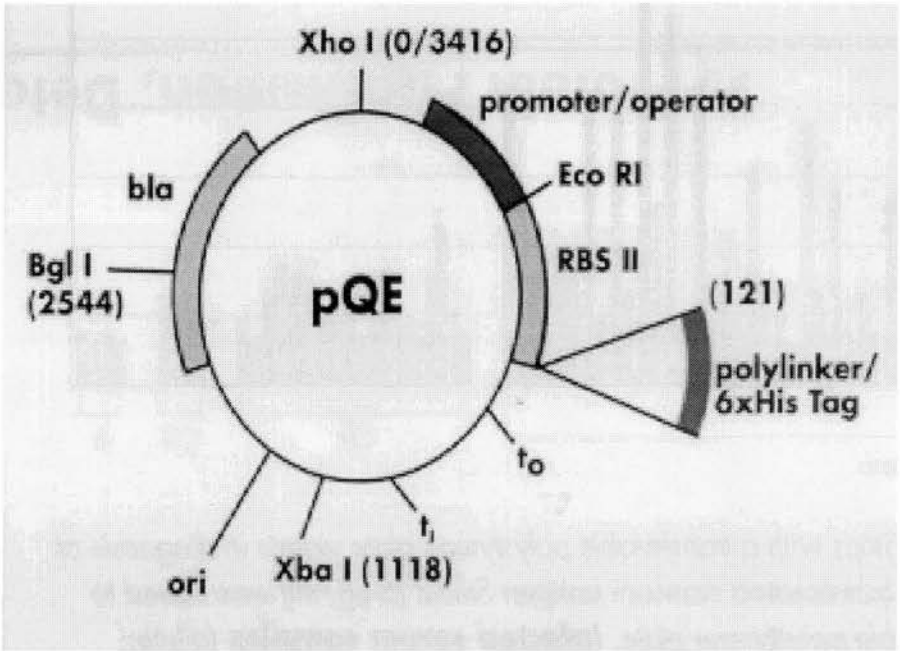

The above figure shows the Qiagen QIA*express*™ expression vector that was used to express the cloned light chains of the toxins BoNTD and TeTX. Two lac operator sequences ensured tightly-controlled repression of the powerful T5 promoter present. There are 6 histidine residues tagged onto the expressed proteins, to enable efficient affinity purification, and two transcriptional terminators to prevent read-through transcription. The β-lactamase gene (bla) confers ampicillin resistance, and allows selection of the transformed *E.coli*.

The plasmids were a generous gift from Dr. Heiner Neimann (Tubingen, Germany) and the constructs are as detailed in *Hayashi et al., 1994*.

(B) NSF expression vectors and design of primers

The plasmid used as a template for the NSF mutagenesis reaction was based on the pQE plasmid detailed in (A). This was also used for propagation of the plasmid in order to obtain enough DNA for experiments, by transforming NM522 cells and using a Qiagen mini-prep kit. The NSF was cloned from a Chinese Hamster Ovary cell line and details of the plasmid can be found in *Whiteheart et al., 1993*. Flanking primers and mutagenic primers were designed using the CHO cell gene sequence, as obtained from the Swiss-prot website. Below is a brief description of how this 4 primer method of mutagenesis works. The primers are then shown, along with the relevant areas of the NSF gene.

Schematic diagram of site-directed mutagenesis by overlap extension

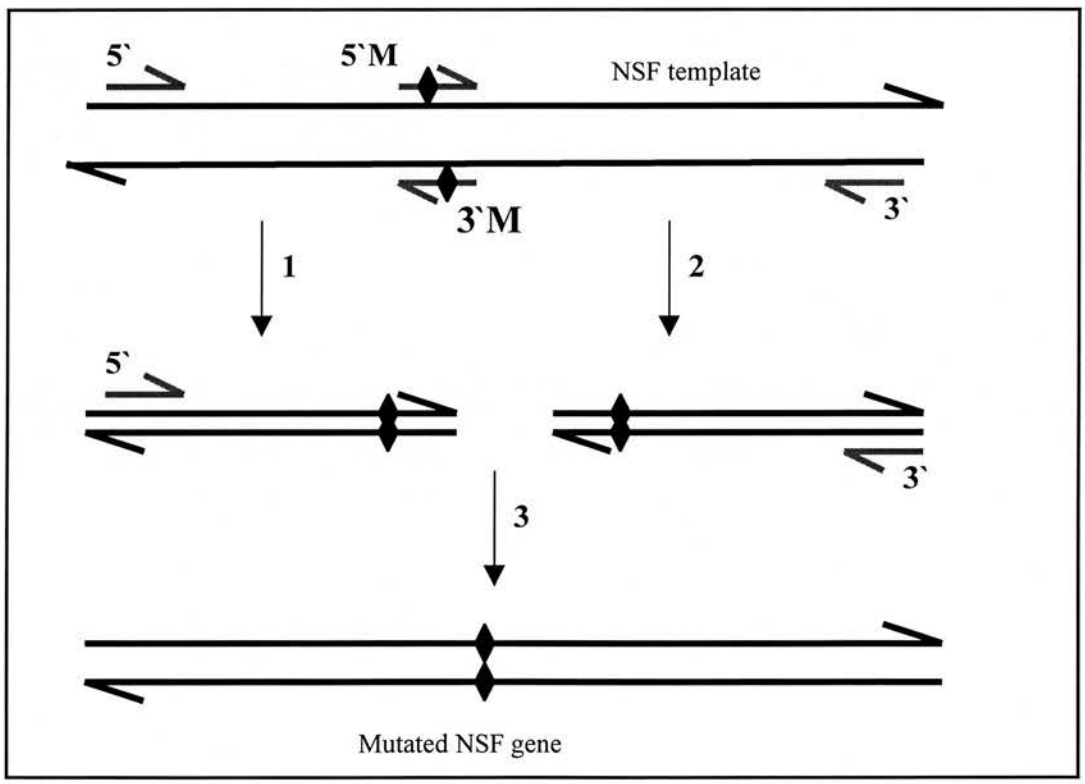

The method used was based on that described by *Ho et al., 1989*. Two separate PCR reactions were used (1 &2) to generate two DNA fragments: PCR 1 used primers 5` and 5`M; PCR 2 used primers 3` and 3`M. The resulting DNA products were purified from an agarose gel using a Qiagen gel DNA extraction kit, to ensure that none of the original template was present in the final reaction. PCR 3 was used to extend the two

mutated pieces of DNA, to obtain a whole mutated gene. This reaction used only the flanking primers 5` and 3`.

NSF primer design

5` primer:

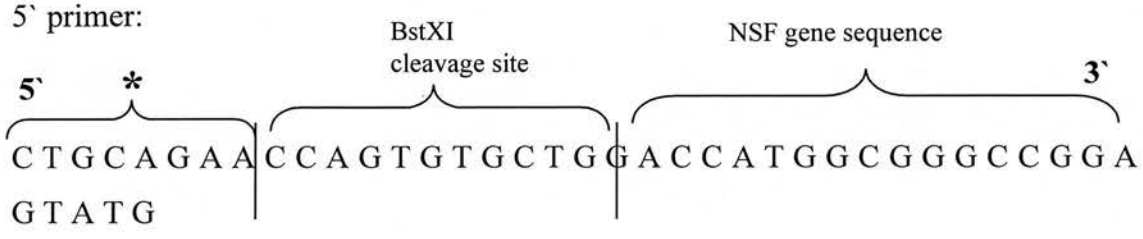

3` M primer:

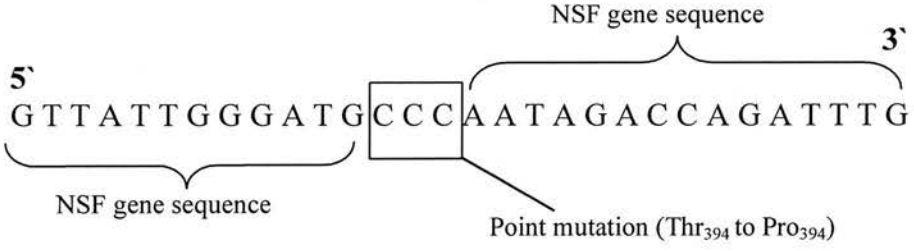

3` primer:

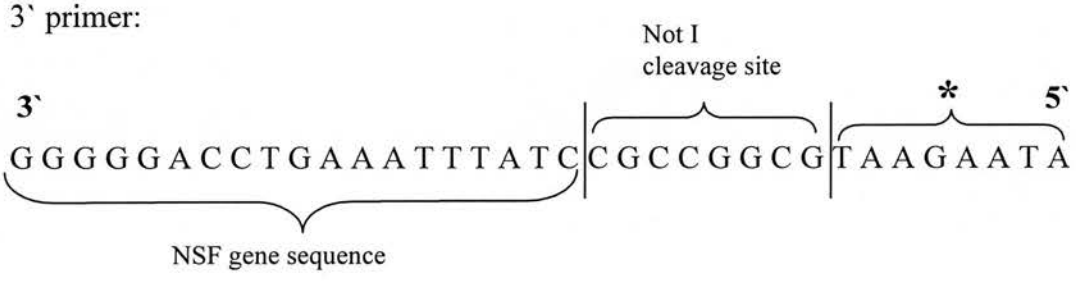

The primers used were as shown above. The 5` and 3` primers were designed using the 5` and 3` ends of the NSF gene, with additional sites added on to allow for cloning into a mammalian expression vector. * Denotes additional nucleotides which were added to improve the efficiency of cutting by the restriction enzymes. The mutational primers contained a single point mutation (ACC to CCC), in the centre. The 5` primer was not shown as it was simply complementary to the 3`M primer.

(C) SEAP and HGH-SEAP expressing plasmids

pSEAP-control plasmid

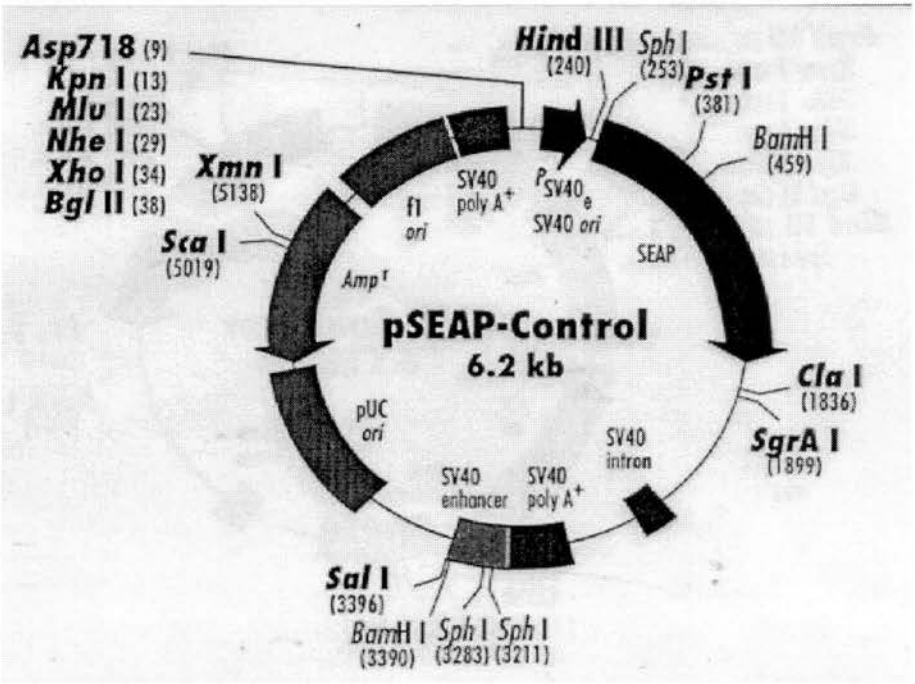

The SEAP-Control plasmid was obtained from Clontech laboratories, Inc. It has an SV-40 promoter and enhancer which allow the expression of SEAP in most mammalian cell types. The SV-40 intron and SV-40 polyadenylation signal ensure proper processing of the transcript in eukaryotic cells. There is a pUC19 origin of replication (along with an ampicillin resistance gene) for propogation in *E.coli*. The sequence can be obtained in GenBank, and further information can be found in the following references: *Berger et al., 1988*; *Araki et al.,1988*; *Chen & Okayama, 1988*; *Sambrook, 1989*.

The SEAP-HGH plasmid was kindly donated by Alan Colley (Biochemistry Dept., University of Edinburgh). The pSEAP-control plasmid was used as a source of DNA from which the SEAP gene was cloned as a HindIII/NotI fragment, and inserted into the pRc/CMV2 plasmid shown below. Cloned HGH gene (including the leader sequence) was then fused to the beginning of the SEAP gene as a NotI/XbaI fragment.

PRc/CMV2 expression vector

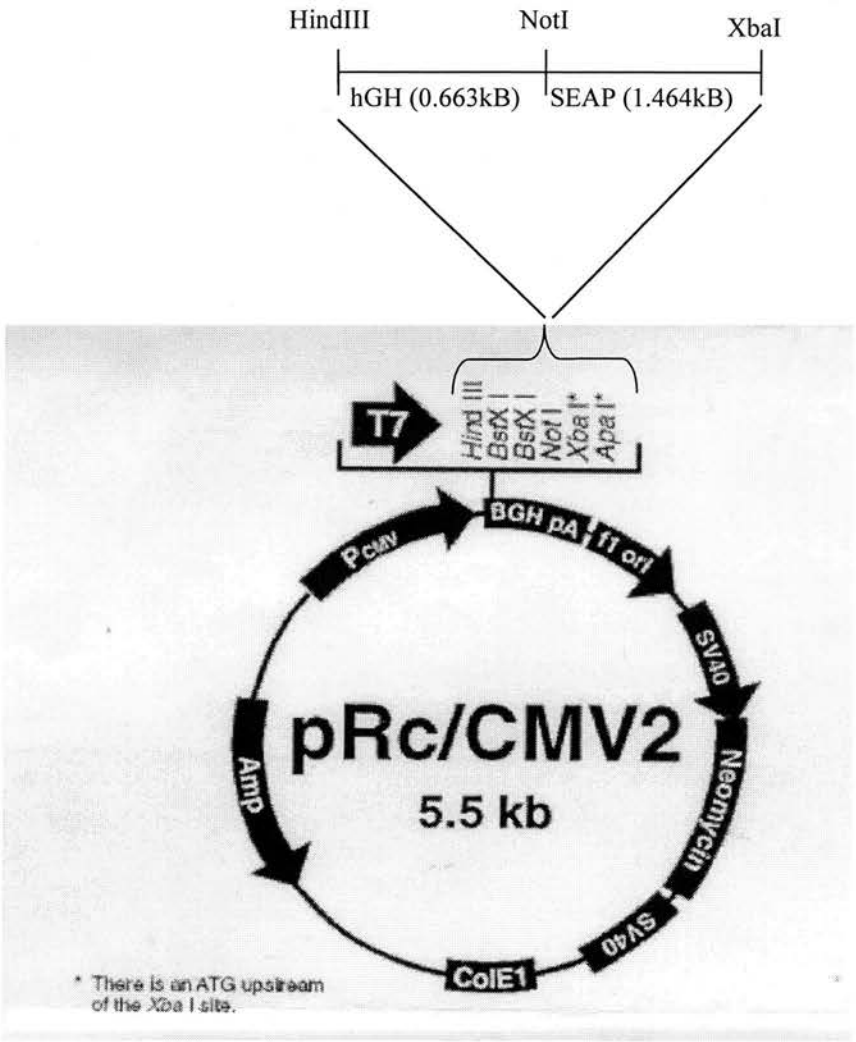

The pRc/CMV2 plasmid was obtained from Invitrogen, and its full sequence can be obtained from the Invitrogen website. It has a CMV promoter to allow for efficient expression of the protein in mammalian cells. It also has a T7 promoter, polylinker, BGH polyA signal, f1 origin, SV40 promoter, SV40 origin of replication, Neo ORF, SV40 polyA, ColE1 origin and ampicillin resistance gene. The above diagram shows the original expression vector, along with the hHG/SEAP fusion gene and its position of insertion into the vector. Neomycin denotes the gene which expresses the G418 resistance of the plasmid.

(D) RT-PCR PRIMER DESIGN

The following shows the primers which were used in an attempt to detect the presence of synaptobrevin and syntaxin in AtT-20 cells using RT-PCR. The RT part of the reaction was done using random primers, but the second PCR amplification of the cDNA used the primers detailed below.

Syntaxin Primers

5` primer

5`** A T •A A G•G A C•C G A•A C C•C A G•G A G•C T C•C G C **3`

3` primer

3`** T C C•T T C•T T C•T A G•T A C•T A G•T A G•T A A•A C G• A C A **5`

These were designed using the 5` and 3` ends of rat syntaxin A, the gene sequence of which was obtained from the internet DNA database.

Synaptobrevin primers

5` primer

5`** A T G•T C T•G C T•C C A•G C T•C A G **3`

3` primer

3`** C A C•C A T•C A A•T A A•C A T•T A G•A T G•A A A•A A A•T G A **5`

These were designed using the 5` and 3` ends of human synaptobrevin 1, the gene sequence of which was obtained from the internet DNA database.

(E) lacZ plasmid map

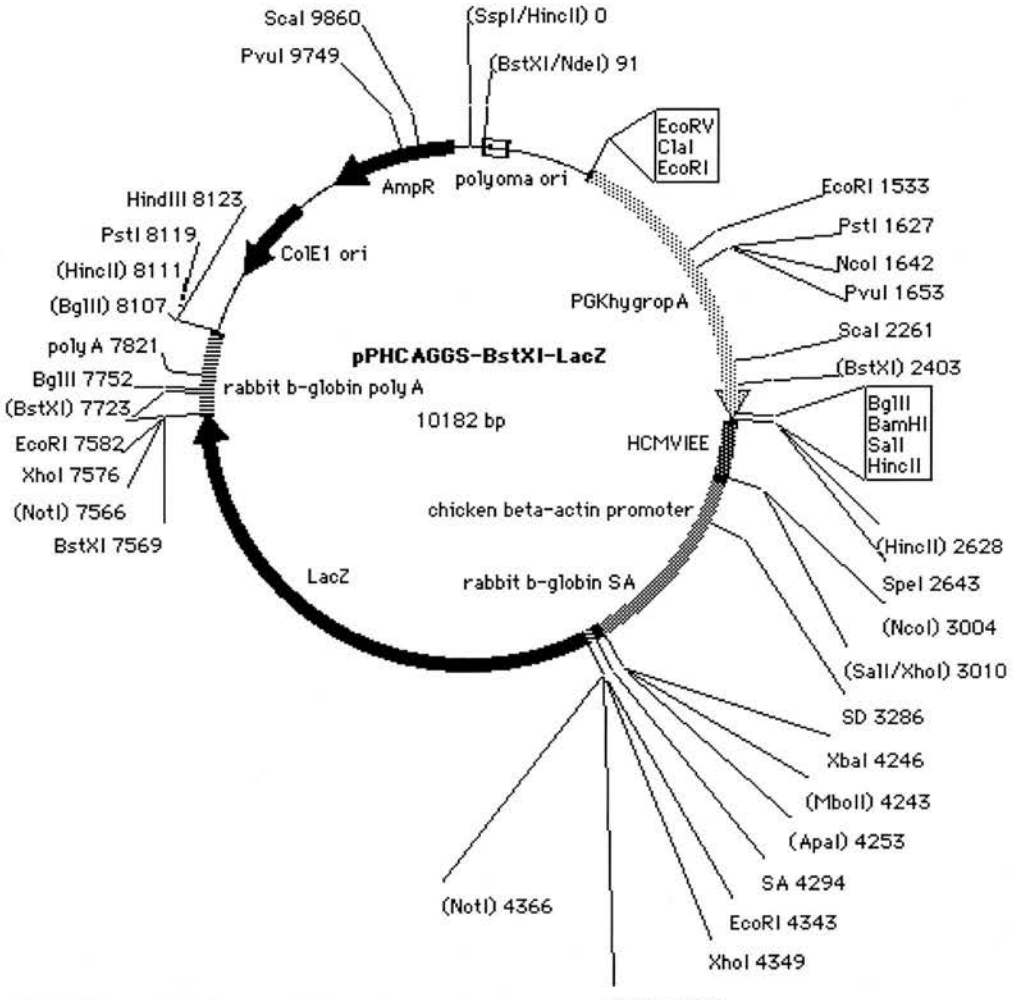

Plasmid name : pPHCAGGS-BstXI-LacZ
Plasmid size : 10182 bp
Constructed by : Hitoshi Niwa
Construction date : Sep. 1994
Comments/References : NotI fragment from pSVlacZ cloned into pPHCAGGS-BstXI (HN68) using BstXI adapters

The lacZ plasmid was a generous gift from Nick Gilbert (Dept. of Biochemistry, Edinburgh University), as were all reagants used for detection of β-galactosidase activity.

Chapter 3

Characterisation of AtT-20 cells using immunoblotting

3.1 Introduction

Many proteins have been identified, mainly in chromaffin and neuronal cells, that are thought to be involved in Ca^{2+}-regulated exocytosis. However definite functional evidence has not yet been obtained for all such proteins, and many have implicated through their interactions with synaptic vesicles or synaptic vesicle proteins. The aim of this project was to examine the exocytotic machinery in AtT-20 cells, and to assess whether similar mechanisms were at work. The starting point for this project was therefore to fully characterise the cells, and to discover whether these proteins were present and what their intracellular distribution was. Due to the huge number of putative exocytotic proteins that have now been discovered, it was decided to concentrate on several well-established ones, for which there was definite functional evidence. These were synaptobrevin, SNAP-25, syntaxin, αSNAP, NSF, rab3A, synaptotagmin and CAPS. It was also decided to study the role of actin in exocytosis from AtT-20 cells, therefore western blotting was used to look for two actin-depolymerising proteins, ADF (actin-depolymerising factor) and cofilin.

Wendland & Scheller, 1994 have previously shown the presence of synaptotagmin, VAMP and synaptophysin in AtT-20 cells, by subcellular fractionation and immunoblotting, while *Martelli et al., 1995* showed the presence of both Rab3A and Rab3D by similar methods.

3.2 Fractionation of AtT-20 cells

AtT-20 cells were grown, harvested and homogenised, as described in section 2.1, after which they were fractionated using various sucrose density gradients, as detailed in 2.1.3. The fractions were run on 10-12% or 10%, 12% and 13% polyacrylamide gels (section 2.2) and then stained with Coomassie blue R. Each fraction was assayed for protein (section 2.1.5), and sucrose concentrations were estimated using a refractometer (section 2.1.4). In order to monitor the distribution of organelles and proteins, various marker proteins were utilised. Preparations of the various organelles were normally used as positive controls and are detailed in Chapter 2.

- **Golgi** were identified using an assay for the enzyme galactosyl transferase and the assay described in 2.1.6. The unique ability of Golgi fractions to transfer galactose from sugar nucleotide precursors to N-acetylglucosamine residues lead to the identification of galactosyl transferase as a marker for this organelle *(Fleischer & Fleming, 1970).* It is now known to be present on the *trans*-cisternae of the Golgi-complex, its active site being at the luminal side *(Strous et al., 1983).*

- The **endoplasmic reticulum** was detected using the α subunit of the signal recognition particle receptor (SRPRα or 'docking protein') as a marker protein specific to the ER. An antiserum raised against the 60,000kDa fragment of the docking protein of dog pancreas microsomes (gift from David Meyer, EMBL, Heidelberg), was used to localise the ER by western blotting of the cell fractions.

- The **mitochondria** were localised by detection of the F_1 sector of the mitochondrial ATP-ase, containing the subunits α,β and γ. Rabbit anti-bovine F_1 serum was obtained from David Apps (Dept. of Biochemistry, Edinburgh University) and was used to localise the mitochondria by western blotting of the cell fractions.

- **Secretory vesicles** were initially detected using the 57kDa subunit B of V-ATPase as a marker protein. Rabbit antiserum was raised against the 57kDa subunit of Kalanchoe tonoplast V-ATPase by Dr. Mark Warren (Department of Biochemistry, Edinburgh University) and was used to localise vesicles by western blotting of the cell fractions.

- The **plasma membrane** was detected by biotinylating the plasma membrane proteins (section 2.1.7) prior to harvesting and homogenisation (section 2.1.2). Western blotting was then used to detect labelled plasma membrane proteins, using streptavidin-conjugated HRP, in place of antibodies, and subsequent detection by ECL.

- **Cytosol** was assumed to remain in the lightest sucrose fractions and blots using antibodies against soluble proteins such as ADF showed this to be true.

In all blots 20µl of the cell fractions were run on 10-12% or 10%, 12% and 13% polyacrylamide gels and then western blotting was done using the technique described in section 2.2. Equal amounts of proteins were not used in each lane as certain fractions contained very little protein and this would greatly lower the chances of being able to detect the desired proteins. A total of four gradient fractionations were done throughout this project, some with slightly varying conditions. The results of these will now be detailed and discussed with respect to protein and sucrose concentrations, and organelle localisation in the gradients. These preparations were also used for the localisation of the exocytotic proteins, which will be discussed in section 3.3. **Gradient 1**

A gradient of 0.4-1.8M sucrose was used and protein concentrations were estimated by Bradford's assay (section 2.1.5.2), the standard curve of which can be seen in figure 3.1. Results of the protein and sucrose estimations are shown in table 3.1. 20µl of the fractions were run on 10-15% gradient gels which were stained using Coomassie blue, and these are shown in figure 3.2. The protein estimations and gels show the majority of cellular proteins to be distributed over two main areas: fractions 4-5 (1.33 & 1.25M sucrose) and fractions 11-13 (0.18, 0.4 & 0.6M sucrose). These probably represent membrane proteins and cytosolic proteins respectively. Secretory vesicles were identified using an antibody against V-ATPase (see figure 3.3), and were shown to be localised in fractions 4-5. However the subunit used as a marker was not an integral one, and it appeared that much of it had dissociated from the integral segment, and was found in the cytosolic fractions (11-13). Synaptotagmin is also a good vesicle marker and was found to co-localise to the V-ATPase proteins and give better results, therefore future fractionations used synaptotagmin as the vesicle marker. An example of a synaptotagmin blot can be seen in figure 3.10.

The various fractions were tested for a number of proteins involved in exocytosis, which will be discussed in section 3.4. Further analysis of the various organelles was done in a repeat of this experiment (see fractionation 2 below).

3.2.2 Gradient 2

The sucrose gradient used was as above, however protein concentrations were estimated by Peterson's assay (section 2.1.5.1), as there was a possibility that sucrose

may have interfered with the Bradford's assay. Table 3.2 details the protein and sucrose concentrations, whilst figure 3.4 shows the Peterson's assay standard curve. The protein distribution is very similar to that obtained previously. Slightly lower protein concentrations were found, due to the fact that slightly less PNS was loaded onto the sucrose gradient (0.7ml instead of 1ml), rather than interference of sucrose in the last protein assay. Since fractions were collected manually, 1ml being estimated by eye, there were also only 12 fractions collected this time.

This gradient was further analysed by the localisation of some of the organelles, using the techniques detailed above. Figure 3.5 shows the blots obtained for mitochondria, and figure 3.6 the blots obtained for ER. Figure 3.7 shows the galactosyl transferase assay results. Secretory vesicles were identified in fractions 4-5 using synaptotagmin as a marker (data not shown).

3.2.3 Gradient 3

The method used for this fractionation was the same as for fractionations 1 and 2, but the sucrose gradient was changed to 0.6-1.6M. This was to try and separate out the membrane proteins which up until this point had clustered in the same area. The protein and sucrose concentrations are shown in table 3.3. The results obtained from the mitochondria, ER and secretory vesicle blots have been summarised in table 3.4, as have the Golgi assay results. Identification of the vesicles was again by use of the anti-synaptotagmin antiserum.

3.2.4 Gradient 4

As the separation of membrane fractions showed no great improvement with the altered range of sucrose concentrations, the gradient used here was 0.4-1.8M (as in fractionations 1 and 2). The major aim in this experiment was to locate the plasma membrane, so intact cells were biotinylated using the method detailed in section 2.1.7. Table 3.5 details the sucrose and protein concentrations, whilst table 3.6 again summarises the results obtained for the mitochondria, vesicle, ER and Golgi localisation. Figure 3.8 shows the results obtained for plasma membrane localisation, as shown by blotting with streptavidin-peroxidase.

Figure 3.9 summarises the results obtained in the various fractionations of AtT-20 cells.

3.3 Discussion

Gradient 1

Protein estimations of samples from this gradient showed that there were two main regions where many proteins were equilibrating: fractions 4-5 and fractions 12-13. These had respective sucrose concentrations of 1.33-1.25M and 0.40-0.18M, and they would be expected to represent membrane and cytosolic proteins respectively. This gradient was used to detect the presence of various exocytotic proteins, detailed in section 3.4. The secretory vesicle fraction was identified as being in fractions 4-5, using the V-ATPase as a marker. However the subunit recognised by the antiserum is not an integral one and thus appeared also in cytosolic fractions (11-13), presumably as a result of dissociation from the V-ATPase. Thus in subsequent experiments the secretory vesicle fraction was identified using the secretory vesicle marker synaptotagmin.

Gradient 2

In this gradient the same procedure was used, however fewer fractions were collected. This meant that the two main regions of protein accumulation were fractions 3-4 and 11-12, with sucrose concentrations of 1.33 & 1.25M sucrose and 0.50 & 0.12M sucrose respectively. The protein concentrations were also slightly lower, but this was due to the fact that the homogenate was slightly more dilute and therefore less protein was actually loaded on each sucrose gradient. In gradient 2 ER, mitochondria and secretory vesicles were located in fractions 3-4 (1.33 & 1.18M sucrose). The ER showed the majority of SRPR to be in the degraded form, however similar bands also appeared in fractions 11-12. It is probable that these are high concentration cytosolic proteins that are reacting non-specifically with the antiserum, as synaptotagmin is integral. The mitochondrial blot shows (unlike the V-ATPase 57kDa subunit) that no dissociation has occurred, although the F_1 subunits are not integral. The Golgi membranes equilibrated in fractions 4-5 (1.18 & 1.14M sucrose), showing slight membrane separation. There was also a peak of this marker in fraction 10, which may have been due to disruption of the Golgi apparatus. Since most membrane proteins were clustered in the same fractions, it was decided to use a sucrose gradient of narrower range in the hope that this would cause some separation

of the membranes and therefore achieve greater enrichment of the secretory vesicle fraction.

Gradient 3

Although the concentration of the sucrose gradient was adjusted, there was little change in the protein distributions, although there was further distribution of the Golgi into fraction 6 (1.06M sucrose), as well as 10. Secretory vesicles, mitochondria and ER remained in fractions 3-4 (1.37/1.22M sucrose). As a final experiment a fractionation was done in which the plasma membrane proteins were biotinylated, to detect whether they were also equilibrating in these middle fractions.

Gradient 4

In this experiment only 1μg from each fraction was loaded per lane of an acrylamide gel, and the biotinylated proteins were detected using streptavidin-HRP. The reason for loading similar quantities of protein here is that the detection method was very sensitive, and the gradient was not screened for a single specific protein, but for all biotinylated proteins. In all other cases, in which detection of particular proteins was required, it was better to load as much as possible, in order to exceed the threshold of detection by the antibody. The sucrose gradient used was 0.6-1.8M and the protein and sucrose estimations of the various fractions showed very similar distributions to previous fractionations. Secretory vesicles, mitochondria and ER equilibrated in fractions 4-5 (1.37 & 1.22M sucrose), and Golgi membranes were also found here, as well as in fraction 10 (0.77M sucrose). Biotinylated proteins were located in fractions 4-5, showing that little separation of plasma membranes was occurring.

Whilst this fractionation method did not achieve separation of the various organelles, it concentrated membrane and cytosolic proteins in quite different areas. These results could be used to assess whether the proteins were cytosolic (and soluble in the cell) or membrane bound or associated. Whether they are specifically bound to plasma membrane, vesicles or other organelles was determined using immunofluorerscence micrsocopy (see chapter 4), and data on these proteins obtained in other studies. The results of the blots obtained for the various exocytotic proteins are shown in the figures section at the end of this chapter. The gradient

number used in each study is quoted, in order that protein and sucrose concentrations can be obtained from the tables.

3.4 Identification of proteins involved in exocytosis

Antibodies against various proteins thought to be involved in Ca^{2+}-regulated exocytosis, were tested against the AtT-20 cell fractions discussed above. Figures 3.10 to 3.22 show the results of the blots, and details of the antibodies (and source) can be found in the appropriate figures. The fractionation number and dilution of the antibody have also been detailed here. Chromaffin membrane granules were usually run beside the AtT-20 cell fractions as a comparison. Whilst these do not always represent ideal positive controls (e.g. for cytosolic/plasma membrane proteins), they serve to show whether differences could be seen in the two cell types. Antibodies were usually tested and titrated using rat brain synaptosomes (for plasma membrane proteins) and rat brain cytosol (for cytosolic proteins), however the data for this is not shown. The following list summarises the proteins examined:

Figure 3.10 synaptotagmin (65kDa; integral vesicle protein)

Figure 3.11 syntaxin (36kDa; integral plasma-membrane protein)

Figure 3.12 SNAP-25 (25kDa; plasma membrane associated protein)

Figure 3.13 αSNAP (36kDa; cytosolic protein)

Figure 3.14 NSF (76kDa; cytosolic protein)

Figure 3.15 ACTH precursors (various molecular weights; major secretory peptide in the dense granules)

Figure 3.16 synaptotagmin (detected using a monloclonal antibody; details as above)

Figure 3.17 Normal rabbit serum (negative control)

Figure 3.18 synaptobrevin 2 (18kDa; integral vesicle protein)

Figure 3.19 Rab 3A (17kDa; vesicle-associated/cytosolic protein)

Figure 3.20 CAPS (145kDa; phospholipid/vesicle associated protein)

Figure 3.21 ADF (20kDa; cytosolic protein)

Figure 3.22 cofilin (17kDa; cytosolic protein)

3.5 Discussion

Synaptotagmin (figures 3.10 & 3.16)

Synaptotagmin was identified in the membrane-rich fractions 4-5, peaking in 4. A degradation product of around 52kDa can also be seen in these fractions as well as in fractions 12-13. However it is unlikely that this is the same product, as a protein of this size would still be an integral membrane component. It is more likely that this is a highly-concentrated cytosolic protein that shows non-specific reactivity with the synaptotagmin antibody. Synaptotagmin has been shown to be present in synaptic vesicles, catecholaminergic granules and peptidergic granules (*Wendland & Scheller, 1994*). AtT-20 cells contain two distinct types of vesicles: small clear synaptic vesicles and dense-core peptidergic vesicles. The small clear synaptic vesicles contain acetylcholine (ACh), which has been shown to be released in response to 100mM potassium (*Matsuuchi et al, 1988*). However these must not be directly equated to the rapid neuronal communication, as it is thought that the ACh release from AtT-20 cells actually mediates paracrine actions (*Reetz et al., 1991*). The dense-core peptidergic vesicles contain ACTH. Synaptotagmin is presumably a marker for both of these, although as yet we cannot separate them.

Syntaxin (figure 3.11)

Syntaxin is an integral plasma membrane protein, and was positively identified (although the band was faint) in the membrane fraction of AtT-20 cells (fraction 4). In agreement with the marker protein results this indicated that all membranes equilibrate around this region. It can also be seen in the chromaffin granule membranes, which suggests contamination with plasma membrane or that syntaxin is also found on vesicle membranes, about which there has been some debate. *Kretzschmar et al., 1996* reports the existence of syntaxin and SNAP-25 on synaptic vesicles, whilst *Tagaya et al., 1995* showed the presence of syntaxin on chromaffin granules only.

SNAP-25 (figure 3.12)

SNAP-25 is a t-SNARE that is anchored to the plasma membrane via multiple palmitoylation of its C-terminal cysteine residues. It therefore appears in the

membrane fractions (4 & 5), and the cytosolic fractions (11-13), where it exists due to dissociation from the plasma membrane. However SNAP-25 can also be recognised (at lower concentrations) in fractions 6-10, where previously no organelles have been localised. Possibly this is simply due to the fractionation process, in that SNAP-25 travels down the gradient to fraction 4 where it equilibrates. It may be that the nature of its linkage to the vesicles causes dissociation from them as it moves down the gradient, thus producing a trail of SNAP-25 protein. Interestingly SNAP-25 can also be seen in the chromaffin granule membranes, which as for syntaxin, could suggest contamination of the granules with plasma membrane, or the existence of a vesicle-bound form (as reported *by Tagaya et al., 1996*).

αSNAP (figure 3.13)

αSNAP is a 36kDa cytosolic protein that associates with the SNARE complex, although at which stage is still under debate. It has been shown that permeabilisation of chromaffin cells causes a run down in the exocytotic response to Ca^{2+}, which can be rectified by the introduction of αSNAP *(Morgan & Burgoyne, 1995)*. This in itself suggests that in a normal cell situation it exists in a soluble form, however this blot shows it to be present in the membrane fractions (4-5). Thus it must be associated with the membranes, or most likely to an integral/associated membrane protein (a SNARE). This is in contrast to the chromaffin granule membranes where it cannot be seen at all. It is also present in the expected cytosolic fractions (11-13), where bands of 66 kDa can alse be seen. It is unlikely that this band represents a SNARE complex of any sort, as this is an SDS-containing gel and the band is not seen with any of the other SNARE proteins. Again it is likely that this is due to the high protein concentration of the cytosolic fractions and non-specific binding as a result of this.

NSF (figure 3.14)

NSF is a cytosolic protein, which binds to the SNARE complex and has ATPase activity. It was identified in the membrane fractions (4-5) and the cytosolic fractions (11-13). Like αSNAP it is therefore associated with membranes, or more likely to integral/associated membrane proteins. In this instance the NSF can also be seen in the chromaffin granule membranes which is interesting with respect to the

aforementioned permeabilisation assay. In this assay, whilst αSNAP rescued the cells from rundown, NSF had no effect, and this was postulated to be because it existed in a membrane-bound form which provided the cell with a plentiful supply (*Morgan & Burgoyne, 1995*). An association with synaptic vesicles was also reported by *Hong et al.,1995* who described co-localisation of NSF with the SV marker synaptophysin.

ACTH propeptides (figure 3.15)

ACTH is one of several peptide hormones derived from the precursor POMC, which gets processed into a 4.5kDa mature ACTH peptide before release on Ca^{2+} stimulation. *Tanaka et al., 1991* showed that the mature form of the hormone is processed to POMC within the Golgi cisternae and RER. The POMC is then processed as the granules mature and move to the periphery of the cell, and much of the cleavage of the POMC into mature ACTH will actually occur within the mature dense core granules. A true marker of the mature dense core granules would be mature 4.5kDa ACTH, however the resolution of the 12% polyacrylamide gel was not great enough to show this band accurately. Subsequent attempts using a tricine based gel system (*Schagger & Jagow, 1987*) also failed to provide accurate identification (data not shown). Thus the propeptides were located in the membrane fractions (4-5) and also in the cytosolic fractions (11-13), probably due to lysis of the granules. However, in a similar way to the synaptotagmin blot, we can assume that the POMC would be present in both immature and mature dense-core vesicles, thus again suggesting a general clustering of the membranes. It is concluded that the ACTH-containing dense-core vesicles are in the membrane fractions, along with many of the other proteins involved in exocytosis.

Normal Rabbit Serum (figure 3.17)

This was simply used as a negative control, to identify any false positives, and show up any major cross-reactive proteins. Little reactivity was seen in fractions 1-8, with an increasing density of bands in fractions 9-11, and slightly less in 12. This shows the potential of the cytosol for giving non-specific reactive bands, some of which have been mentioned previously. In general a band has been considered to be a

positive result only when it is the major and most dense band present.

Synaptobrevin 2 (figure 3.18)

Synaptobrevin is an integral vesicular membrane marker, and has been shown to be present on SVs (*Trimble et al., 1988*), catecholaminergic granules (*Papini et al., 1995*) and peptidergic dense core vesicles (*Halpern et al., 1990*). It localised to the membrane fraction 4 in AtT-20 cells, however some very strong bands were seen in fractions 10-12 at around 116kDa. High molecular weight bands have been seen in this region in previous blots, and could be attributed to a complex that was not dissociated by SDS. Different loading conditions were therefore tried, such as increased or decreased SDS and DTT concentrations and heating of the sample to 25°C, 37°C or 90-100°C, however no difference was seen. As the high-molecular weight bands varied between blots it is doubtful that it is a SNARE complex, and probably represents non-specific reactivity. Previously mentioned was that a positive result was inferred by the existence of a band of the expected mobility, and the highest density. However the different amounts of protein loaded must also be taken into account, as 3-5 times the amount was loaded in fractions 11-13 (cytosolic fractions) compared to fractions 4-5 (membrane fractions).

Rab 3A (figure 3.19)

This protein is vesicle-associated in its GTP bound form, and cytosolic in its GDP bound form. It is thus found in membrane fractions (3-4) and cytosolic fractions (11-13).

CAPS (figure 3.20)

This protein has been shown to bind phospholipids, and has been postulated, from cytosolic rundown experiments in PC12 cells, to be involved in late stage triggering of fusion (*Walent et al., 1992*). In AtT-20 cells all of the protein was identified in the cytosolic fractions (11-12), perhaps indicating a later role for it in Ca^{2+}-regulated exocytosis. The degraded form (seen around 85kDa) is common and can also be seen in the references cited above.

ADF (figure 3.21)

ADF and cofilin are very similar actin-depolymerising proteins, and have been found to be abundant in neuronal and secretory tissues. Both sever actin filaments in a Ca^{2+}-independent manner, are pH-dependent *(Hawkins, 1993)*, and transients in intacellular pH have been noted in various cells on stimulation of exocytosis *(Stella, 1995)*. This and the relatively recent suggestion that actin acts as a barrier to exocytosis prompted the study of these two proteins. ADF was found in cytosolic fractions 11-12 only.

Cofilin (figure 3.22)

Cofilin was located in the cytosolic fractions only, and was most concentrated in fraction 12.

3.6 Triton X-114 fractionation

The results obtained using conventional fractionation of AtT-20 cells followed by SDS-PAGE and Western blotting show the presence of the majority of exocytosis-related proteins tested, however they could only be separated into membrane-bound and cytosolic fractions. In addition, the blots obtained for certain proteins, in particular syntaxin and synaptobrevin, gave very weak signals. RT-PCR and immunofluorescence were used as alternative methods of further characterising the AtT-20 cell line, and these results are presented in chapter 4. It was also decided to use fractionation with Triton X-114, in the hope that it would yield more information about the proteins, and give more definite results in western blotting. The technique used is detailed in section 2.1.9.2, and each gel had 15µg protein loaded per lane. All antibodies used were as described in the gradient blots (figures 3.10-3.22). However the antibodies to synaptobrevin and syntaxin were new, and were obtained from Timothy Whalley (Stirling University). Both were rabbit antisera, raised against the recombinant cytoplasmic domains of the proteins, and they were used at a dilution of 1/1000. The fractionation was performed on the pellet from 6 x 150cm^2 confluent flasks, which corresponds to approximately 4 x 10^6 cells.

Integral membrane proteins, in order that they can exist as such, have hydrophobic domains that anchor them within the lipid bilayer. Non-ionic detergents with polyoxethylene heads such as Triton-X-100, can replace the lipid environment of these proteins. Triton-X-114 has the added advantage of having a low 'cloud-point', thus on warming a solution of TX-114 to 30°C it forms two phases: detergent rich and aqueous. Intrinsic proteins partition into the lower phase, whilst extrinsic and soluble proteins partition into the upper phase *(Pryde, 1986).*

TX-114 was homogenised with the cell pellet at 0°C, in order to solubilize the membranes. Having centrifuged, a TX-114 insoluble fraction was obtained, containing membrane proteins in their original phospholipid environment that the TX-114 was unable to solubilise. The supernatant was then warmed, allowing the separation into 2 phases: aqueous and detergent-rich. These generated two more fractions: the aqueous layer (S) containing the hydrophilic proteins, and the detergent-rich fraction (P2) containing the hydrophobic integral membrane proteins.

The proteins which were tested for using this technique were synaptobrevin, syntaxin, αSNAP, NSF, SNAP-25 and synaptotagmin. The results are shown in figure 3.24 and are discussed in section 3.7. All blots included chromaffin granule membranes (C) and the various fractions are labelled S, P1 and P2. Molecular weight markers are shown in kDa. A Coomassie-stained gel was also run to show the general protein concentrations and distributions (figure 3.23).

3.7 Discussion

The majority of **syntaxin** was found in fraction S, which is expected to contain the soluble, hydrophilic proteins. Only a small fraction of syntaxin was detected in the expected P2 fraction (hydrophobic membrane proteins). A similar result was obtained for **synaptobrevin** and **synaptotagmin,** in that the main bands were in the S fraction, with minor bands detected in the P2 fraction. Possibly these proteins have very hydrophilic domains, outside their hydrophobic membrane spanning domains, which cause them to fractionate in this way (*Fischer-Colbrie et al., 1982*). Another explanation may be that multimeric complexes may form, which shield the

hydrophobic domains, thus causing the protein to behave in a more hydrophilic manner (*Tanford & Reynold, 1976*). Another possibility is that the traces of TX-114 remaining in the S fraction were sufficient to maintain the proteins in solution. This problem can be overcome on removal of the detergent by dialysis against XAD-2 resin *(Pryde & Phillips, 1986)*, but this approach was not practical in such a small-scale fractionation. In contrast SNAP-25 was found in fraction P2 only presumably by virtue of its behaving as a typical membrane protein.

The soluble proteins **NSF** and **αSNAP** were both found in the membrane fraction P2, as was also observed in the previous fractionation by sucrose density gradient. The TX-114 fractionation may also suggest their binding (in non-stimulated cells) to membrane components, however not via synaptobrevin, synaptotagmin or syntaxin. The other possibility is that they are binding to SNAP-25 and co-localising with it, although most evidence has suggested the need for a SNARE complex, before αSNAP/NSF binding will occur (*Goda, 1997*). It must be remembered that the TX-114 fractionation does not produce a realistic cellular environment, and the soluble proteins could be dissociating and re-associating with other membrane proteins, after solubilzation.

3.8 Conclusions

The presence of the proteins synaptotagmin, syntaxin, synaptobrevin, SNAP-25, NSF, αSNAP, ADF cofilin, CAPS and rab3A has been cofirmed in AtT-20 cells. Syntaxin, synaptobrevin, synaptotagmin, SNAP-25, NSF, αSNAP and rab3A were all found to be membrane-bound, with NSF, αSNAP, rab3A and SNAP-25 also being found in the cytosolic fractions. ADF, cofilin and CAPS were found only in the cytosolic fraction. These results demonstrate that αSNAP, NSF and rab3A are associated with membranes or membrane-bound proteins in AtT-20 cells that have not been stimulated with Ca^{2+}. This may suggest a much earlier role for them in Ca^{2+}-regulated exocytosis, in that they attach to the SNARE complex before the influx of Ca^{2+}.

TX-114 fractionation was useful in showing more positive bands in Western blots for many of the proteins, particularly synaptobrevin and syntaxin. These same antibodies, when used with the original sucrose density gradient fractions gave no definite bands. Thus the TX-114 fractions provided an enrichment of proteins, which the previous approach was unable to match. However TX-114 fractionation does not really provide any additional information as to the localisation of the proteins in the cell.

Table 3.7 summarises the results obtained using these two techniques (sucrose density gradient sedimentation and TX-114 fractionation), and gives details of the fractions in which the proteins were found.

Chapter 3 shows the presence in AtT-20 cells of many of the proteins believed to be involved in exocytosis, in neuronal and chromaffin cells. The next aim was twofold: (1) Further characterisation of AtT-20 cells (especially with respect to actin and the cytoskeleton). (2) To assess the role (if any) of these proteins in exocytosis from AtT-20 cells.

Figure 3.1 Bradford assay standard curve for protein determination (gradient 1)

A standard curve was constructed using BSA standards ranging from 0 to 20μg and the absorbance was read at 595nm. The cell fractions were diluted until on the scale of the graph and the protein concentrations calculated accordingly, using the standard curve. The standard curve was plotted as A_{595} against μg BSA.

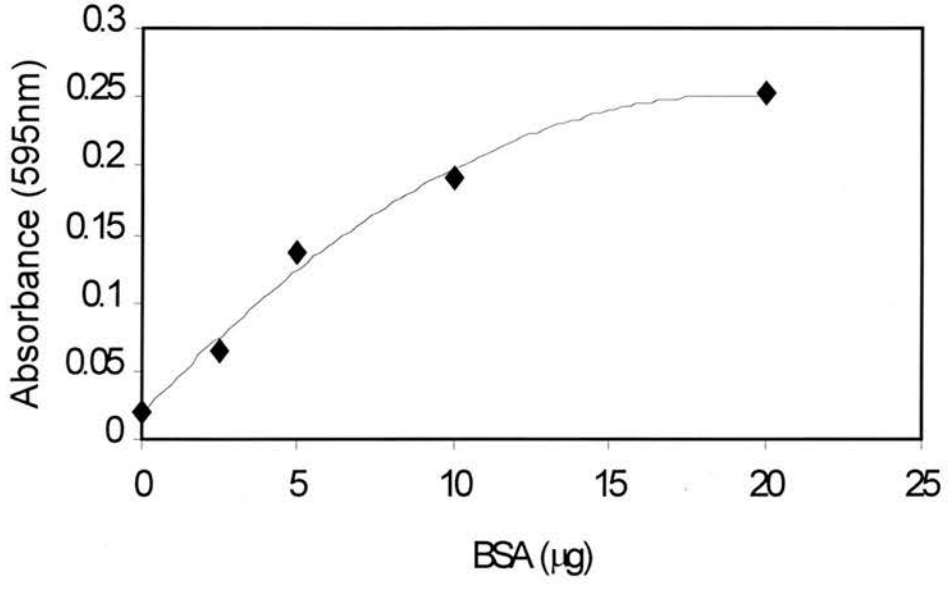

Table 3.1 Protein and sucrose concentrations in gradient 1

Protein concentrations were estimated using Bradford's assay and calculated using the standard curve shown in figure 3.1. Sucrose estimations were obtained by refractometry.

Fraction number	Protein concentration (mg/ml)	Sucrose concentration (M)
1	0.15	1.71
2	0.15	1.58
3	0.17	1.46
4	3.05	1.33
5	2.21	1.25
6	0.32	1.10
7	0.19	0.99
8	0.21	0.88
9	0.27	0.77
10	0.46	0.63
11	1.70	0.60
12	9.00	0.40
13	3.80	0.18

Figure 3.2 10-15% gradient gels of fractions from gradient 1

20µl of each cell fraction were run on 10-15% gradient gels (labelled 1-13), along with DaVII/SDS-6H markers, chromaffin granule membranes (CGM), rat brain synaptosomes (S) and cytosol (C). Approximately 20µg of each of these were run per lane. 20µl of each cell fraction correlates to the following total quantity (µg) of protein per fraction loaded onto the gel: (1) 3.0, (2) 3.0, (3) 3.4, (4) 61.0, (5) 44.2, (6) 6.4, (7) 3.8, (8) 4.2, (9) 5.4, (10) 9.2, (1) 34.0, (12) 180.0, (13) 76.0.

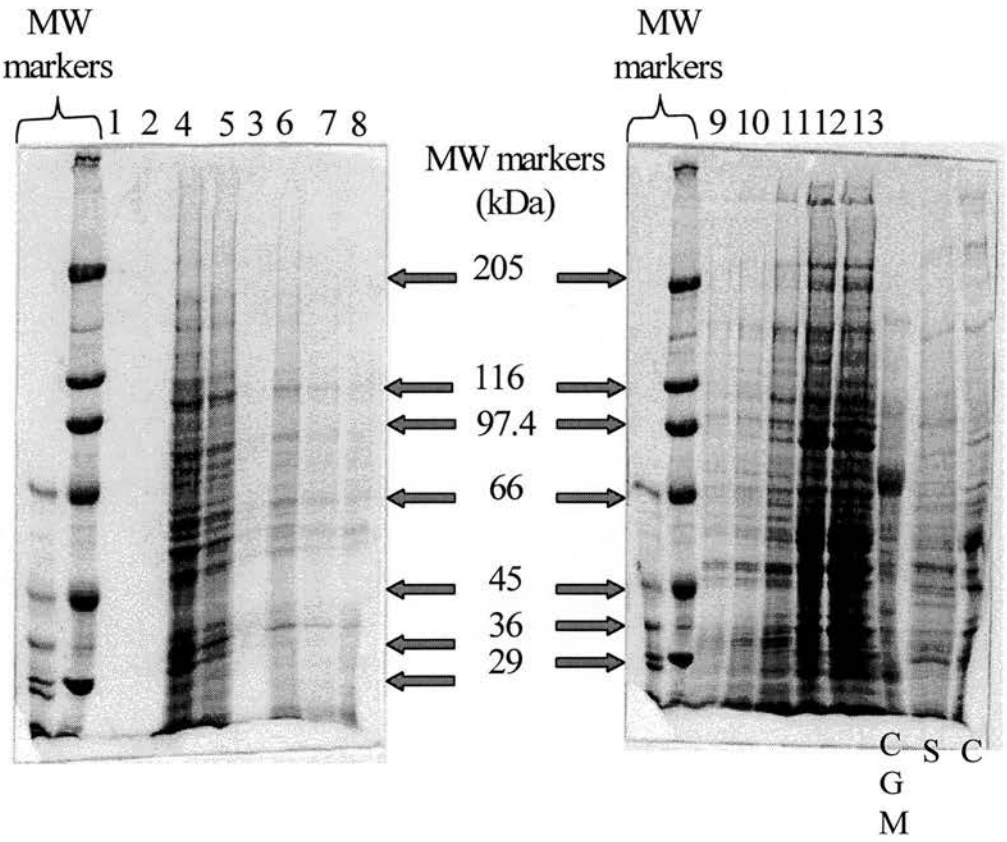

Figure 3.3 Localisation of secretory vesicles in gradient 1

The diagram below shows the blots obtained when using the anti-V-ATPase antibody (at a dilution of 1/2000), as described previously. The molecular weight of the V-ATPase antigen is 57kDa, the positive control used here is chromaffin granule membranes (labelled as C). H represents AtT-20 cell homogenate, and the various AtT-20 cell fractions are labelled 1-13.

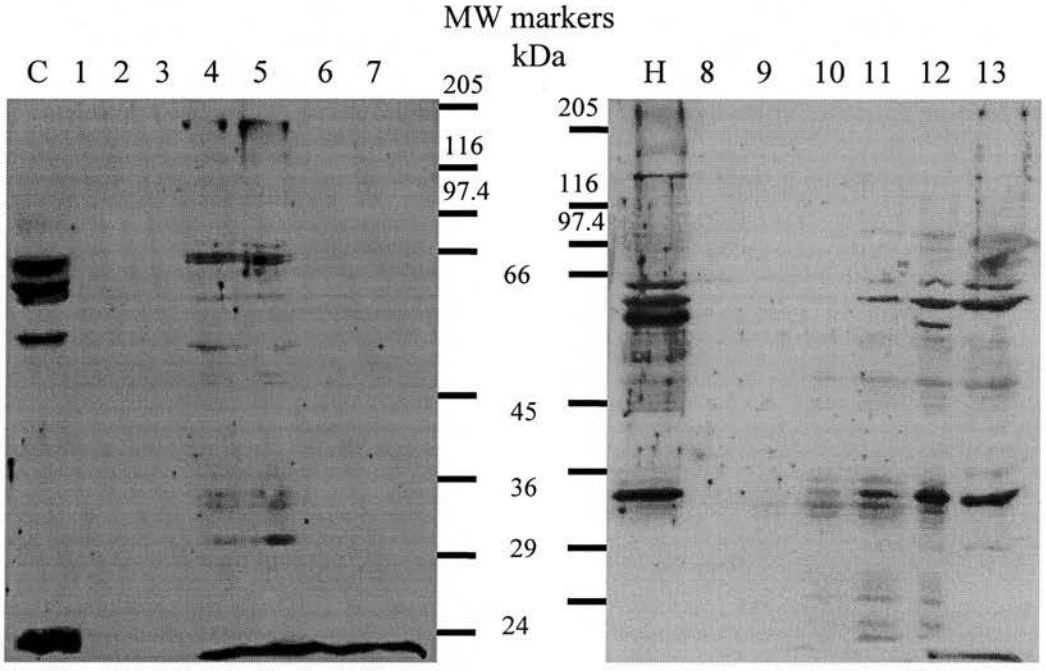

Figure 3.4 Peterson's assay standard curve for protein determination (gradient 2)

A standard curve was constructed using BSA standards ranging from 0 to 100μg and the absorbance was read at 750nm. Appropriate volumes of the cell fractions were diluted, until on the scale of the graph, and the protein concentrations calculated accordingly, using the standard curve. The standard curve was plotted as A_{750} against μg BSA.

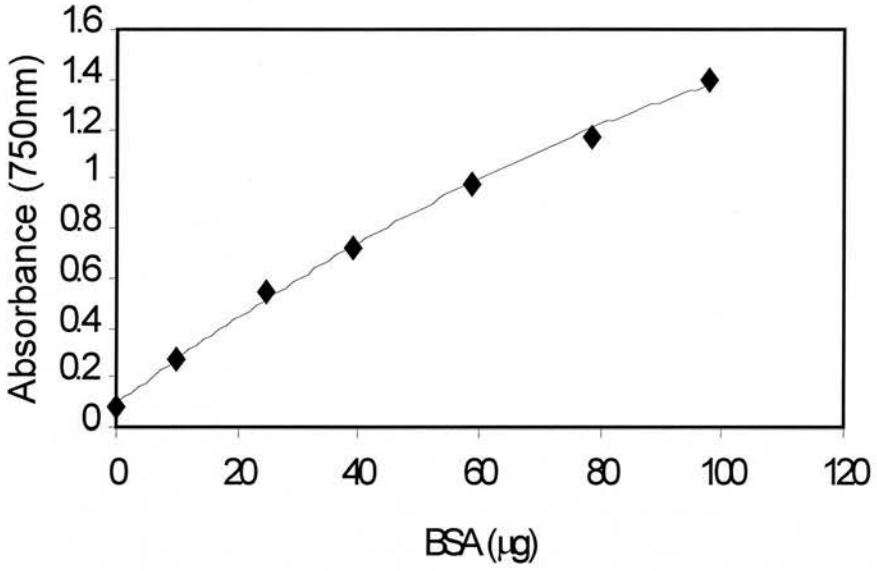

Table 3.2 Protein and sucrose concentrations in gradient 2

Protein estimations were done using a Peterson's assay and calculated using the standard curve shown in figure 3.4.

Fraction Number	Protein concentration (mg/ml)	Sucrose concentration (M)
1	0.06	1.67
2	0.09	1.50
3	1.18	1.33
4	0.91	1.18
5	0.58	1.14
6	0.49	1.02
7	0.31	0.84
8	0.28	0.77
9	0.38	0.67
10	0.66	0.63
11	3.34	0.50
12	6.44	0.12

Figure 3.5 Localisation of mitochondria in gradient 2

The diagram below shows the blots obtained using the anti-F_1 antibody (at a dilution of 1/1000), as described previously. The F_1 sector of the mitochondria contains 3 subunits: α and β having a molecular weight of 55 and 51kDa and γ of 30kDa. Molecular weights are shown in the centre of the two gels. The positive control (bovine heart mitochondria) is labelled M and the various fractions are labelled 1-12. H represents a sample of AtT-20 cell homogenate.

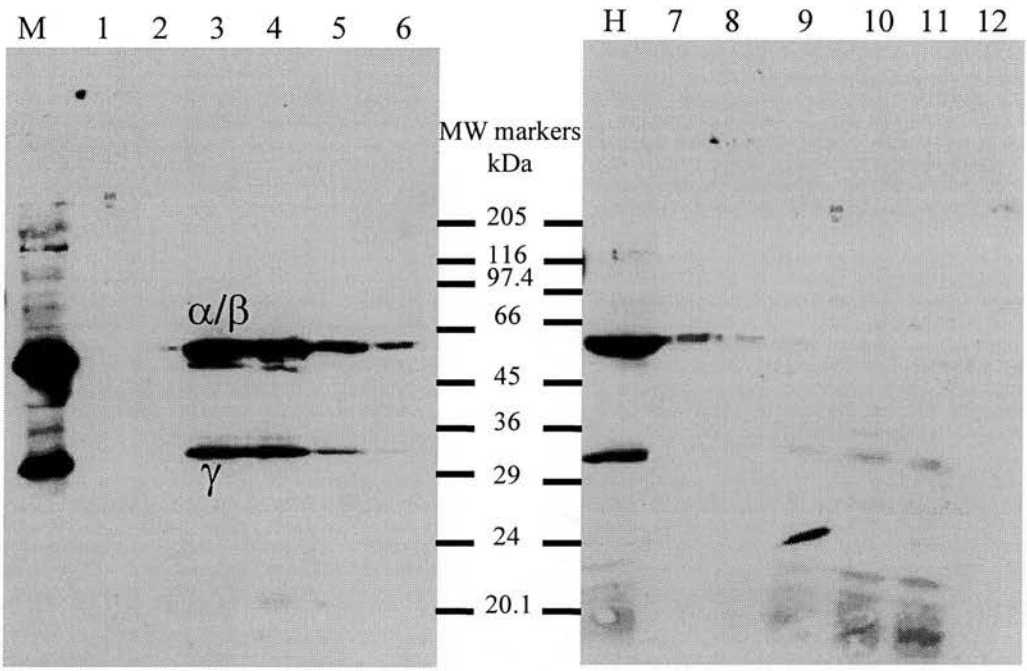

Figure 3.6 Localisation of endoplasmic reticulum in gradient 2

The diagram below shows the blots obtained when using the anti-SRPR antibody (at a dilution of 1/1000), as described previously. The molecular weight of the docking protein is 72kDa, however it is very easily degraded to a smaller (60kDa) product which is what is detected in the AtT-20 cell fractions. This degradation can also be seen in the microsome preparation that was used as a positive control, labelled M. AtT-20 cell fractions are shown 1-12 and AtT-20 cell homogenate is shown as H.

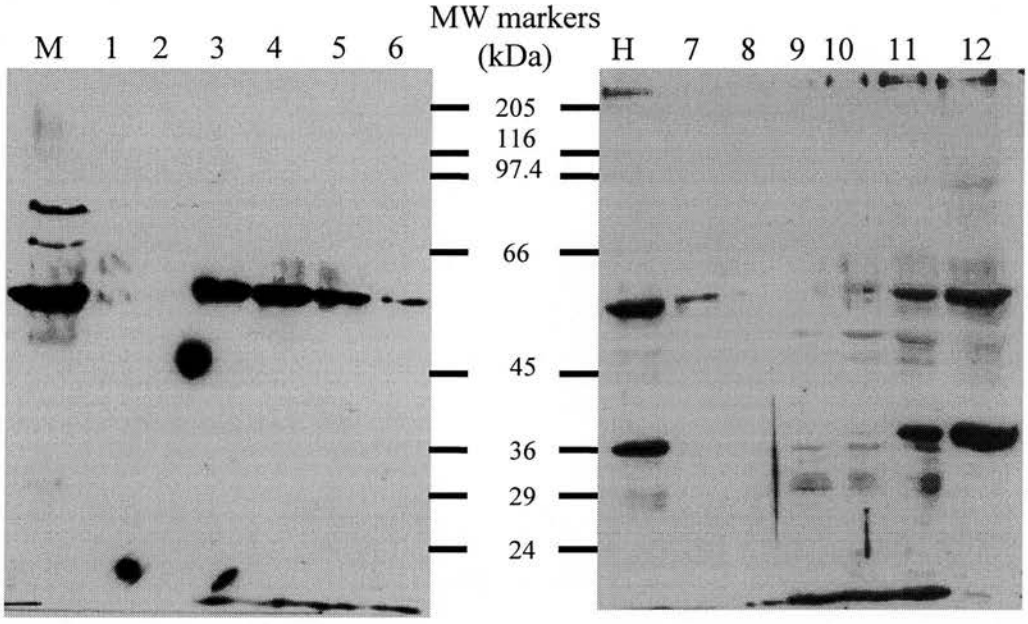

Figure 3.7 Localisation of Golgi membranes in gradient 2

Galactosyl transferase was assayed in order to identify Golgi membranes in the AtT-20 cell fractions. The presence of galactosyl transferase (and hence Golgi) was indicated by the transfer of galactose from [^{3}H]-UDP-galactose to ovomucoid, and this was expressed in dpm. The graph below shows [^{3}H] measured as dpm (i.e. presence of galactosyl transferase) plotted against sucrose concentration.

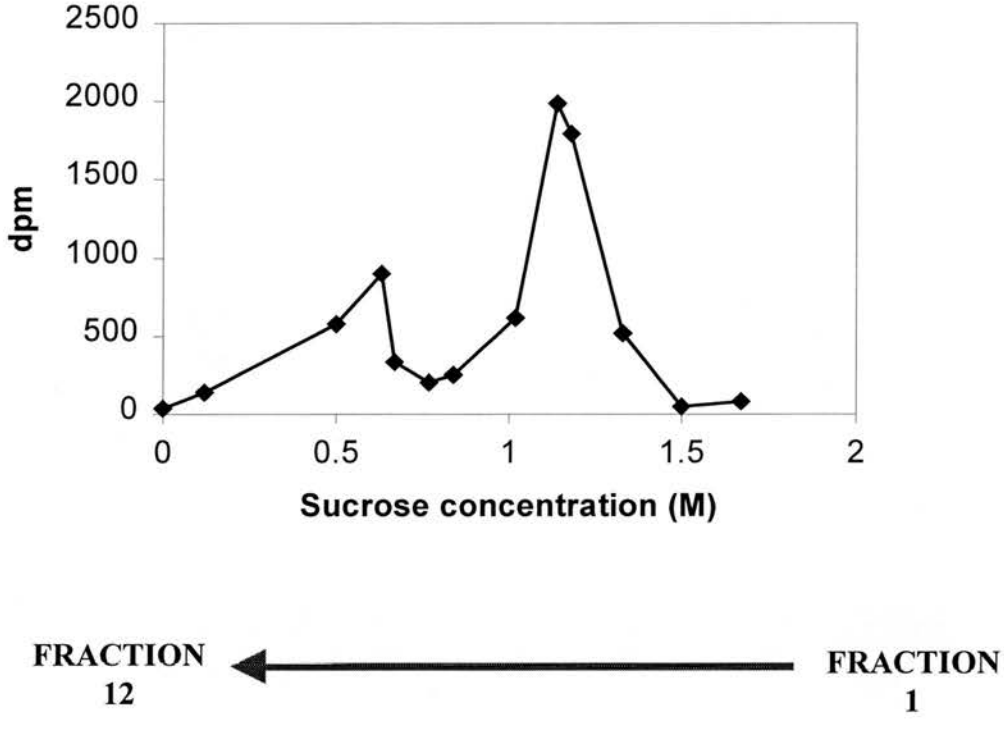

Table 3.3 Protein and sucrose concentrations in gradient 3

Sucrose concentrations were estimated by refractometry, and protein concentrations by Peterson's assay. The sucrose gradient used was 0.6-1.6M.

Fraction number	Protein concentration (mg/ml)	Sucrose concentration (M)
1	0.05	1.50
2	0.2	1.54
3	0.62	1.37
4	0.65	1.22
5	0.42	1.18
6	0.32	1.06
7	0.3	0.95
8	0.35	0.84
9	0.77	0.84
10	1.15	0.77
11	3.2	0.56
12	4.8	0.00

Table 3.4 Localisation of organelles in gradient 3

Mitochondria, secretory vesicles, ER and Golgi were localised using methods previously described. Their position is summarised below in a table using – to show a negative finding in that fraction, and a scale of + , ++ and +++ to show the presence of the organelle, and its increasing concentration.

Fraction number	Golgi	Vesicle	ER	Mitochondria
1	-	-	-	-
2	-	+	++	++
3	-	+++	+++	+++
4	-	++	++	++
5	-	+	-	-
6	++	+	-	-
7	-	+	-	-
8	-	-	-	-
9	-	-	-	-
10	+++	-	-	-
11	-	-	-	-
12	-	-	-	-

Table 3.5 Sucrose and protein concentrations in gradient 4

Sucrose and protein concentrations were determined using refractometry and Peterson's assays respectively. The sucrose gradient used was 0.6-1.8M.

Fraction number	Protein concentration (mg/ml)	Sucrose concentration (M)
1	0.1	1.80
2	0.26	1.71
3	0.35	1.54
4	1.77	1.37
5	1.87	1.22
6	0.69	1.14
7	0.25	0.99
8	0.45	0.91
9	0.81	0.84
10	1.52	0.77
11	6.25	0.19
12	5.1	0.07

Figure 3.8 Localisation of plasma membrane in gradient 4

The plasma membrane was localised in this final fractionation by biotinylating the cell surface antigens. Biotinylated proteins were detected using streptavidin-HRP, at a dilution of 1/4000. Unlike all the other blots so far, 1μg of protein was loaded on each lane, due to the sensitivity of the detection method. The AtT-20 cell fractions are labelled 1-12, and molecular weight markers are shown at the side.

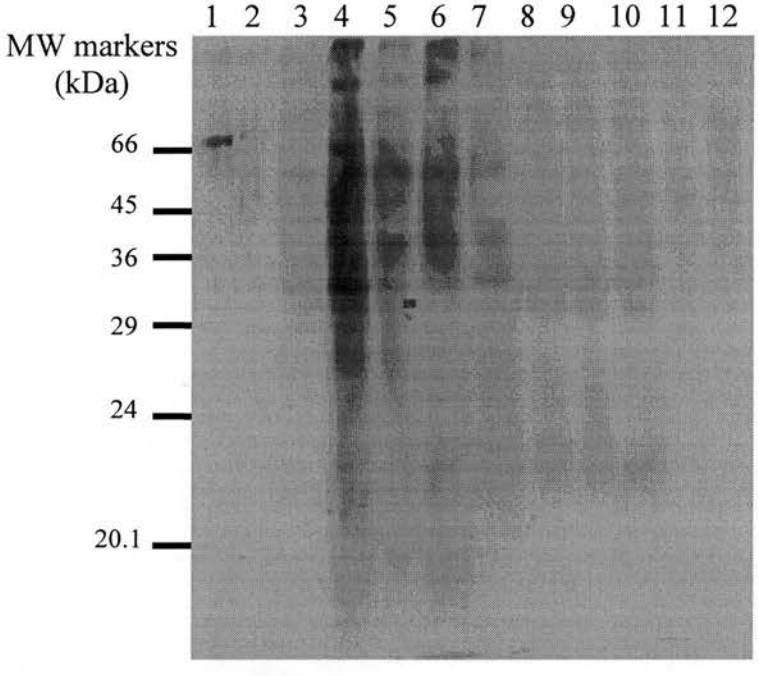

Table 3.6 Localisation of organelles in gradient 4

The following table summarises the results obtained for gradient 4 in the same manner as table 3.4 (gradient 3).

Fraction number	golgi	vesicle	ER	mitochondria
1	-	-	-	-
2	-	-	-	-
3	-	-	-	-
4	+++	+++	+++	+++
5	+++	++	+++	+++
6	++	+	++	++
7	-	-	-	-
8	-	-	-	-
9	-	-	-	-
10	++	-	-	-
11	-	-	-	-
12	-	-	-	-

Figure 3.9 Summary of protein estimations and sucrose estimations of gradients 1-4

This summarises the organelle localisation results and the sucrose/protein concentrations for gradients 1-4 (the compositions of which are shown in the table). The fractions marked are the ones with the highest concentration of organelle.

gradient	golgi	ER	vesicle	mitochondria	Plasma-membrane
1 (0.4-1.8M)			4, 5		
2 (0.4-1.8M)	4, 5, 10	3, 4	3, 4	3, 4	
3 (0.6-1.6M)	6, 10	3, 4	3, 4	3, 4	
4 (0.6-1.6M)	4, 5, 10	4, 5	4, 5	4, 5	4, 5

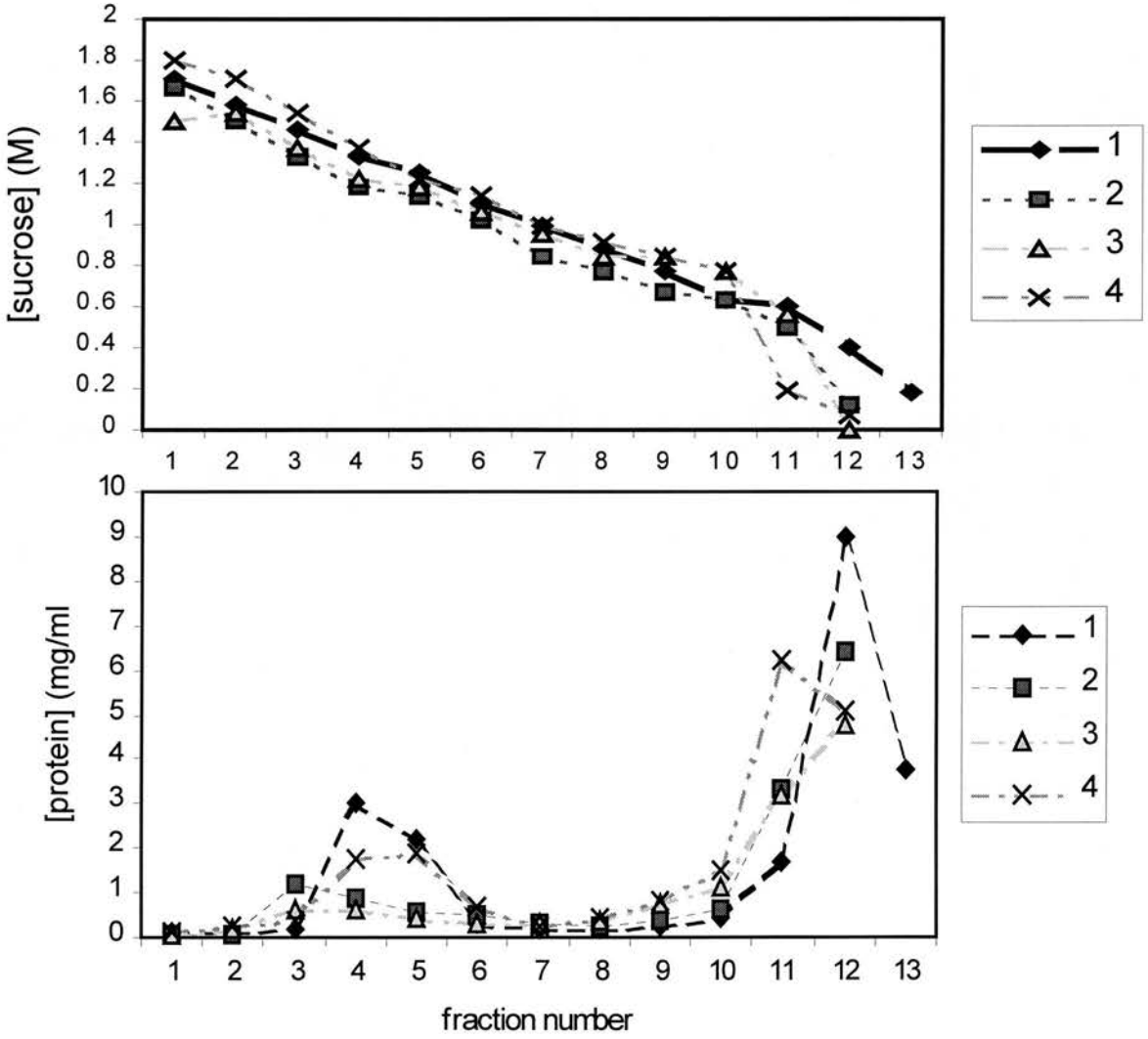

Figure 3.10 Synaptotagmin

Rabbit anti-synaptotagmin serum was raised against a recombinant fusion protein, consisting of the cytoplasmic domain of bovine synaptotagmin I linked to protein A, and was kindly donated by Leonora Ciufo (Dept. of Biochemistry, Edinburgh University). It was used at a dilution of 1/1000, and the positive control used was bovine adrenal chromaffin granule membranes (CGM). Synaptotagmin is a 65kDa integral vesicular membrane protein. C represents CGM, H is homogenate (with H/2 representing a 1:2 dilution of homogenate), and gradient fractions are shown as 1-12 (high to low sucrose concentration). The gradient used here was F1. Molecular weight markers are shown in the centre in kDa.

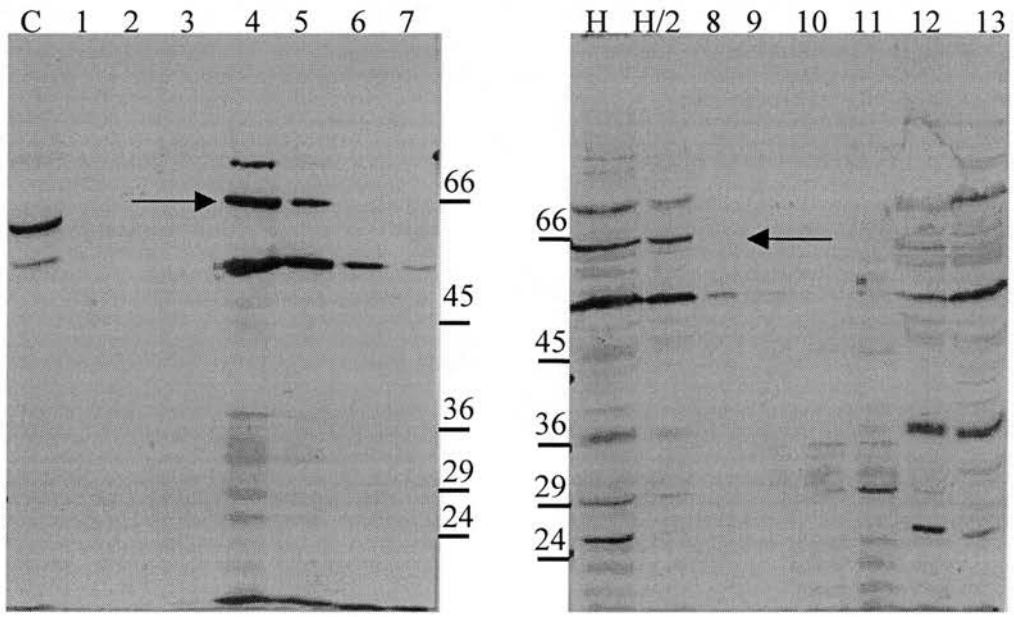

3.11 Syntaxin

The antibody used in this case was an ascites mouse monoclonal (HPC-1) available from Sigma. The immunogen used was a synaptosomal plasma-membrane fraction from adult rat hippocampus, and the monoclonal recognizes an epitope in the extracellular domain of the 36kDa membrane protein syntaxin. The antibody was used at 1/2000 and chromaffin granule membranes were also blotted (denoted by C). AtT-20 cell fractions are shown 1-13, with homogenate and 1:2 diluted homogenate shown as H and H/2 respectively. Molecular weight markers are shown in the centre in kDa, and this blot used fractions from gradient 1.

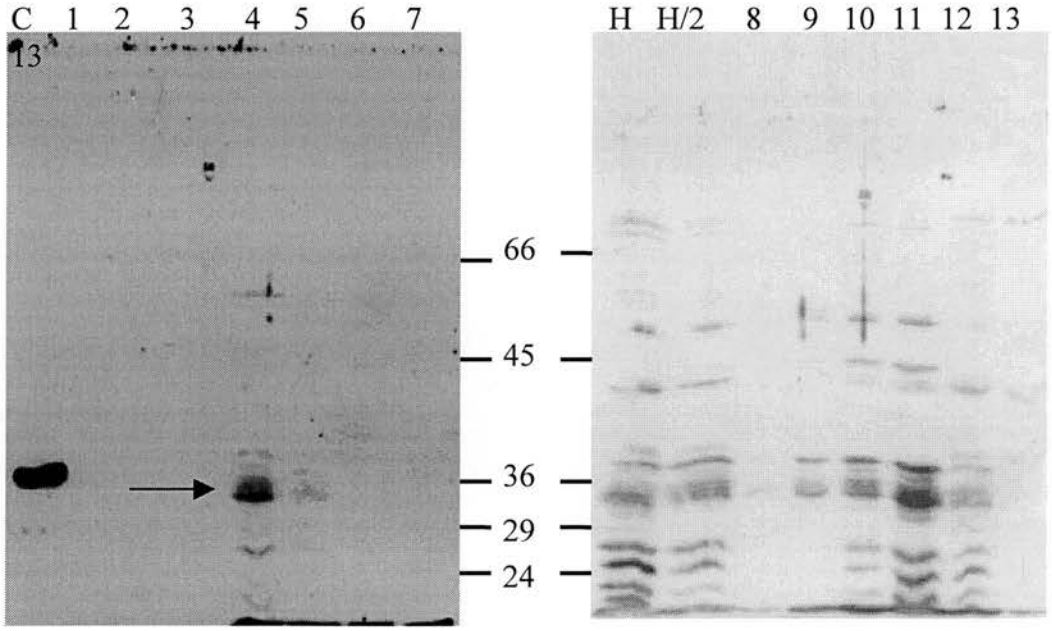

3.12 SNAP-25

The rabbit anti-SNAP-25 serum used was a gift from Prof. R. Burgoyne (University of Liverpool), and was raised against a synthetic peptide of SNAP-25. The antibody was used at a 1/1000 dilution, and chromaffin granule membranes were also run. 1-13 represent the various fractions, C the chromaffin granule membranes and H and H/2 the homogenate and homogenate diluted 1:2. Fractions from gradient 1 were used for this blot.

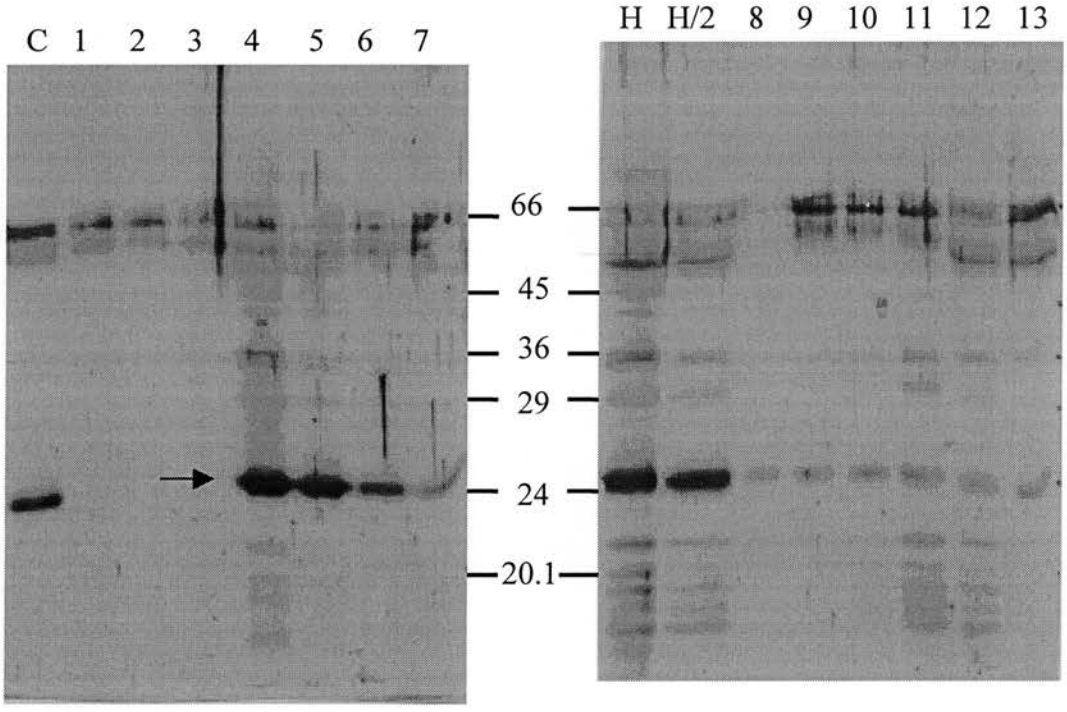

Figure 3.13 αSNAP

The rabbit anti-αSNAP serum was kindly donated by Dr. Tim Levine (ICRF, London). It was raised against the his-tagged αSNAP recombinant protein, and then affinity-purified against the same protein. αSNAP is a 35kDa cytosolic protein. The antibody was used at a dilution of 1/1000, and again gradient 1 was used. 1-13 denotes the AtT-20 cell fractions, H and H/2 are AtT-20 cell homogenates neat and diluted 1:2, and C is chromaffin granule membranes.

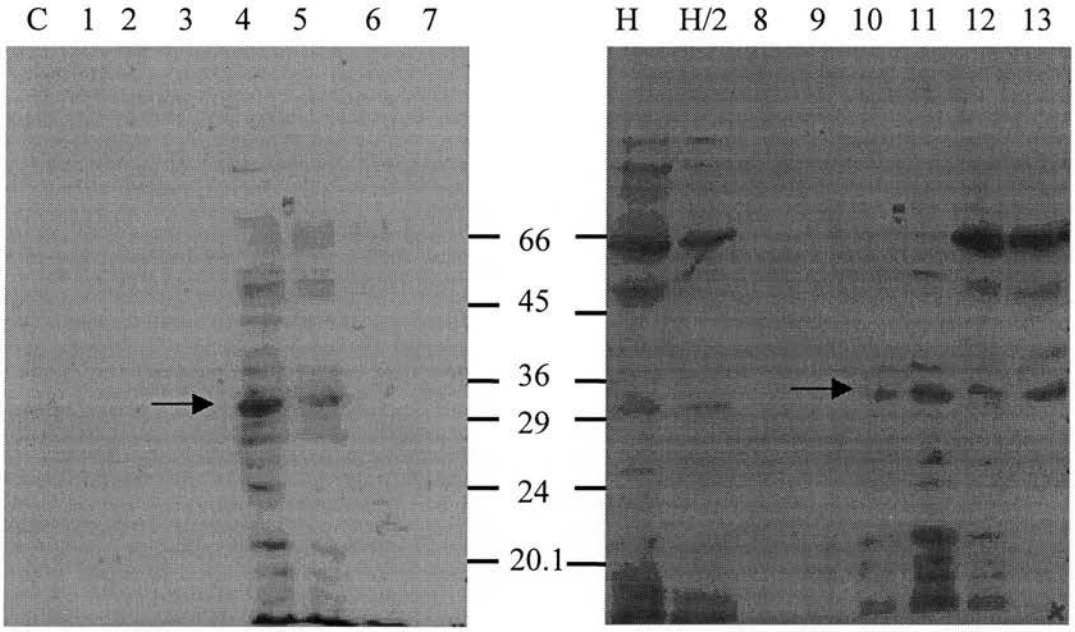

3.14 NSF

The rabbit anti-NSF serum was donated by Prof. R. Burgoyne (University of Liverpool), and was raised against his_6-tagged recombinant NSF (cloned from a chinese hamster ovary cell line). The antibody was used at a dilution of 1/1000, and again gradient 1 was used in these blots. C denotes chromaffin granule membranes, H and H2 show AtT-20 cell homogenate neat and at a dilution of 1:2, and AtT-20 cell fractions are numbered 1-13.

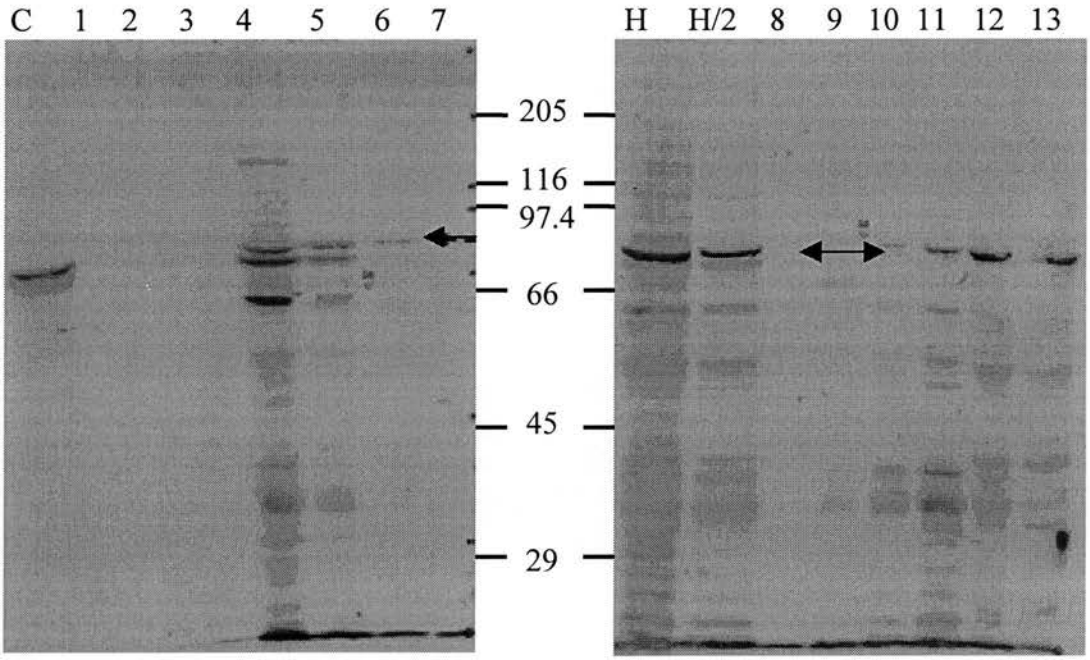

3.15 ACTH propeptides

Anti-human ACTH serum, developed in rabbit using ACTH(18-39)-KLH as the immunogen, was obtained from Sigma. This gel will not detect the mature form due to its acrylamide concentration, however it shows the various stages of processing, which are labelled below. Chromaffin granule membranes were run as a negative control (C), AtT-20 cell homogenate is shown as H (neat) and H/2 (1:2 dilution), fractions are labelled 1-13 (gradient 1 again having been used). The antiserum was used at a dilution of 1/1000.

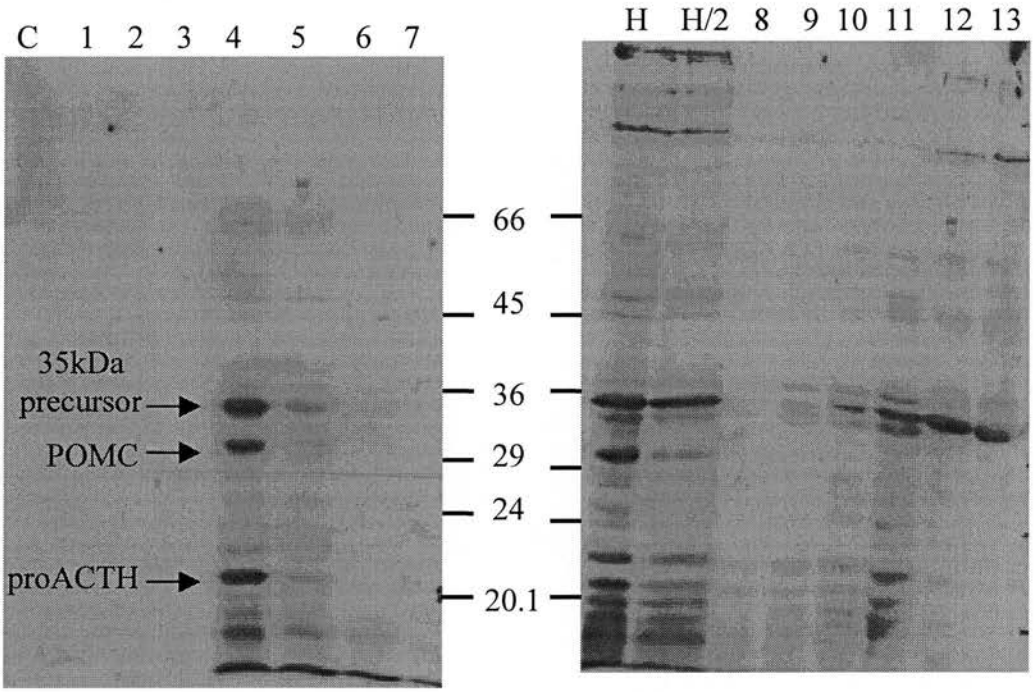

Figure 3.16 Synaptotagmin

The antiserum used here was a mouse monoclonal (hybridoma culture medium) which recognised an epitope near the C terminus of synaptotagmin. It was raised by Dr. Bulent Tugal (Department of Biochemistry, Edinburgh University) and was used as neat, sterile filtered culture medium. CGMs (C) were used as a postivive control and AtT-20 homogenate was run at a dilution of ½ (H/2). Fractions are labelled 1-12, and gradient 2 was used in this case. The positions of the molecular weight markers are shown in the centre labelled as kDa.

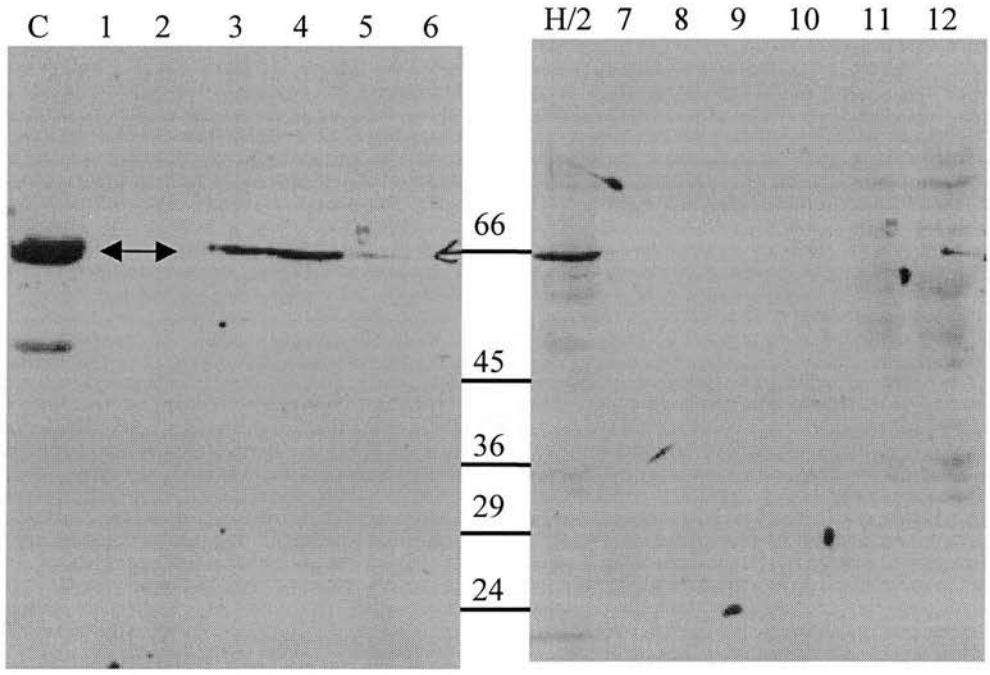

Figure 3.17 Normal Rabbit Serum

Normal rabbit serum (NRS) was obtained from Sigma, and was used at a dilution of 1/100, as a negative control. In particular it was hoped that this would show up any major proteins (present at high concentrations) which which showed non-specific reactivity. It should also help to verify that results obtained for exocytotic proteins were true and specific. Chromaffin granule membranes were run (C) and neat AtT-20 cell homogenate (H), as well as AtT-20 cell fractions 1-12 (labelled as such, from gradient 2). The positions of molecular weight markers are shown in the centre labelled as kDa.

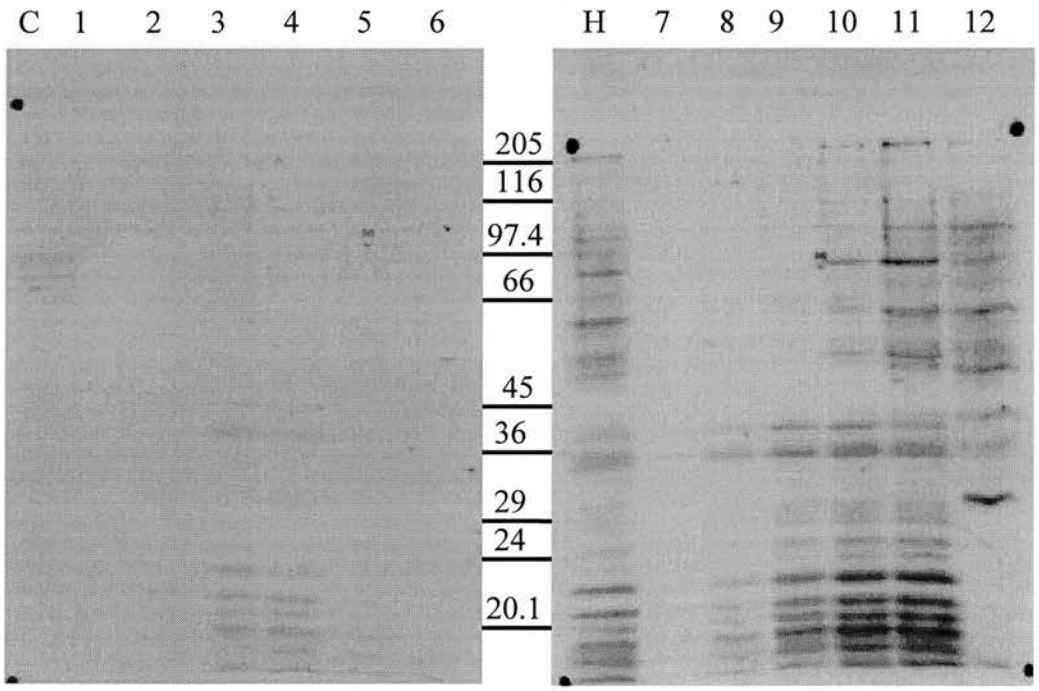

Figure 3.18 Synaptobrevin 2

This rabbit antiserum was raised against recombinant synaptobrevin 2, and was donated by Cliff Shone (Porton Down). Synaptobrevin 2 is an integral vesicular protein of 18kDa. The antiserum was used at a dilution of 1/1000 against fractions from gradient 2. Chromaffin granule membranes (C) acted as a positive control, AtT-20 cell homogenate was run neat (N), and fractions were labelled 1-12. The positions of molecular weight markers are shown in the centre labelled as kDa.

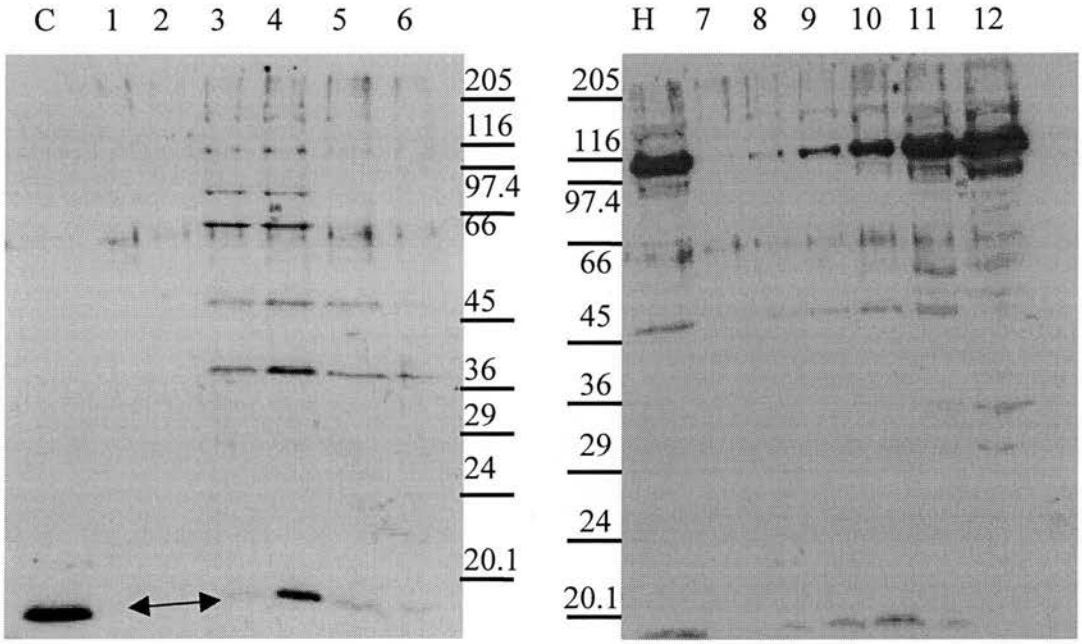

Figure 3.19 Rab3A

Rabbit antiserum was raised against recombinant human Rab3A, and was specific in that it did not cross react with Rab3B, however its cross-reactivity with Rab3C and 3D had not yet been determined. It was donated by Dr. Francois Darchen (Institute of Biology and Physiology, Paris), and was used at a dilution of 1/500. Chromaffin granule membranes (C) were also run, as well as rat brain synaptosomes (S). Fractions are from gradient 3 and are labelled 1-12. The position of molecular weight markers are shown in the centre labelled as kDa.

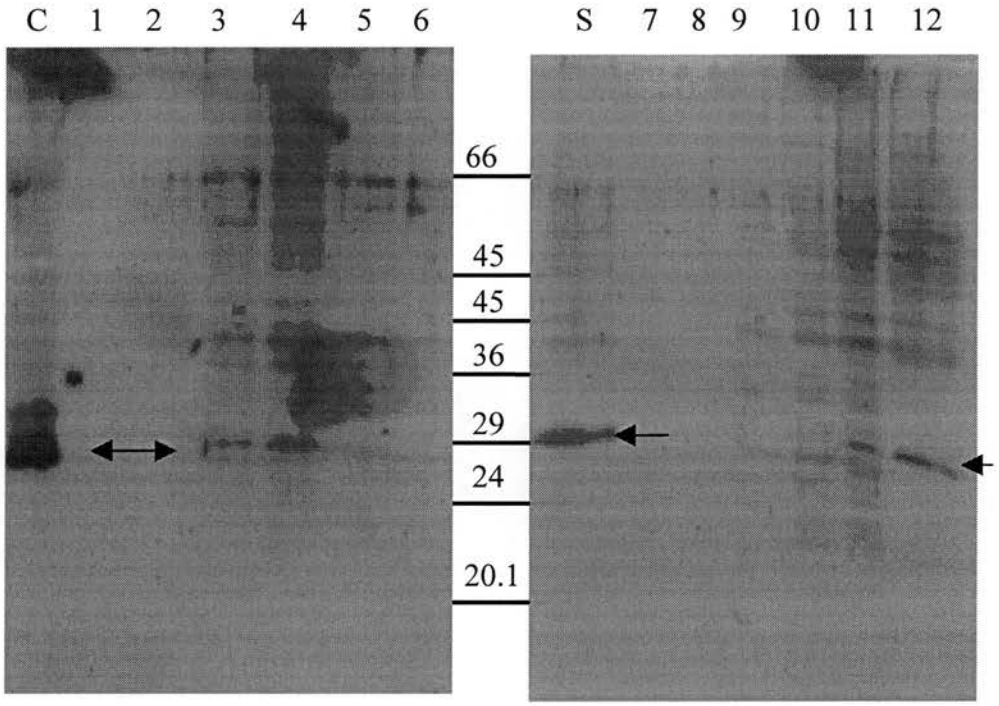

Figure 3.20 CAPS

This rabbit antiserum, raised against the CAPS protein, was donated by Dr. Thomas Martin (University of Wisconsin, Madison, USA) and was used at a dilution of 1/1000. A PC12 cell pellet was used as a positive control, and fractions were from gradient 3, and are labelled 1-12. The position of molecular weight markers are shown in the centre labelled as kDa.

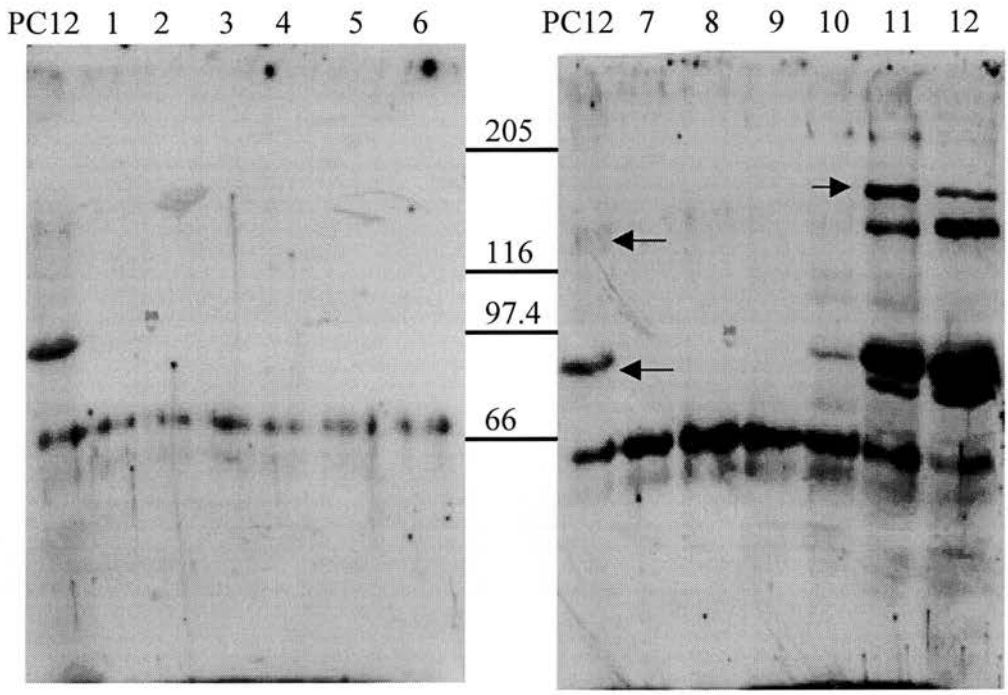

Figure 3.21 ADF

Rabbit antiserum was raised against recombinant human cytoplasmic ADF, and was donated by Dr. Sutherland MacIver (Department of Biochemistry, Edinburgh University). The antibody was used at a 1/500 dilution and a cell pellet of the human T-cell line (hsp2) was used as a positive control (L), Chromaffin granule membranes were also run (C), and the AtT-20 cell fractions used were from gradient 4 and are labelled 1-12. The position of molecular weight markers are shown in the centre labelled as kDa.

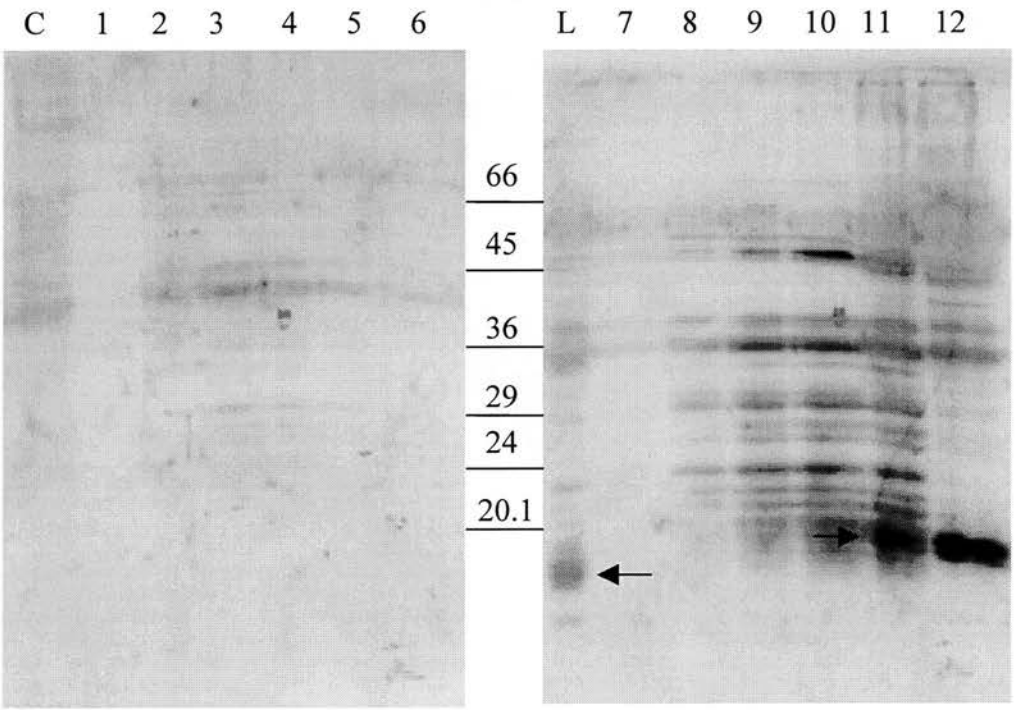

Figure 3.22 Cofilin

Rabbit antiserum was raised against human recombinant cytoplasmic cofilin, and was donated by Dr. Sutherland Maciver (Department of Biochemistry, Edinburgh University). It was used at a dilution of 1/1000, against AtT-20 cell fractions from gradient 4 (labelled 1-12). A pellet of cells from the human T-cell line (hsp2) was run as a control (L), and chromaffin granule membranes were also run (C). The position of molecular weight markers are shown in the centre labelled as kDa.

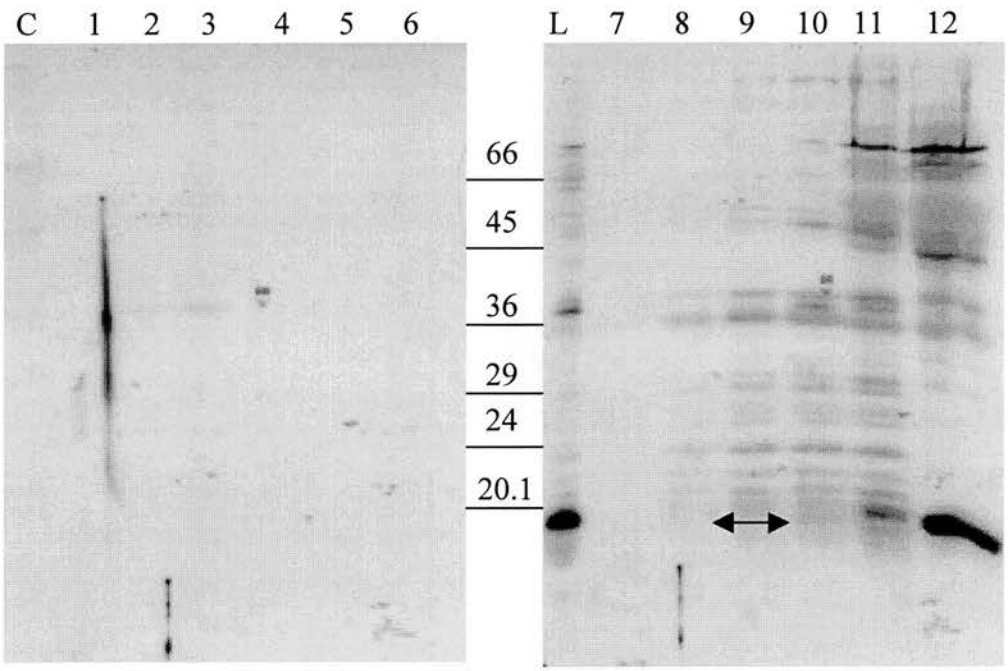

Figure 3.23 Coomassie stained gel of Triton X-114 fractions

10µl samples of the TX-114 fractionation detailed in 2.1.8 were run on an acrylamide gel. The fractions are displayed as P1, P2 and S, details of which can be found in 2.1.8.2. Molecular weights are displayed on the left hand side in kDa.

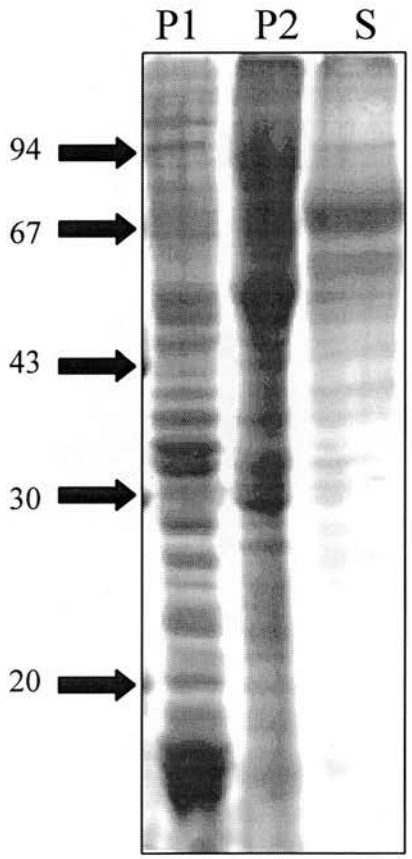

Figure 3.24 Blots of TX-114 fractions

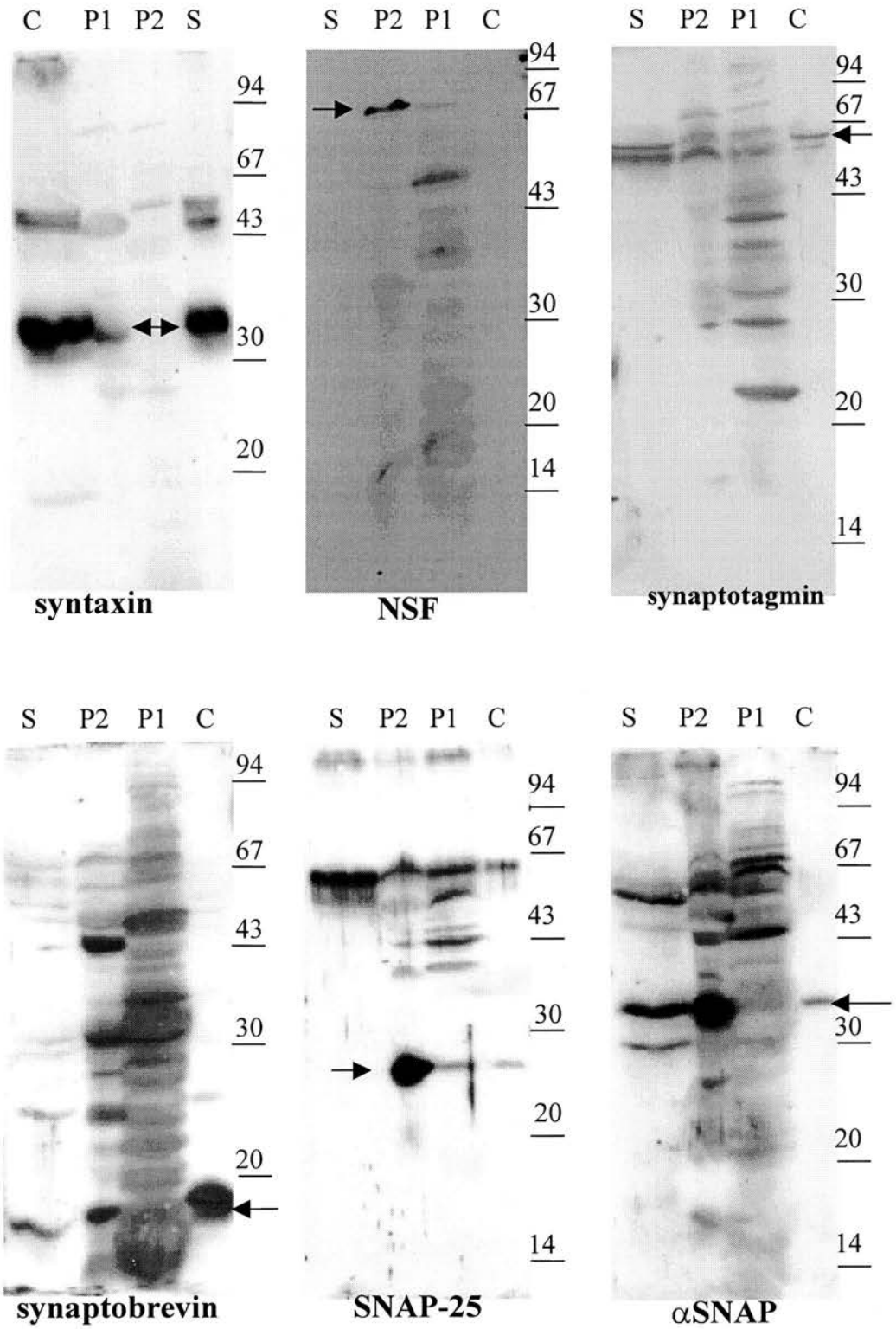

Table 3.7 Summary of fractionation results

The table below summarises the results obtained using the different methods of fractionation. The presence of the protein in a fraction is shown by +, and its absence by -. A blank space has been left when it has not been tested in a particular fraction. The fraction where the protein was most concentrated (for that particular fractionation) is marked *. If no asterisk is present, the distribution between the two or three fractions is similar.

PROTEIN	Sucrose gradient fractionation		TX-114 fractionation results		
	Membrane	Cytosolic	P1	P2	S
Synaptotagmin	+	-	-	+	+
Syntaxin	+	-	-	+	+*
Synaptobrevin	+	-	-	+	+
SNAP-25	+*	+	-	+	-
αSNAP	+	+	-	+*	+
NSF	+	+	-	+*	-
Rab3A	+	+			
CAPS	-	+			
ADF	-	+			
Cofilin	-	+			
ACTH propeptides	+*	+			

Chapter 4

Further characterisation of AtT-20 cells using indirect immunofluorescence microscopy and RT-PCR

4.1 Introduction

Chapter 3 reported the presence in AtT-20 cells of many of the proteins thought to be involved in exocytosis (*Martin, 1997)* however it was only possible to localise them to the extent of being cytosolic or membrane-bound. Indirect immunofluorescence microscopy was used as the cells could be studied *in situ*, in order that the localisation of the various proteins could be described in greater detail.

The second method of further characterising AtT-20 cells was that of RT-PCR. This was used alongside the western blotting technique, and prior to the TX-114 fractionation, to try to detect mRNA for particular proteins. Its aim was to strengthen the results obtained using western blotting, and in particular to confirm the presence of syntaxin and synaptobrevin. The blots obtained for these proteins (prior to those obtained via the TX-114 fractionation) had been poor, and further validation by this method was sought.

A further aim was to look at the structure of actin within AtT-20 cells, and to use Ba^{2+} to stimulate exocytosis in the cells, to examine any consequent changes in the cytoskeletal structure. Ba^{2+} triggers exocytosis in a number of cell types, and it has been shown that this process causes true vesicular release as shown by its sensitivity to the clostridial neurotoxins (*M^{c}Mahon et al., 1992*). It is thought that Ba^{2+} influences transmitter release at various stages, first undergoing uncontrolled influx into the cell, which may have inhibitory effects on K^+ channels. It then may exchange with intracellular Ca^{2+} in internal stores, and react with factors other that calmodulin to trigger transmitter release (*Augustine and Eckert, 1984; Verhage et al., 1995)*. These properties make Ba^{2+} a useful tool, in that it enters the cell without the need for permeabilisation and causes rapid and massive release of secretory products.

It is proposed that in many secretory cell types, a network of actin beneath the plasma membrane acts to prevent the docking of granules with fusion sites in resting cells (*Burgess & Kelly, 1987*). In chromaffin cells re-organisation of cortical actin occurs in parallel with catecholamine release (*Cheek & Burgoyne, 1987; Cheek & Burgoyne, 1986*), and similar effects have been seen in mast cells (*Koffer et al., 1990*). It is thought that such reactions may be catalysed by actin-severing proteins (*Vitale et al., 1991*), and indeed agents which stabilise or de-stabilise actin filaments

have been shown to inhibit or potentiate secretion respectively (*Holm-Nielson et al., 1989; Orci et al., 1972*). Actin organisation has also been studied in exocytosis from AtT-20 cells by *Castellino et al., 1992.* They concluded that the ACTH-containing vesicles are held *within* an actin network, which *may* have to be disconnected from the vesicles before exocytosis can occur. They found that glucocorticoids inhibited ACTH release by stabilisation of this actin network, and they postulated that this was its main inhibitory effect.

4.2 Indirect immunofluorescence with antibodies to exocytotic proteins

Many of the antibodies used to detect proteins by western blotting were also used for indirect immunofluorescence microscopy. It is important to bear in mind that immunofluorescence is used to detect fixed, native proteins within cells, whereas western blotting detects SDS-denatured proteins. This means that antibodies yielding positive results in western blotting, may not do so in immunofluorescence. The results that have been included in this chapter are those that show strong, distinct and specific staining of the cells (e.g. punctate, plasma-membrane, cortical etc.), and are obviously significant when compared to the normal rabbit serum (NRS) control. Many of the antibodies used displayed a general increase in brightness of cytosolic staining, when compared to NRS. These results have not been included as they were not considered significant. Even with NRS immunofluoresence, the intensity of the staining will vary, as different areas of the slide were viewed. It was therefore difficult to select typical areas, and to accurately compare them to the staining obtained with specific antibodies. The control used was therefore NRS, with the same exposure and development time as the specific antibody, but little emphasis has been put on variation in intensities, and more on variation of staining patterns. All antisera used in this section were the same as those used for western blotting (but were diluted 1/100), and all cells were processed as detailed in section 2.3. Any variations in this protocol is detailed in the appropriate figure legend. The results are shown in figures 4.2 to 4.9, along with the appropriate control.

4.3 Discussion

Polyclonal anti-ACTH (figure 4.2)

Strong punctate staining can be seen, showing localisation of ACTH to organelles. There is perinuclear RER staining, followed by strong Golgi staining of the propeptide hormone as it passes through the various processing stages. Towards the periphery of the cell the staining becomes less dense, and very small punctate bodies can be seen. These are very probably the ACTH-containing mature secretory vesicles, and similar ACTH staining has been shown by *Wendland & Scheller, 1994.*

Monoclonal anti-ACTH (figure 4.3)

A staining pattern very similar to that obtained with polyclonal anti-ACTH was seen here, however the background was slightly lower and the staining slightly stronger. It was therefore decided that this antibody would be used for future experiments.

Anti-αSNAP (figure 4.4)

Staining with anti-αSNAP was very punctate and strong, and unlike typical diffuse cytosolic staining. There was little RER or Golgi staining, but much peripheral staining, which greatly resembled that of ACTH, in quantity, position and size. This suggests that αSNAP is pre-docked to ACTH-containing vesicles, and confirms results obtained with subcellular fractionation and western blotting.

Anti-NSF (figure 4.5)

The staining obtained with this antiserum was weak, but unlike that obtained for αSNAP, in that no punctate staining was seen. However plasma membrane staining can be seen, in agreement with the results of subcellular fractionation and western blotting. Both of these results taken together suggest that NSF is indeed bound to membranes in non-stimulated cells, but to the plasma-membrane as opposed to secretory vesicles.

Anti-SNAP-25 (figure 4.6)

Anti-SNAP-25 antiserum displays strong plasma membrane staining, as would be expected from this membrane associated t-SNARE.

Anti-Cofilin (figure 4.7)

The staining seen with anti-cofilin was very unusual in that very strong punctate bodies were seen on the periphery of the cell. The number of these cofilin-rich bodies (CRBs) varied from cell to cell, ranging from zero to approximately 12. Aside from the difference in quantity, they also differed from the vesicles that stained for αSNAP and ACTH, in that they were larger in size.

Affinity purified anti-cofilin (figure 4.8)

The anti-cofilin antiserum was affinity-purified (section 2.3.4) in an attempt to decrease background staining. Staining similar to that obtained with unpurified antibody was seen, however the background staining was lower. The cell shown here has the highest level of staining found, the average being only 2-3 CRBs per cell.

Actin staining with phalloidin (figure 4.9)

The actin structure was analysed using the actin-stabilising drug phalloidin conjugated to rhodamine. Actin was present throughout the cytosol, in a network-like arrangement, but that the strongest staining was obtained at the plasma-membrane. Thus it appears that most filamentous actin in AtT-20 cells is at or adjacent to the plasma-membrane. This type of staining, with its lack of stress fibres, was also reported by *Castellino et al., 1992.*

4.4 Co-localisation studies using immunofluorescence

It was decided to investigate the role of actin in exocytosis, first by looking at its position in relation to the ACTH vesicles. In many regulated secretory cell types a definite cortical actin ring exists, below which the majority of the vesicles appear to lie (*see review - Morgan, 1995*). The CRBs were also investigated, because of the very unusual staining pattern, and the fact that cofilin is an actin de-polymerising protein. The double staining patterns of ACTH/actin, cofilin/actin and cofilin/ACTH were studied using a combination of FITC- and rhodamine-conjugated antibodies and phalloidin. Figures 4.10-4.12 show the results obtained.

4.5 Discussion

ACTH & actin

Figure 4.10 suggests that the ACTH-containing secretory vesicles are not located in a distinct zone below the cortical actin. Instead they show that the vesicles exist within the overall actin network, and that vesicles can be seen within actin at the very periphery of the cells. These results agree with those of *Castellino et al., 1992* who made a similar finding using electron microscopy. As mentioned before, many secretory cells show a more distinct pattern, in which the vesicles lie well below this cortical actin layer, and in this aspect AtT-20 cells appear to differ.

Cofilin & actin

Figure 4.11 shows that the CRBs very definitely co-localise with the filamentous cortical actin, suggesting that their role is connected with this actin. Further experiments will need to be done to assess whether actin is involved in exocytosis in AtT-20 cells and if so, whether cofilin is involved, possibly by triggering de-polymerisation.

Cofilin & ACTH

This experiment was to assess whether the CRBs were directly linked to the ACTH vesicles, and the results clearly demonstrated that they were not. All photographs in these co-localisation studies were taken on the same plane of focus, and in this instance the CRBs were focused upon. This is why the peripheral ACTH-containing vesicles are not well defined, and much of the staining is of the Golgi. When the ACTH-containing peripheral vesicles were focused upon, few CRBs were seen, and those that were did not co-localise with the ACTH vesicles.

4.6 RT-PCR as a method of characterisation of the proteins present in AtT-20 cells

RT-PCR was used in an attempt to obtain a more convincing demonstration of the presence of synaptobrevin and syntaxin. These proteins could not be detected in western blots using a number of different antisera, the best results having been

detailed in chapter 3. As they form a major part of the SNARE apparatus, more definite proof of their presence in AtT-20 cells was needed. Synaptobrevin was detected in AtT-20 cells by Wendland & Scheller, but it was necessary to show its existence specifically in the cell line that was being used in the present work. The alternative methods used were immunofluorescence microscopy, RT-PCR and TX-114 fractionation. Synaptobrevin and syntaxin antibodies gave no significant staining in immunofluorescence microscopy, although western blotting after TX-114 fractionation did produce positive results. However it was the last technique to be used, and the results obtained by RT-PCR are worth mentioning.

The primers used were as detailed in the appendix to chapter 2. The initial method used was to isolate AtT-20 cell mRNA using a Qiagen kit (section 2.9.1). RT-PCR was then attempted using the specific primers only, to try and amplify the specific cDNAs encoding synaptotagmin, synaptobrevin and syntaxin. Synaptotagmin was used as a control as the primers had already been used for cloning purposes, and synaptotagmin had been detected by western blotting. This technique met with little success as no bands could be seen when the products were run on agarose gels. With all RT-PCR one of the major problems is the degredation of the RNA by contaminating RNase. Although precautions were taken, the amounts of mRNA obtained were so small that they could not be detected on a gel or by spectrophotometry. It was therefore decided to use a total RNA preparation a different approach would be taken, in that a total RNA prep would be used. Messenger RNA constitutes 1-5% of the total RNA in a cell, thus total RNA levels should be high enough to detect.

The total RNA preparation was done as detailed in section 2.9.2 and the A_{260}/A_{280} ratio was 2.1. mRNA can display secondary structures which may interfere with specific primer binding, and this can be a reason for failure of RT-PCR. It was decided to do the RT-PCR in two stages: the first stage involved the use of random primers to obtain double stranded cDNA of all the cellular mRNAs. The specific primers were then used in the second stage, to amplify the synaptotagmin, synaptobrevin or syntaxin cDNAs (section 2.9.3). The result of the synaptotagmin RT-PCR is shown in figure 4.13, whilst figure 4.14 shows the results obtained using the synaptobrevin and syntaxin primers.

Synaptotagmin gave a strong positive result, which was not seen in the negative controls. No positive result was obtained with the synaptobrevin primers as the bands that can be seen were also obtained with the 5' primer alone, and must therefore be due to a non-specific reaction. 2µl of cDNA from reaction 1 was used in 100µl the second-stage PCR, so it is possible that random primers present has interfered and caused non-specific amplification of some cDNA.

However a band of the correct size (864bp) was seen in the correct lane for syntaxin, but not in the negative control lanes, showing that it is specific. As it was a fairly faint band, a further PCR reaction was performed with the same primers. The product was run on an agarose gel, to check that the same band was being obtained (figure 4.15), and then 100µl of the product was run on an agorose gel with larger lanes (figure 4.15). The band was subsequently excised using a Qiagen gel extraction kit, and the product was sent to be sequenced by Oswel. The sequence obtained is given in figure 4.16, and discussed in 4.7.

4.7 Discussion

The synaptotagmin primers gave a strong band of the expected size (1kb), presumed to be the synaptotagmin cDNA. However the synaptobrevin primers gave a non-specific result, which was obtained with the 5' primer only. The syntaxin primers gave a band of the expected size, which was not seen in any of the negative controls. However when this band was sequenced, the result was not syntaxin as expected. The homology of the sequence with that of syntaxin, and the percentage match was very low, showing that the cDNA obtained was not syntaxin, and that it was not even related. The failure of this technique to show the presence of the mRNA of syntaxin or synaptobrevin could be due to many reasons. The primers were not designed using the mouse gene as this was not available from the database (see Appendix). They were designed against conserved regions at the ends of the gene, but it is possible that some difference existed which prevented efficient primer binding, and subsequent amplification. Other possibilities are that the mRNA displayed a secondary structure which interfered with even the random primer binding, or that RNase had destroyed these particular mRNAs.

4.8 Ba^{2+} stimulation studies

On stimulation of many types of secretory cell a change in the distribution of filamentous actin can be seen. *Cheek & Burgoyne, 1986* showed disassembly of the cortical actin 15s after stimulation with nicotine, and re-assembly at 30s, all of which was independent of external Ca^{2+}. *Roth & Burgoyne, 1995* used the drug cytochalasin, which prevents the assembly of actin filaments. They reported that it had no effect on the cortical actin in resting chromaffin cells, but that acted to hinder the re-assembly of filamentous actin, after cellular stimulation with 14-3-3 proteins and PMA. Actin disassembly and re-assembly can be rapid and transient, and in this study cytochalasin was used to arrest re-assembly, thus 'freezing' the disassembled actin structure.

In the present work the distribution of ACTH, actin and cofilin in AtT-20 cells has been studied at various stages, following stimulation with Ba^{2+}. The time points shown are 15s, 1min and 5min; however 5s, 30s, 2min, 5min and up to 1 hour were also used, but gave the same results, and the data has not been included. The cells were grown in 6-well plates on coverslips and then stimulated with Ba^{2+} as detailed in 2.5.1.1. Following addition of the Ba^{2+}, the cells were stopped by immediately fixing with formaldehyde at the various time points. The cells were then processed for immunofluorescence microscopy as detailed in 2.3. This was done for the results shown in figures 4.17 & 4.18. Cytochalasin D was also used in an effort to ensure that any transient change in actin re-organisation was not missed. In these experiments (figure 4.19) 2.5μM cytochalasin D was included in the Ba^{2+} stimulation buffer, and the cells then processed as before. Figures 4.17-4.19 show the results obtained. All experiments and time points used controls of Locke's buffer without the addition of Ba^{2+}.

4.9 Discussion

No significant changes in the distribution of actin, ACTH or cofilin were seen at any of the time points studied. Double labelling was used to enable detection in the relative localisation of particular proteins, but none were noticed. These results

suggest that in AtT-20 cells stimulation of exocytosis (at least by Ba^{2+}) does not cause any large-scale change in the distribution of actin; nor does it cause a change in CRBs, or indeed in vesicle distribution. This latter result suggests that AtT-20 cells release a relatively small percentage of their granules during a single stimulatory event, so these small changes cannot be detected by immunofluorescence microscopy at this level. An alternative explanation may be that the process of vesicle release is a relatively dynamic one, and released vesicles are constantly being replace by new mature vesicles. This in turn would mean that the docked αSNAP/NSF would recycle between the membranes of newly released vesicles and the population replacing them. This matter has been investigated and discussed further in Chapter 5, where radioimmunoassay was used to measure the total ACTH content in AtT-20 cells, compared with levels released during Ba^{2+} stimulations.

The fact that no changes in actin or cofilin occur during stimulation of the cells does seem to point towards their having no major regulatory role in exocytosis from AtT-20 cells. Although such a transient event is inherently hard to detect, the inclusion of cytochalasin D makes it less likely that it was overlooked. Furthermore, differences in actin localisation, in relation to secretory vesicles, do not appear to appear to be as distinct as in other cells. As with all negative results it is difficult to reach an absolute conclusion, and this subject is further investigated in Chapter 5, in which the time course of Ba^{2+}-stimulation is further studied. Phalloidin and cytochalasin were also introduced into permeabilised AtT-20 cells, in order to assess whether these agents inhibited or potentiated secretion.

4.10 Conclusions

Immunofluorescence microscopy showed the presence of SNAP-25, cofilin, NSF, αSNAP, ACTH (propeptides and mature forms) and showed the structure of filamentous actin within the cell. It suggested that SNAP-25 and NSF were localised on the plasma membrane, and αSNAP and ACTH on secretory vesicles. Cofilin directly co-localised to cortical actin, but not to the ACTH-containing vesicles. These vesicles were localised within the actin network, as opposed to being in an area below the actin and distinct from it. Ba^{2+} stimulation studies did not reveal any

rearrangements of cortical actin on stimulation of the AtT-20 cells, nor were any changes in redistribution of secretory vesicles or cofilin detected using this technique. Cytochalasin D had no effect on this process, or indeed on the cortical actin structure itself. These results are further validated in chapter 5, where radioimmunoassay data will be shown corresponding to the Ba^{2+} stimulation study, to prove that exocytosis was occurring in the cells studied by immunofluorescence microscopy.

RT-PCR detected bands of the expected size, for synaptotagmin and syntaxin mRNAs, but not for synaptobrevin, however the sequence of the latter showed it not to be syntaxin. Although the synaptotagmin result may be a true positive, this product would also have to be sequenced in order to confirm this.

The results obtained in the present chapter are in accord with those obtained in chapter 3 which showed αSNAP and NSF to be membrane bound. They extend them by suggesting that αSNAP is bound to secretory vesicles, and NSF to the plasma membrane. They also suggest that the actin/vesicle structure differs from that seen in many secretory cells, in that there appears to be a network as opposed to a definite barrier. Stimulation studies failed to show any involvement of actin or cofilin in exocytosis, and showed little changes in the detectable vesicle distribution.

The next chapter uses radioimmunoassay of ACTH and a permeabilised cell system to look at the mechanisms of exocytosis in more detail.

Figure 4.1 AtT-20 cells

This is a high-powered phase contrast micrograph of AtT-20 cells, which have been plated on coverslips, fixed and processed as they would be for immunofluorescence microscopy. Calibration bar = 12.5μm. Photographs were taken on slightly different planes of focus in order that the overall cell structure can be seen (a), and the nuclear structure can be seen (b).

(a)

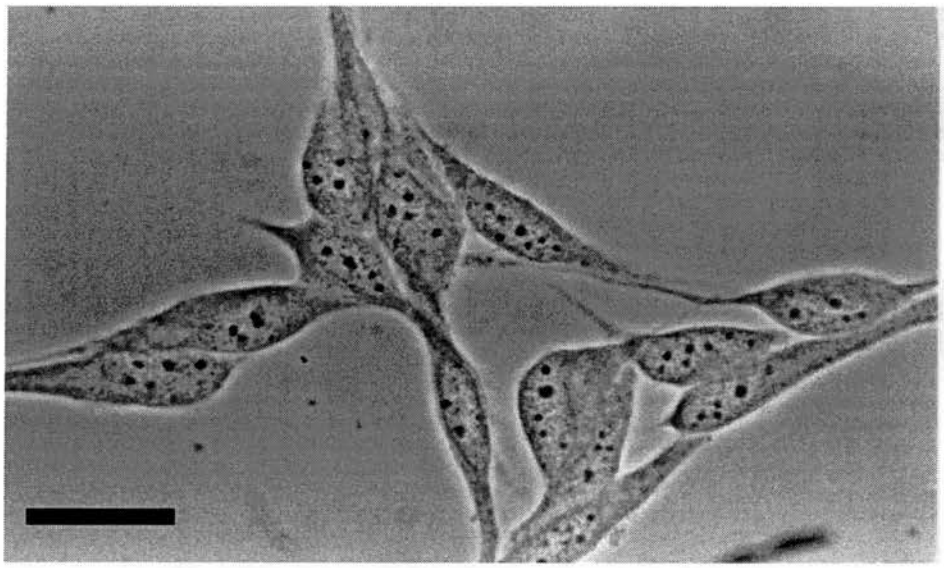

(b)

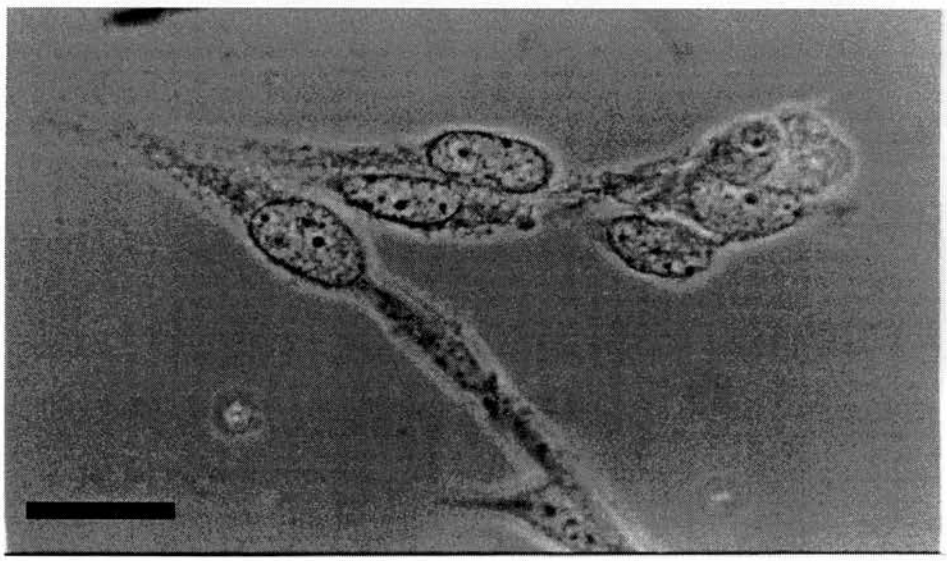

4.2 Immunofluorescence microscopy using polyclonal anti-ACTH

The antibody used here was rabbit polyclonal anti-ACTH antiserum, as detailed in figure 3.15, at a dilution of 1/100. (a) shows anti-ACTH staining, whilst (b) shows the NRS control at the same dilution, using the same exposure/development times respectively. The secondary antibody used was anti-rabbit conjugated to rhodamine, at a dilution of 1/100. Calibration bar = 12.5μM.

(a)

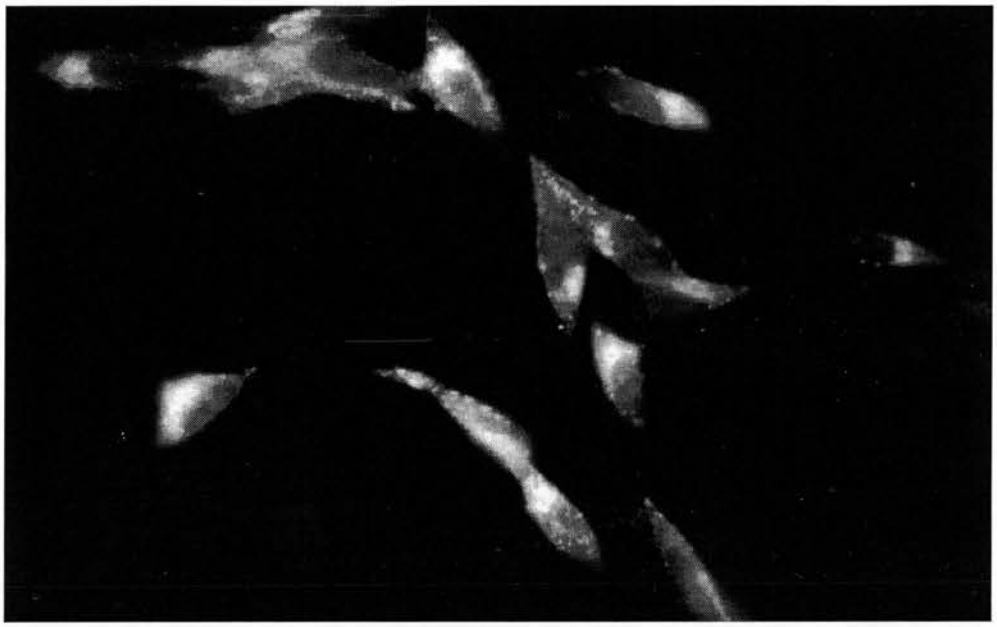

(b)

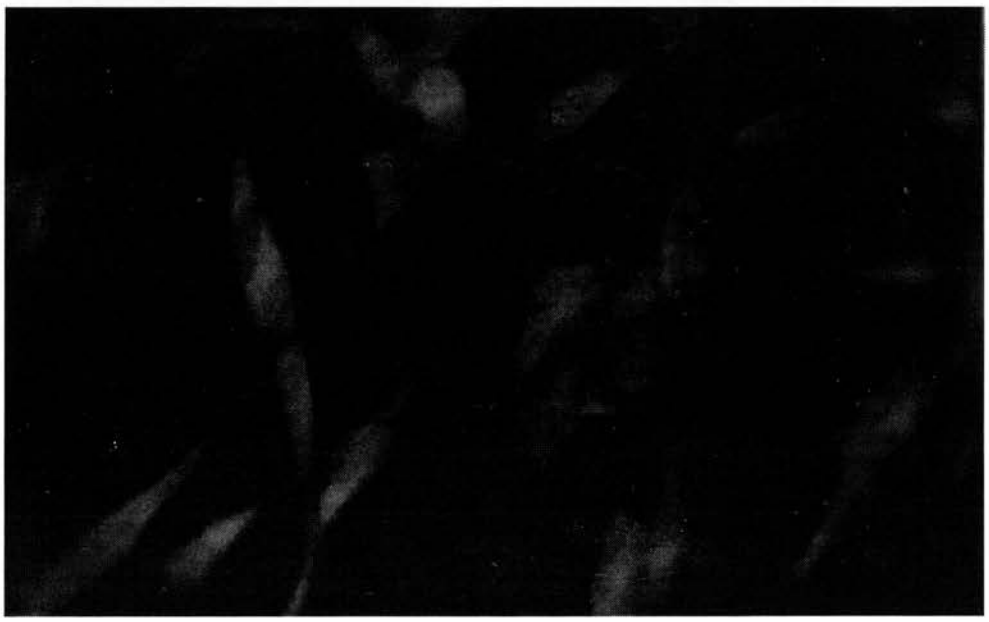

4.3 Immnuofluorescence microscopy using monoclonal anti-ACTH

The monoclonal antibody obtained here was from a hybridoma cell line, and the culture supernatant was used neat. The secondary antibody used here was therefore anti-mouse conjugated to rhodamine, at a dilution of 1/100. Calibration bar = 12.5μM.

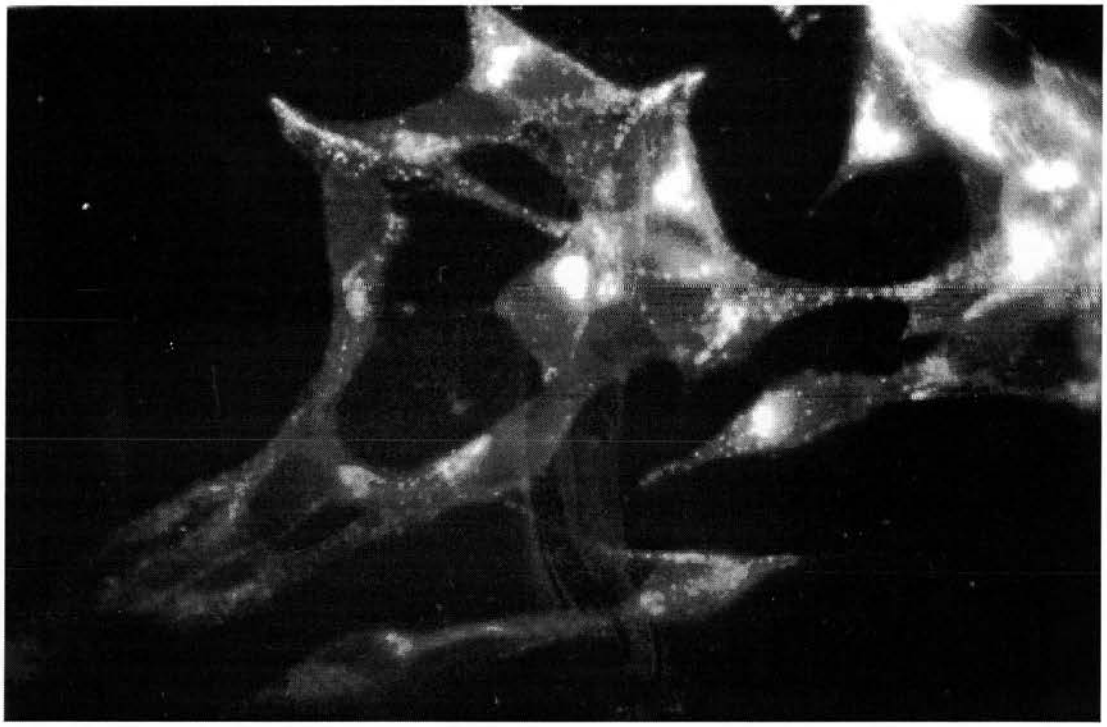

4.4 Immnuofluorescence microscopy using anti- αSNAP antiserum

The antibody used was as described in figure 3.13, and was used at a dilution of 1/50. As it was an affinity-purified antibody no NRS control has been shown. (a) shows anti-αSNAP staining, whilst (b) shows a control of secondary antibody only. The secondary antibody used was anti-rabbit conjugated to rhodamine, at a dilution of 1/100. Calibration = 12.5μM.

(a)

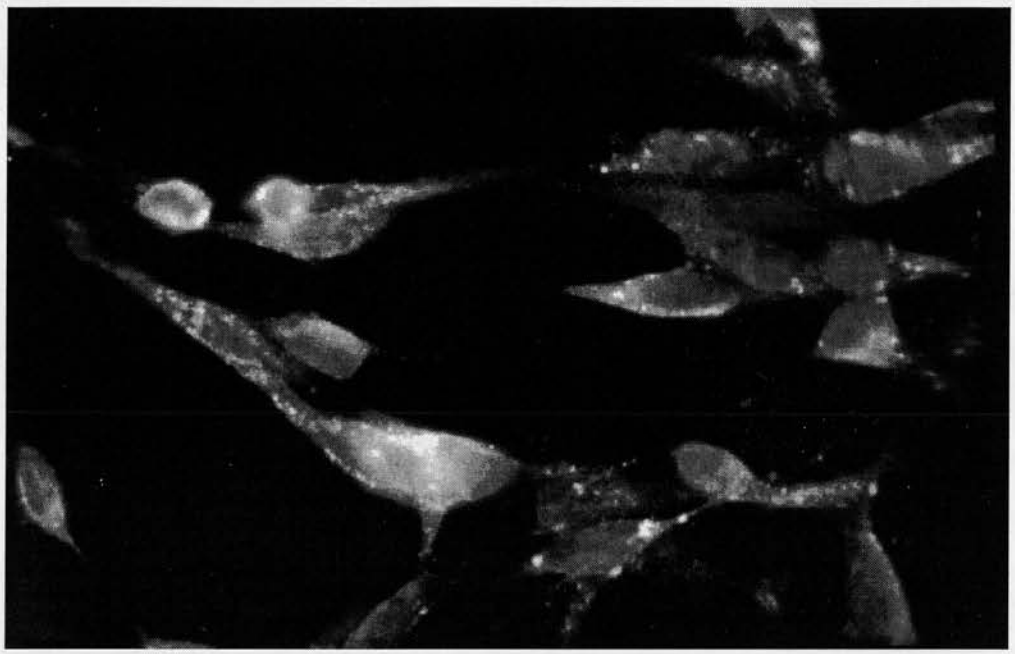

(b)

4.5 Immnuofluorescence microscopy using anti-NSF antiserum

The antiserum used was as described in figure 3.14, and was used at a dilution of 1/100. A control of NRS has been shown, using the same dilutions, exposure and development times. (a) shows anti-NSF staining, whilst (b) shows the control of NRS. The secondary antibody used was anti-rabbit conjugated to rhodamine, at a dilution of 1/100. Calibration bar = 12.5μM.

(a)

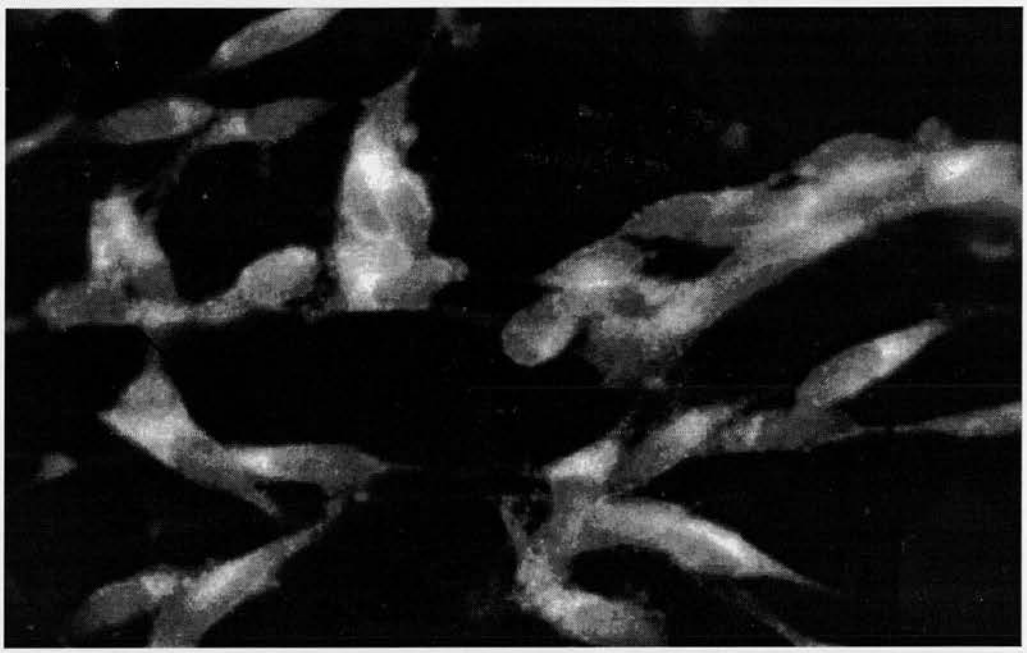

(b)

4. 6 Immunofluorescence microscopy using anti-SNAP-25 antiserum

The antiserum used was as described in figure 3.12, and was used at a dilution of 1/100. A control of NRS is shown, using the same dilutions, exposure and development times. (a) shows anti-SNAP-25 staining, whilst (b) shows the control of NRS. The secondary antibody used was anti-rabbit conjugated to rhodamine, at a dilution of 1/100. Calibration bar = 12.5μM.

(a)

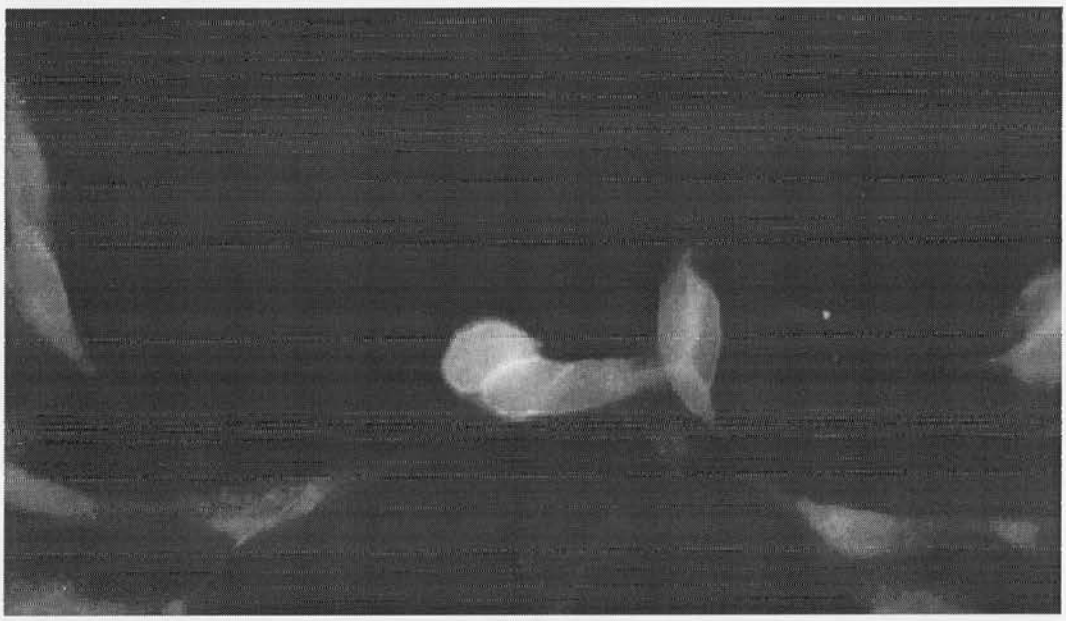

(b)

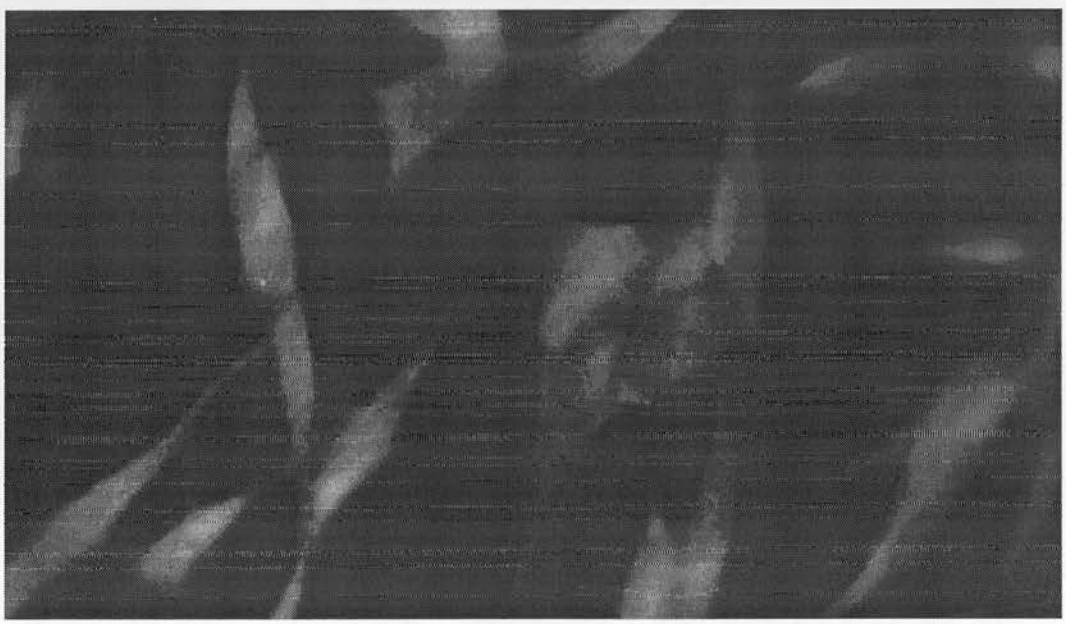

4.7 Immunofluorescence microscopy using anti-cofilin antiserum

The antiserum used was as described in figure 3.22, and was used at a dilution of 1/100. A control of NRS has been shown, using the same dilutions, exposure and development times. (a) shows anti-cofilin staining, whilst (b) shows the control of NRS. The secondary antibody used was anti-rabbit conjugated to rhodamine, at a dilution of 1/100. Calibration bar = 12.5μM.

(a)

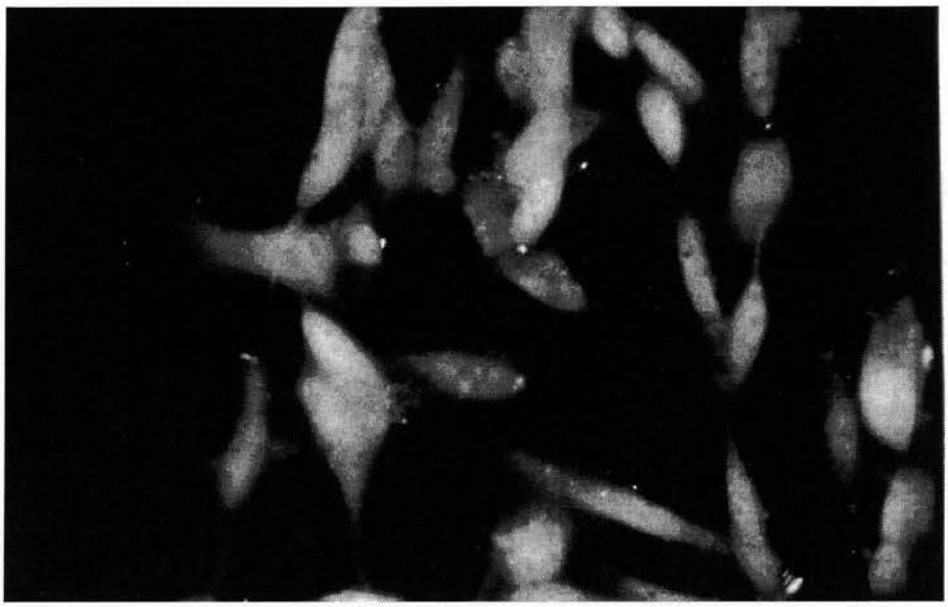

(b)

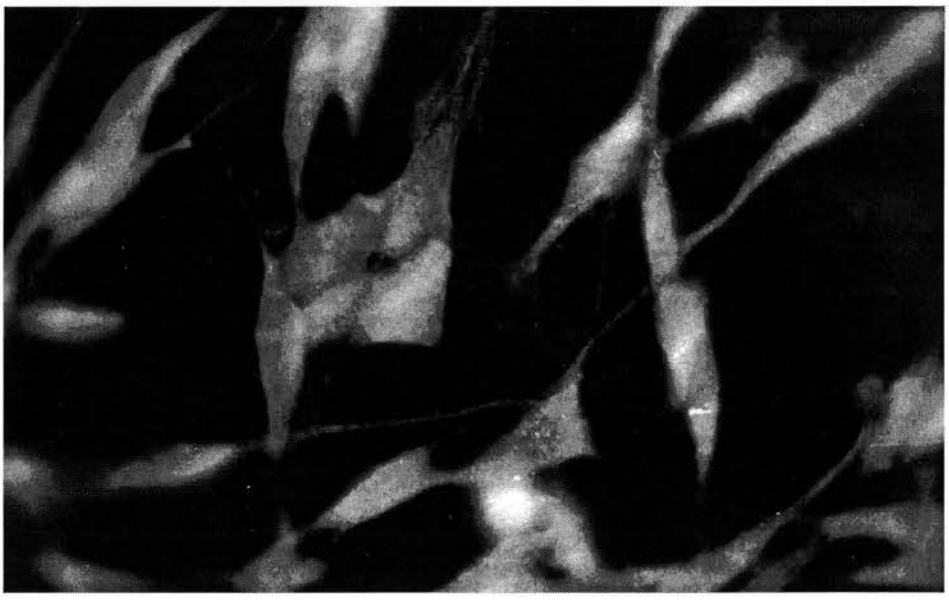

4.8 Immunofluorescence microscopy using affinity purified anti-cofilin

The cofilin antibody used in figure 4.7 was affinity-purified as detailed in 2.3.4. It was used at a dilution of 1/50, and the secondary antibody used was anti-rabbit conjugated to rhodamine, at a 1/100 dilution.

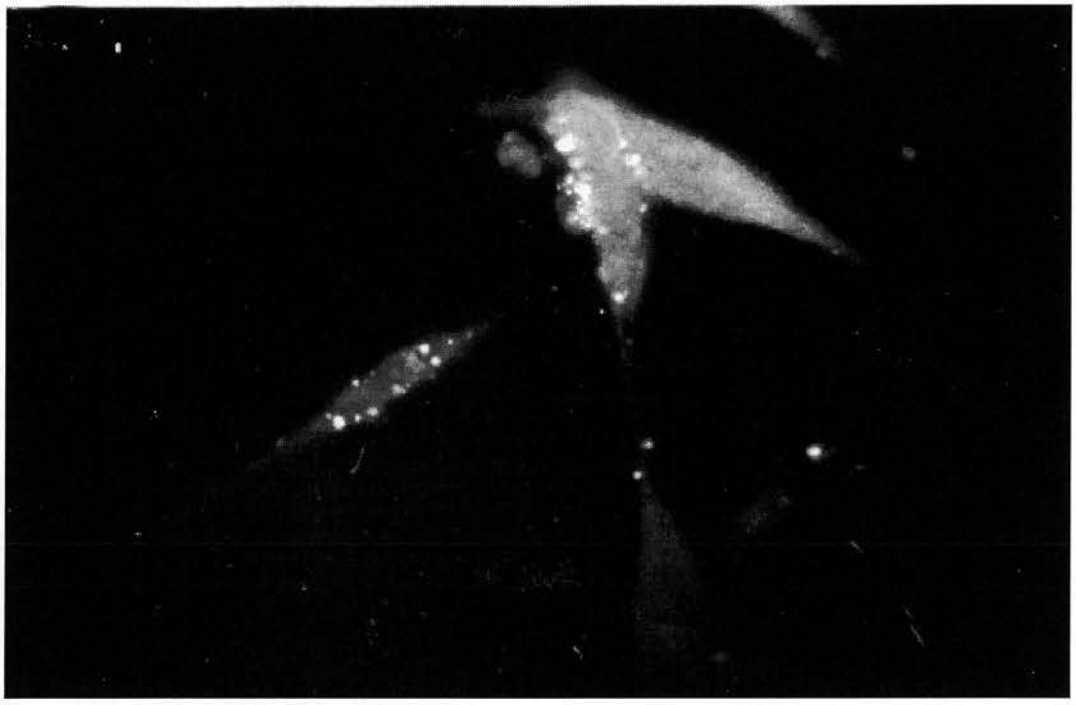

4.9 Actin staining with phalloidin

These cells were directly stained with the actin-stabilising drug phalloidin, conjugated to rhodamine. It was used at a concentration of 2μg/ml.

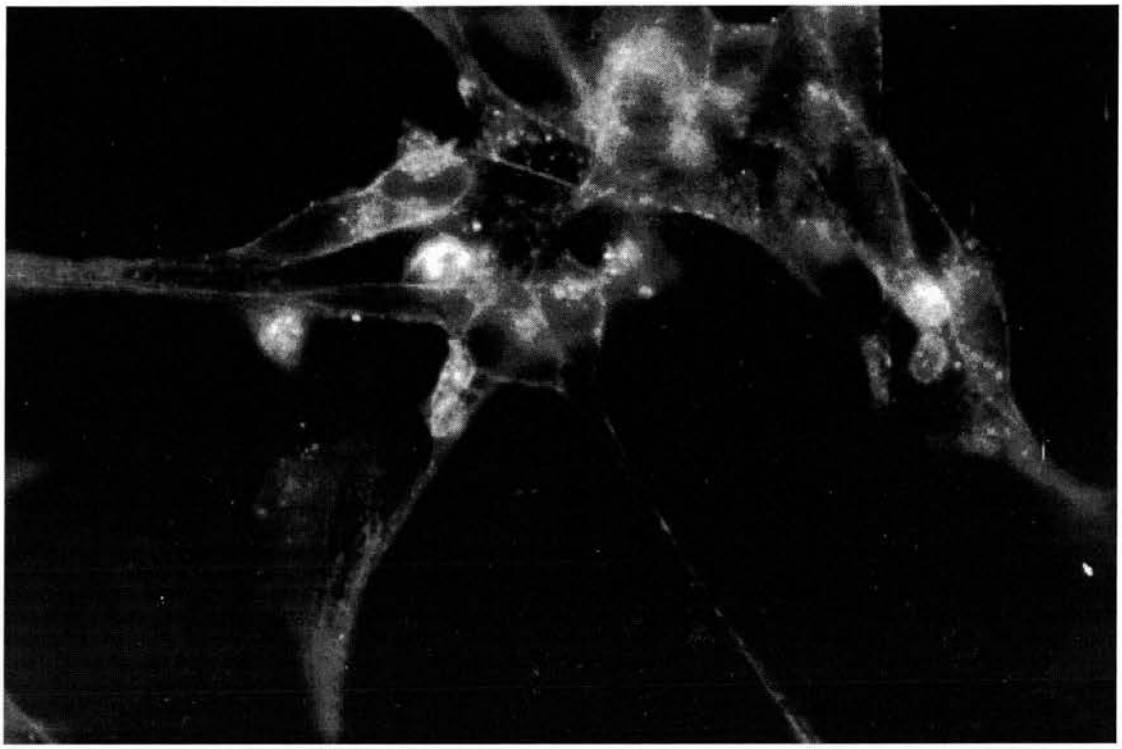

4.10 Colocalisation of ACTH and actin using immunofluorescence microscopy

Cells were labelled as detailed in figures 4.3 and 4.9, except that the actin was labelled with phalloidin conjugated to FITC. Two different areas are shown: (a)/(b) and (c)/(d). (a) and (c) are stained for ACTH, (b) and (d) are stained for actin. Calibration bars = 12.5μM.

(a)

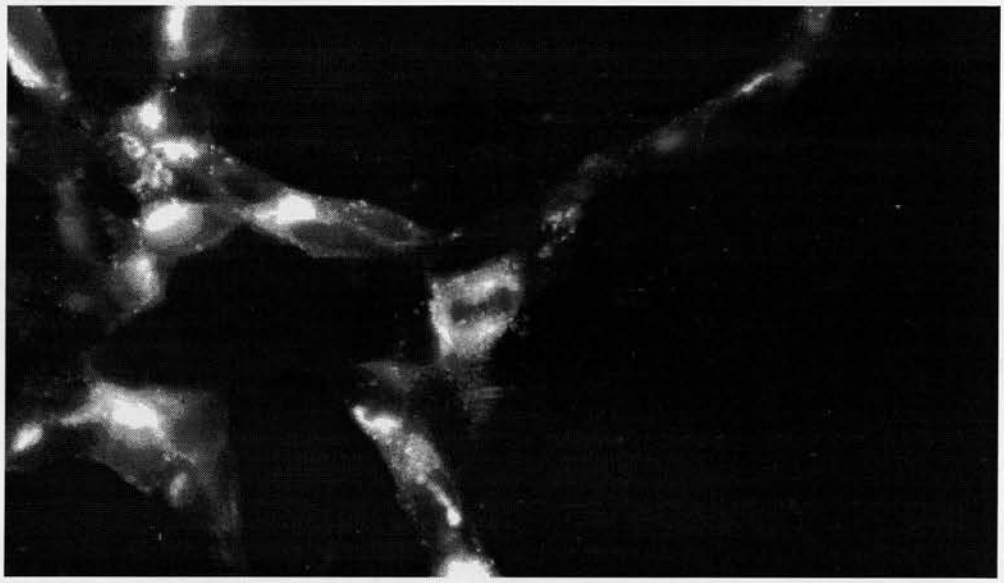

(b)

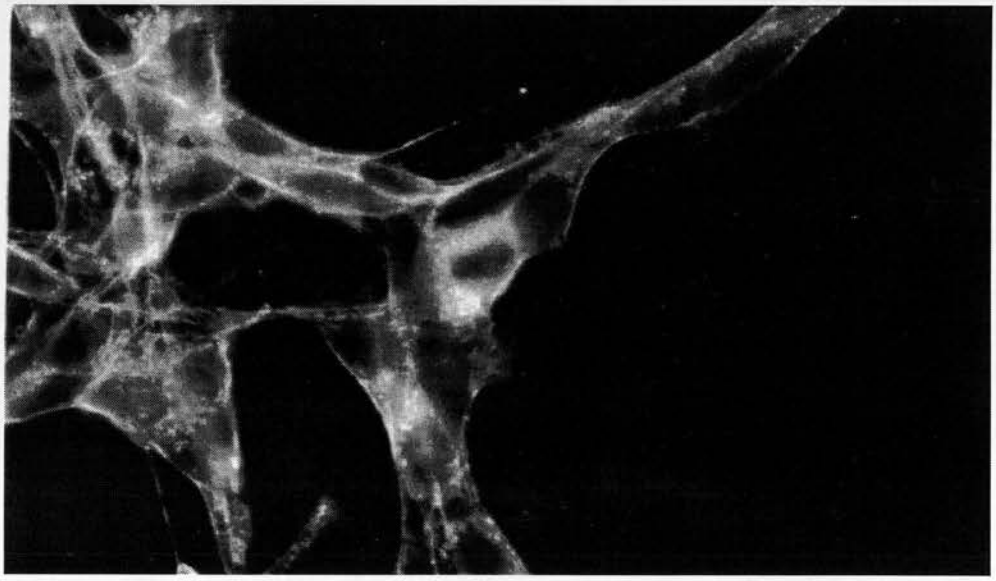

(c)

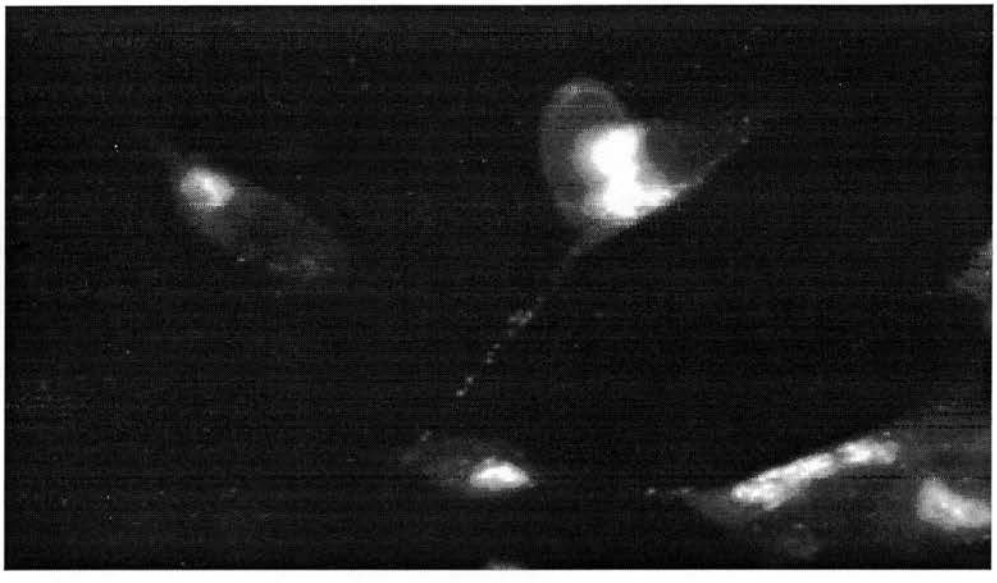

(d)

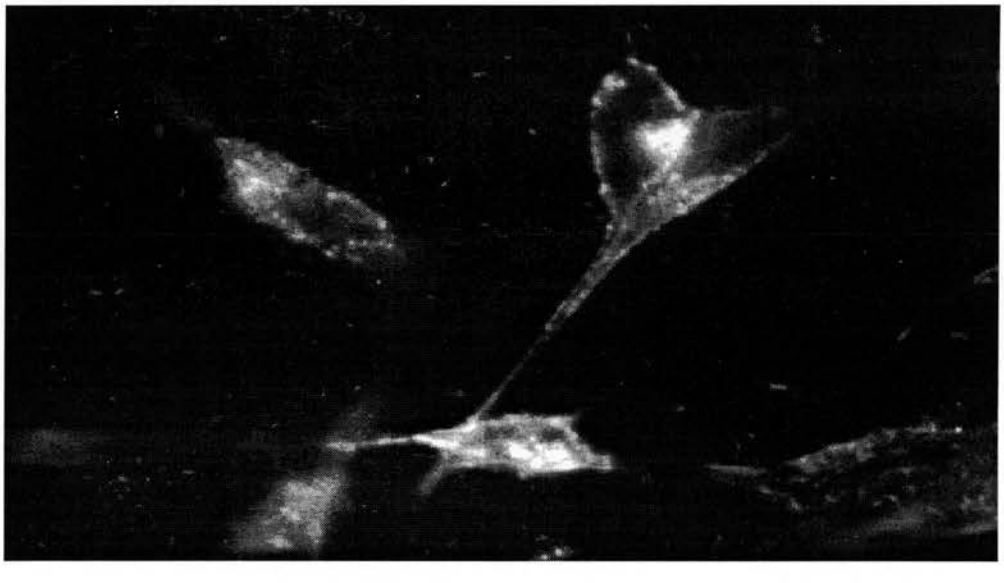

4.11 Colocalisation of cofilin and actin using immunofluorescence micrsocopy

Cells were labelled as detailed in figures 4.8 and 4.9, except that the phalloidin used to label the actin was conjugated to FITC. Two different areas are shown: (a)/(b) and (c)/(d). (a) and (c) are stained for cofilin, (b) and (d) are stained for actin. Calibration bars = 12.5μM.

(a)

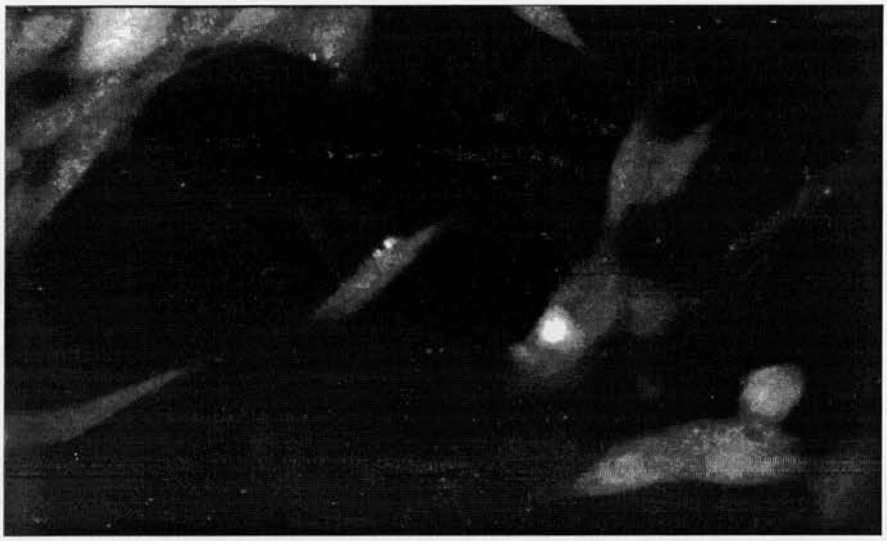

(b)

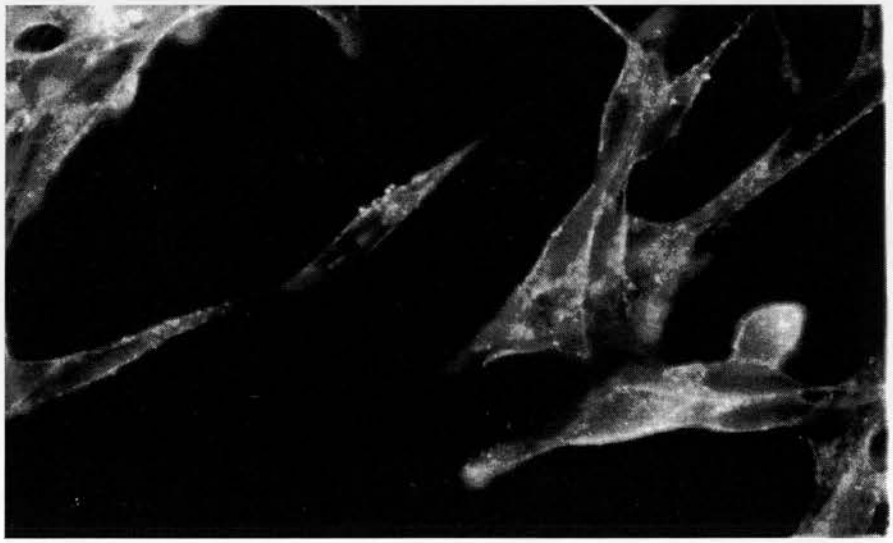

(c)

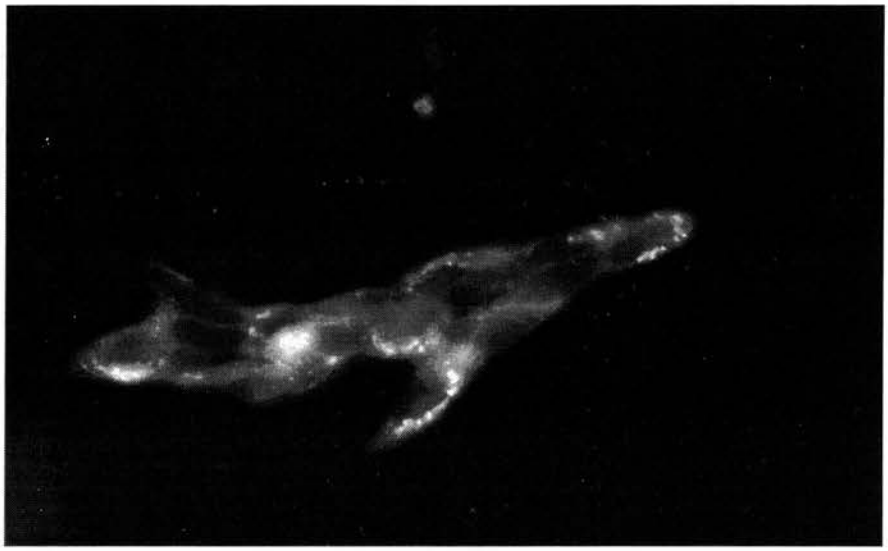

(d)

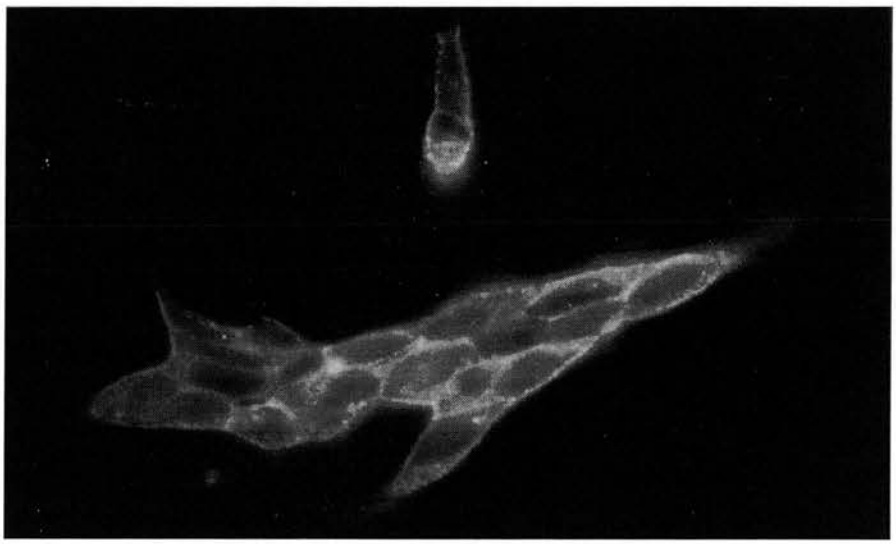

4.12 Colocalisation of ACTH and cofilin using immunofluorescence microscopy

Cells were labelled as detailed in figures 4.8 and 4.3, except that the anti-rabbit antisera used to detect cofilin, was conjugated to FITC. Two different areas are shown: (a)/(b) and (c)/(d). (a) and (c) are stained for cofilin, (b) and (d) are stained for ACTH. Calibration bars = 12.5μM.

(a)

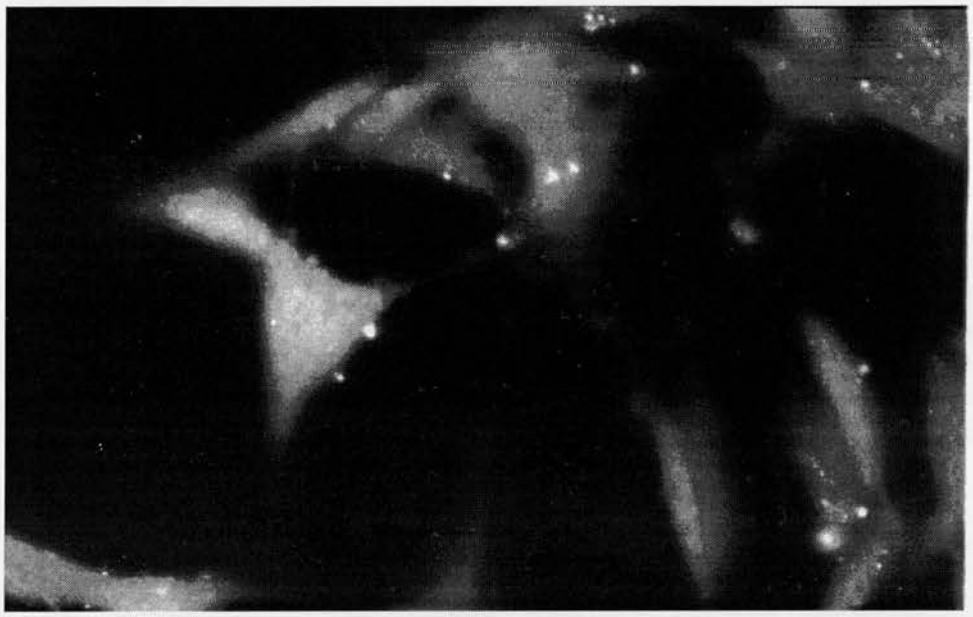

(b)

(c)

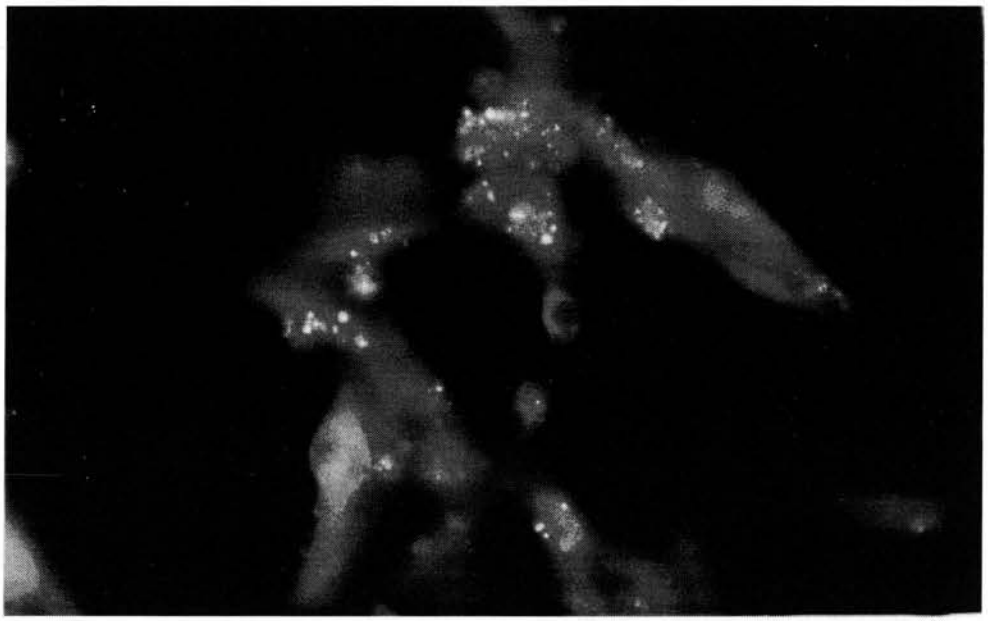

(d)

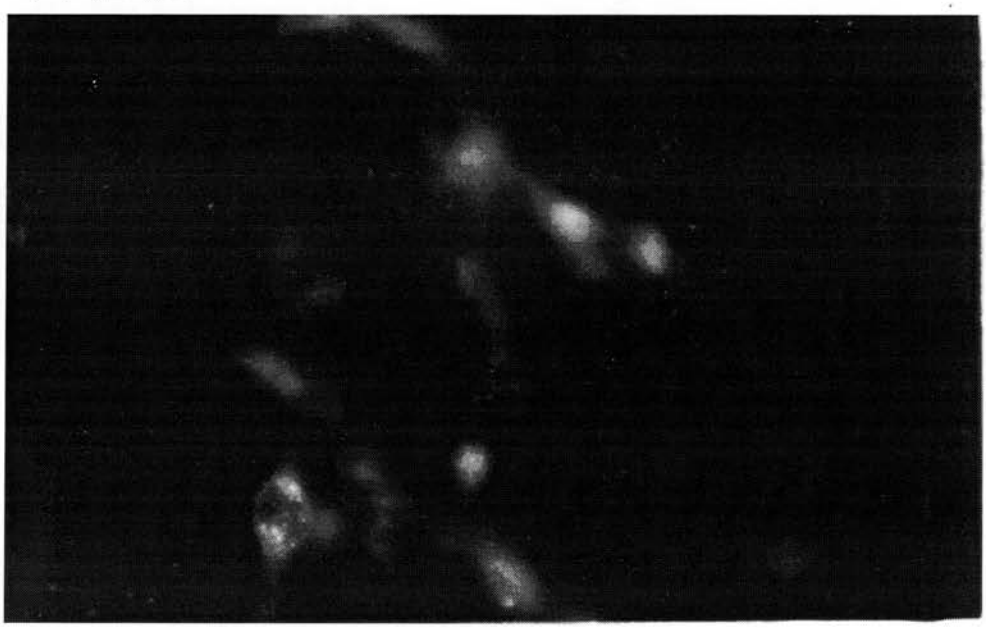

4.13 RT-PCR with synaptotagmin primers

Lanes 1 and 6 show a 1kb DNA ladder (detailed on left hand side in base pairs) and lane 2 a PCR control. Lane 3 shows the RT-PCR rection with the 5'primer only, whilst lane 4 is the RT-PCR reaction with the 3' primer only. Lane 5 shows the band obtained when both the 5' and the 3' primers were present. All samples were run on agarose gels as described in section 2.7.2.2.

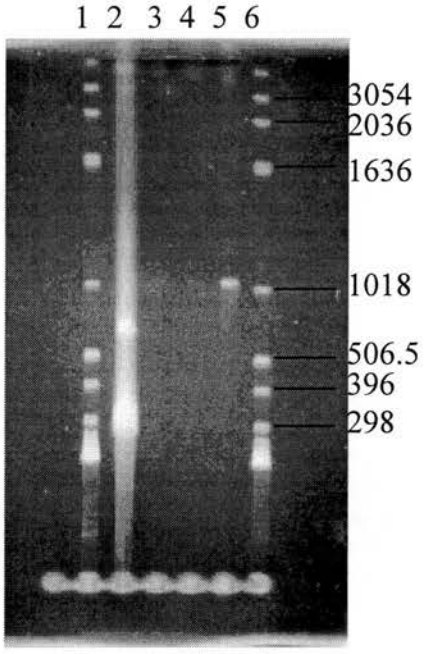

4.14 RT-PCR with synaptobrevin and syntaxin primers

Lane 1 shows a 1kb ladder, and the DNA fragment sizes are given on the left hand side in base pairs. Lane 2 shows the RT-PCR product in the presence of both synaptobrevin primers, while lanes 3 and 4 show the RT-PCR product in the presence of the 5' synaptobrevin primer and the 3' synaptobrevin primer respectively. Lane 5 shows the RT-PCR product in the presence of both the 5' and the 3' syntaxin primers, while lanes 6 and 7 show the RT-PCR product in the presence of the 5' syntaxin primer and the 3' syntaxin primer respectively. All samples were run on agarose gels as described in section 2.7.2.2.

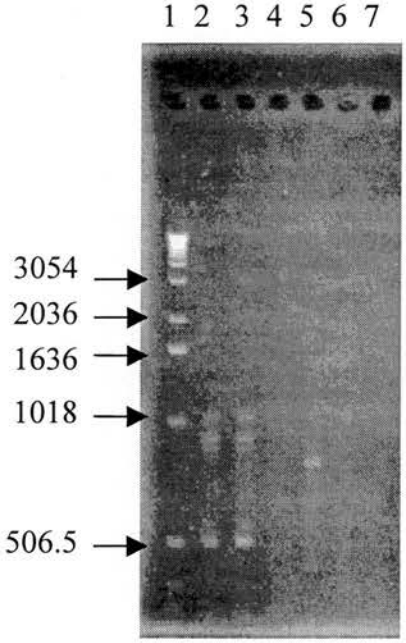

4.15 Amplification and gel extraction of syntaxin RT-PCR product

Gel 1 shows the RT-PCR product obtained in figure 4.11, amplified up by subsequent rounds of PCR. Lane 1 shows 1kb markers, lane 2 a positive PCR control and lane 3 the product obtained with syntaxin primers. Gel 2 shows 100µl of this PCR product run on an agarose gel, and the arrow indicates the band which was cut out and purified. Gel 3 shows 10µl of the purified product, and which was then sent for sequencing. All samples were run on agarose gels as described in section 2.7.2.2.

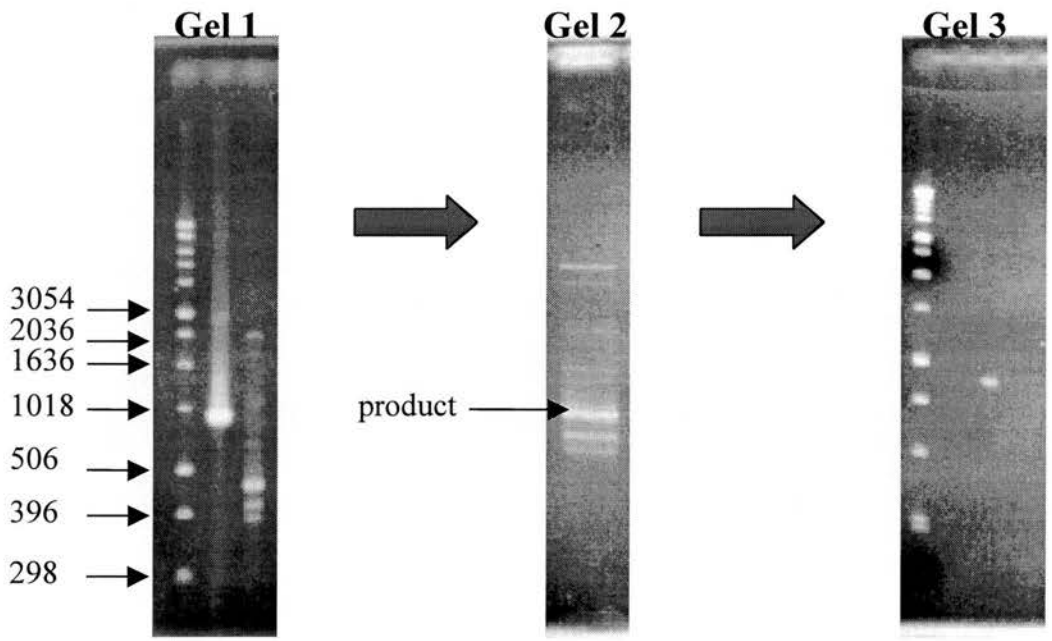

4.16 RT-PCR product sequence

The sequence below represents that obtained from Oswell, for the sequencing of the RT-PCR product. N is a base of unknown identity. A sequence was obtained for the first 210 bases.

NTNTNAACTT GGTNCCANCT CCCCNACCNN

NTANNCTAGN GCCTNTNGTA TCANCCNNCC

NGCATCACTC CTTGNCANCA GGNNCGACAG

GTGGTNANGC ACCTGGCCTC TCACTCCTGG

ACCTNCTGAG TAGGGTGTNN NNN

4.17 Staining for ACTH and actin after Ba^{2+} stimulation

AtT-20 cells were stimulated as detailed in section 2.5.1.1, and then double-labelled for ACTH and actin, as previously described (figure4.10). (a)-(f) show Ba^{2+}-stimulated cells, whilst (g)-(l) show control cells, incubated in Lockes buffer. (a)-(c) and (g)-(i) show staining for ACTH, whilst (d)-(f) and (j)-(l) show actin staining. (a)-(c), (d)-(f), (g)-(i) and (j)-(l) represent the same time course of 15s, 1min and 5min. Calibration bars = 12.5μM.

(a) ACTH Ba^{2+} 15s

(b) ACTH Ba^{2+} 1min

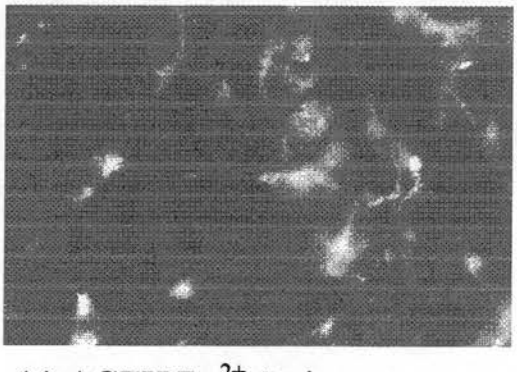

(c) ACTH Ba^{2+} 5min

(g) ACTH control 15s

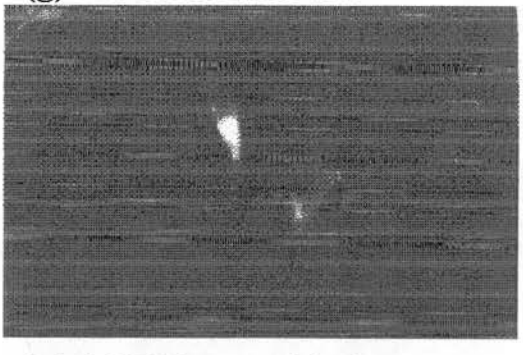

(h) ACTH control 1min

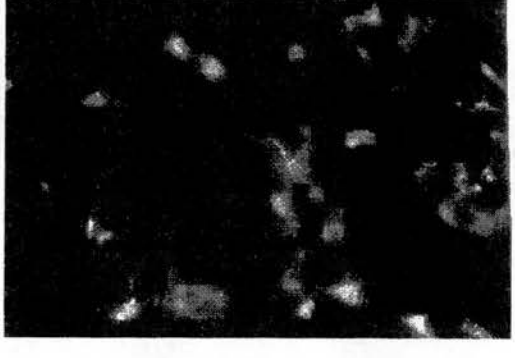

(i) ACTH control 5min

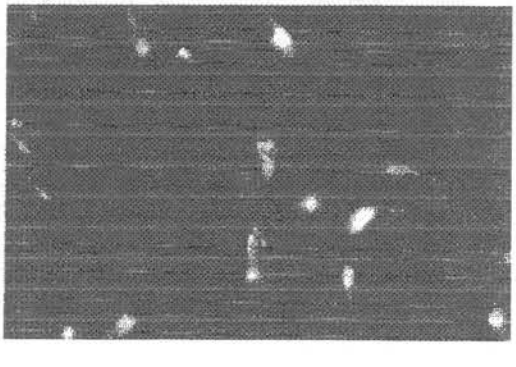

(d) actin Ba^{2+} 15s —

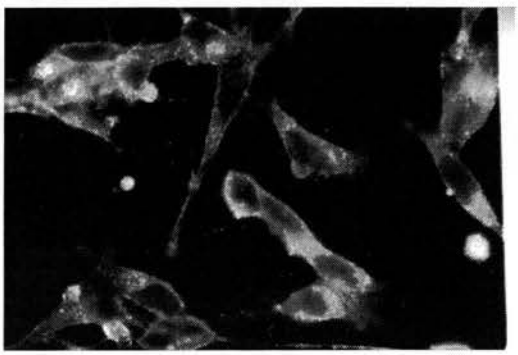

(j) actin control 15s —

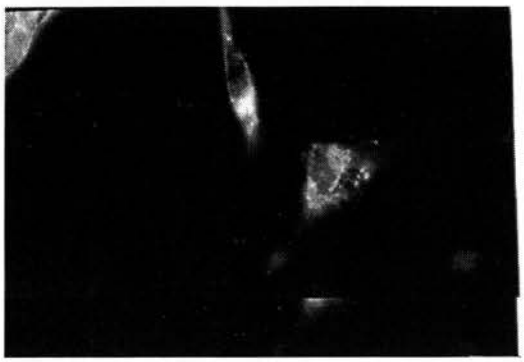

(e) actin Ba^{2+} 1min —

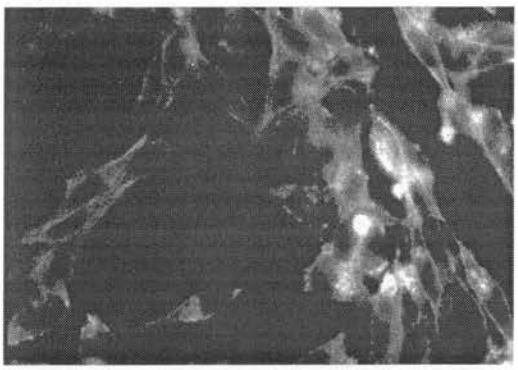

(k) actin control 1min —

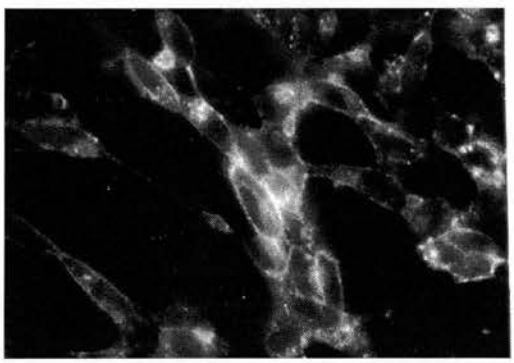

(f) actin Ba^{2+} 5min —

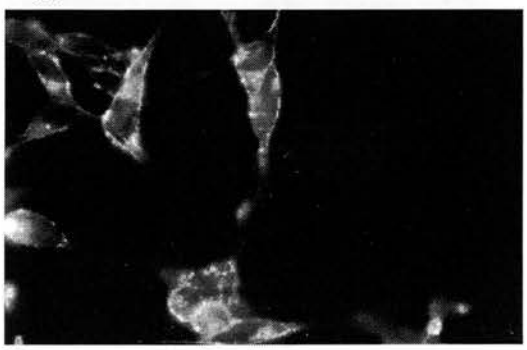

(l) actin control 5min —

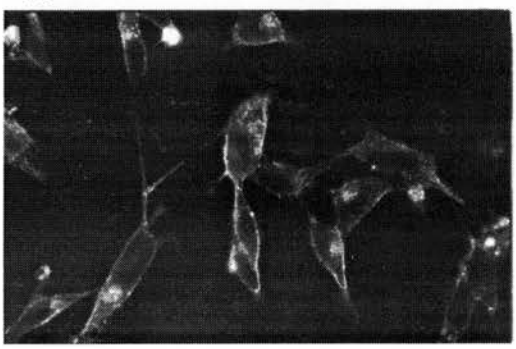

4.18 Staining for cofilin and actin after Ba^{2+} stimulation

AtT-20 cells were stimulated as detailed in 2.5.1.1, and then double-labelled for cofilin and actin, as previously described. (a)-(f) show Ba^{2+}-stimulated cells, whilst (g)-(l) show control cells, incubated in Lockes buffer. (a)-(c) and (g)-(i) show staining for cofilin, whilst (d)-(f) and (j)-(l) show actin staining. (a)-(c), (d)-(f), (g)-(i) and (j)-(l) represent the same time course of 15s, 1min and 5min. Calibration bars = 12.5μM.

(a) Ba^{2+} cofilin 15s

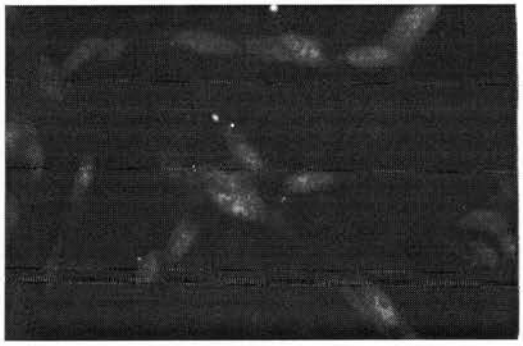

(g) control cofilin 15s

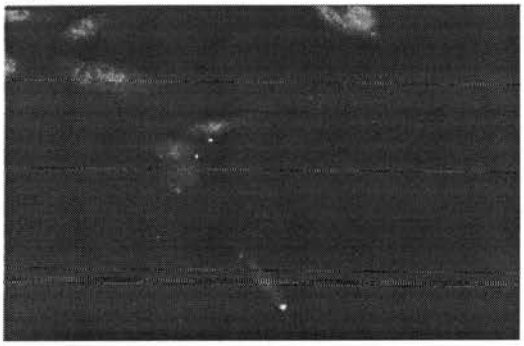

(b) Ba^{2+} cofilin 1min

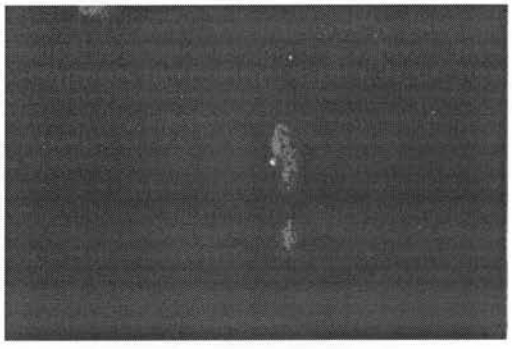

(h) control cofilin 1min

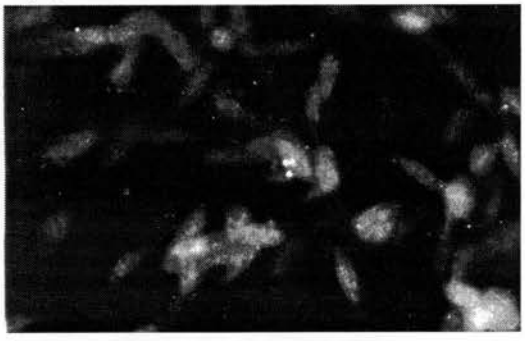

(c) Ba^{2+} cofilin 5min

(i) control cofilin 5min

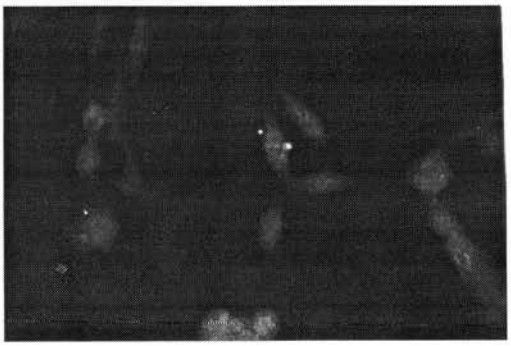

(d) Ba^{2+} actin 15s

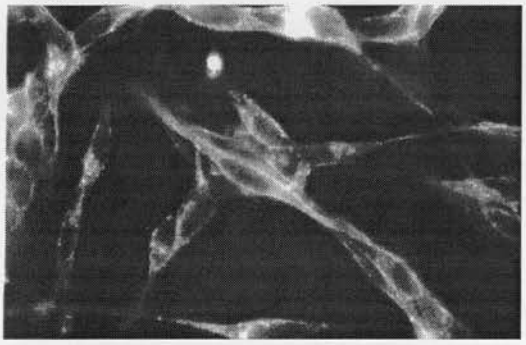

(j) control actin 15s

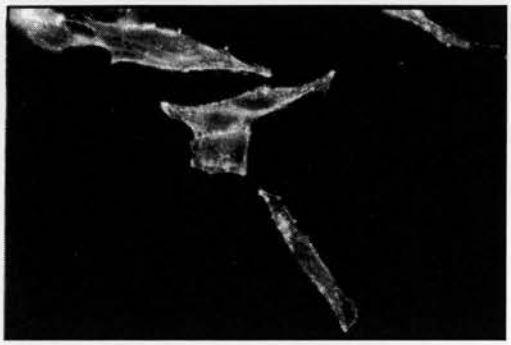

(e) Ba^{2+} actin 1min

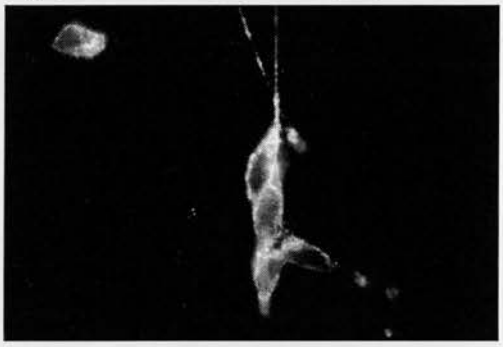

(k) control actin 1min

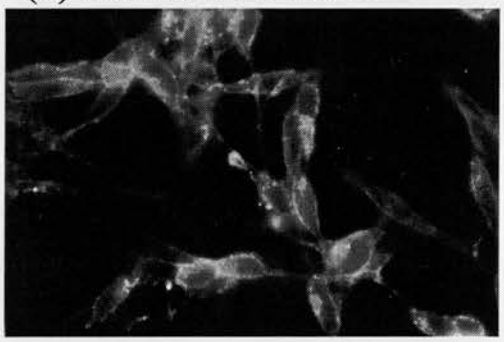

(f) Ba^{2+} actin 5min

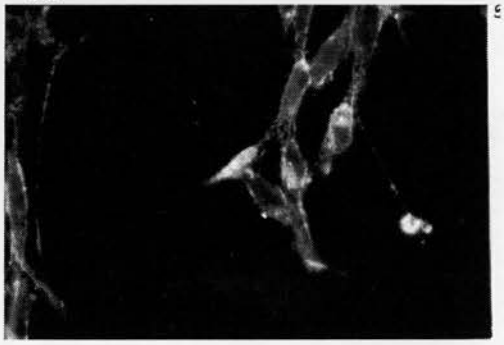

(l) control actin 5min

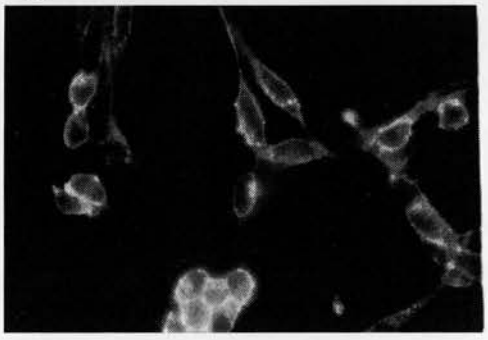

4.19 Staining actin after Ba^{2+} stimulation (in the presence of cytochalasin)

AtT-20 cells were stimulated as detailed in section 2.5.1.1, and then labelled for actin as previously described (figure 4. 9). (a)-(c) show the Ba^{2+}-stimulated cells, whilst (d)-(f) show control cells, incubated in Lockes buffer. In each case 2.5μM cytochalasin D, was including in within the Ba^{2+} stimulation or control buffer. Calibration bars = 12.5μM.

(a) Ba^{2+} actin 15s

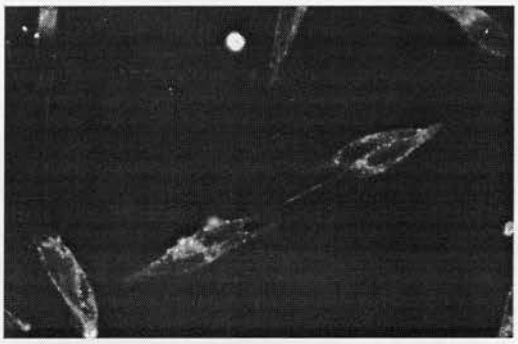

(d) control actin 15s

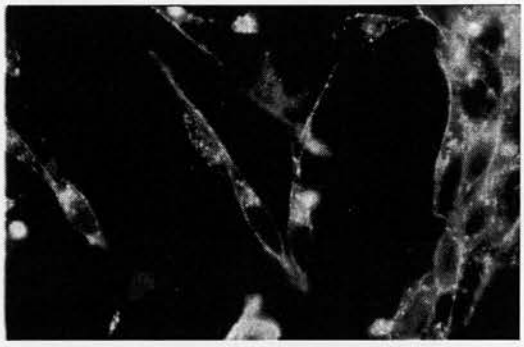

(b) Ba^{2+} actin 1min

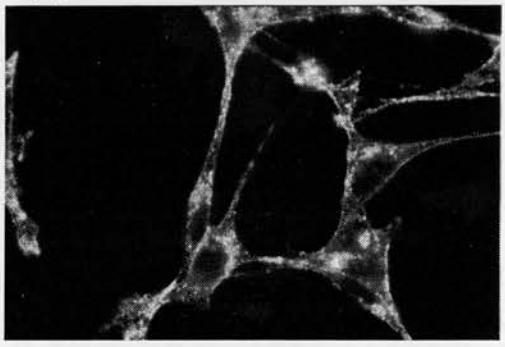

(e) control actin 1min

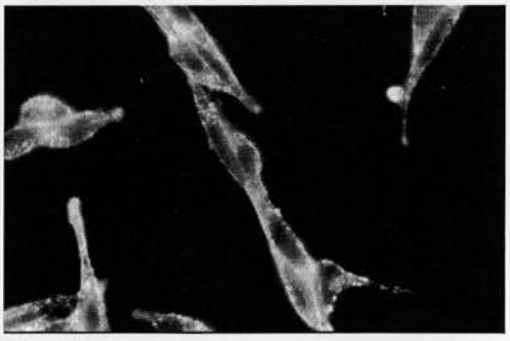

(c) Ba^{2+} actin 5min

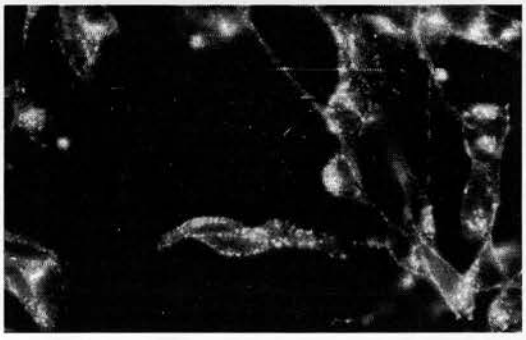

(f) control actin 5min

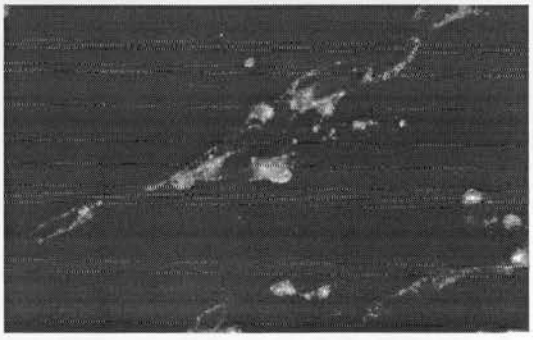

Chapter 5

A study of Ca^{2+}-regulated exocytosis, using permeabilised AtT-20 cells and ACTH radioimmunoassay

5.1 Introduction

The aim of the work described in this chapter was to study Ca^{2+}-regulated exocytosis in permeabilised AtT-20 cells into which antibodies, proteins, toxins or drugs had been introduced. Buffered Ca^{2+} could then be used to stimulate exocytosis, and the secreted ACTH measured using a radioimmunoassay (RIA). This would allow detection of any changes in Ca^{2+}-regulated exocytosis, as a result of the various factors which had entered the cells.

The radioimmunoassay was set up with reagents obtained from NIDDK (National Institute of Diabetes and Digestive and Kidney Diseases). It was then used to check that the cells were secreting in a normal, regulated way as reported by *Sabol, 1980, Hook et al., 1982; Phillips & Tashjian, 1982; Loechner et al., 1996*. For these studies non-permeabilised AtT-20 cells were used with K^+, 8`-bromo-cAMP, CRH and Ba^{2+} to stimulate secretion, whilst dexamethasone was used as an inhibitor of secretion. The digitonin permeabilisation conditions were optimised, ensuring that excessive levels of ACTH were not being lost, but that the incubation times allowed the entry of a number of different factors.

Having developed a permeabilised cell assay, a number of different approaches were used. Antibodies directed against proteins involved in secretion, purified recombinant proteins (normally involved in secretion), actin stabilising or destabilising drugs and recombinant clostridial neurotoxin light chains were all added to the permeabilised AtT-20 cells, and their effects on secretion measured using the ACTH RIA.

5.2 ACTH radioimmunoassay

ACTH and anti-ACTH were obtained from NIDDK, and iodination of the ACTH was done as detailed in section 2.4.1. The protocol for the ACTH RIA was obtained from Dr. John Bennie (Royal Edinburgh Hospital, Edinburgh), however the anti-ACTH antiserum was from a different source, and it was necessary to re-optimise the assay using this new antiserum. The assay was performed as detailed in section 2.4.2. The anti-ACTH antiserum dilutions used in this experiment were 1/20000, 1/30000,

1/40000, 1/50000 and 1/60000 with standards ranging from 0-80ng/ml ACTH. All data were fitted using a third order polynomial curve to the order of three. The aim was to obtain an anti-ACTH concentration that gave a well-fitted curve, with a B_0/TC value of around 20-25%, as this part of the curve allows for the most accurate calculations of ACTH concentrations. The B_0 value is the count obtained in the presence of approximately 10,000cpm iodinated ACTH, but no standard ('cold') ACTH. The TC (total counts) value is the cpm in 50µl (i.e. a normal sample) of iodinated ACTH, with no subsequent treatment, and this is approximately 10,000cpm. B_0/TC is simply used to optimise the assay within the correct area of the curve. As the total counts were around 10000cpm, and the B_0 values were around 2500-3000cpm, samples were read on the gamma counter for 3min in order to give sufficient accuracy. Doubling dilutions were not used to produce the standards for the standard curve, as this can lead to inaccuracies, and all standards were diluted separately from a stock solution. Figure 5.1 shows the standard curves and B_0/TC values obtained for each concentration of antiserum. Normal samples and standards are plotted as shown on this curve, as $\%B/B_0$, that is percentage bound iodinated ACTH (in the presence of sample or standard 'cold' ACTH) over bound iodinated ACTH (in the absence of any standard or sample 'cold' ACTH).

5.3 Discussion

It was decided to use an antiserum concentration of 1/60000, as this gave a very reproducible curve with a B_0/TC value of 23%. All standards were assayed in triplicate, whilst actual samples were assayed in duplicate. ACTH standards were obtained from the Royal Edinburgh Hospital, and assayed using this system. In this work they all gave values within 2-3 times the values obtained using the Royal Edinburgh assay.

The calculation of the ACTH concentration of unknown samples was done using the polynomial equation obtained for each assay. The equation was used to produce an iterative formula which allowed the calculation of unkown values. A standard curve and formula was calculated for each single radioimmunoassay, however these are not

all given in the results chapters. Figure 5.2 shows a representative standard curve and the formula used to calculate values from it. Having obtained an accurate and reproducible method of measuring ACTH secretion, the next stage was to assess whether the AtT-20 cells used were secreting ACTH normally fashion, and whether the levels were measurable by RIA.

In all subsequent experiments where ACTH concentration has been measured standard error bars have been shown, and unless otherwise stated n=4. In this case 'n' refers to the number of wells assayed, however to further increase accuracy these samples were all assayed twice and the mean values used for further calculation, and calculation of standard errors. Each set of results reported in this chapter was obtained within the same radioimmunoassay to avoid the problem of variations in standard curves giving rise to differences in results, between assays. Each assay was done using cells grown to 70-80% confluency in 24-well plates, and the volumes used were always 1ml per well. The results are reported as ACTH concentration in ng/ml, rather than per number of cells, as this varied slightly between assays. As a rough guide, one well of a 24-well plate contained 10,000 – 20,000 cells, therefore the ACTH release could be calculated as ng/10,000-20,000 cells.

5.4 Secretion of ACTH by non-permeabilised AtT-20 cells, in response to various secretagogues.

A time course was obtained for release stimulated by CRF, KCl and Ba^{2+}, to assess the optimum time for measuring ACTH secretion, all stimulations being done as detailed in section 2.5.1. Two time courses were obtained for the Ba^{2+} stimulations, in order that these could be compared to the experiments detailed in figures 4.17-4.19. A dose-response curve was also obtained for CRF, and the various secretagogues were then used at their optimal concentrations to stimulate the AtT-20 cells. The inhibitory effect of dexamethasone on CRF-, K^+- and 8`-bromo-cAMP-mediated exocytosis was examined in parallel. Figures 5.3-5.7 detail the results obtained in these experiments.

5.5 Discussion

The time course of CRF-stimulated ACTH secretion (figure 5.3a) showed that maximal release was obtained at 30-40min, in that the largest difference was seen between basal and CRF-stimulated samples, as well as the smallest standard errors. The dose response (figure 5.3b) confirmed that 100nM CRF was optimal, as lower CRF concentrations lead to increased standard errors. Thus in subsequent CRF-stimulation experiments 30 minute incubations with 100nM CRF were used, at 37°C. Although the differences between basal levels of secretion and CRF-stimulated levels of secretion were not large, they are similar to those previously found. Reports on the extent of stimulation range from 2 to 5 times the basal level of stimulation *(Reisine et al., 1985; Hook et al., 1982)*. In the system used here CRF stimulation produced 1.5-2 times the levels of basal secretion, and although this is fairly low the results were consistent and reproducible. However it is important to note such variations as they may be due to differentiation of the cells, or the use of slightly different methods of culture.

The time course of K^+-stimulated ACTH secretion (figure 5.4) also showed the optimum time of assay to be around 30min, and to produce approximately twice the basal levels of ACTH secretion.

Figure 5.5 shows the results obtained when the effect of dexamethasone on ACTH secretion was measured, after stimulating the cells with 100nM CRF or 50mM K^+. The results showed that both CRF and K^+ stimulated the cells to secrete around 2 times the basal level of ACTH. Dexamethasone reduced CRF-stimulated and K^+-stimulated ACTH secretion by approximately 65% in both cases, and almost returned them to basal levels. The basal level itself was also reduced by 55%. Again reports vary with respect to the effect of dexamethasone on ACTH secretion, with many suggesting that it inhibits CRF-, but not K^+- stimulated secretion *(Phillips & Tashjian, 1982)*. However *Sabol, 1980* showed that K^+-stimulated endorphin secretion was significantly decreased with dexamethasone. These differences suggest that cell lines may differentiate and behave slightly differently. Dexamethasone was stored in a stock solution at a concentration of 10mM in DMSO, and the experiment

was repeated using controls with the same levels of DMSO only. The same results, were seen thus any inhibitory effect was due a specific effect of the dexamethasone.

The effects of 8-bromo-cAMP on AtT-20 cells were also investigated, and are detailed in figure 5.6. A time course has not been included in this experiment as preliminary work identified optimal incubation times of 30min. The basal level of ACTH secretion was 6.3ng/ml, and 5mM 8-bromo-cAMP increased this to 13.2ng/ml. Dexamethasone inhibited both basal and stimulated levels of ACTH secretion, bringing them down to 5.3ng/ml and 6.5ng/ml respectively, an effect commonly reported in AtT-20 cells *(Phillips & Tashijan, 1982)*.

The time course of Ba^{2+}-stimulated release (figure 5.7) was determined in order to further analyse the immunfluorescence results obtained in figures 4.17-4.19**.** These results did not show any change in actin or cofilin distribution, over a time course of Ba^{2+}-stimulation (15s, 1min and 5min). The time course of Ba^{2+}-stimulation measured by RIA was done in two parts to increase the accuracy of the times at which the samples were taken: (a) shows 5min-60min and (b) shows 15s-5min. There is little Ba^{2+}-stimulation between 15s and 2min, after which there is a large increase to 3-4.5 times that of the basal levels. Graph (a) shows a maximal stimulated level of 3.4ng/ml ACTH, whilst graph (b) shows a maximal stimulated level of 8.7ng/ml. As the ACTH concentration was assessed on separate occasions using different RIAs the discrepancy could simply be due to variation between the assays. However it is also possible that 5 min represents the point where ACTH secretion has only just begun, in which case any variation in taking samples would have a large effect. It was therefore decided that in subsequent Ba^{2+}-stimulation experiments 10 minute incubation times would be used.

These results are important in that they show that the immunofluorescence studies were performed within the correct time scale. At 15s and 1min, there is little ACTH secretion, however at 5min ACTH secretion has just begun. No changes in actin or cofilin distribution could be seen at any of these time points, and even the addition of cytochalasin D failed to slow any re-polymerisation and reveal any changes. Immunofluorescence microscopy was performed at various time points between 10-60mins, however these results were not been included as they were the same as at the

time points shown. Again there was no evidence for the involvement of actin or cofilin in Ca^{2+}-regulated exocytosis in AtT-20 cells, unless the changes were so small that the techniques used were not sensitive enough to detect them.

These experiments have shown that the AtT-20 cell line used in these studies secretes ACTH in a regulated manner, in response to CRF, K^+, Ba^{2+} and 5`-bromo-cAMP. Dexamethasone inhibits release stimulated by CRF, $K^+$ and 5`-bromo-cAMP, in disagreement with many reports but agreement with others, suggesting variations between cell lines or culture techniques. The different methods of action of these various secretagogues can also be seen in that CRF, K^+ and 5`-bromo-cAMP all gave maximal levels of secretion at around 30 min, whereas Ba^{2+} acts at the much faster time of 5min.

5.6 Permeabilisation of AtT-20 cells and subsequent stimulation of ACTH secretion by Ca^{2+}

5.6.1 Optimisation of digitonin permeabilisation

Streptolysin-O was initially used for cell permeabilisation, however trypan blue staining showed little permeabilisation to be occurring, and when chicken red blood cells were used as a control, similar results were seen. When digitonin was used the results were much more reproducible and trypan blue showed permeabilisation of a high percentage of the AtT-20 cells. Various intracellular buffers were also tested, for preventing loss of AtT-20 cells from the wells, and the best was found to be the K^+-glutamate/PIPES buffer detailed in section 2.5.2. The assay involved the cells being washed in 1ml intracellular buffer, followed by permeabilisation in the intracellular buffer containing digitonin. This was then removed and 0.5ml of intracellular buffer was added including any factors that were required to enter the cells. Ca^{2+}-stimulated ACTH secretion was evoked by adding an additional 0.5ml intracellular buffer, containing the appropriate concentration of Ca^{2+}. Initial experiments showed that significant cell loss was occurring on removal of the digitonin permeabilisation buffer, however when the cells were plated on to poly-L-lysine coated 24-well plates (section 2.5.2), this problem was eliminated. Varying

digitonin concentrations were used (5-50μg/ml), and trypan blue was used to stain permeabilised cells and assess the percentage cell permeabilisation. It was found that below 10μg/ml digitonin, only approximately 50% of AtT-20 cells were permeabilised, however at 10 and 20μg/ml digitonin (for 5-10min), greater than 80% of cells were permeabilised. In subsequent experiments, 20μg/ml digitonin (for 10min) was found to produce the most reliable results and to cause greater than 90% of cells to be permeabilised. The ACTH RIA was then used to assess the amount of ACTH that was leaking into the digitonin buffer during permeabilisation. This latter value should be as low as possible, as it is in effect a measure of intracellular membrane damage. The amount of Ca^{2+}-stimulated secretion that occurred in these permeabilised cells was also measured, as well as ACTH release on total lysis (section 2.5.4), in cells prior to digitonin permeabilisation and after digitonin permeabilisation. The ACTH levels that were found are shown in figure 5.8.

At this stage it is necessary to introduce some terminology to clarify the descriptions of any variations in the process. The buffer used for washing, digitonin incubation (10min), incubation with proteins and drugs (15min) and subsequent Ca^{2+} stimulation (10min) was based on the PIPES/K^+ glutamate buffer previously described. In the presence of digtonin, proteins or drugs, and stimulatory Ca^{2+} it will be respectively referred to as permeabilisation buffer, pre-Ca^{2+} incubation buffer and Ca^{2+}-stimulation buffer. The assay stages i.e. digitonin permeabilisation of the cells, incubation of the cells with proteins or drugs and stimulation of the cells with 10μM Ca^{2+} will be respectively detailed as permeabilisation stage, pre-Ca^{2+} incubation stage and Ca^{2+}-stimulation stage. All experiments were done using the above protocol and incubation times, unless otherwise stated. All experiments used AtT-20 cells, grown to 70-80% confluency in 24-well plates, the incubation stages using 1ml buffer, and the ACTH being assayed in 1ml buffer.

5.6.2 Optimisation of Ca^{2+}-stimulated ACTH secretion in AtT-20 cells

Up until this point, 10μM free Ca^{2+} was used to stimulate ACTH secretion in AtT-20 cells, as this was the level used in most of the work here. However as every experimental system varies, it was necessary to assess the optimal Ca^{2+} concentration which should be used to stimulate secretion, as well as the optimal time at which to

measure release. The dose-response curve for Ca^{2+}-stimulation, and the time course of release are shown in figure 5.9. The effect of temperature on Ca^{2+}-mediated ACTH secretion was measured and is displayed in figure 5.10.

5.6.3 Evaluation of the viability of the permeabilised cell system

Having optimised the permeabilisation system, it was necessary to prove that proteins and drugs could actually enter the permeabilised AtT-20 cells. To assess this, a number of agents were incubated with the permeabilised AtT-20 cells for 15min, and the results were assessed by immunofluorescence microscopy. This was done by fixing the cells (as detailed in 2.5.2), immediately on removal of the pre-Ca^{2+} incubation buffer (including the proteins or drugs), and following the immunofluorescence protocol from this point on. The following were used in this experiment: phalloidin-conjugated rhodamine (to label actin), affinity-purified anti-cofilin antiserum and a plant-actin binding protein (ZMAPB3) conjugated to GFP. The molecular weights of these were 0.5kDa, 150kDa and 50kDa respectively, and figure 5.11 shows the results.

5.7 Discussion

Trypan blue staining of permeabilised cells indicated that 20μg/ml digitonin was necessary to obtain reproducible permeabilisation of greater than 90% of AtT-20 cells. Although the leakage of ACTH into the digitonin buffer (indicating intracellular membrane damage) was increased at this digitonin concentration, it was decided that reproducible and efficient permeabilisation was essential. Total lysis values showed that AtT-20 cells in one well of a 24 well plate contained 9.7ng/ml ACTH, which decreased to 6.2ng/ml ACTH following digitonin permeabilisation. The 1.6ng/ml lost during permeabilisation corresponds fairly well with these figures, and represents 13% of the total ACTH content (taking into account basal levels of leakage). Although this is significant, later Ca^{2+}-stimulation results showed that the cells still secreted in a regulated manner, and it was considered a tolerable loss.

The corresponding Ba^{2+}-stimulation results (obtained using the same RIA) showed that during a 10min stimulation the cells released 71% of their total ACTH content.

Considering the immunofluorescence results, in which the ACTH staining was examined following a Ba^{2+}-stimulation, it it is surprising that no change in granule distribution was seen. One explanation for this is that the cells might produce and replace ACTH in a very efficient manner, ready for the next stimulatory event. Another might be that the lysis buffer gave inaccurate readings using the RIA, and indeed the B_0 values did vary, however these were taken into account in calculations of the ACTH concentration. It may be that a combination of the buffer and lysis process caused general degradation of the ACTH.

The Ca^{2+}-mediated release of ACTH from these permeabilised cells was 2.5ng/ml (3 times that of basal levels), thus the cells were releasing 40% of their total ACTH content after permeabilisation. Although these levels were lower than those produced by Ba^{2+}-stimulation, the standard errors were small and the results very reproducible. This indicates differences in the mechanisms of Ca^{2+}- and Ba^{2+}-stimulated ACTH release, and should be considered when interpreting results obtained using this method of stimulation. The actin distribution was also examined following Ba^{2+}-stimulation, and as this is not a physiological stimulatory event, it will be important in the following section to look at the role of actin during Ca^{2+}-stimulated ACTH release.

The time-course and dose-response curves of Ca^{2+}-stimulated ACTH release were typical, in that the optimal Ca^{2+} concentration was 10μM and the optimal time of sampling was around 10min. These conditions were used in all subsequent experiments.

The effect of temperature was examined to assess whether it was possible obtain secretion at room temperature, as opposed to the more physiological 37°C. ACTH secretion at room temperature was 2.9 times the basal level, and at 37°C was 3.2 times the basal level. As the difference was not significant it was decided that it would be possible to incubate all samples at room temperature, as this allowed for greater accuracy, particularly with respect to the time at which the samples were taken.

Immunofluorescence microscopy proved that factors of varying molecular weight could efficiently enter the permeabilised AtT-20 cells and bind, in the 15min pre-

incubation stage before the addition of the Ca^{2+}. A 15min incubation was used during subsequent experiments, unless otherwise stated. The real value of such a result was that it added validity to any negative results obtained with recombinant proteins, antibodies or drugs such as phalloidin.

Having fully optimised and validated the permeabilised cell assay, the next stage was to examine the effects of possible interfering factors, on Ca^{2+}-stimulated ACTH secretion in AtT-20 cells.

5.8 Introduction of antibodies and recombinant proteins into permeabilised AtT-20 cells

5.8.1 Introduction of antibodies to permeabilised AtT-20 cells

AtT-20 cells were permeabilised as detailed in 2.5.2, and diluted antiserum was included in the pre-Ca^{2+} incubation buffer. All subsequent experiments used this same protocol unless otherwise stated. Antisera to cofilin, syntaxin and synaptotagmin were used to assess the involvement of these proteins in exocytosis. All antisera were used at a dilution of 1/100 and results are shown in figure 5.12. NRS was used as a control, and basal levels of secretion without any additions were also measured.

5.8.2 Introduction of recombinant proteins into permeabilised AtT-20 cells

Recombinant cofilin and synaptotagmin were introduced into AtT-20 cells in the pre-Ca^{2+} incubation buffer. BSA at similar concentrations was used as a control, and basal levels with no additions were also measured. Figures 5.13 & 5.14 show the results obtained for cofilin and synaptotagmin.

Another approach was to assess the effect of adding recombinant cofilin on the kinetics of ACTH secretion. Following a pre-Ca^{2+} incubation stage with cofilin, AtT-20 cells were stimulated with 10μM Ca^{2+} for 2, 5 and 10min, and then samples removed and ACTH levels measured. The control was BSA, as this was shown in figure 5.13 to be the most appropriate. Figure 5.15 shows the results of this time course experiment.

5.9 Discussion

The introduction of antibodies to synaptotagmin, syntaxin and cofilin into permeabilised AtT-20 cells had negligible effects on Ca^{2+}-stimulated ACTH secretion. Although anti-cofilin caused a small decrease in Ca^{2+}- stimulated ACTH secretion, NRS had the same effect, suggesting that the effect was non-specific. Anti-synaptotagmin and anti-syntaxin had no significant effect on either Ca^{2+}-stimulated or basal levels of secretion, when compared to ACTH secretion in cells incubated with intracellular buffer containing no antibodies. Whilst these results could suggest that cofilin, synaptotagmin and syntaxin have no role in ACTH secretion, results of similar experiments in chromaffin cells, in which such proteins are known to have a role, were also negative *(Vitale et al., 1995)*. However there are other experimental systems in which the introduction of antibodies into permeabilised chromaffin cells, has pronounced effects *(Ohara-Imaizumi et al., 1997)*. The other explanation for the lack of effect of anti-synaptotagmin and anti-syntaxin is that vesicles are already docked at the plasma membrane, and the antibodies are either unable to bind, or do not affect a rate-limiting step, although this would rule out a role for synaptotagmin as a Ca^{2+}-sensor.

Similar results were obtained on the introduction of recombinant cofilin and synaptotagmin, in that they had no significant effect on ACTH secretion. Both cofilin and synaptotagmin caused a slight increase in ACTH secretion, but this was mimicked by the BSA control and therefore was deemed non-specific. The explanation for this lack of effect is similar to those offered on introduction of the antibodies; that these proteins do not have a major role in this particular stage of exocytosis. It seems likely that adding an excess of functional recombinant cofilin had no effect as there was already a plentiful reservoir of cytosolic protein. The explanation for synaptotagmin is not as simple, since it is an integral membrane protein, and only the recombinant cytosolic domain was being introduced to the cells. The presumption was that this recombinant protein would act as a dominant negative effector of the exocytotic machinery, for example by competing with native synaptotagmin for interactions with other proteins. As no effect was seen, this protein may not have a rate-determining role in Ca^{2+}-regulated exocytosis in AtT-20 cells. A similar result was reported by *Wendland & Scheller, 1994*, who used AtT-20

cells that were stably transfected with the gene for the cytoplasmic domain of synaptotagmin, and found no effect on Ca^{2+}-regulated exocytosis. Another possibility is that there is an alternative pathway which can be utilised when the synaptotagmin pathway is blocked. These explanations imply that synaptotagmin may be a Ca^{2+}-sensor, but if its main role were as a v-SNARE, the lack of effect of the cytoplasmic domain may simply be due to the fact that the vesicles are already docked at the plasma-membrane. This idea has already been proposed by *Schiavo et al., 1997* to explain the fact that vesicles remain docked at the plasma membrane after treatment with botulinum toxins A and E, which proteolytically digest SNAP-25. The time course of ACTH secretion in the presence of cofilin showed no effect on the kinetics of ACTH secretion. If actin has a rate-determining role in Ca^{2+}-stimulated ACTH secretion, the introduced cofilin might stimulate ACTH secretion, by increasing actin de-polymerisation. Since no change in the kinetics was seen an adequate pool of functional protein may already have been present in the cells.

5.10 Further investigation of the role of actin in Ca^{2+}-stimulated ACTH secretion in AtT-20 cells

Phalloidin and cytochalasin D were also used to study the role of actin in Ca^{2+}-regulated exocytosis in AtT-20 cells. Figure 5.16 shows the results obtained when phalloidin was incubated with AtT-20 cells prior to Ca^{2+}-stimulation, and samples were taken at varying times (2, 5 and 10min), to assess whether the actin-stabilising drug had any effect on the kinetics. Finally cytochalasin D (an actin de-stabilising drug) was used to assess whether destabilisation of the actin had any effect on ACTH secretion, and these results are shown in figure 5.17.

5.11 Discussion

Neither phalloidin nor cytochalasin D appeared to have any effect on Ca^{2+}-stimulated or basal ACTH secretion in permeabilised AtT-20 cells (figures 5.16-5.17). Immunofluorescence studies showed that phalloidin binds to the actin in such cells (figure 5.11), so the lack of effect cannot be explained by its failure to enter and bind.

Figures 4.17-4.18 showed that no changes could be seen in actin distribution, following Ba^{2+}-stimulation of ACTH secretion. The inclusion of cytochalasin D, to slow down the re-polymerisation of the actin (figure 4.19) was also investigated in these experiments. A slight change in the actin distribution could be seen, in that it appeared more 'patchy', however this effect occurred in both control and Ba^{2+}-stimulated cells and thus was not a consequence of ACTH secretion. Cytochalasin D had no effect, producing no significant change in ACTH secretion (figure 5.17). One could say that the Ba^{2+}-stimulation experiments may not be physiologically relevant, however the same explanation cannot be offered for experiments in which ACTH secretion was stimulated with Ca^{2+}. Furthermore, measurements of ACTH release do not rely on qualitative judgement, but on statistically-analysed data. These findings (as well as those reported in chapter 4) do not prove any role for actin in Ca^{2+}-stimulated ACTH secretion in AtT-20 cells. Many similar studies of different cell types produced different results. For example *Lelkes et al., 1986* reported that 5μM cytochalasin D caused a large increase in Ca^{2+}-stimulated catecholamine release from chromaffin cells, while phalloidin had the opposite effect in the same system.

5.12 Investigation of cytosolic rundown and the introduction of recombinant αSNAP into permeabilised AtT-20 cells

Much work has been done on the role of αSNAP in Ca^{2+}-regulated exocytosis, particularly in chromaffin cells, and in relation to the cytosolic rundown seen in permeabilised cells. The leakage of soluble proteins from permeabilised cells has been used as a means to identify cytosolic proteins involved in Ca^{2+}-regulated exocytosis. Introduction of cytosol to rundown cells can reconstitute efficient secretion in response to Ca^{2+}, as can the introduction of various proteins involved in exocytosis, and one of these proteins is αSNAP. This section repeats studies of the extent to which cytosolic rundown occurs in AtT-20 cells, as assesssed by the rundown of the exocytotic response to Ca^{2+}, and the leakage of the cytosolic enzyme LDH. Further experiments tested whether this rundown could be reversed by the addition of rat brain cytosol or αSNAP. Rat brain cytosol was obtained from Dr. Leonora Ciufo (University of Edinburgh), and was a by-product of the preparation of

rat brain synaptosomes, whilst recombinant αSNAP was obtained from Professor Burgoyne (University of Liverpool) and was prepared as detailed in *Morgan & Burgoyne, 1995.*

Figure 5.18 shows exocytotic rundown in permeabilised AtT-20 cells. This rundown was produced by permeabilising AtT-20 cells in the normal way (i.e. 20μg/ml digitonin for 10min), and then varying the time of the pre-Ca^{2+} incubation stage (15, 30, 60, 90 min), before stimulation of secretion with 10μM Ca^{2+} for 10min. This was repeated and expanded in figure 5.19, with the introduction of rat brain cytosol to assess whether any increase in secretion was seen. AtT-20 cells were also permeabilised for increasing lengths of time, followed by incubation with or without rat brain cytosol before Ca^{2+}-stimulation. Figure 5.20 shows cytosolic leakage manifested as leakage of LDH under varying conditions (section 2.5.5). Figure 5.21 shows the results obtained when αSNAP was introduced to cells with varying incubation times prior to Ca^{2+}-stimulation. Figure 5.22 shows the effect of introducing αSNAP into cells permeabilised for extended periods of time, followed by the usual 15min pre-Ca^{2+} incubation period, prior to Ca^{2+}-stimulation. Rat brain cytosol was present at a concentration of 3mg/ml in a buffer containing 25mM Hepes-KOH and 0.32M sucrose. This was diluted in intracellular buffer to 1.5mg/ml, however the intracellular buffer was modified so that it would be iso-osmotic with the AtT-20 cells, lowering the potassium glutamate concentration from 150mM to 70mM. Control experiments without added cytosol used this intracellular buffer diluted with the Hepes/sucrose buffer only. αSNAP was equilibrated with the required intracellular buffer by passage through Biogel P-6 DG. A 15% loss occured during this process, as judged by A_{280} measurements and the final concentration of αSNAP was 53μg/ml. Figure 5.21 shows a polyacrylamide gel of αSNAP.

5.13 Discussion

Figure 5.18 shows the effects of increasing the pre-Ca^{2+} incubation time, prior to Ca^{2+}-stimulation. It has already been demonstrated that factors can enter and bind in AtT-20 cells (figure 5.11), and one would expect that if unbound cytosolic factors

were important in ACTH secretion in AtT-20 cells there would be a decrease in ACTH secretion with increasing pre-Ca^{2+} incubation times. In fact, little decrease was seen from 15min to 60min, after which point there was a small drop. This drop at 90 min may have been due to reduced cell viability as opposed to true exocytotic rundown. Figure 5.19 expands on this and shows the effects of adding cytosol, with an attempt to increase the exocytotic rundown by using increased permeabilisation times. These results show that there is a decrease in ACTH secretion when the pre-Ca^{2+} incubation times, prior to Ca^{2+}-stimulation is increased from 0min to 15min. Rat brain cytosol had no effect on the Ca^{2+}-stimulated zero-time sample, but it caused a 37% increase in the basal sample. Cytosol also had no effect on the Ca^{2+}-stimulated 15min sample, but it caused a 33% increase in the basal 15min sample. These results suggest that the 'rundown' seen between 0 and 15min is cellular damage rather than cytosolic or exocytotic rundown. The increase in basal levels of secretion is probably due to the an effect on the levels of free Ca^{2+}, and some factor may be present which slightly elevates these levels, so that the control cells show a degree of Ca^{2+}-stimulated ACTH secretion. Addition of cytosol does have an effect on the Ca^{2+}-stimulated sample at 90min causing a 21% increase and restoring the level of secretion to that seen at 15min. It continues to have an effect on the basal level, which displays a 12% increase. Thus it appears that true exocytotic rundown only begins much later, at around 90min. The permeabilisation time was increased to 45min to try to accelerate rundown, and indeed the ACTH secretion dropped to basal levels. On the introduction of cytosol for 15min prior to Ca^{2+}-stimulation, ACTH secretion was increased 62%, whilst basal levels were only increased by 25%. Thus cytosolic rundown also appears to occur with a 45min permeabilisation, and the effect can be reversed to some extent by the addition of cytosol. This protocol provided a quicker method of assaying cytosolic rundown, produced lower standard errors than the in 90min rundown experiment and proved more reproducible.

Figure 5.20 shows true cytosolic rundown, as opposed to a decrease in Ca^{2+}-stimulated ACTH secretion, measured as LDH leakage from AtT-20 cells. After 10min the permeabilisation buffer contained 145U/ml LDH, and after 45min 446IU/ml, showing that cytosolic components leak out of the cells during permeabilisation, and increasing the permeabilisation time increases this effect. It

also shows that leakage occurs during the pre-Ca^{2+} incubation stage (using a 10min permeabilisation), the pre-Ca^{2+} incubation buffer containing 48IU/ml LDH. When this pre-Ca^{2+} incubation was increased to 30 and 60min the buffer contained 119U/ml and 123U/ml LDH respectively. In cells permeabilised for 45min, followed by the normal 15min pre-Ca^{2+} incubation, the pre-Ca^{2+} incubation buffer contained no significant levels of LDH, suggesting that all the LDH had leaked out during the 45min permeabilisation period. These results confirm that cytosolic leakage occurs in these cells, but at a much faster rate than the exocytotic rundown. Leakage of LDH is significant at 15min and plateaus at 30min, unlike the exocytotic rundown which is not significant at 15min, but significant at 90min. This again suggests that that the exocytotic machinery is docked and in place.

The inclusion of αSNAP during the pre-Ca^{2+} incubation for 15, 30 or 60min had no effect on Ca^{2+}-stimulated ACTH secretion (figure 5.21). This is consistent with the demonstration that no significant exocytotic rundown occurs over this period of time (figure 5.18), however numerous other studies have shown αSNAP to have the ability to increase Ca^{2+}-stimulated exocytosis. *Morgan & Burgoyne, 1995* showed an increase from 25% total catecholamine release to 31% total catecholamine release in chromaffin cells. As shown in figure 5.22, αSNAP (unlike whole brain cytosol), had no effect when the cells were permeabilised for 45 min, in that it could not re-constitute Ca^{2+}-stimulated secretion. Morgan & Burgoyne, 1995 showed αSNAP to have this ability in chromaffin cells, when they showed αSNAP to increase in Ca^{2+}-stimulated catecholamine secretion in chromaffin cells under similar conditions.

In summary these results suggest that exocytotic rundown does occur in permeabilised AtT-20 cells, but only after a fairly long period of time, whereas leakage of cytosolic proteins occurs over a shorter period of time. Rat brain cytosol can reverse this exocytotic rundown, whereas recombinant αSNAP does not appear to have any effect.

5.14 Introduction of Botulinum and Tetanus toxins into permeabilised AtT-20 cells

One of the most effective ways of studying Ca^{2+}-regulated exocytosis is by using Clostridial neurotoxins. Many studies have shown these toxins to greatly inhibit Ca^{2+}-regulated exocytosis in both neuronal and chromaffin cells and the inhibition has been related to the specific proteolytic degradation of synaptobrevin, syntaxin or SNAP-25 by particular toxins *(Hayashi et al., 1994; Niemann et al., 1994)*.

Little effect on Ca^{2+}-regulated exocytosis was found, on the introduction of antibodies, recombinant proteins, actin-stabilising drugs or actin de-stabilising drugs into AtT-20 cells. The recombinant protein and antibody results were attributed to the fact that in AtT-20 cells secretory vesicles are already docked at the plasma membrane, thus preventing these factors from interfering. The use of toxins should allow proteolysis of t-SNAREs or v-SNAREs, even in docked vesicles, and thus inhibit exocytosis. Toxin-mediated inhibition of Ca^{2+}-regulated exocytosis in AtT-20 cells would also prove that the susceptible protein had a definite role in ACTH secretion. It was decided initially to use recombinant light chains of Botulinum neurotoxin D (BoNTD-LC), Tetanus toxin (TeTX) and Botulinum neurotoxin C (BoNTC-LC), the former two being specific for synaptobrevin, and the latter for syntaxin, as these proteins are the main SNARE proteins. However preliminary experiments failed to detect expression of the BoNTC-LC by transfected NM522 cells, and due to time constraints efforts were concentrated on BoNTD-LC and TeTX-LC expression, as preliminary work showed expression of these recombinant proteins.

5.14.1 Preparation of recombinant light chains of tetanus toxin (TeTX-LC) and Botulinum toxin D (BoNTD-LC)

The optimised protocols for the production and purification of TeTX-LC and BoNTD-LC are detailed in 2.6; in this section some of the preliminary work on toxin production production is described. The purification conditions were initially varied in order to optimise yield and purity, mainly by varying the number of washes and wash buffer concentration and composition. Ni-agarose was used throughout the procedure, in conical glass tubes. Washing and sample collection stages were done

by re-suspension of the Ni-agarose and centrifugation to collect the supernatant. It was found that TeTX-LC was best eluted using a pH change and a number of washing stages, while BoNTD-LC was best eluted using an imidazole gradient. Ni-agarose bound TeTX was washed with SE buffer (pH8.0), followed by SE buffer (pH6.5), and then a number of washes with SE buffer (pH5.0). The most concentrated and purest fraction was wash 10 of the SE buffer (pH5.0), and this was used in subsequent experiments. Figure 5.23 shows the various TeTX fractions obtained during the washing stages, and run on an acrylamide gel. BoNTD was initially eluted using a stepwise imidazole gradient, however BoNTD-LC could be seen in any of the fractions following the 30mM wash, none of which were particularly pure (figure 5.24 shows a gel of the fractions). It was therefore decided to extend the number and the volume of the 10mM and 30mM imidazole washes, to remove contaminating bacterial proteins, without losing any of the BoNTD-LC. At this point it was also concluded that the use of non-transfected bacterial NM522 cells, grown in non-selective media, and then treated in exactly the same way as the transfected bacterial cells, was necessary to show this 50kDa band to be specific. Figure 5.25 shows a gel of the fractions from the purification of BoNTD-LC (using the 10mM and 30mM imidazole washes), and also the fractions obtained with the non-transfected bacterial cells. Passage through Biogel P-6DG was used to change the buffer of the BoNTD-LC and BoNTD-LC control to that of the intracellular buffer used in permeabilisation experiments. The same control (i.e. non-transformed bacterial cells fractionated in the same way as the TeTX-LC transfected cells) was used for TeTX-LC, and figure 5.26 shows a gel of the fractions obtained for both of these.

5.14.2 Introduction of TeTX-LC and BoNTD-LC into permeabilised AtT-20 cells

Optimisation of the purification of BoNTD-LC and TeTX-LC, was based on the acrylamide gels that were run of the various fractions. BoNTD-LC and TeTX-LC were identified by the presence of a 50kDa band that was absent, or greatly reduced, in the control cell fractions. A preliminary experiment was performed as follows: toxin purification was as detailed in 2.6, and two 0.5ml fractions were obtained for each toxin, which were equilibrated with intracellular buffer. 0.4ml of the BoNTD-

LC fraction was then added to 4.5ml intracellular buffer, and 0.5ml of the resulting mixture was used per sample in a 20min pre-Ca^{2+} incubation stage (prior to Ca^{2+}-stimulation of the cells). The control was BSA (2.5μg/ml), which was around the concentration expected for the BoNTD-LC. In this preliminary experiment exact estimates were not made of the BoNTD-LC concentration, but rough estimates could be made from the acrylamide gels (figure 5.25). The results of the Ca^{2+}-stimulation and ACTH RIA for this experiment have been displayed in figure 5.27. The introduction of TeTX-LC (figure 5.28) was done at a slightly later stage in the project, and used a control of non-transformed bacteria fractionated in the same way, as opposed to BSA. In this experiment 200μl or 20μl of the 0.5ml fraction after passage through BioGel, was added to 4.3ml or 4.48ml respectively of intracellular buffer, and 0.5ml of the resulting mixture was used per sample in the 20min incubation preceding the Ca^{2+}-stimulation stage. The concentration of the toxin was not accurately assayed at this stage, and again could be roughly estimated using fractions run on acrylamide gels (figure 5.26). An additional control was used that contained no bacterial fraction, in order to assess basal ACTH secretion. The results of this experiment are shown in figure 5.28.

Having confirmed the activity of the BoNTD-LC and TeTX-LC fractions being used, it was decided to repeat the experiment using properly quantitated toxin samples, varying toxin concentrations and all the necessary controls. To quantify the toxins a combination of Peterson's assay (detailed in 2.5.1.1) and densitometry were used. The Peterson assay allowed the total protein concentration to be calculated, whilst the densitometry allowed other protein bands to be taken into account, as the samples were not totally pure. The percentage of 50kDa protein compared to total protein was obtained by densitometry and then this percentage was used to calculate the concentration of protein that was toxin. Figure 5.29 shows the acrylamide gel of the samples used for densitometry, and shows how the toxin concentrations were calculated.

These toxins were then introduced into permeabilised AtT-20 cells, as in the previous experiments. Figure 5.30 shows the results for TeTX-LC, and figure 5.31 the results obtained for BoNTD-LC.

5.15 Discussion

The protocol for purification of TeTX-LC (see 2.6), was chosen as there was a strong 50kDa band seen in fraction 18 (diagram 5.23) which was relatively pure. Further experiments on a non-transformed bacterial control showed the absence of this 50kDa band (figure 5.26). The initial protocol using stepwise increases in imidazole concentrations to purify BoNTD-LC resulted in elution of BoNTD-LC after 30mM imidazole (figure 5.24). It was therefore decided to increase the washing stages up to this point and then elute the BoNTD-LC immediately with 100mM imidazole, and this proved to be more successful (figure 5.25).

The introduction of BoNTD-LC into permeabilised AtT-20 cells, followed by stimulation with Ca^{2+}, produced a reduction in ACTH secretion, although the basal (Ca^{2+}-independent) ACTH secretion was unaltered (figure 5.27). The highest TeTX-LC concentration reduced ACTH secretion to 65% of the control, and there was no effect on basal ACTH secretion.

The concentrations of the toxins were quantified using a combination of Peterson's assays and densitometry. After buffer equilibration the concentrations of BoNTD-LC and TeTX-LC were 48µg/ml and 38µg/ml respectively (the recovery after Biogel treatment being about 70%). The toxins comprised approximately 25% of the total protein present in the active fractions.

These toxin preparations were introduced into permeabilised AtT-20 cells, prior to Ca^{2+}-stimulation. One of the main problems of these experiments was that the toxins could not be frozen, even in the presence of glycerol, without extensive loss of activity. The low yield of from each preparation also caused problems, as the dose used had to be kept to a minimum, in order that sufficient numbers of samples could be tested to ensure that the results were statistically significant and accurate. The introduction of 38nM TeTX-LC caused a drop in ACTH secretion to 78% of the control level, whilst 17nM TeTX-LC caused no detectable reduction. The introduction of 30nM BoNTD-LC caused a drop in ACTH secretion to 77% of the control level, whilst 15nM BoNTD-LC caused a similar drop to 74% of its control level. It is interesting to note that in the BoNTD-LC control ACTH secretion is reduced to 85% of the normal levels obtained in the absence of any bacterial

proteins, suggesting that even 15nM BoNTD-LC produces maximal effects. Other experiments tested the buffer only, by passing it through BioGel P-6DG, and found it to have no effect on ACTH secretion. Thus it appears that this drop is not due to incomplete buffer equilibration (and subsequent effects on free Ca^{2+} concentrations), but to proteins present in the non-transformed bacterial cells that interfere with ACTH secretion. In this second experiment slightly lower inhibition of secretion was seen, however this is most likely due to differences in the toxin concentrations being used. The results are statistically significant, reproducible, and exhibit a dose response, thus suggesting a definite role for synaptobrevin in Ca^{2+}-stimulated ACTH secretion in AtT-20 cells. Another important finding is the lack of effect of either of these toxins on the basal levels of secretion in AtT-20 cells. Much of the literature suggests that basal secretion in AtT-20 cells is not simply constitutive secretion, but due to the regulated pathway (*Matsuuchi & Kelly, 1991*). These results would suggest this not to be true and show that vesicles are being released via a completely different, synaptobrevin-independent pathway.

5.16 Introduction of α–latrotoxin to non-permeabilised AtT-20 cells

α-Latrotoxin (the neurotoxin in black widow spider venom) is a potent stimulator of neurosecretion, through its binding to high-affinity pre-synaptic receptors. It can stimulate massive vesicle release in the presence or absence of Ca^{2+}, in both neuronal and PC12 cells, and this may be due to the presence of two distinct receptors (*Davletov et al., 1996; Krasnoperov et al., 1997*). The effects of α-latrotoxin were investigated in intact AtT-20 cells, using Locke's buffer as the extracellular buffer, with EGTA used to remove extracellular Ca^{2+} in some experiments. The cells were washed with Locke's buffer, after which they were incubated with 5nM α-latrotoxin, with Ca^{2+} or EGTA for 10 or 40min, at room temperature. Supernatants were then removed and assayed for ACTH, the results for which are seen in figure 5.32.

5.17 Discussion

There was no increase in secreted ACTH in the presence of α-latrotoxin, but rather a slight decrease, compared to the control samples. The samples containing the α-latrotoxin in the absence of Ca^{2+} showed an even larger decrease, and increasing the time of incubations (in either the absence or the presence of calcium) had little effect on either. Exactly what caused this decrease is open to discussion, and may be some other factor within the α-latrotoxin preparation. Certainly the results are statistically significant, however further work is required to elucidate mechanisms involved.

The α-latrotoxin sample that was used in this set of experiments was kindly donated by Dr. Robert Chow (Dept. of Physiology, University of Edinburgh), who had also tested it on chromaffin cells. In his experiments massive secretion was seen both in the presence and in the absence of calcium, confirming that the toxin preparation was active. However the experiments on AtT-20 cells show that α-latrotoxin has no effect on ACTH secretion, and if anything actually reduces basal secretion slightly. This indicates a lack of α-latrotoxin receptors, indicating a significant difference between the AtT-20 cell line and chromaffin or neuronal cells.

5.18 Conclusions

The results presented in this chapter confirm that the AtT-20 cells were behaving appropriately in response to various secretagogues, and that the radioimmunassay was sensitive enough to yield reproducible and accurate measurements of these levels of ACTH secretion.

The cells could be permeabilised with digitonin, and subsequently stimulated with 10μM Ca^{2+} to secrete around 26% of the total ACTH content (3 times the basal levels of secretion). Immunofluorescence microscopy was used to prove that under these conditions, with a 15min incubation prior to Ca^{2+}-stimulation, various proteins or drugs could enter the cells and bind to intracellular components.

In this permeabilised cell system, antibodies to synaptotagmin, cofilin and syntaxin had no effect on basal or Ca^{2+}-stimulated levels of ACTH secretion. Recombinant

cofilin, synaptotagmin or αSNAP also had no effect on basal or Ca^{2+}-stimulated ACTH secretion. The introduction of actin-stabilising or -destabilising drugs produced no change in basal or Ca^{2+}-stimulated ACTH secretion, nor in the kinetics of ACTH secretion.

These results suggest that neither actin nor cofilin has a major rate-determining role in ACTH secretion from AtT-20 cell. Antibodies and non-functional recombinant proteins also showed no effect on ACTH secretion, suggesting a lack of involvement of synaptotagmin, syntaxin, αSNAP or synaptotagmin in rate-determining steps, or an inability to interfere with the process. The latter is more likely, particularly in view of the immunofluorescent staining patterns, which suggest that vesicles are docked and soluble factors such as αSNAP have already bound.

Cytosolic rundown (the loss of cytosolic proteins from permeabilised cells) and exocytotic rundown (the loss of Ca^{2+}-stimulated ACTH secretion from permeabilised cells) were also investigated. True exocytotic rundown was only seen at around 90min after permeabilisation, and this could be inhibited by the addition of cytosol. This rundown was also seen by increasing the permeabilisation time to 45min, and again cytosol inhibited this. LDH leakage was assayed as a measure of cytosolic leakage and indicated that cytosolic leakage was much faster and more complete than exocytotic rundown. αSNAP had no effect on exocytotic rundown in that it failed to increase ACTH secretion in cells permeabilised for 45min.

These results are consistent with the idea that secretory vesicles are pre-docked, and αSNAP is pre-bound. Exogenous αSNAP caused no inhibition of exocytotic rundown, suggesting that the drop in secretion is not due to the leakage of αSNAP. The effect of cytosol by no means proves that the drop in secretion seen at 90min is even due to loss of proteins specific to exocytosis. The drop may simply be due to a loss of cell viability over this period of time, which cytosol may protect against in a manner unrelated to effects on exocytosis.

The introduction of Tetanus toxin and Botulinum neurotoxin D light chains into permeabilised AtT-20 cells caused a significant drop in secretion, indicating an important role for synaptobrevin in Ca^{2+}-regulated exocytosis in AtT-20 cells. In

contrast α-latrotoxin, when introduced into intact AtT-20 cells did not cause exocytosis, but slightly reduced basal levels of ACTH secretion.

These results suggest that the cellular machinery involved in Ca^{2+}-regulated exocytosis in AtT-20 cells has similarities to that used by neuronal and chromaffin cells, but that the mechanism of vesicle release may vary in some respects.

Figure 5.1 Optimisation of radioimmunoassay for ACTH

(a) standard curves obtained using different anti-ACTH concentrations. These were plotted as % bound/bound zero (% B/B0) against log ACTH (ng/ml). 'Bound' is the measurement of iodinated ACTH (in cpm) present in the pellet of samples containing 'cold' non-iodinated ACTH. 'Bound zero' is the measured iodinated ACTH (in cpm) in the pellet of samples containing no 'cold' non-iodinated ACTH. The data were all fitted with a third order polynomial curve. (b) shows the B_0 over total counts (TC) obtained for each anti-ACTH concentration.

(a)

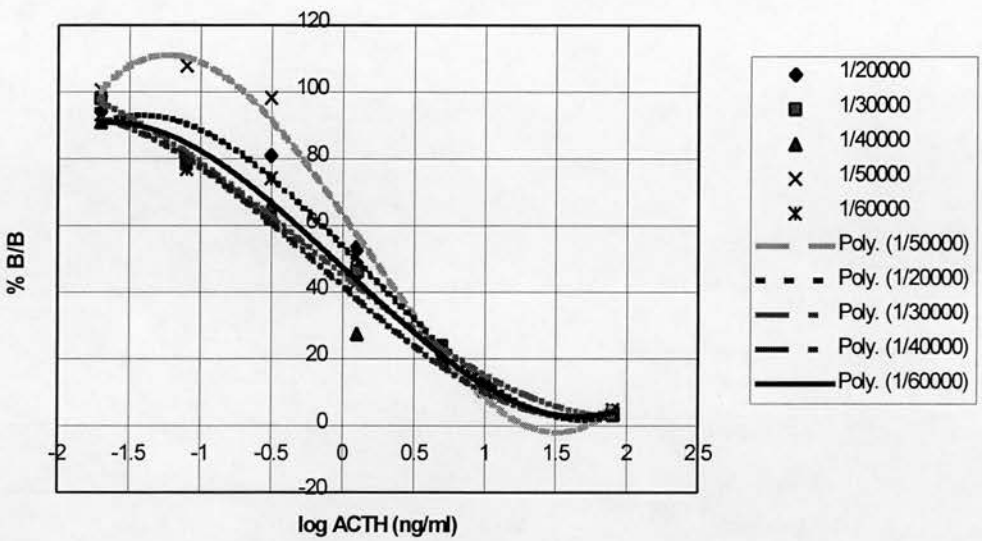

(b)

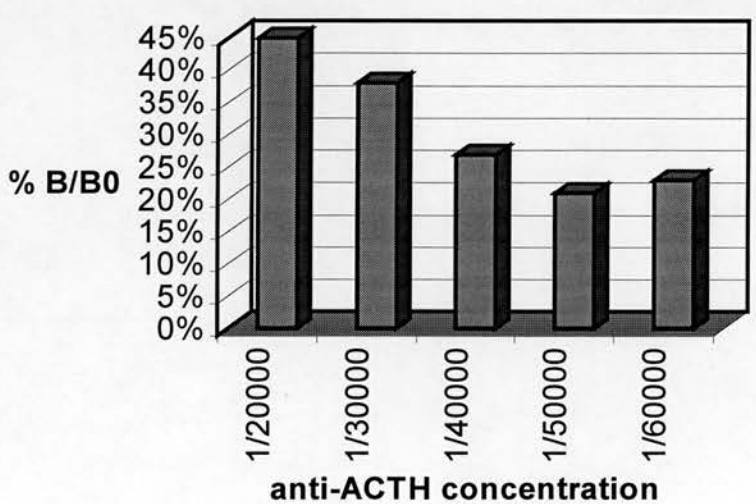

Figure 5.2 Standard curve and formula used to calculate unknown ACTH concentrations of samples.

(a) mean standard curve obtained in an ACTH radioimmunoassay. The values were always plotted $\%B/B_0$ against log ACTH. The equation obtained was as shown and the R value is given below. (b) shows the derivation of the formula of this equation and explains how this was used to calculate ACTH concentrations of samples from their $\%B/B_0$ values.

(a)

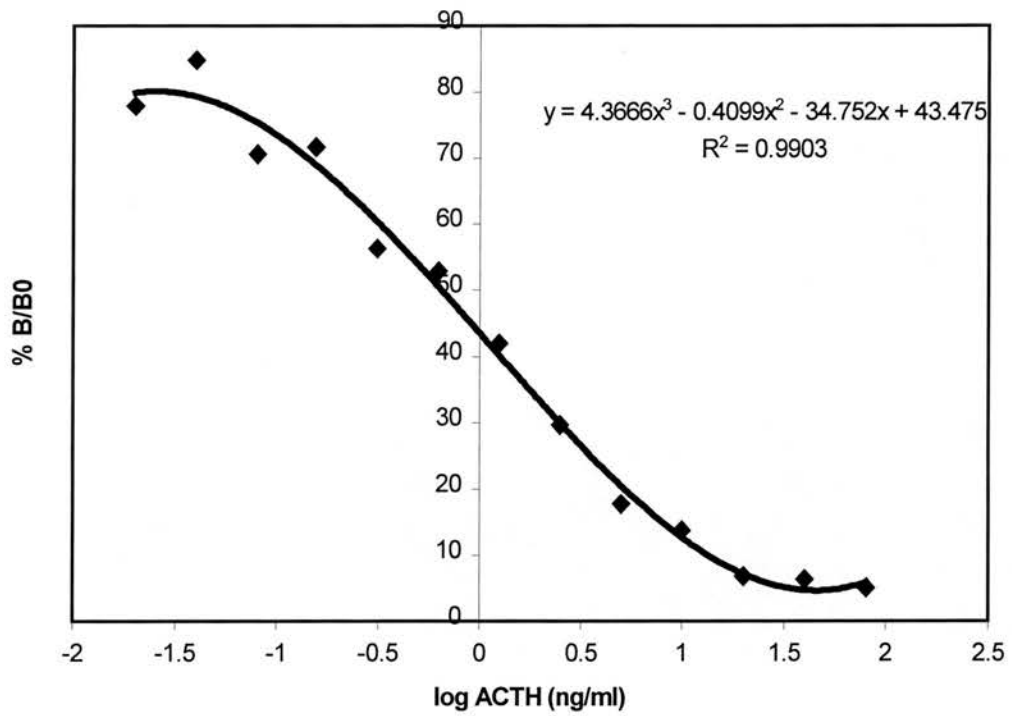

(b)

$f(x) = 4.3666x^3 - 0.4099x^2 - 34.752x + 43.475 = f(x)$

differentiating with respect to x: $f`(x) = 13.0998x^2 - 0.8198x - 34.752$

The value of x cannot be directly found from this equation, however the following expansion of the equation allows substitution of "guess values" into the expanded equation, and x is then determined by an iterative procedure.

The following formula was used:

log ACTH (ng/ml) = $x + (y - f(x)) / f`(x)$

Thus the 'guess value' of x can be 0. This gives a value of 0.249626. This new value of x is then substituted back into the formula, and another value obtained. Eventually the same value is consistently obtained and this is transformed from log ACTH to ACTH concentration (ng/ml). The table below shows an example from the spreadsheets used for all these assays, and shows the calculation for a B/B_0 value of 34.8%, using the previous standard curve and equation. The ACTH concentration obtained was 1.782ng/ml (1.8ng/ml).

y	x	f(x)	f'(x)	log ans	ans
34.8	0	43.475	-34.752	0.249626	1.776748
34.8	0.249626	34.84238	-34.1404	0.250867	1.781834
34.8	0.250867	34.80001	-34.1332	0.250867	1.781835
34.8	0.250867	34.80001	-34.1332	0.250867	1.781835

[where log ans = $x + (y - f(x)) / f`(x)$]

N.B Please note that all subsequent graphs of results within this chapter are based on single experiments however duplicate or triplicate experiments were carried out and gave similar results.

Figure 5.3 Time-course and dose-response of CRF-stimulated exocytosis

(a) time course of ACTH secretion, stimulated with 100nM CRF. (b) dose response curve obtained with increasing concentrations of CRF, all samples having been taken at 30 minutes. All media were pre-warmed to 37°C, and all incubations were at 37°C.

(a)

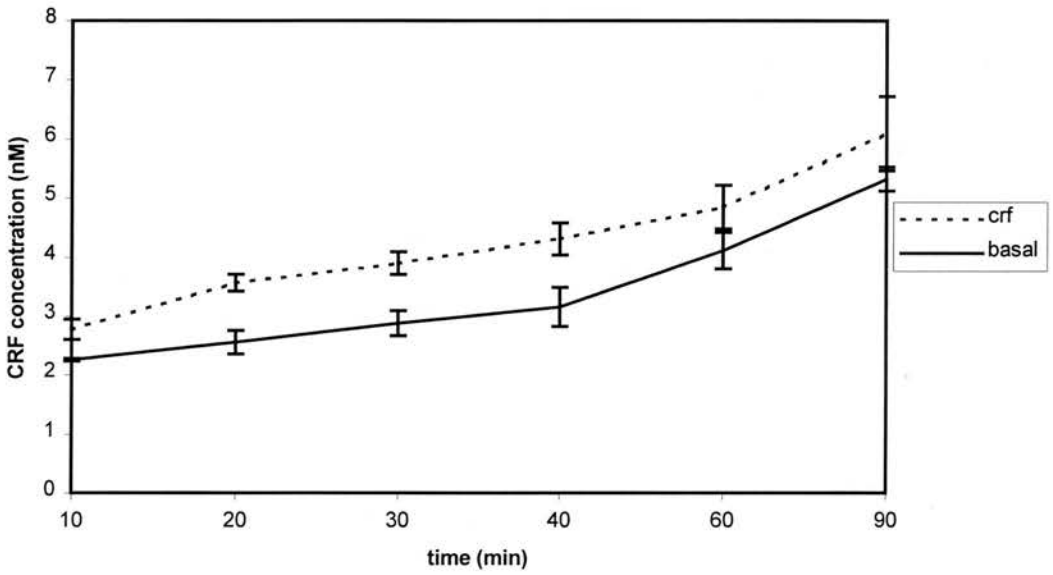

(b)

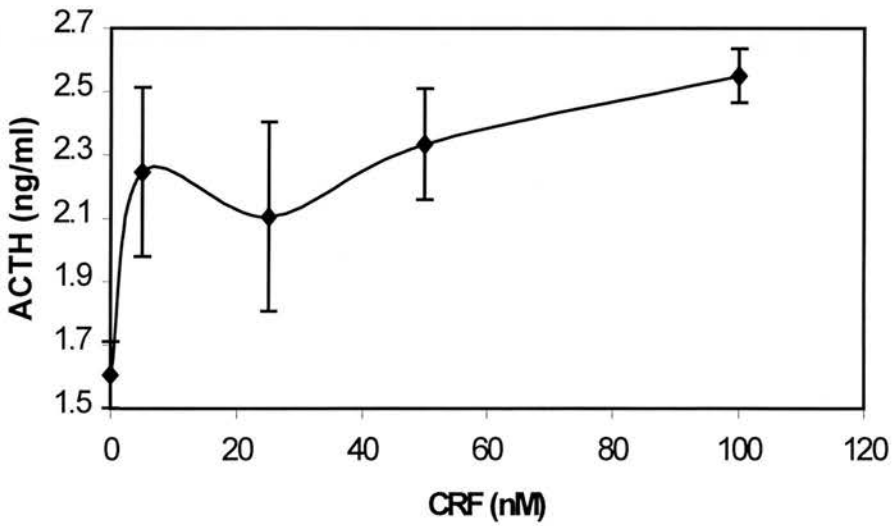

Figure 5.4 Time-course of K^+-stimulated exocytosis

Time course obtained when ACTH secretion was stimulated by depolarisation of AtT-20 cells with 50mM K^+.

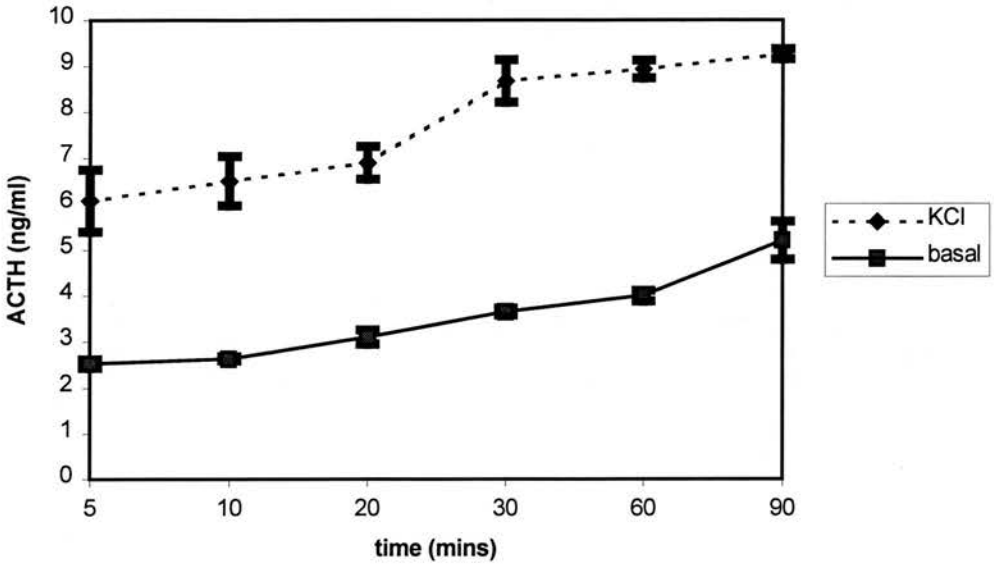

Figure 5.5 Effects of dexamethasone on ACTH secretion stimulated with CRF or K^+

The bar chart shows ACTH secretion in response to 100nM CRF (CRF) or 50mM K^+ (KCl), all over 30min and at 37°C. To assess the effects of the glucocorticoid analogue dexamethasone, the cells were pre-incubated with 100nM for 60min, after which the appropriate secretagogue was used.

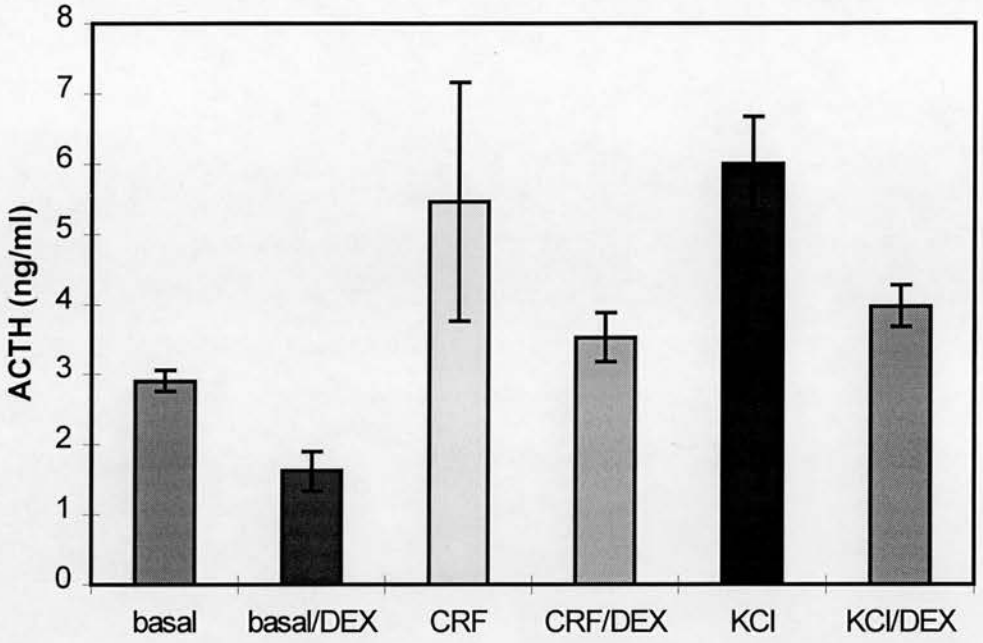

Figure 5.6 Effects of dexamethasone on ACTH secretion stimulated with 8-bromo-cAMP

The bar chart shows the levels of ACTH secretion obtained on stimulation of AtT-20 cells with 5mM 8-bromo-cAMP (1hour incubation at 37°C). Basal levels represent control cells incubated with media only, and dexamethasone was used as in figure 5.5.

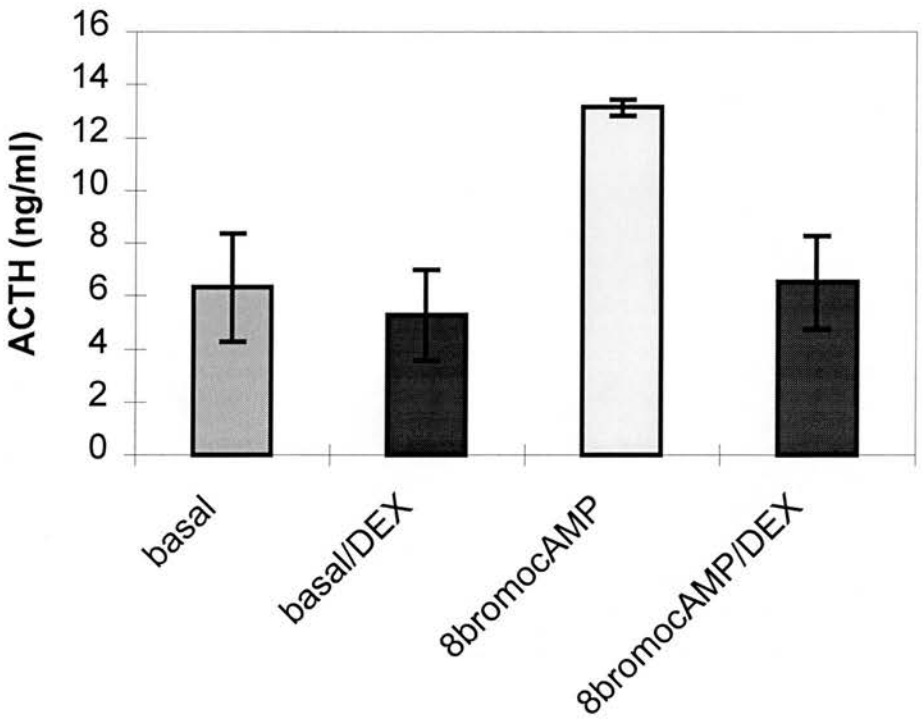

Figure 5.7 Time course of Ba^{2+}-stimulated ACTH secretion

(a) time course of Ba^{2+}-stimulated ACTH secretion up to 5min. (b) a similar time course up to 60 min. All incubations were at room temperature. Ba^{2+} stimulation is labelled Ba, whilst basal levels (i.e. cells incubated with Locke's buffer) are labelled as Bactrl

(a)

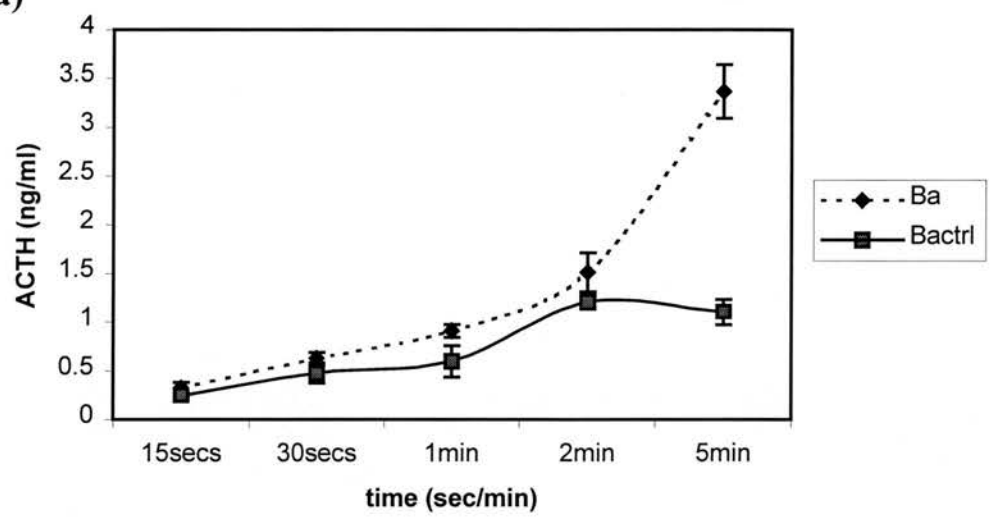

(b)

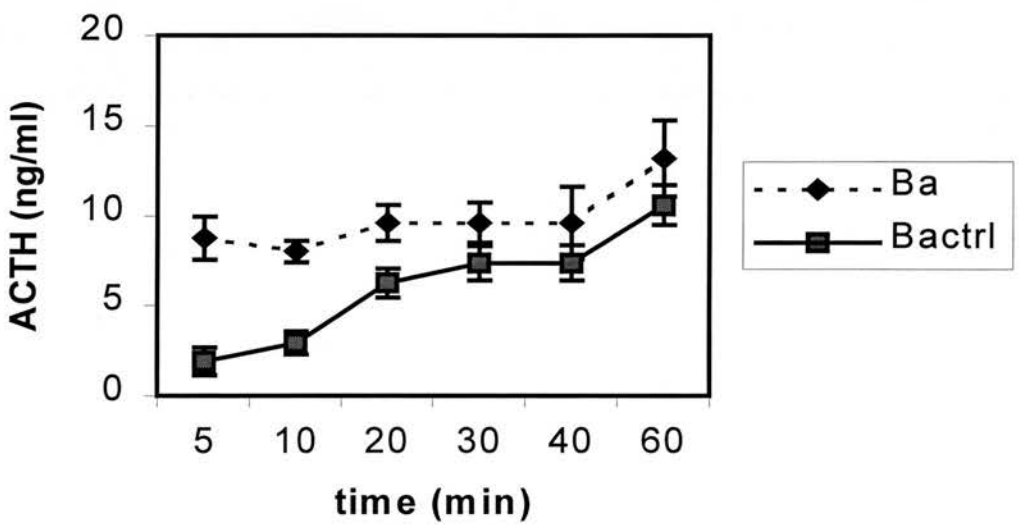

Figure 5.8 Effects of digitonin permeabilisation on AtT-20 cells

(a) concentration of ACTH measured in the permeabilisation buffer after removal from the cells. Cells were permeabilised for 5 or 10min, with the concentrations of digitonin shown. (b) total lysis values for AtT-20 cells before digitonin permeabilisation (TL (pre-dig)) and after digitonin permeabilisation (TL (post-dig)), compared to typical values released by Ba^{2+}-stimulation (Ba stim) and Ca^{2+}-stimulation (Ca stim). Two basal levels of ACTH secretion are shown (Ba ctrl and ca ctrl) as the buffers vary in these two types of stimulation. The Ca^{2+}-stimulation used 20mg/ml digitonin for 10min.

(a)

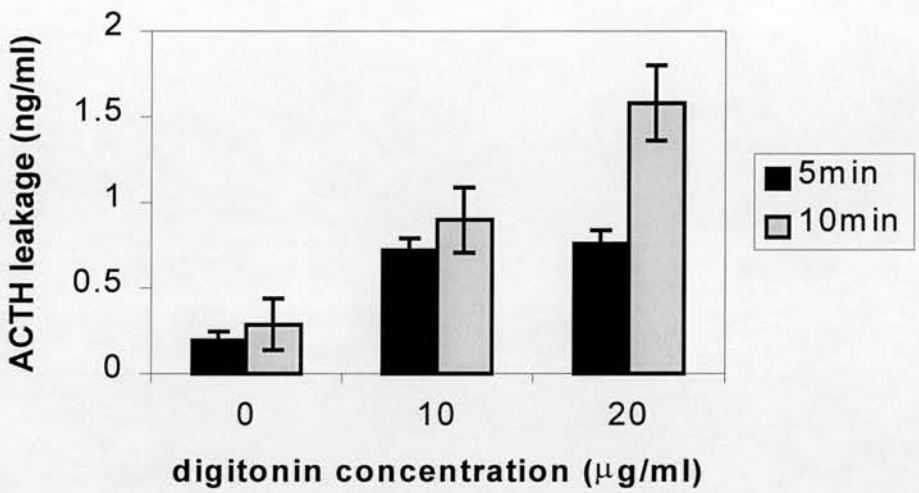

(b)

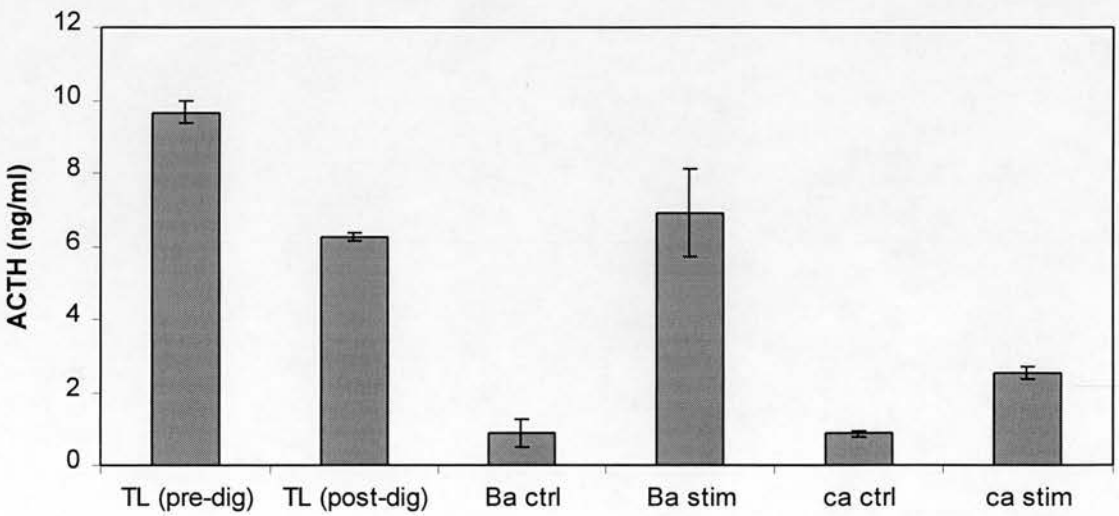

Figure 5.9 Dose-response curve and time-course of Ca^{2+}-stimulated ACTH secretion

(a) ACTH secretion obtained using varying Ca^{2+} concentrations. All samples were taken at 10min. (b) Time course of ACTH secretion after stimulation with 10μM Ca^{2+} (+Ca), or in the presence of 0mM Ca^{2+} (-Ca).

(a)

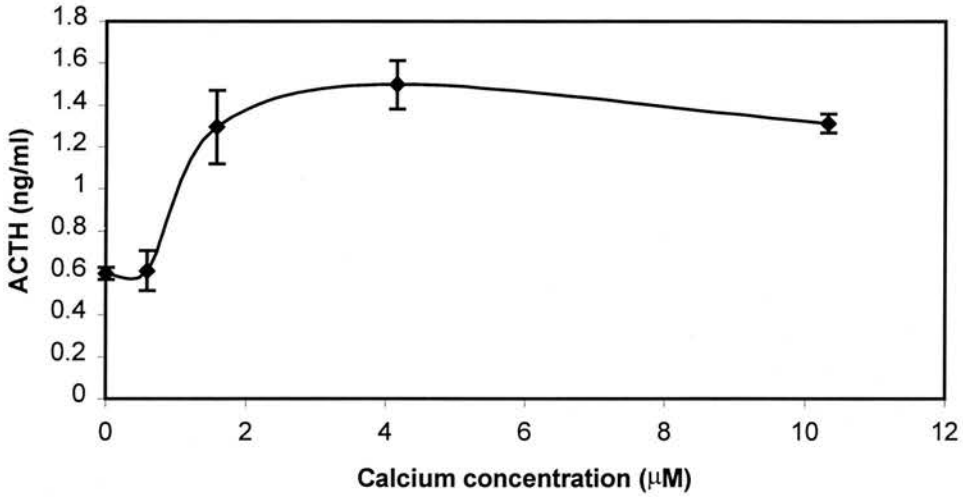

(b)

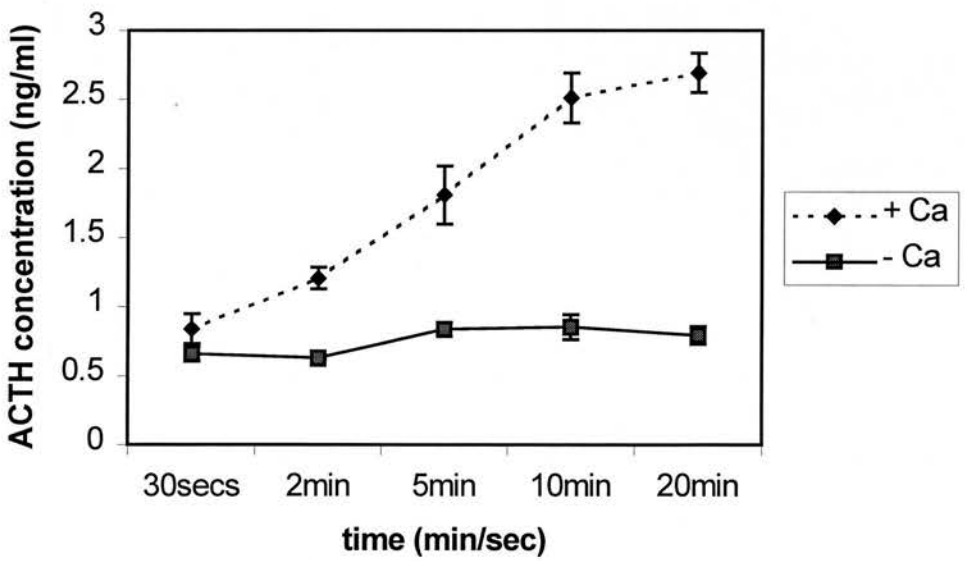

Figure 5.10 Effect of temperature on Ca^{2+}-stimulated ACTH secretion

The bar chart shows the effect of temperature variation on the levels of ACTH secretion obtained using 10μM Ca^{2+} for 10min. Cells were permeabilised at room temperature as usual, after which they were incubated at room temperature or 37°C for 15min, followed by a 10min stimulation with 10μM Ca^{2+} at room temperature or 37°C. Basal levels are represented by -Ca, stimulated cells are shown by +Ca; at room temperature (RT), or 37°C (37).

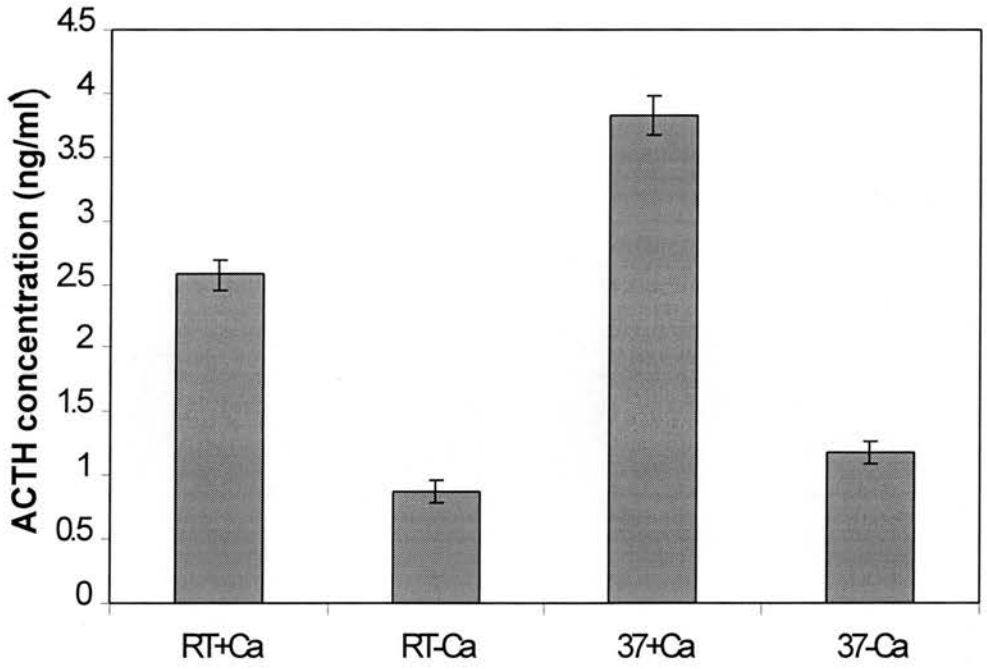

Figure 5.11 Immunofluorescence microscopy as a method to test the entry of various factors into permeabilised AtT-20 cells

The figures below show the staining patterns obtained with digitonin-permeabilised AtT-20 cells labelled with with various immunofluorescent probes. (a) staining with a plant actin-binding protein ZMAP-B3 conjugated to GFP, (b) phalloidin conjugated to FITC and (c) anti-cofilin rabbit antiserum followed by goat anti-rabbit serum conjugated to rhodamine. All concentrations and dilution were as detailed in Chapter 4, and ZMAP-B3 was used at a concentration of 100μg/ml.

(a)

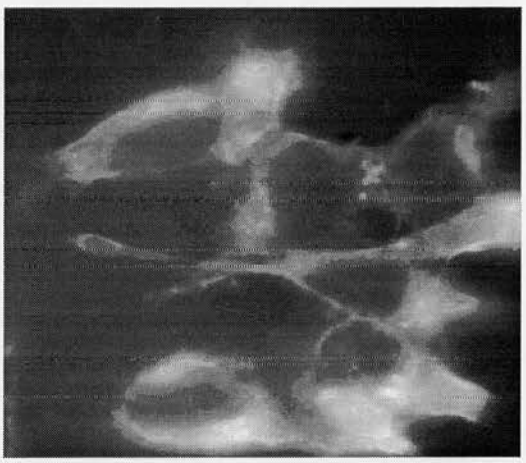

(b)

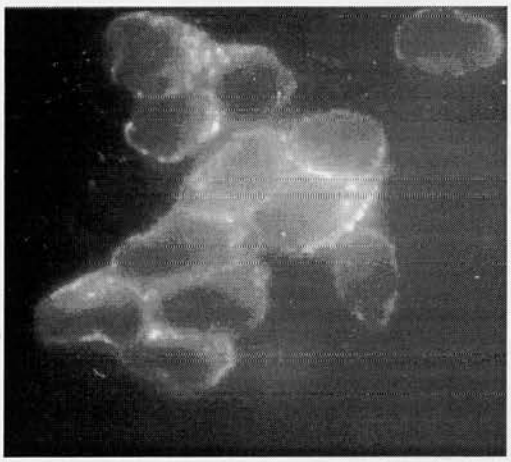

(c)

Figure 5.12 Effect of antibodies on ACTH secretion from permeabilised AtT-20 cells

The bar chart below shows ACTH secretion obtained from permeabilised AtT-20 cells which had been incubated with various antisera, prior to stimulation with 10μM Ca^{2+}. Anti-cofilin, anti-synaptotagmin, anti-syntaxin and NRS antisera were as previously described in figures 3.22, 3.10, 3.11 and 3.17 respectively, and anti-cofilin was used without affinity purification. All antisera were diluted 1/100 in the pre-incubation buffer. Ca^{2+}-stimulation is represented by (+), and the control by (-), normal rabbit serum (nrs), anti-cofilin (C), anti-synaptotagmin (p65),anti-syntaxin (S) and no antiserum (N).

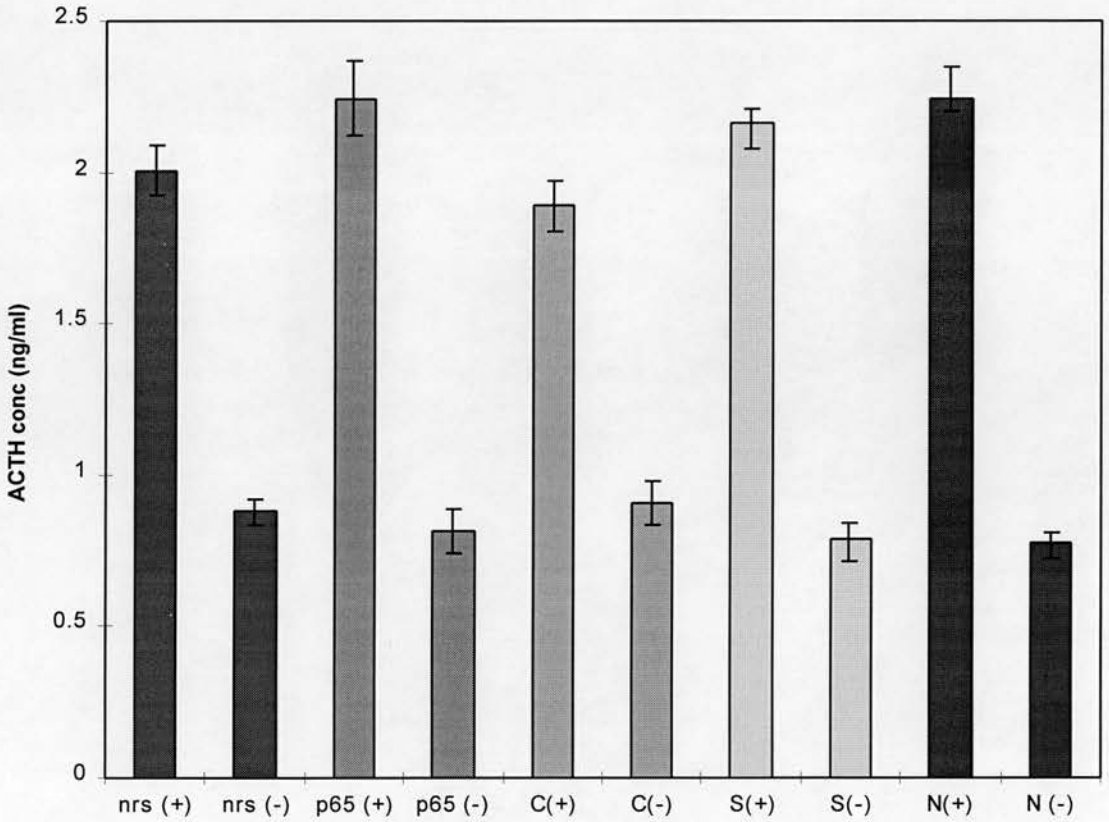

Figure 5.13 Effects of recombinant cofilin on ACTH secretion from permeabilised AtT-20 cells

(a) secretion obtained from cells incubated with 100μg/ml recombinant cofilin for 15min prior to the addition of the Ca^{2+}-stimulation buffer. Recombinant human cofilin (21kDa) was obtained from Dr. Sutherland Maciver. (b) Gel of a sample of cofilin (20μg); molecular weight markers are shown in kDa at the side. Cofilin was stored as a stock solution in 10mMTris-HCl buffer containing DTT and NaN_3, at a concentration of 100mg/ml. This was diluted in the pre-incubation buffer, to a concentration of 100μg/ml. A control of 100μg/ml BSA was used, as well as a control with no protein additions, however both these controls contained the equivalent amounts of Tris buffer, without cofilin. The presence of 10μM Ca^{2+} is shown by (+), and its absence as (-), whilst BSA is the BSA control, N the control with no protein additions, and cof is recombinant cofilin.

(a)

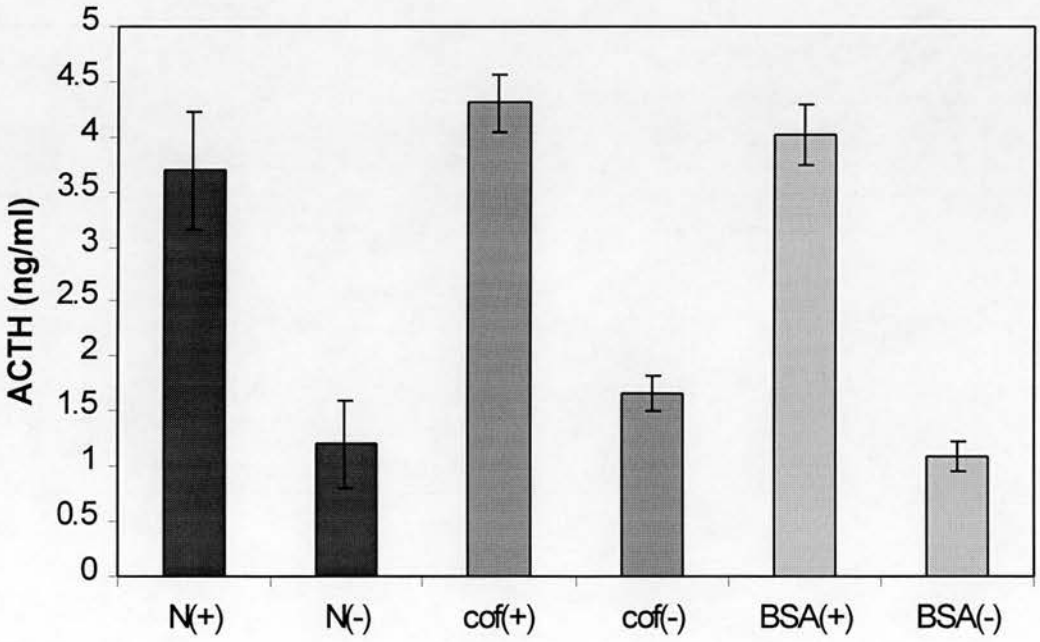

(b)

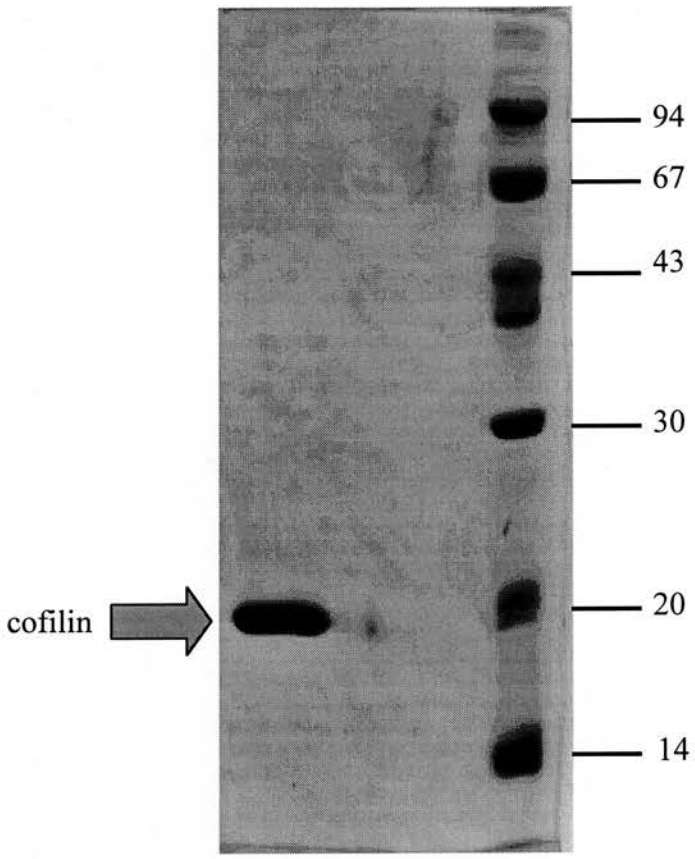

Figure 5.14 Effects of recombinant synaptotagmin on ACTH secretion from permeabilised AtT-20 cells

(a) secretion obtained from cells incubated with 100μg/ml recombinant synaptotagmin (cytoplasmic domain) in the 15min incubation stage prior to the addition of the Ca^{2+}-stimulation buffer. Recombinant bovine synaptotagmin I cytoplasmic domain was obtained from Leonora Ciufo (Biochemistry Department, University of Edinburgh). (b) gel of synaptotagmin; molecular weight markers are shown in kDa at the side. Passage through BioGel P-6DG was used to transfer synaptotagmin into the correct intracellular buffer. Lanes 1 and 2 respectively show 20μg synaptotagmin before and after equilibration with BioGel. A control of 100μg/ml BSA was used, as well as a control with no protein additions, and both contained the equivalent amounts of intracellular buffer and were also equilibrated with BioGel. The presence of 10μM Ca^{2+} is shown as (+), and its absence as (-), whilst BSA represents the BSA control, N the control with no protein additions, and p65 the presence of recombinant synaptotagmin.

(a)

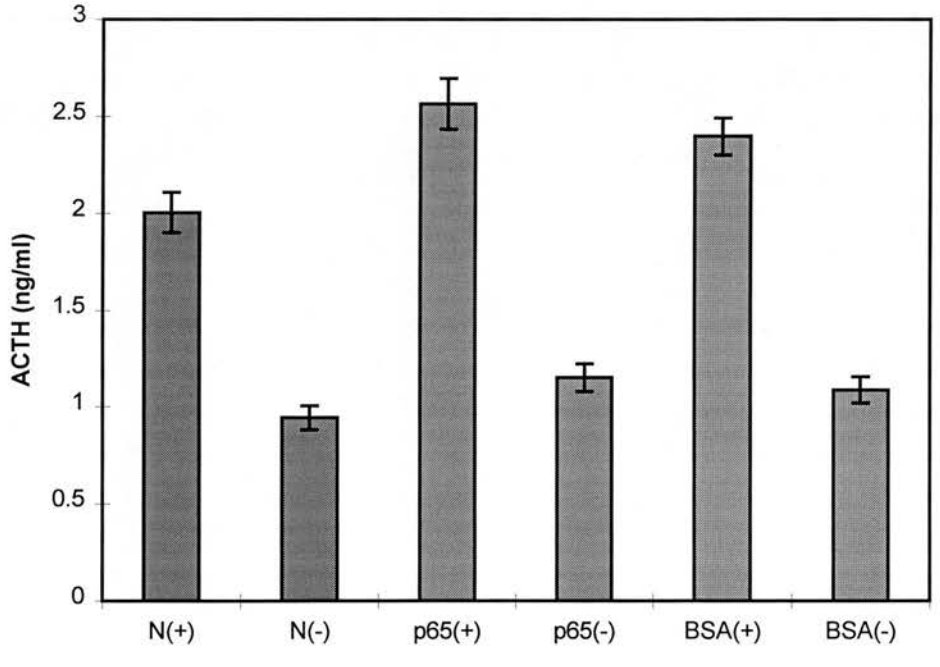

(b)

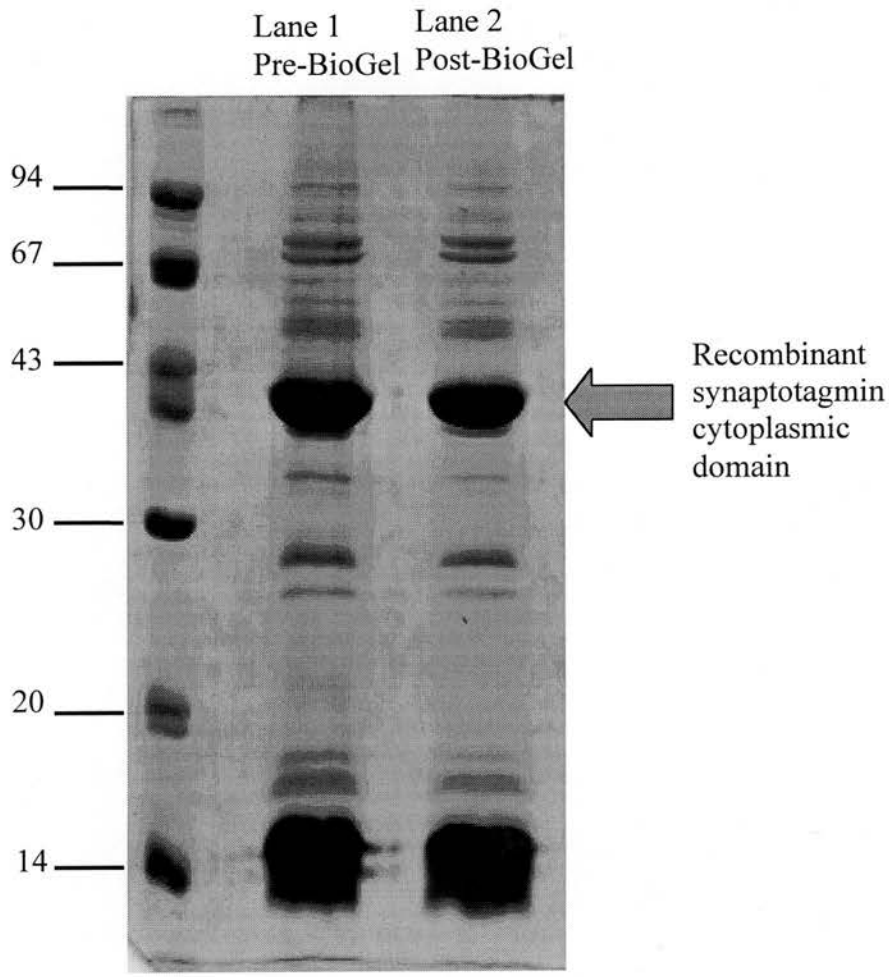
Lane 1
Pre-BioGel
Lane 2
Post-BioGel
94
67
43
30
20
14
Recombinant
synaptotagmin
cytoplasmic
domain

Figure 5.15 Time course of ACTH release from permeabilised AtT-20 cells, incubated with recombinant cofilin

The details of this experiment were exactly as in figure 5.12, except that following addition of the Ca^{2+}-stimulation buffer, samples were taken at 2, 5 and 10min. The control for this experiment was intracellular buffer containing 100μg/ml BSA. Samples taken from cells incubated with cofilin are labelled as cof with (+) or (-) showing the presence or absence of 10μM Ca^{2+} respectively. Samples taken from cells incubated with BSA are labelled as BSA with (+) or (-) showing the presence or absence of 10μM Ca^{2+} respectively.

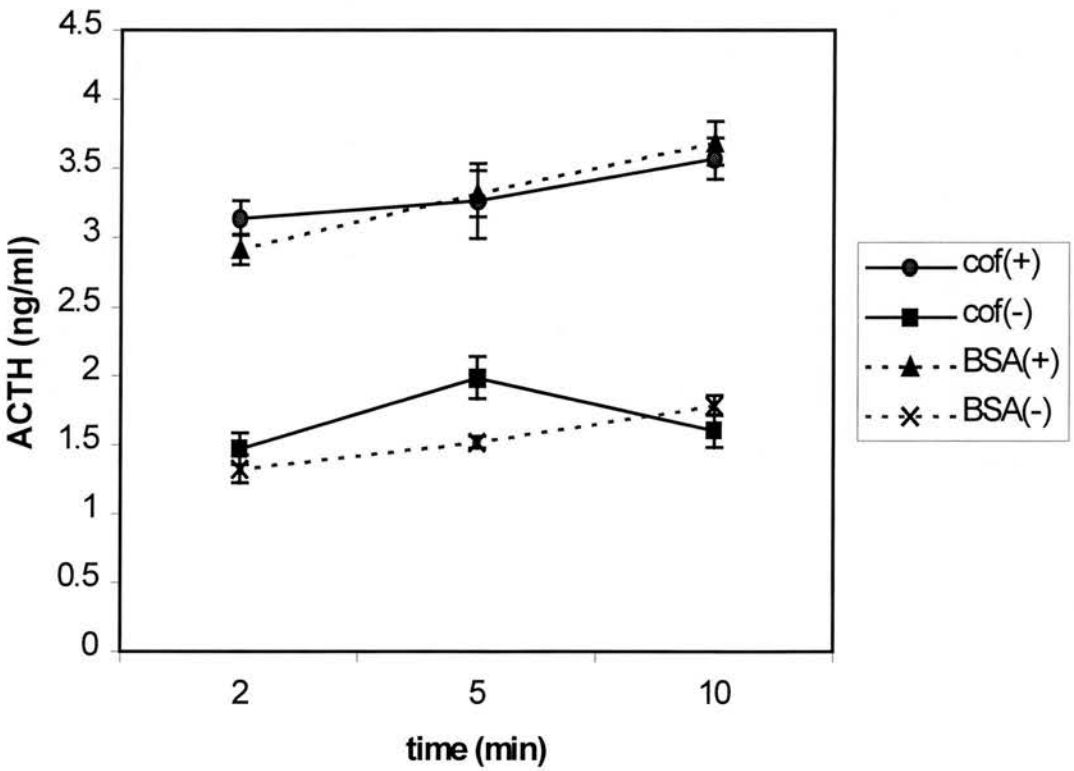

Figure 5.16 Effect of phalloidin on ACTH secretion from permeabilised AtT-20 cells

Permeabilised AtT-20 cells were incubated with phalloidin (27μg/ml), prior to Ca^{2+}-stimulation. As the stock was stored in ethanol, the control was the intracellular buffer containing the appropriate volume of ethanol. Following Ca^{2+}-stimulation samples were taken at 2, 5 and 10 min. The presence of 10μM Ca^{2+} is shown as (+), its absence as (-), control levels are shown as CTRL, and samples containing phalloidin as PHAL.

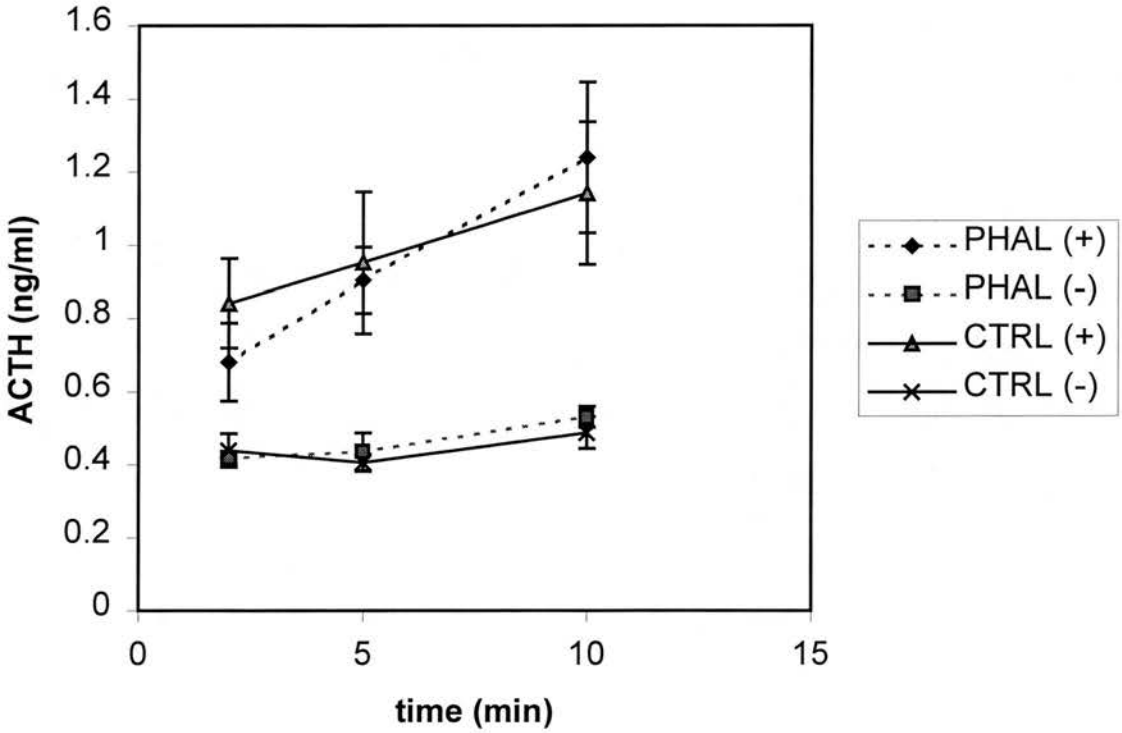

Figure 5.17 Effect of cytochalasin on ACTH secretion from permeabilised AtT-20 cells

Permeabilised AtT-20 cells were incubated with Cytochalasin D (10μM) prior to stimulation with 10μM Ca^{2+}. Cytochalasin was stored as a stock solution in DMSO, so the control contained the appropriate concentration of DMSO. The presence or absence of Ca^{2+} is indicated as (+) or (-) respectively, whilst cytochalasin samples are shown as CYCH, and controls as CTRL.

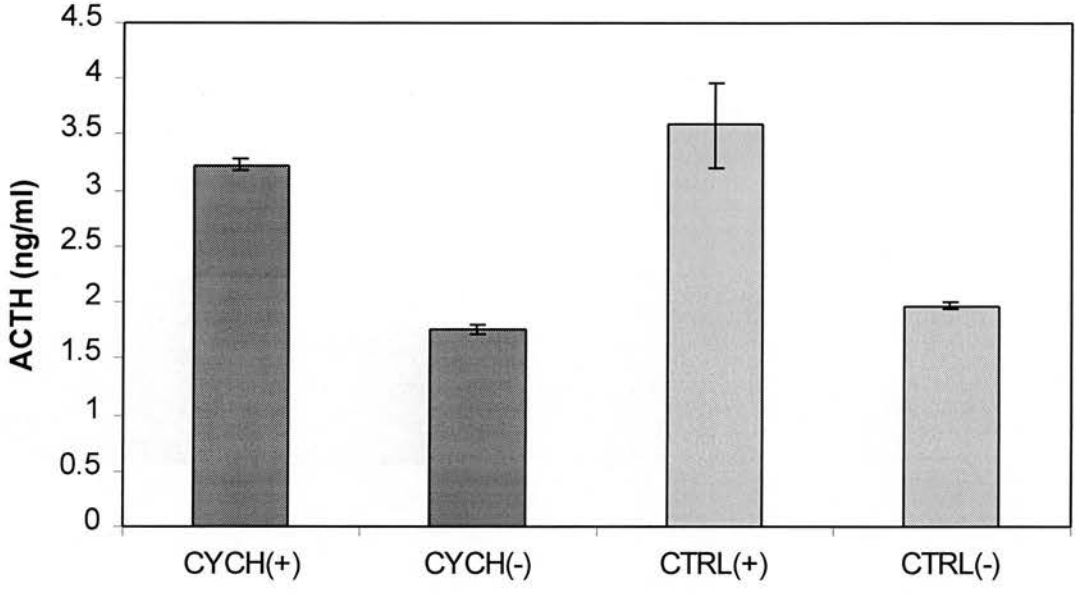

Figure 5.18 Exocytotic rundown in permeabilised AtT-20 cells

The graph below represents the effect on ACTH release of increased incubation times, prior to Ca^{2+}-stimulation of ACTH secretion. The presence of Ca^{2+} is shown as CALCIUM, while its absence is shown as BASAL.

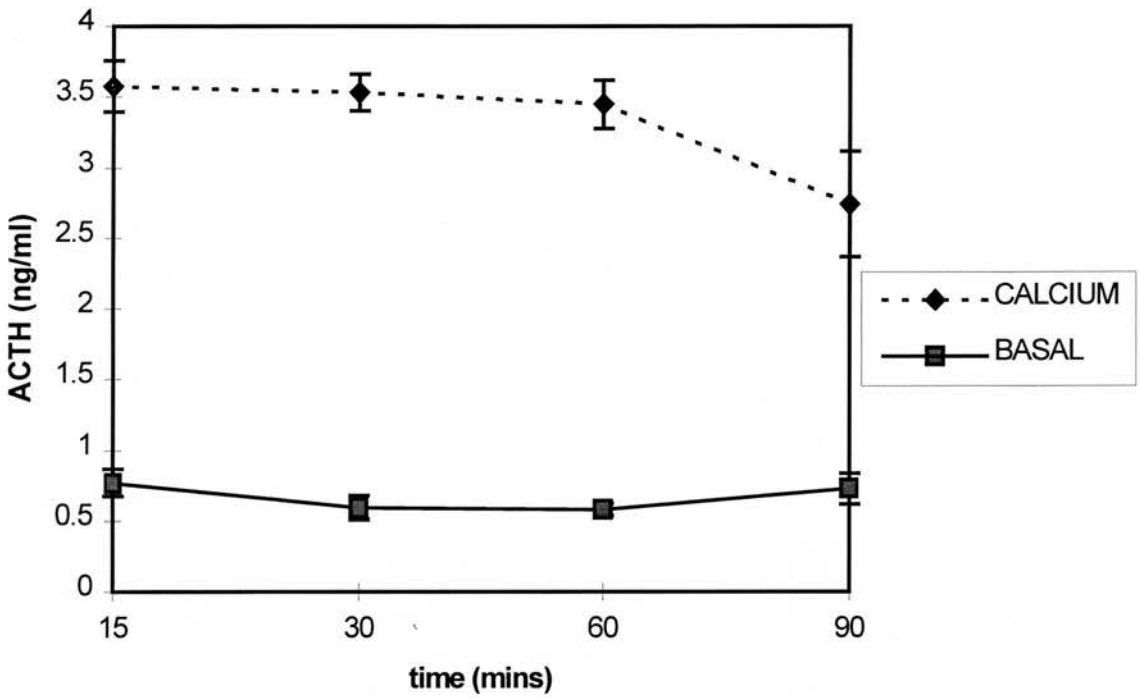

Figure 5.19 Exocytotic rundown in permeabilised AtT-20 cells and introduction of rat brain cytosol

The barchart below shows the effect of increasing both the pre-Ca^{2+} incubation times prior to Ca^{2+}-stimulation, the permeabilsation time itself, and the effects of the introduction of cytosol. Rat brain cytosol was used at a concentration of 1.5mg/ml protein and is shown as CYT, and the presence and absence of Ca^{2+} is shown as (+) or (-) respectively. The various incubation times prior to Ca^{2+}-stimulation were 0, 15 and 90min respectively, and are shown as the first three groups of columns. The increased permeabilisation time was 45min, and is displayed in the last group of columns.

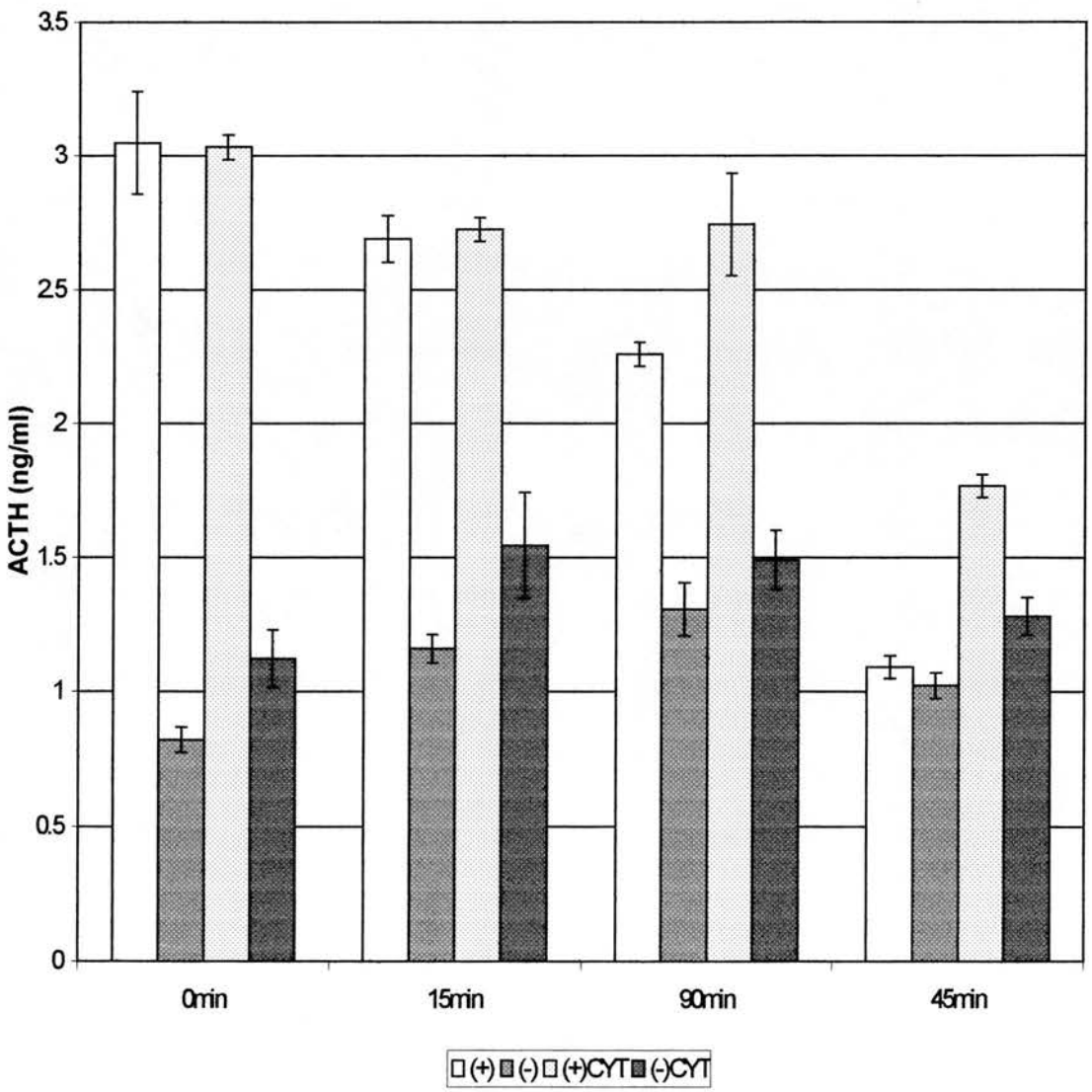

Figure 5.20 Cytosolic rundown in permeabilised AtT-20 cells

The bar chart below shows the leakage of LDH (measured in arbitory units) from permeabilised AtT-20 cells. AtT-20 cells were permeabilised in 24 well plates with 20μg/ml digitonin for 10min as usual, and then incubated in the usual pre-Ca^{2+} incubation buffer for 15, 30 and 60min. An additional permeabilisation time of 45min was also used, following which the cells were incubated with pre-Ca^{2+} incubation buffer for 15min (shown as 45min/15min). LDH activity was estimated in the digitonin-containing permeabilisation buffer (PB) and in the pre-Ca^{2+} incubation buffer (intracellular buffer; IC). Controls were these buffers without the presence of digitonin (-D), permeabilised samples being shown as (+D).

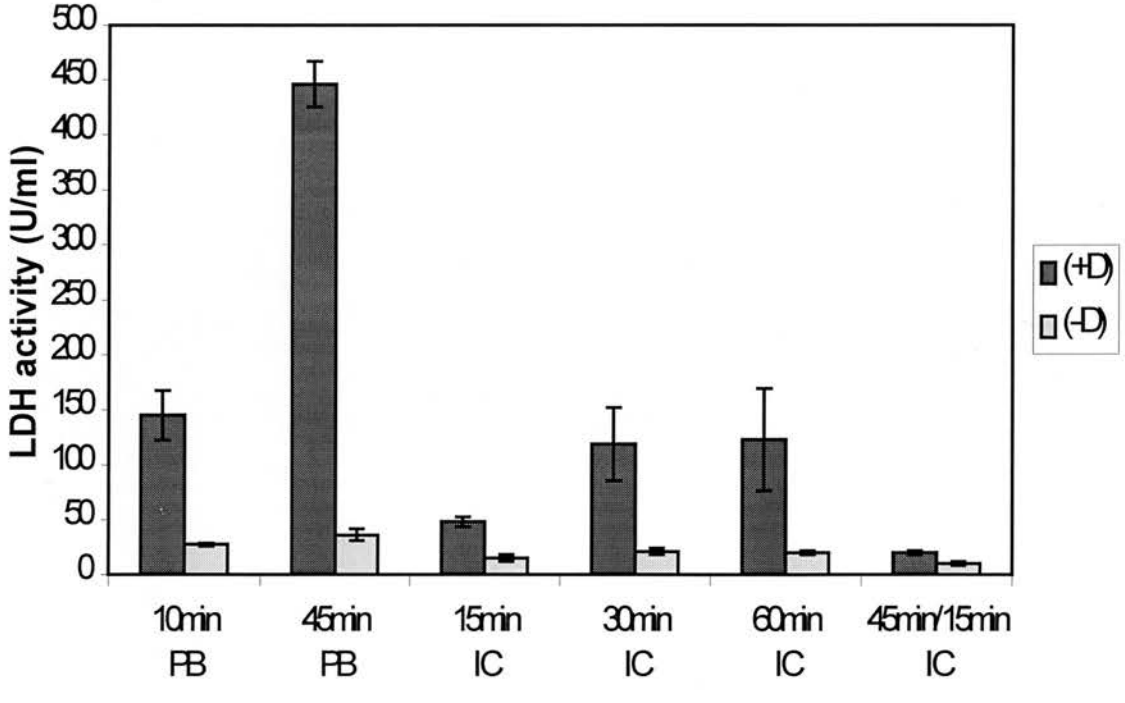

Figure 5.21 Effect of introduction of recombinant αSNAP on secretion from permeabilised AtT-20 cells

(a) the effect of recombinant αSNAP, on Ca^{2+}-stimulated ACTH secretion in permeabilised AtT-20 cells. The cells were permeabilised with 20μg/ml digitonin for 10min, and then incubated with pre-Ca^{2+} incubation buffer containing 53μg/ml αSNAP or BSA, for 15, 30 or 60min, before stimulation with Ca^{2+}. The presence or absence of 10μM Ca^{2+} is indicated by (+) or (-) respectively. (b) gel of recombinant αSNAP (20μg); molecular weight markers are shown on the left hand side in kDa, and 36kDa recombinant αSNAP is also labelled. * is some spill-over from an adjacent lane in the gel, and not contamination the recombinant αSNAP sample. αSNAP was obtained from Professor R. Burgoyne and Richard Barnard (University of Liverpool).

(a)

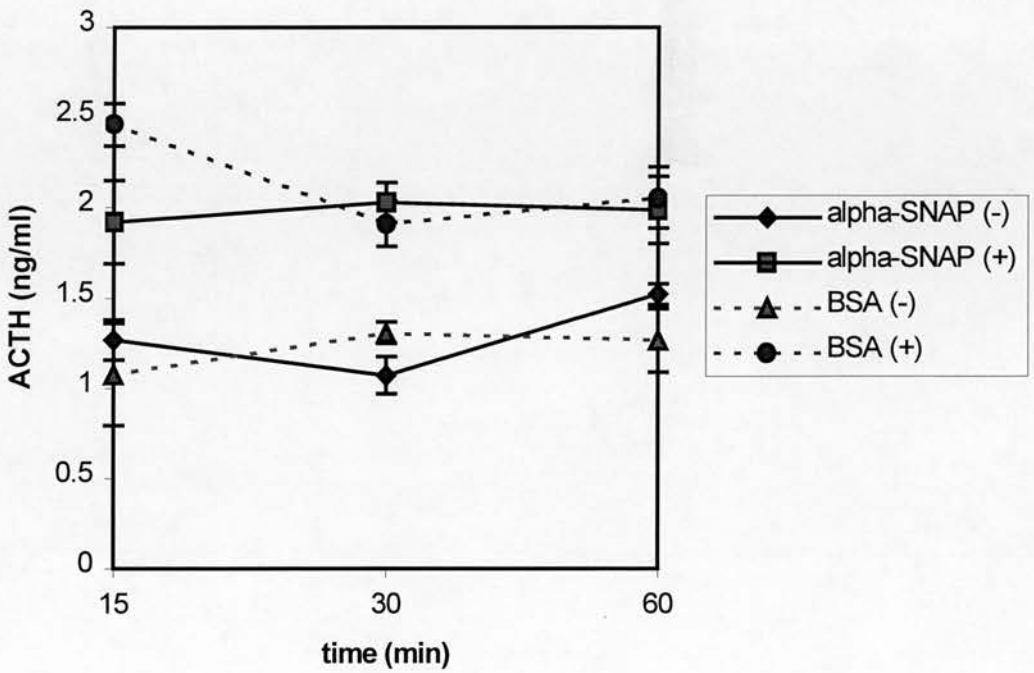

(b)

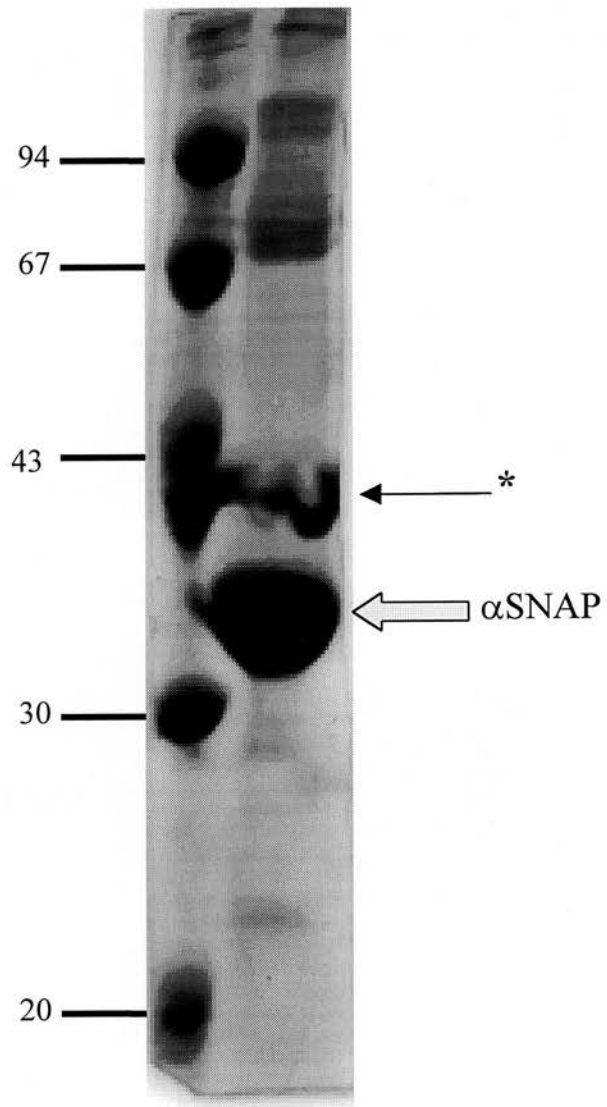

Figure 5.22 Introduction of αSNAP into extensively permeabilised AtT-20 cells

The bar chart below displays the results obtained on the introduction of recombinant αSNAP into AtT-20 cells that had been permeabilised with 20μg/ml digitonin for 45min. 53μg/ml αSNAP or BSA included in the pre-Ca^{2+} incubation buffer before stimulation with 10μM Ca^{2+}. The presence or absence of Ca is indicated by (+) or (-).

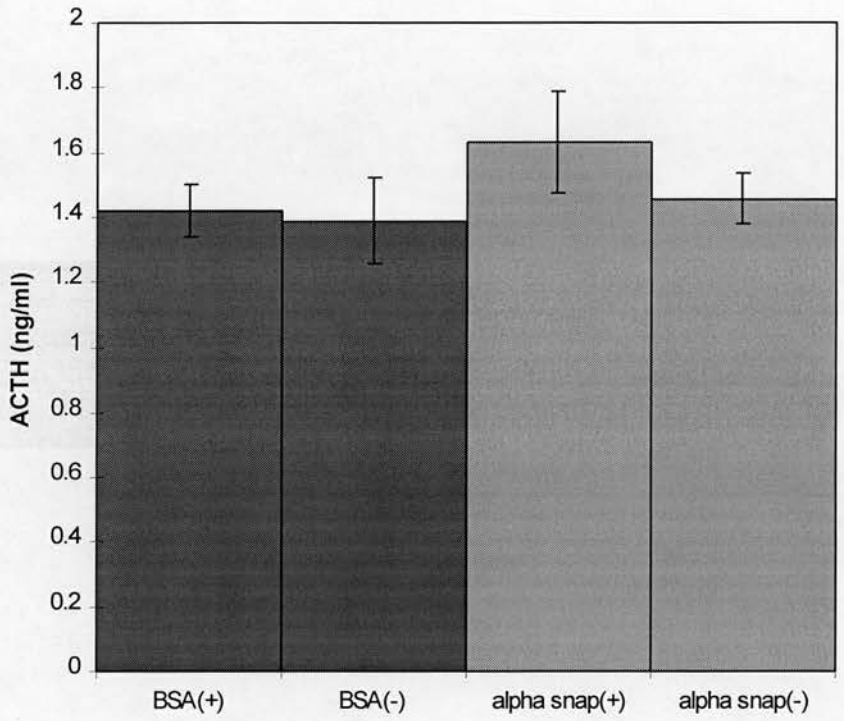

Figure 5.23 Optimisation of TeTX-LC purification

Following overnight incubation with 9ml lysate, the Ni-agarose was washed 5X with 4ml SE buffer (pH8.0), 10X with 4ml SE buffer (pH6.5) and 14X with 0.5ml SE buffer (pH5.0). 20µl samples of each fraction were loaded on an polyacrylamide gel in the following order: Lane 1 – molecular weight markers (kDa); lane 2 – supernatant of sonicated NM522 cells (before binding to Ni-agarose); lane 3 – supernatant of sonicated NM522 cells (after binding to Ni-agarose); lane 4 – first wash with SE buffer (pH8.0); lane 5 – last wash with SE buffer (pH8.0); lane 6 – first wash with SE buffer (pH6.5); lane 7 – last wash with SE buffer (pH6.5); lanes 8-10 – washes 1-3 with SE buffer (pH5.0); lane 11 – molecular weight markers; lanes 12-22 – washes 4-14 with SE buffer (pH5.0). Lanes 2 and 3 were heavily over-loaded but serve to show the small percentage of bacterial protein which bound to the Ni-agarose. The fraction which was tested on permeabilised cells has been marked with an arrow.

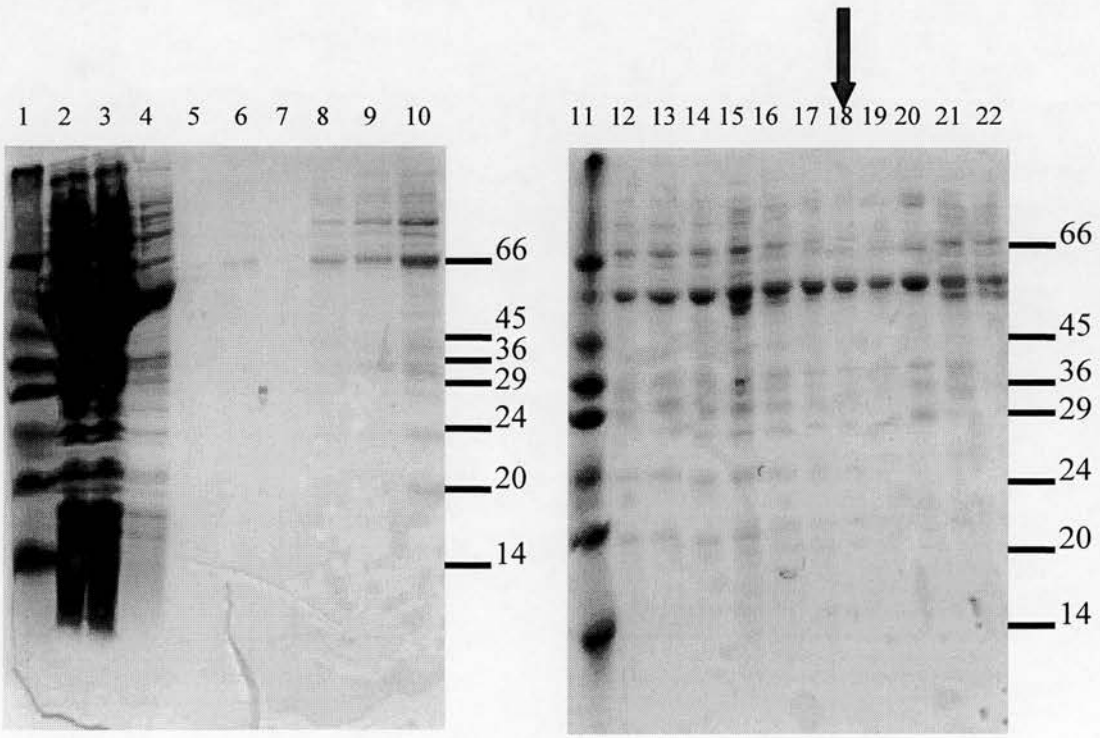

Figure 5.24 Development of purification protocol for Botulinum neurotoxin D light chain

Following overnight incubation with 9ml lysate, Ni-agarose was washed 5X with 1ml SE buffer (pH8.0) and once with 0.5ml SE buffer containing 10, 20, 30, 40, 50, 60, 70, 80 or 90mM imidazole (9 washes in total). This was then followed by three washes with 0.5ml SE buffer containing 100mM imidazole. All buffers were pH8.0. 20µl samples of each fraction were loaded on a polyacrylamide in the following order: Lane 1 – molecular weight markers (kDa); lane 2 – last wash with SE buffer (pH8.0); lanes 3-11 – washes with SE buffer containing increasing imidazole concentrations of 10,20,30,40,50,60,70,80 and 90mM respectively; lanes 12-14 – washes 1-3 with SE buffer containing 100mM imidazole; lane 15 – first wash with SE buffer (pH8.0); the first wash with SE buffer (pH8.0) was loaded out of order, and this wash was in fact the first to be done.

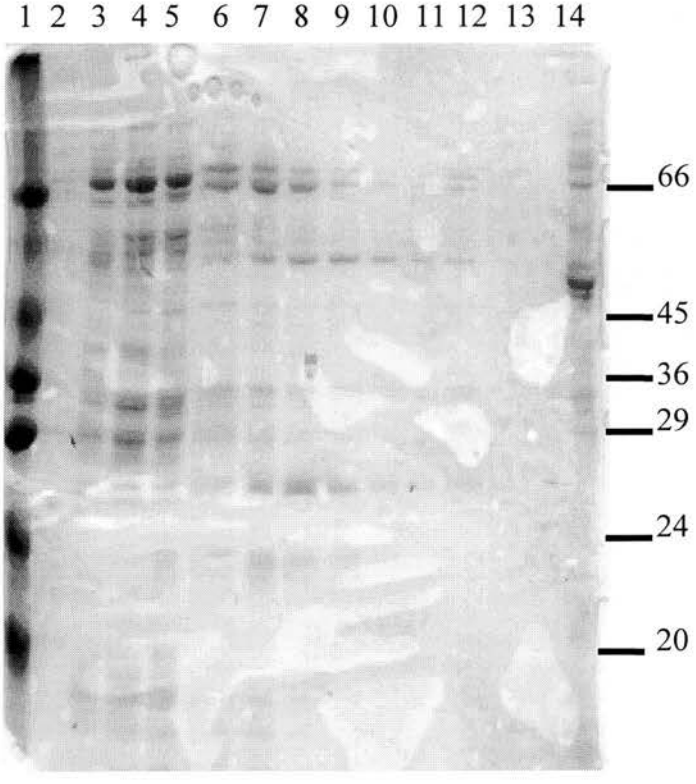

Figure 5.25 Purification of BoNTD-LC

The protocol used in figure 5.23 was modified, in that washing was restricted to an imidazole concentration of 30mM, and elution with 100mM imidazole. The Ni-agarose was washed 10X with 4ml SE buffer (pH8.0), 10X with 4ml SE buffer containing 10mM imidazole, 10X with 4ml SE buffer containing 30mM imidazole, and 5X with 0.5ml SE buffer containing 100mM imidazole; all buffers were pH8.0. 20µl samples of fractions were run on polyacrylamide gels and were loaded as follows: lane 1 – molecular weight markers (kDa); lane 2 – supernatant of sonicated NM522 cells before binding to Ni-agarose; lane 3 – supernatant of sonicated NM522 cells after binding to Ni-agarose; lane 4 – first wash with SE buffer (pH8.0), lane 5 – last wash with SE buffer (pH8.0); lane 6 – first wash with SE buffer containing 10mM imidazole; lane 7 – last wash with SE buffer containing 10mM imidazole; lane 8 – first wash with SE buffer containing 30mM imidazole; lane 9 – last wash with SE buffer containing 30mM imidazole; lane 10 – first wash with SE buffer containing 100mM imidazole (pre-BioGel treatment); lane 11 – as for 10 but after BioGel equilibration; lanes 12-15 – washes 2-5 with SE buffer containing 100mM imidazole. Gel 1 shows an experiment with BoNTD-LC transformed cells, and gel 2 shows the same for control (non-transformed) cells.

Gel 1

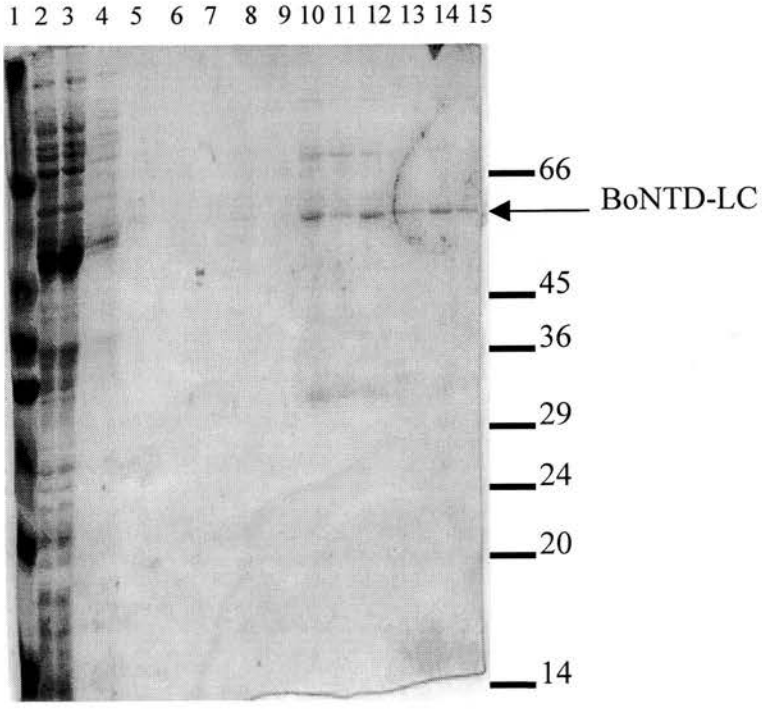
1 2 3 4 5 6 7 8 9 10 11 12 13 14 15
66
BoNTD-LC
45
36
29
24
20
14

Gel 2

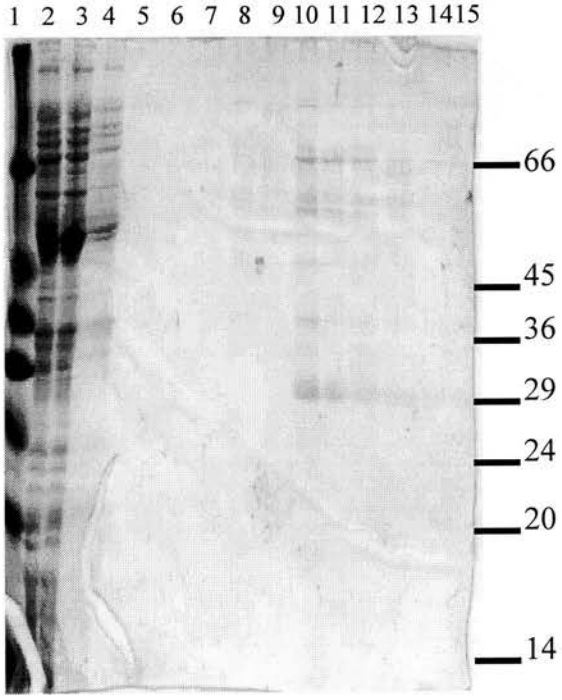
1 2 3 4 5 6 7 8 9 10 11 12 13 1415
66
45
36
29
24
20
14

Figure 5.26 Purification of TeTX-LC

This purification was carried out as detailed in 2.6, but non-transformed NM522 cells were used as a control, and were treated in the same way. 20µl samples of fractions were run on polyacrylamide gels. The gels were loaded as follows: lanes 1 & 16 – molecular weight markers (kDa); lane 2 – supernatant of sonicated cell extract prior to Ni-agarose binding; lane 3 – supernatant of sonicated cell extract after Ni-agarose binding; lane 4 – first wash with SE buffer (pH8.0); lane 5 – last wash with SE buffer (pH8.0); lane 6 – first wash with SE buffer (pH6.5); lane 7 – last wash with SE buffer (pH6.5); lanes 8-15 – washes 1-9 with SE buffer (pH5.0); lanes 17-22 – as for lanes 2-7 above, but with control cells; lanes 23-25 – first, third and ninth wash with SE buffer (pH 5.0); lane 26 – control cells tenth wash with SE buffer (pH5.0) pre-BioGel equilibration; lane 27 – as for lane 26 but after BioGel equilibration; lanes 28 and 29 – as for lanes 26 and 27 but transformed cell samples.

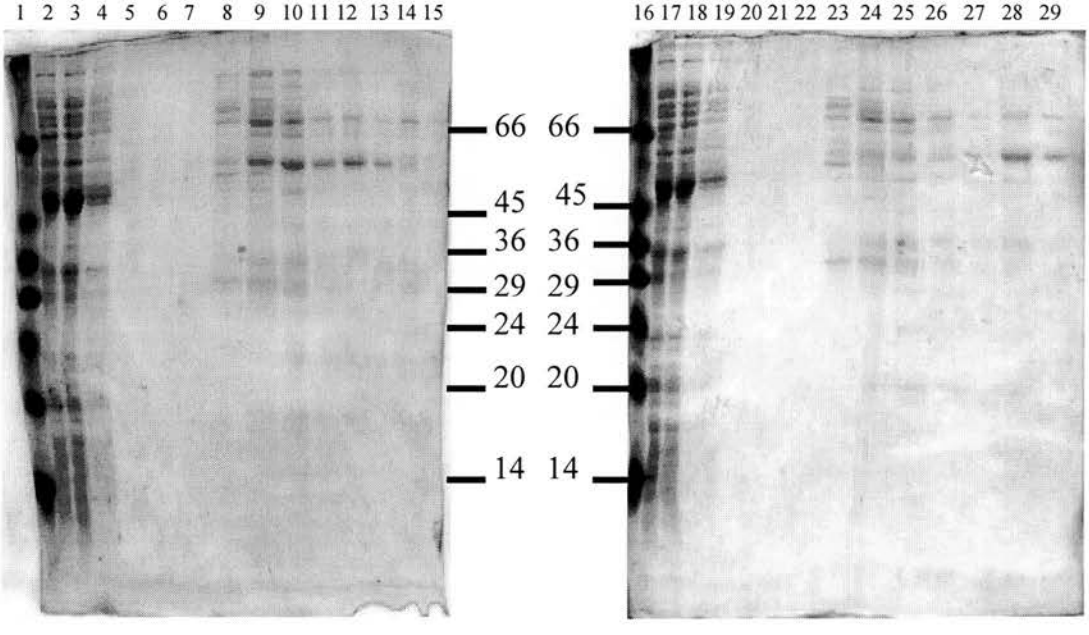

Figure 5.27 Introduction of BoNTD-LC into permeabilised AtT-20 cells, followed by Ca^{2+}-stimulation of ACTH secretion

The barchart shows secretion from permeabilised cells after introduction of the recombinant BoNTD-LC (prepared as in 2.6). The cells were incubated with the toxin for 20min and then stimulated with 10μM Ca^{2+}. BoNTD shows samples taken from cells incubated with BoNTD-LC, and then incubated with (+) or without 10μM Ca^{2+} (-). The control samples are shown as BSA (100μg/ml), and were again stimulated with Ca^{2+} (+) or not (-).

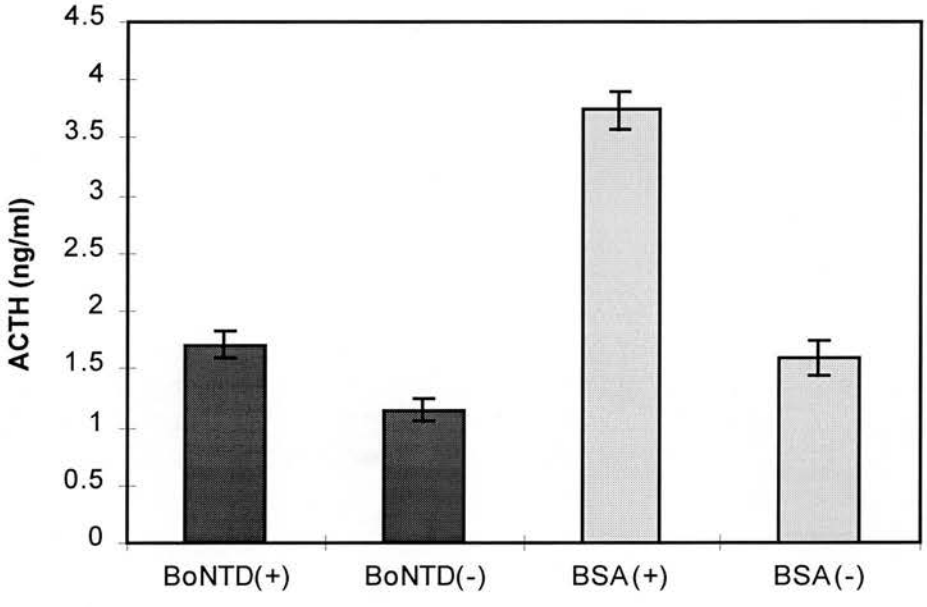

Figure 5.28 Introduction of TeTX-LC into permeabilised AtT-20 cells, followed by Ca^{2+}-stimulation of ACTH secretion

The bar chart below shows the results obtained on incubation of permeabilised AtT-20 cells with TeTX-LC for 20min, followed by stimulation of the cells with 10μM Ca^{2+}. In all cases (+) shows the presence of Ca^{2+}, whereas (-) shows the absence of Ca^{2+} (i.e. basal levels of secretion), and ctrl shows normal secretion levels. The presence of TeTX-LC is shown as TeTX whilst the control of non-transformed bacterial cells is shown as TeTXctrl. Two different concentrations of TeTX/TeTXctrl were used: 200 indicates the addition of 200μl TeTX/TeTXctrl to 4.8ml intracellular buffer, and 0.5ml of this was used per well; 20 indicates the addition of 20μl TeTX/TeTXctrl to 4.98ml intracellular buffer, and 0.5ml of this was used per well. 'buff' was a control in which the SE buffer (pH5.0) was passed through BioGel P-6DG and then added to the pre-Ca^{2+} incubation buffer at the aforementioned concentrations. This was to check that it was having no effect on normal AtT-20 cell secretion and that buffer exchange was occurring efficiently, thus causing no change in free Ca^{2+} concentrations.

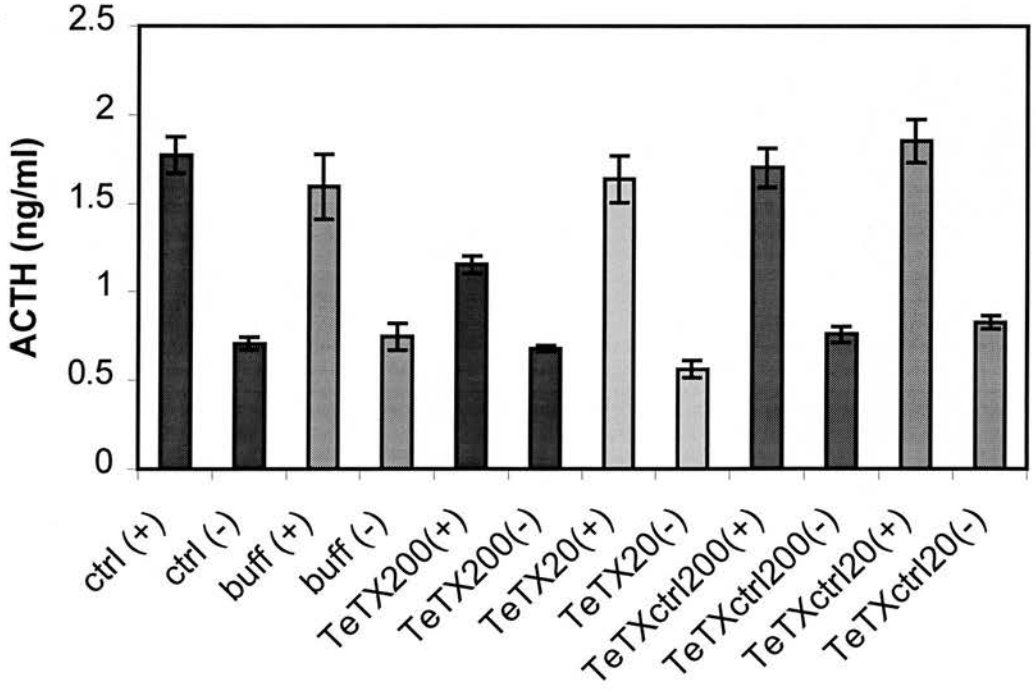

Figure 5.29 Quantitation of BoNTD-LC and TeTX-LC

(a) 20µl samples of toxin fractions were run on a 10% acrylamide gel in the following order: lane 1 – molecular weight markers (kDa); lane 2 – TeTX-LC before BioGel; lane 3 TeTX-LC after BioGel; lane 4 TeTX-LC control before BioGel; lane 5 TeTX-LC control after BioGel; lane 6 – BoNTD-LC control before BioGel; lane 7 – BoNTD-LC control after BioGel; lane 8 – BoNTD-LC before BioGel; lane 9 – BoNTD-LC after BioGel. (b) shows the figures obtained using densitometry and Peterson's assay.

(a)

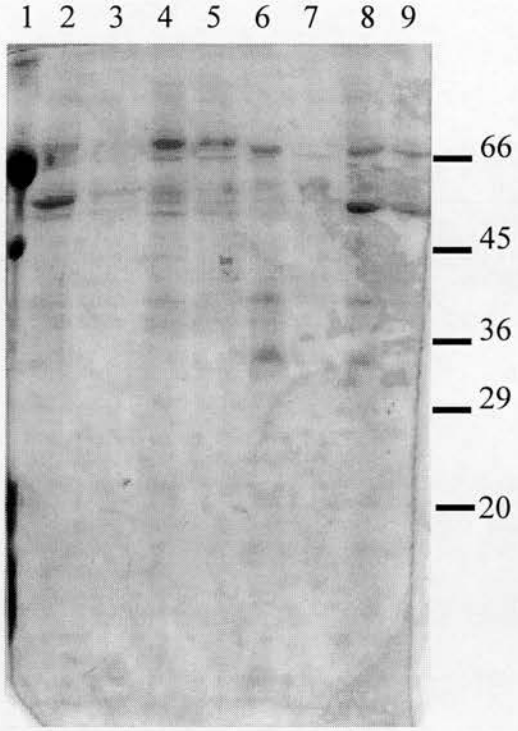

(b)

Total protein concentration (lane 3) = 140µg/ml
% TeTX-LC of total protein = 27%
TeTX-LC concentration = 37.8µg/ml (following a 20% loss due to BioGel treatment)
Total protein concentration (lane 8) = 209mg/ml
% BoNTD-LC of total protein = 23%
BoNTD-LC concentration = 48.07µg/ml (following a 37% loss due to BioGel treatment)

Figure 5.30 Introduction of quantitated TeTX-LC into permeabilised AtT-20 cells

The effect of quantitated TeTX-LC on Ca^{2+}-stimulated ACTH secretion from AtT-20 cells. Stimulation with 10μM Ca^{2+} is shown as (+), whilst basal secretion (no Ca^{2+} present) is shown as (-). Normal stimulation is displayed as normal, the presence of TeTX-LC as TeTX, and the presence of TeTX-LC control as TeTXctrl. Toxin concentrations are shown in nM. Control samples are also shown as nM, and this relates to the volume of control preparation added to the pre-Ca^{2+} stimulation buffer, i.e. the same as for the toxin preparation.

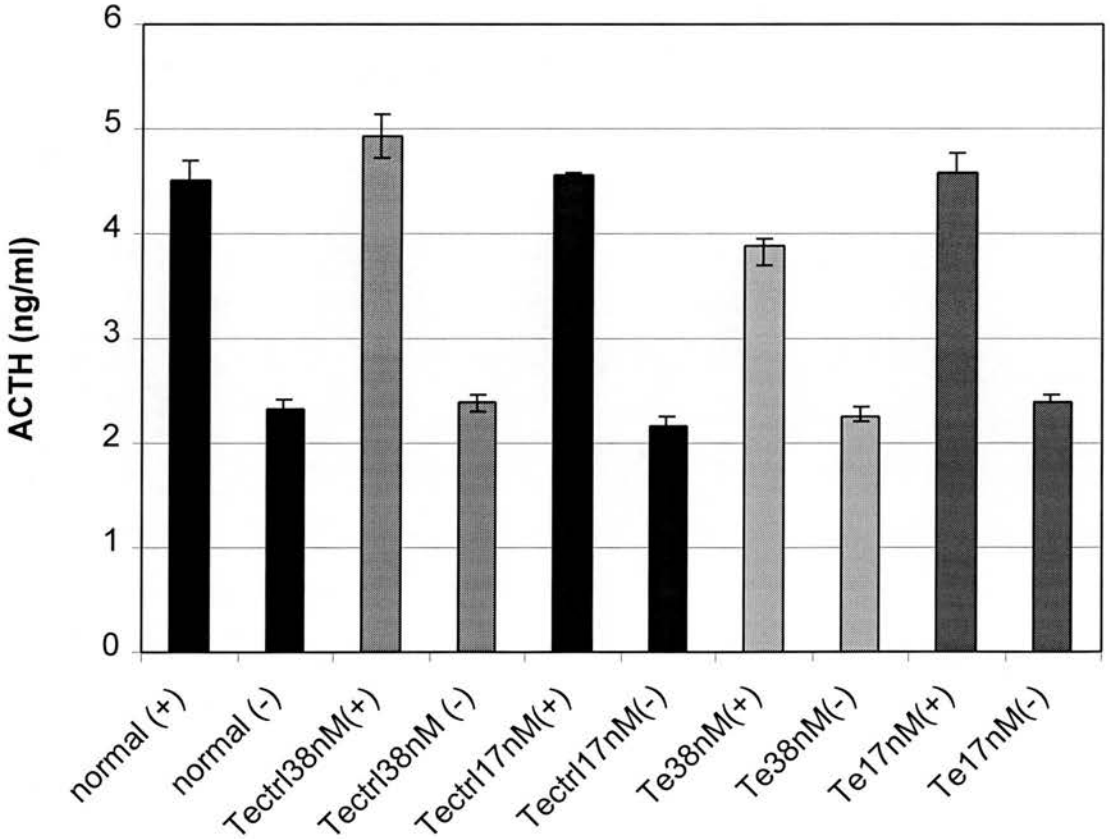

Figure 5.31 Introduction of quantified BoNTD-LC into permeabilised AtT-20 cells

The effect of quantitated BoNTD-LC on Ca^{2+}-stimulated ACTH secretion from AtT-20 cells. Stimulation with 10μM Ca^{2+} is shown as (+), whilst basal secretion (no Ca^{2+} present) is shown as (-). Normal stimulation is displayed as normal, the presence of BoNTD-LC as BoNTD, and the presence of BoNTD-LC control as BoNTDctrl. Concentrations used are shown in nM. Control samples are also shown as nM, and this relates to the volume of control preparation added to the pre-Ca^{2+} stimulation buffer, i.e. the same as for the toxin preparation.

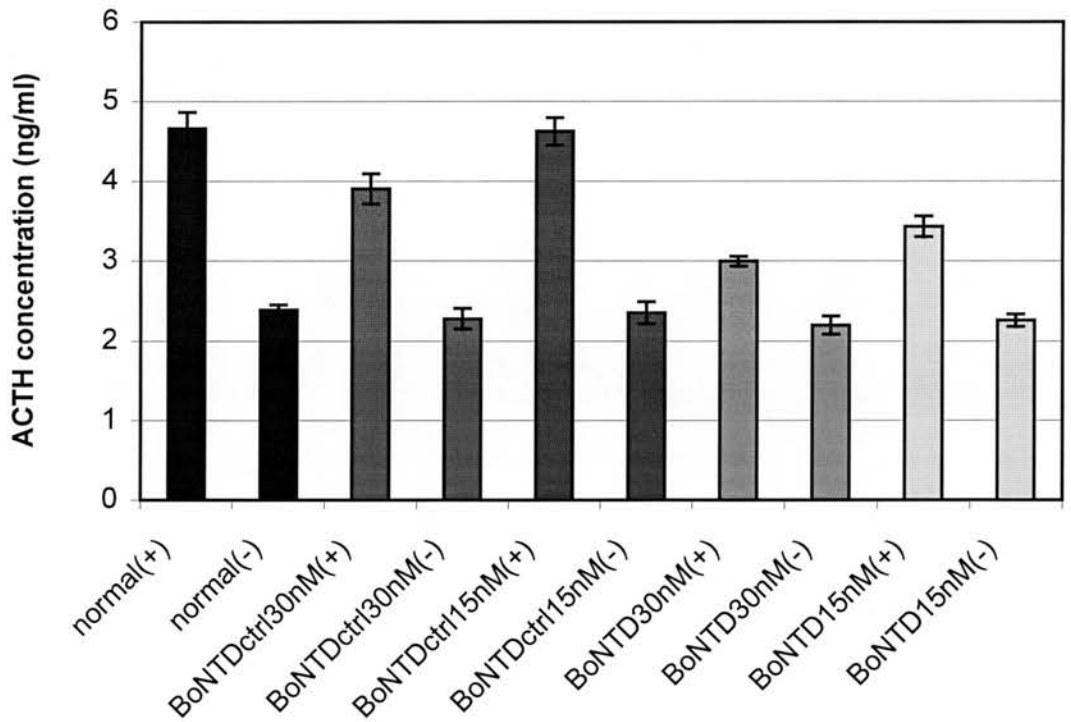

Figure 5.32 Treatment of intact AtT-20 cells with α-latrotoxin

AtT-20 cells were washed with Locke's buffer (see 2.5.1.1), and then incubated with the same buffer for 10 or 40min, in the presence or absence of 5nM α-latrotoxin. The bar chart below shows the resulting ACTH secretion, the time points being shown as 10 or 40, and the presence or absence of α-latrotoxin as 'latro' or 'ctrl' respectively. Two types of Lockes buffer were used: calcium free (-), containing 10mM EGTA, or standard Locke's buffer containing calcium (+). The α-latrotoxin was prepared from black widow spiders and was obtained from Dr. Robert Chow (Dept. of Physiology, Edinburgh University).

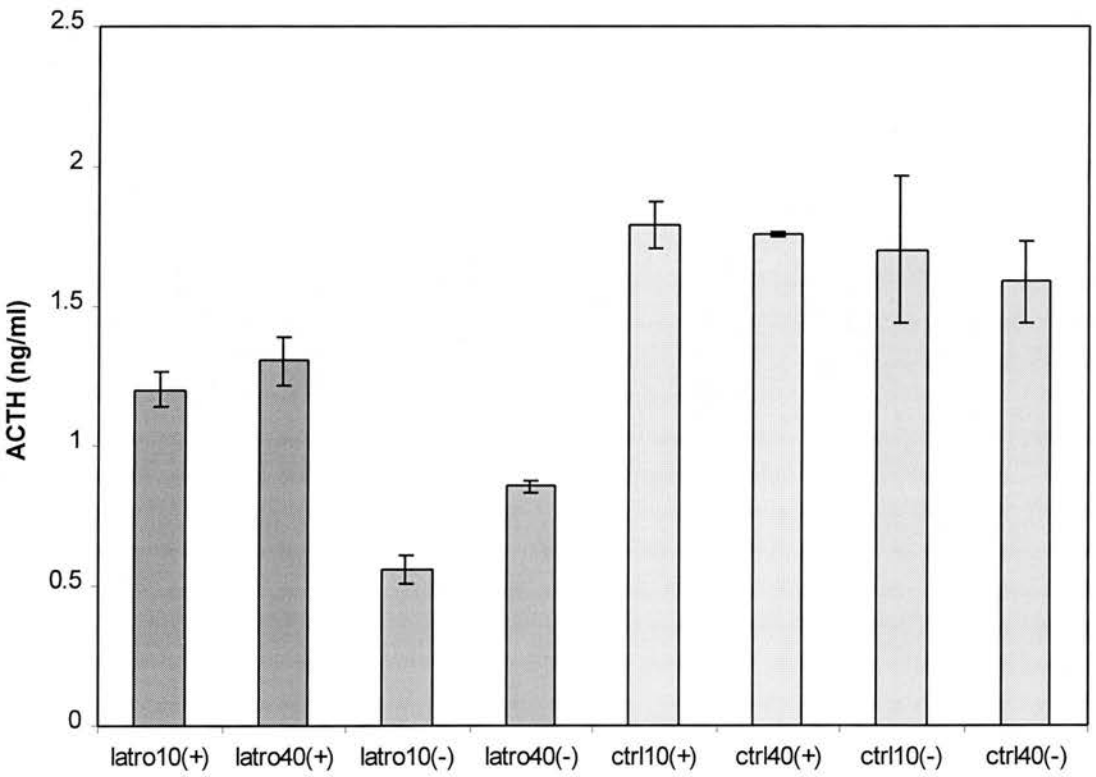

Chapter 6

Investigation of alternative methods of measuring ACTH secretion in AtT-20 cells and further molecular work

6.1 Introduction

This chapter is divided into two main sections. **Section I** describes results obtained when molecular biological techniques were used to try and produce an alternative system of measuring Ca^{2+}-regulated exocytosis in AtT-20 cells. **Section II** describes the results obtained when molecular biological techniques were used to try and produce an alternative way of studying the mechanism of Ca^{2+}-regulated ACTH secretion in AtT-20 cells.

Section I

One of the major difficulties encountered in this project was the need to use a radioimmunoassay (RIA) to measure ACTH secretion from AtT-20 cells. This assay was very time-consuming, taking two full days to obtain results. The iodinated ACTH was also very unstable and was only usable for 3-4 weeks after iodination, and the centrifugation step limited the number of samples that could be handled in one RIA. It was decided to try to produce an alternative method of assaying regulated secretion in AtT-20 cells, by transfecting the cells with the gene for an easily-measured secretory protein. The reporter gene used was secreted alkaline phosphatase (SEAP), a human placental enzyme, with the unusual and useful properties of high temperature stability and highly restricted species and tissue expression. All samples can therefore be heated to 65°C before assaying, thus removing any non-SEAP alkaline phosphatase and providing a very specific assay.

Two plasmid types were used in this section, the maps for which are in the appendix section (C). The first plasmid (SEAP-ctrl) produced constitutive secretion of alkaline phosphatase when transfected into cells, and contained no G418 resistance gene. The second plasmid (HGH-SEAP) was constructed by excision of the SEAP gene from SEAP-ctrl and construction of a fusion protein by joining it to human growth hormone (HGH) gene. This fusion product would enter the regulatory secretory pathway of AtT-20 cells and be secreted in a Ca^{2+}-regulated manner. All cDNA manipulation and plasmid construction was performed by Dr. Allan Colley (Dept. of Biochemistry, University of Edinburgh). Transfections have previously been performed on AtT-20 cells, to examine pro-hormone targeting and processing. Several studies have shown that exogenous hormones can be transfected into these

cells and are correctly processed and released in a regulated manner (*Jung et al., 1993; Chavez & Moore, 1997*). A plasmid called pPHCAGGS-BstXI-LacZ (see appendix E), was used as a control for optimisation of the lipofectamine transfection. This was a high-expression plasmid which on transfection of mammalian cells expressed the enzyme β-galactosidase, which could then be detected using the protocol detailed in 2.7.1, that resulted in transfected cells being stained blue.

Section II

The second technique used was an extension of the work described in Chapter 4, in which the mechanisms of exocytosis in AtT-20 cells were investigated. A major problem in this work was that the introduction of several recombinant proteins thought to be important in exocytosis had little effect on Ca^{2+}-regulated exocytosis. The best explanation is that the secretory vesicles are docked and ready to be released on Ca^{2+}-stimulation, thus introduction of proteins would have no effect on measured secretion. The transfection of cells with plasmids encoding mutant forms of proteins involved in exocytosis might be a way to overcome this problem. NSF has long been known to be involved in Ca^{2+}-regulated exocytosis in many cell types, through experiments similar to those done with αSNAP *(Banarjee et al., 1996)*. NSF exists within the cell as a homotrimer of 76kDa units and has ATPase activity reported to be involved in Ca^{2+}-regulated exocytosis *(Morgan & Burgoyne, 1995)*. *Carol Harley, 1994* reported a point mutation (obtained using mutagenic polymerase chain reaction; *Muhlrad et al., 1992*) of Thr_{394} to Pro_{394} in SEC18 (the yeast NSF homologue). This mutant form of the SEC18 protein interacts with wild type SEC18 monomers to produce trimers, and acts in a dominant negative fashion. The mutation was not within the region of NSF containing ATPase activity, nor did it have any effect on secondary structure of the protein. When the mutant SEC18 was expressed in yeast, it caused a decrease in the growth rate of the yeast culture and an internal accumulation of secretory proteins. It was decided to try to make the same point mutation in mammalian NSF cDNA (obtained from chinese hamster ovary cell line), and then to clone this into the mammalian expression vector pRC/CMV2 (see appendix C) and transfect AtT-20 cells. The template used for the mutation was a

generous gift from Professor R. Burgoyne, University of Liverpool, and is shown in appendix (A).

Section I Investigation of alternative methods of measuring Ca^{2+}-regulated secretion in AtT-20 cells

6.2 Optimisation of lipofectamine transfection conditions using lacZ expression vector

AtT-20 cells were plated in 6-well plates and grown until they were approximately 60% confluent, at which point they were used for transfection. The method of transfection was as detailed in 2.7.1 and the ratios of DNA (μg) to lipofectamine (μl) used were 0:2, 1:4, 1:6, 1:8, 1:10, 1:12. The cells were then tested for β-galactosidase activity as detailed in 2.7.1.1, and transfected cells stained blue. The plates were then photographed, the results of which are shown in figure 6.1.

6.3 Discussion

The results show well 5 to have the greatest percentage of transfected cells, and this was obtained at a ratio of 1: 10 DNA (μg):lipofectamine (μl). Control cells (well 1) showed no staining. Although this result was specific to a particular vector, it provided a starting point for the transfections. It also was a useful and quick method of assessing that this particular method of transfection was working efficiently, allowing the identification of any future problems as plasmid-specific.

6.4 Investigation of transient transfections with SEAP-ctrl and HGH-SEAP vectors

Before attempting to study AtT-20 cells stably transfected with HGH-SEAP it was necessary to show that the cells could be transiently transfected with SEAP-ctrl and HGH-SEAP vectors, and that SEAP activity could be seen. AtT-20 cells were first

transfected with SEAP-ctrl and SEAP-HGH vectors, and transiently transfected cells assayed for SEAP using cytochemistry, chemiluminescence and spectophotometric assays. The standard ACTH RIA was also used to ensure that these cells were secreting in the normal way. The cytochemistry experiments were done using cells grown to 70% confluency in on glass coverslips in 6-well plates, containing 2ml medium. The chemiluminescence experiments used medium from cells grown in 6 well plates to 70% confluency, in 2ml medium. The spectrophotometric assays were all done using cells grown in 24-well plates to 70% confluency in 1ml medium, or the equivalent volume of buffer for Ba^{2+}-stimulation experiments. This was used for all subsequent experiments. In all cases vectors were prepared as detailed in 2.7.1.1 and appropriate restriction enzyme digests done at all stages, to ensure that the correct DNA was present.

6.4.1 Transient transfection of AtT-20 cells with HGH-SEAP and SEAP-ctrl, followed by detection using cytochemistry

AtT-20 cells were transfected as detailed for transient transfections in 2.7.1.4 using DNA (μg):lipofectamine (μl) ratios of 1:10 and 5.88:10, along with a negative control containing no DNA. Both vector types were used and the cells were then cytochemically stained for alkaline phosphatase activity after 24-72 hours using the kit described in 2.9.2.

On examination of the cells no staining for alkaline phosphatase could be seen, so the chemiluminescence assay was used.

6.4.2 Transient transfection of AtT-20 cells with HGH-SEAP, followed by detection using chemiluminescence

AtT-20 cells were transfected as detailed for transient transfections in 2.7.1.4 using DNA (μg):lipofectamine (μl) ratios of 1:10 and 1:1 with a negative control containing no DNA. Only the HGH-SEAP vector was used in this case (due to a shortage of reagents) and the medium from the cells was assayed for SEAP activity after 72 hours using the kit described in 2.9.1. The detection of the chemiluminescent reaction was by exposure of 96 well plates, containing the reaction mixture, to X-ray film for 30min. The results are shown in figure 6.2.

6.4.3 Transient transfection of AtT-20 cells with HGH-SEAP and SEAP-ctrl, followed by detection using an enzymatic assay

AtT-20 cells were transfected as detailed for transient transfections in 2.7.1.4 using a DNA (μg):lipofectamine (μl) ratio of 1:1, with a negative control containing no DNA. Both vector types were used and the medium from the cells was assayed after 72hours using the enzyme assay described in 2.9.3. The results for this are shown in figure 6.3.

It was then necessary to assess whether the HGH-SEAP could be released in a regulated manner, and whether the SEAP could be detected, and this was done by stimulating the transiently-transfected cells with Ba^{2+} (as detailed in 2.5.1.1). The SEAP-ctrl plasmid was used as an additional control in these experiments, as in this case the SEAP should be constitutively expressed and Ba^{2+}-stimulation should have no effect. The results for this are shown in figure 6.4.

Finally the transiently-transfected cells were stimulated with Ba^{2+} as before, and the secreted ACTH measured by RIA, to check that the regulated secretion was normal. The results for this are shown in figure 6.5.

All the results shown are for cells that had been transiently transfected for 72hours. Cells transfected for different times were also assayed and very similar results obtained.

6.5 Discussion

Cytochemistry was unsuccessful as a method of detection of alkaline phosphatase secreted from transfected cells, probably due to a lack of sensitivity. The chemiluminescence assay (figure 6.2) proved much more successful and indicated that the optimal ratio of HGH-SEAP DNA (μg): lipofectamine (μl) was 1:1. This was in contrast to the lacZ expression vector results which showed a DNA (μg): lipofectamine (μl) ratio of 10:1 to be best, and demonstrated that the optimal ratio for

transfection was dependent on the particular plasmid being used. The main problem with chemiluminescence was that the reagents were very costly as they were intended for use in a typical reporter gene assay, as opposed to an assay that requires the processing of numerous samples. The spectophotometric assay used gave good results in that it detected SEAP in the media of AtT-20 cells transiently transfected for 72 hours (figure 6.3). The HGH-SEAP vector gave an increase in absorbance of around 1.7 times that of non-transfected cells, whilst the SEAP-ctrl vector gave an increase of nearly 2.3 times that of non-transfected cells. This shows a difference in basal levels of secretion between the constitutively secreted SEAP (SEAP-ctrl) and the SEAP in the regulated secretory pathway (HGH-SEAP). The enzyme assay was then tested for its ability to detect SEAP secreted from AtT-20 cells stimulated with Ba^{2+} (figure 6.4). In this instance the controls were non-transfected cells and cells transfected with the SEAP-ctrl vector, and both gave very similar absorbance levels. No detectable difference was seen between Ba^{2+}-stimulated and non-stimulated cells, or control and transfected cells, and absorbance levels obtained were background levels. The same samples were assayed for ACTH secretion using the RIA, to ensure that the transfection had not caused any disruption in normal regulated secretion (figure 6.5). The results showed that Ba^{2+}-stimulated ACTH secretion was occurring in AtT-20 cells transfected with both SEAP-ctrl and HGH-SEAP vectors. This eliminates the possibility that SEAP was not detected due to a general transfection-mediated failure of the AtT-20 cells to secrete normally, although it cannot be excluded that the HGH-SEAP had not correctly entered the regulatory pathway.

Although the reporter gene assay appeared satisfactory, it did not permit the measurement of regulated secretion in AtT-20 cells. It was decided to obtain stable HGH-SEAP transfectants using selection with G418 as detailed in 2.7.1.4. The reasoning behind this was to attempt to obtain a higher percentage of transfected cells (i.e. 100%) thus increasing the signal, and allowing the detection of Ba^{2+}-stimulated SEAP secretion.

6.6 Selection of stable HGH-SEAP AtT-20 cell transfectants and subsequent detection of SEAP

AtT-20 cells were transfected with HGH-SEAP and SEAP-ctrl vectors at a DNA (μg): lipofectamine (μl) ratio of 1:1, with an additional control containing no vector DNA. The transfection was done in the usual manner, followed by selection over a period of 4-6 weeks using G418. Only wells transfected with HGH-SEAP contained surviving cells after 2-3weeks, and these were sub-cloned, grown up and a stock frozen down for future use. The following experiments investigated two stably-transfected cell lines, s1 and s2. Throughout these experiments the cells were maintained in G418-containing medium to ensure that loss of expression did not occur.

The spectrophotometric assay was first used to measure the amount of SEAP in the medium after 72 hours, and the results are shown in figure 6.6. The cells were stimulated to secrete using Ba^{2+}, and secreted SEAP measured. Samples of cells were also completely lysed, in order to detect total SEAP. The results for this are shown in figure 6.7. Finally the same samples were assayed for Ba^{2+}-stimulated secretion of ACTH using RIA to ensure that the stable transfectants were still able to secrete in a regulated manner (results shown in figure 6.8).

6.7 Discussion

AtT-20 cell lines s1 and s2 were stably transfected with the HGH-vector and then screened for SEAP activity using the standard spectrophotometric assay. Figure 6.6 shows the amount of SEAP constitutively secreted into the medium. The s1 cell line secreted very large amounts (approximately 4.5 times the control levels), whilst the s2 cell line secreted amounts around 1.5 times the control levels. These results confirmed that stable transfectants had been obtained, that displayed both G418 resistance and SEAP activity.

The next stage was to assess whether SEAP release could be stimulated by Ba^{2+} (figure 6.7). An additional control of lysed cells was also used, in order to measure the total SEAP content. The results indicated a problem in the sensitivity of the system in that the A_{450} values for all samples (including the non-transfected control cells) were very similar. Even the s2 cell line, which previously showed high levels of SEAP activity, displayed no activity above basal levels. Interestingly, when the

same cells were stimulated to secrete ACTH using Ba^{2+}, the s2 cells (which had been shown to produce high levels of SEAP) displayed a significant reduction in the levels of Ba^{2+}-stimulated secretion. This suggested that the HGH-SEAP was causing a reduction in regulated secretion, because of the site of integration of the HGH-SEAP vector DNA within the genomic DNA. Another possibility was that the HGH-SEAP protein was expressed at very high levels, was entering the regulatory secretory pathway and was interfering with the transport and release of ACTH.

6.8 Discussion and Conclusions (Section I)

These experiments showed that the HGH-SEAP vector could efficiently transfect AtT-20 cells, and could be used to select G418-resistant clones. The selection process was lengthy, and the number of clones surviving the 2-3week stage was minimal, although plating the cells at low density improved this. The problem then was to maintain these cells and grow up large enough numbers to passage and eventually freeze. In this particular set of experiments only two stable cell lines actually reached this stage. This indicates the advantages of using transiently-transfected cells for initial stages of assessing the system.

It was found that SEAP could be detected in medium when cells had been grown in it for around 72 hours. However on stimulation of the cells with Ba^{2+}, no difference in SEAP levels could be measured between basal and stimulated samples, in transiently or stably-transfected cells. Even after total lysis of stably transfected cells SEAP was still undetectable using the spectrophotometric assay. It was previously shown that Ba^{2+}-stimulation caused a large fraction of total ACTH to be released, while immunofluorescence revealed no significant granule depletion. This was presumed to be due to the ACTH processing and release being rapid, or to degradation of ACTh in the lysis buffer. These results in which the total SEAP in the cells cannot be detected, but where SEAP released over 72 hours (at basal levels) can be detected, suggests a similar scenario.

These results suggest that the HGH-SEAP vector and spectrophotometric assay do not provide a sensitive enough method for the measurement of regulated exocytosis. The next stage in the process would be to use transiently-transfected cells to study

alternative methods of SEAP detection. A possible alternative to the *p*-nitrophenyl phosphate (pNPP) used in this enzyme assay for the detection of SEAP, was reported by *Huang et al., 1992.* They showed that 3,6-fluorescein diphosphate could be used as a fluorogenic substrate for alkaline phosphatase, and with a sensitivity of 50 times that of the assay with pNPP.

If a detection method could be found in which the levels of sensitivity were such that Ba^{2+}-stimulated secretion of SEAP could be accurately monitored, stable cell lines could then be produced. This would require the large-scale selection of a number of stable cell lines, which could undergo detailed analysis. Immunofluorescence could be used to detect the presence and whereabouts of the HGH-SEAP protein, and its distribution could be compared to that of ACTH. The ACTH RIA could be used to assess the effect (if any) on ACTH secretion. The new system of detection could then be used to check that regulated secretion of HGH-SEAP had the same characteristics as secretion of ACTH. This type of system would result in an assay that would be an enormous improvement on the ACTH RIA, providing the sensitivity was high enough. If it were, a far greater number of samples could be processed in a much shorter period of time, without the constraints of product life-span. One of the main future aims of this project would be to further develop this type of system.

Section II

This section describes a very small section of work that was done within the scope of the project. It represents the beginning of a large project, in that it uses a completely different method to try and further analyse Ca^{2+}-regulated exocytosis in AtT-20 cells. Transfection of AtT-20 cells with a mutated NSF gene should have a dominant negative effect in the cell, regardless of whether vesicles are docked or undocked. The intention was to mutate the NSF gene at the aforementioned site (see appendix) using a plasmid template described in appendix (A) containing the NSF cDNA clone from the Chinese Hamster Ovary cell line. Having done this it would be re-cloned into a mammalian expression vector (along with the non-mutated control) and AtT-20 cells transfected with it. Depending on the results of the transient transfection (i.e.

how deleterious it was to the cells) the mutant NSF would then have been sub-cloned into an expression vector which would allow NSF expression to be controlled.

6.9 Site-directed mutagenesis of the NSF gene

The first stage of the project was to attempt to mutate the NSF gene, and the method used for this has been described in 2.8 and appendix (B). The primers flanking the NSF gene are denoted as 5' and 3', whilst the primers in the centre of the gene containing the point mutation have been denoted as 5'M and 3'M. The plan was to mutate the first half of the gene leaving an overlap of single bases, and then to mutate the other half of the gene and leave the complementary overlap of single bases, all using PCR. These overhangs could then act as long primers, which should anneal to the other overhang, followed by extension using PCR. This 4-primer method of site-directed mutagenesis has previously been reported by *Ho et al., 1989*. The precise method used in each of these experiments has been detailed in 2.8, but an outline of the primers and enzymes used in the reaction is given below.

The first experiment used the 5'M primer only (as this was obtained first), as well as the 5' and 3' primers. The 5' and 3' primers were used to assess whether the primers would give a whole gene product (as this was to be used for control transfections) and the 5'M and 3' primers were used to assess whether a 'mutant' half of the gene could be obtained. The results for this are shown in figure 6.9, which is a gel of the PCR product obtained with Taq polymerase. The same reaction was investigated using VENT-polymerase as this enzyme improves fidelity of the reaction and the results of this are shown in figure 6.10. Both mutated fragments were then produced using the 5'M and 3' primers or the 3'M and 5' primers and VENT-polymerase. Samples of these PCR products were run on agarose gels, and the results are shown in figure 6.11. The next stage was the purification of the mutant fragments, in order to remove any of the original NSF template, which would cause contamination of the mutant product through the 5' and 3' primers causing amplification of non-mutated NSF. This was done by running all of the PCR product on a polyacrylamide gel system set up using a large-toothed comb. The bands were then excised and purified using a Qiagen gel-purification kit, which also resulted in the concentration of the

DNA. A sample of this DNA was run on an agarose gel and the results are shown in figure 6.12. Figure 6.13 shows the results obtained when the 5' and 3' primers were used to try to anneal the two fragments together, with VENT-polymerase and varying Mg^{2+} concentrations.

6.10 Discussion and Conclusions

Figure 6.9 showed that the 5'M, 5' and 3' primers were functional with Taq polymerase and gave bands that were of the expected size (i.e. 2200bp and 1100bp for the whole NSF gene and the mutated fragment respectively). When experiments were done using single primers only, no bands were obtained. Figure 6.10 showed the same experiment with VENT polymerase, and although the bands were less strong, they could easily be seen when run on a gel. Figure 6.11 showed the production of both mutant fragments using VENT polymerase, and these PCR products were then purified and concentrated which resulted in bands of the correct size (around 1100bp for both fragments). However when PCR and the 5' and 3' primers were used to try and join these fragments together and create a whole mutated gene, the reaction was unsuccessful, and no bands of the correct size were obtained. At this point the project had to be abandoned due to time constraints. The fragments would also need to be sequenced to ensure that the correct point mutation had been obtained. A possible problem with this end reaction was the size of the fragments which were being joined together (1100bp). Previous work that reported success using this type of mutagenesis was joining much smaller fragments together (*Ho et al., 1989*), and it may be that we would have to look at an alternative method. This section has been included as it represents the main body of work that would be undertaken (along with the alternative assay work also included in this section), if the project were to be continued. It offers a new approach that would yield information that would greatly improve our understanding of the mechanisms involved in Ca^{2+}-regulated exocytosis in AtT-20 cells.

Figure 6.1 Transfection of AtT-20 cells with lacZ expression vector using lipofectamine

AtT-20 cells were transfected with the lacZ expressing vector, and then stained for β-galactosidase activity 12 hours after transfection. The dark, speckled staining represents positively-stained areas of cells. Wells 1-6 contain cells transfected with DNA (μg):lipofectamine (μl) ratios of 0:2, 1:4, 1:6, 1:8, 1:10, 1:12 (well 1 representing the negative with no lacZ expressing vector).

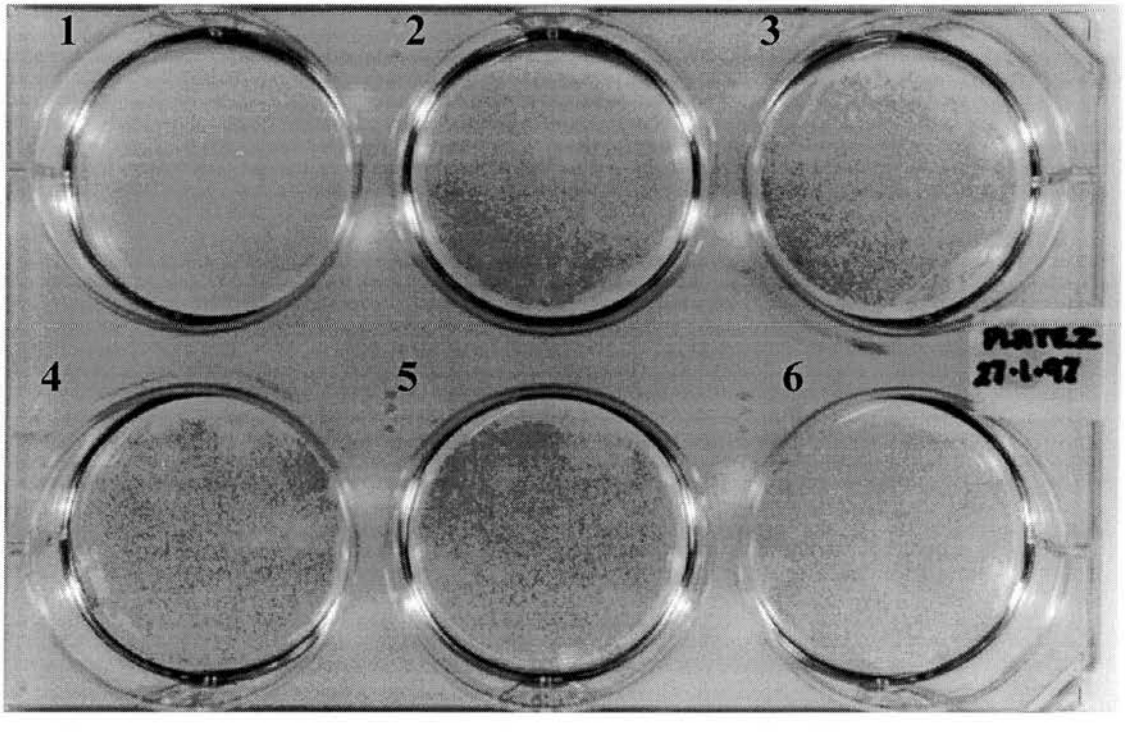

Figure 6.2 Transient transfection of AtT-20 cells with HGH-SEAP and subsequent detection using chemiluminescence

Chemiluminescence assay as a method to detect the transient transfection of AtT-20 cells with the HGH-SEAP vector. Duplicate samples were assayed and these are shown in the same column. The columns are labelled 1-3 and these represent DNA (μg):lipofectamine (μl) ratios of 0:1 (control), 1:1 and 10:1 respectively.

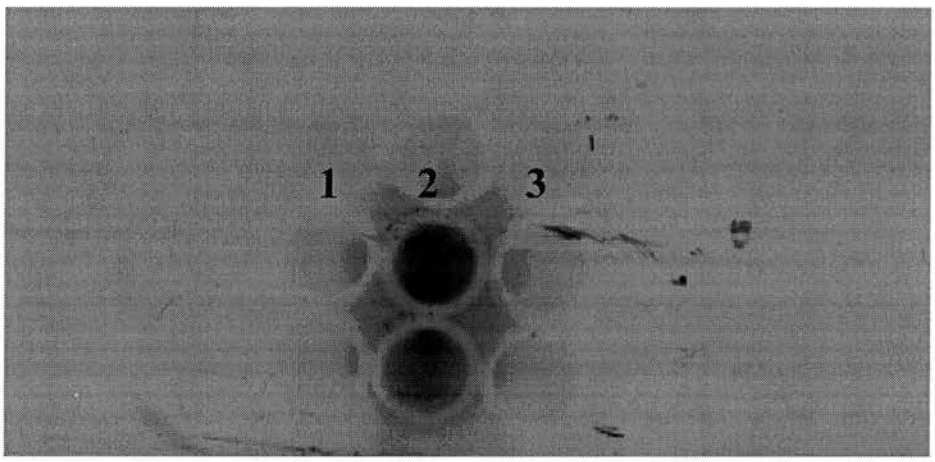

Figure 6.3 Detection of SEAP in transiently-transfected AtT-20 cells using a spectrophotometric assay

Medium from AtT-20 cells transfected 72hours previously with vectors SEAP-ctrl and HGH-SEAP was assayed for SEAP using the spectrophotometric technique described in 2.9.3. The ratios of DNA (μg) to lipofectamine (μl) were 1:1, except in the control sample which contained the same volume of lipofectamine (5μl) but no DNA. The figure below details the A_{450} values obtained when the samples were read using a plate reader, having zeroed on empty wells.

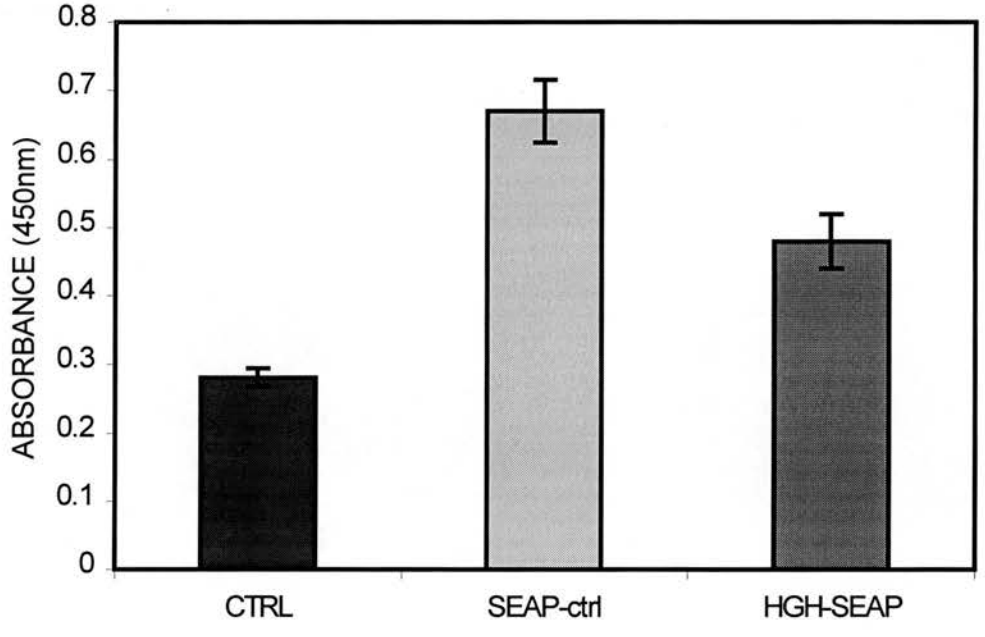

Figure 6.4 Stimulation of transiently-transfected AtT-20 cells with Ba^{2+}, followed by spectrophotometric detection of SEAP

AtT-20 cells were transiently transfected with SEAP-ctrl and HGH-SEAP plasmids, and then stimulated with Ba^{2+} in the normal way after 72hours. The amount of SEAP secreted was then assessed by spectrophotometric assay. Cells incubated in Ba^{2+}-stimulation buffer are shown as (+) barium, whilst cells incubated in the control Locke's buffer are shown as (-) barium.

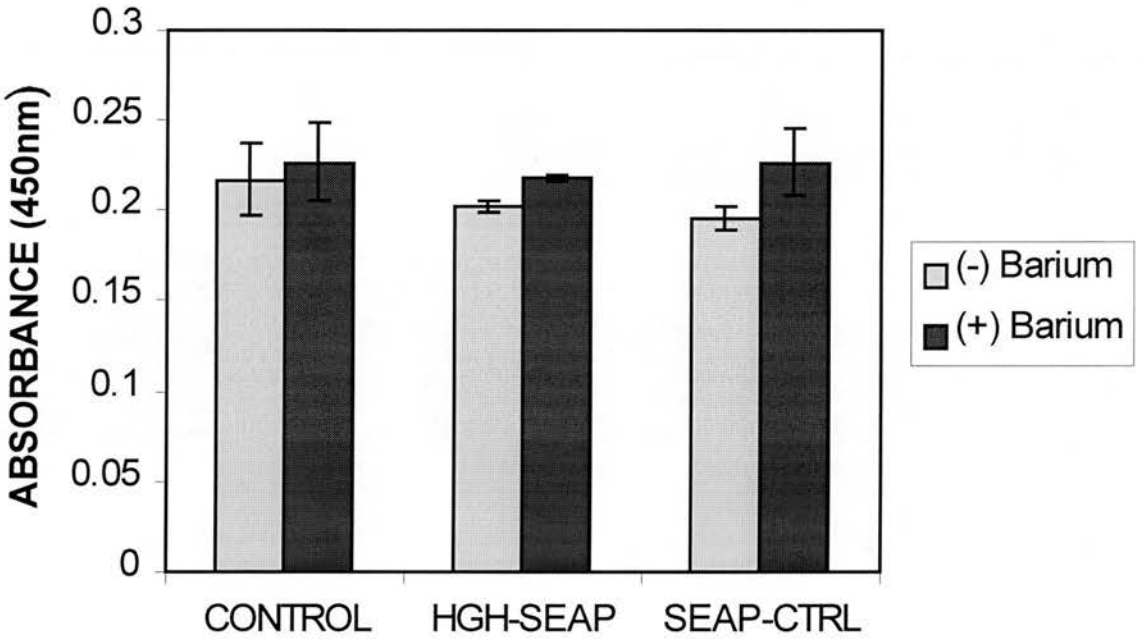

Figure 6.5 Ba^{2+}-stimulation of transiently-transfected cells and measurement of ACTH secretion by radioimmunoassay

The usual ACTH RIA was used to measure ACTH secretion from transiently-transfected AtT-20 cells. Cells incubated with Ba^{2+} are shown as Ba stim, whilst cells incubated in control Locke's buffer are shown as Ba ctrl.

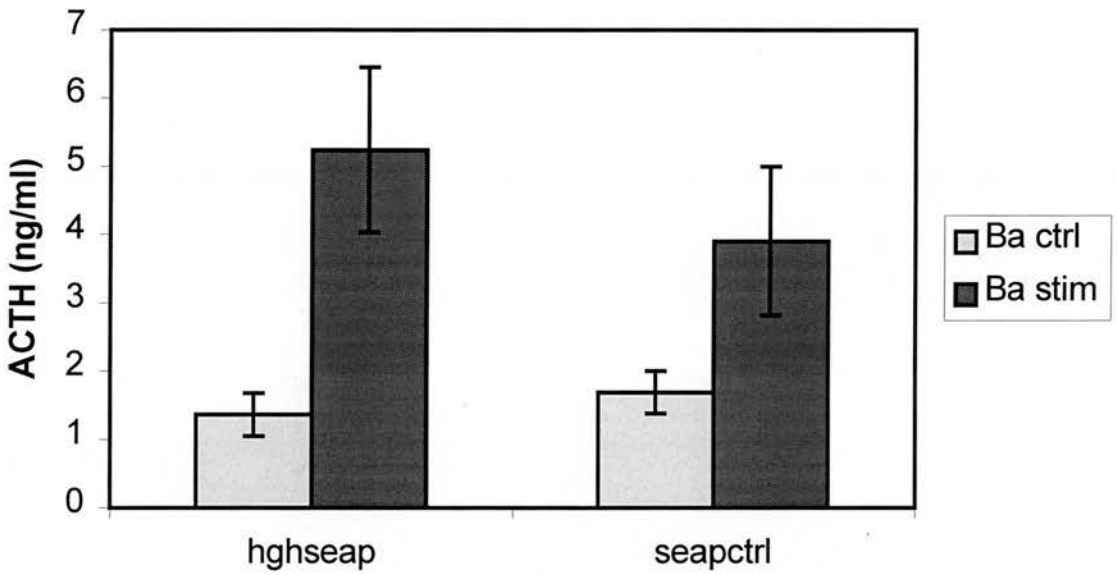

Figure 6.6 Detection of SEAP in stably-transfected AtT-20 cells using spectrophotometry

Secreted SEAP was measured in the medium of AtT-20 cells stably transfected with the HGH-SEAP vector, and grown in the medium for 72hours. Control represents non-transfected cells grown under the same conditions, whilst s1 and s2 represent the two stable cell lines.

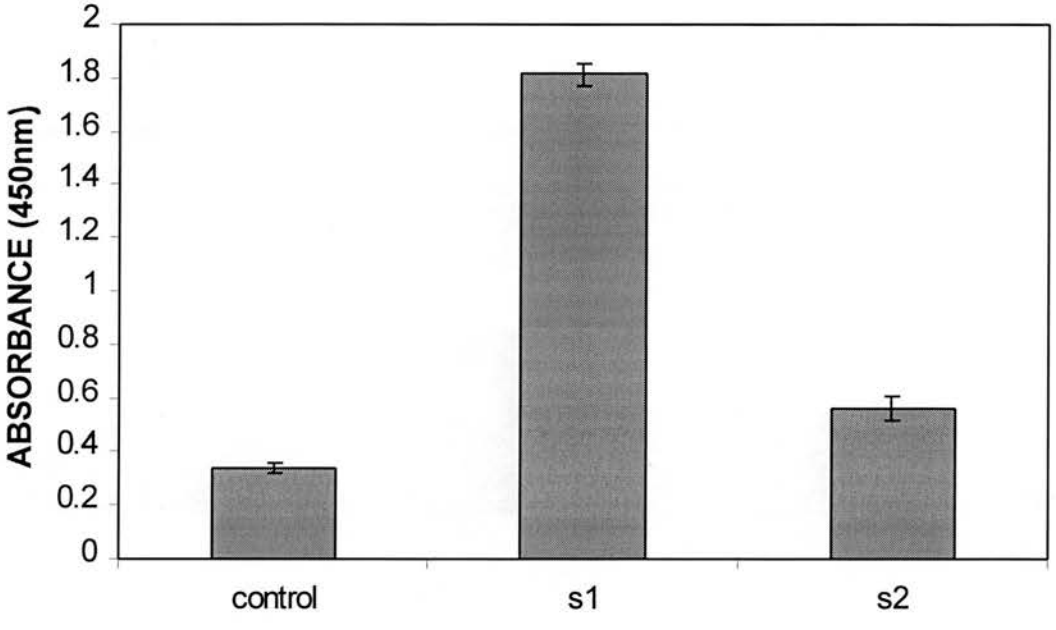

Figure 6.7 Ba^{2+}-stimulation of stably-transfected cells and measurement of SEAP secretion by spectrophotometry

AtT-20 cell lines stably transfected with HGH-SEAP vector were grown until 70-80% confluent, at which point they were stimulated to secrete using Ba^{2+}. The secreted SEAP was measured by spectrophotometric assay. Normal represents non-transfected AtT-20 cells grown and stimulated in the same way, whilst s1 and s2 are the stable cell lines. The samples stimulated with Ba^{2+} are shown as (+) barium, those incubated in the control Locke's buffer as (-) barium, and total lysis samples as total lysis.

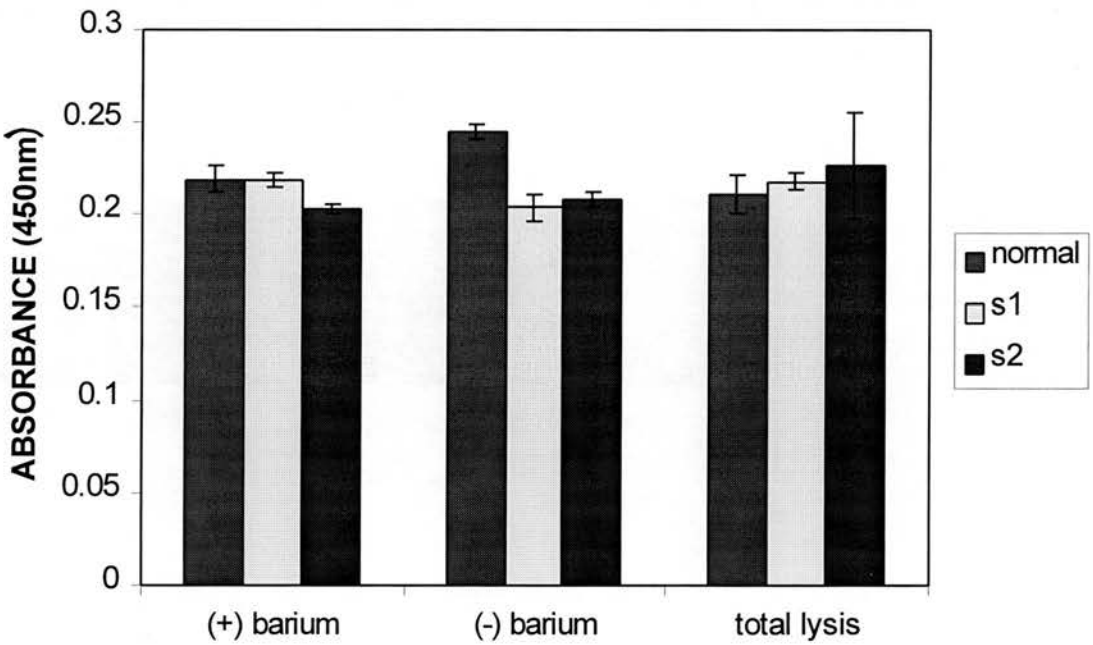

Figure 6.8 Ba^{2+}-stimulation of stably-transfected cells and measurement of ACTH secretion by radioimmunoassay

AtT-20 cells stably transfected with HGH-SEAP vector were grown in 24-well plates until 80% confluent, and were then stimulated to secrete using Ba^{2+}. The ACTH secreted was measured using RIA. Cells stimulated with Ba^{2+} are shown as (+) barium, whilst cells incubated in control Locke's buffer are shown as (-) barium. Non-transfected control cells, treated in the same way are shown as normal, whilst the stable cell lines are displayed as s1 and s2.

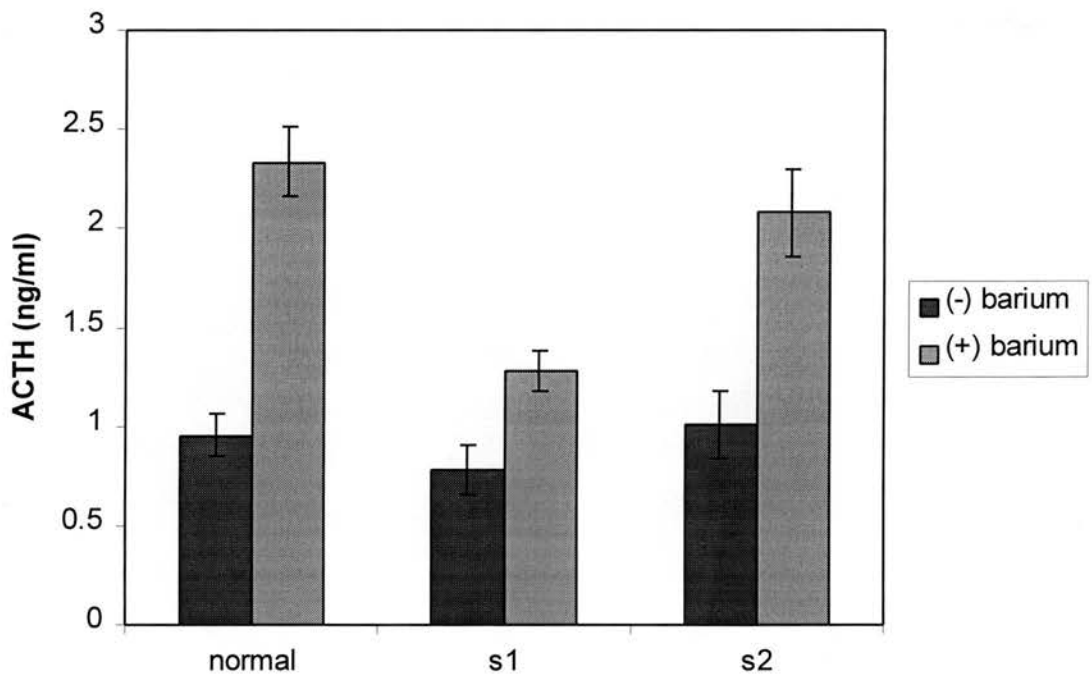

Figure 6.9 Optimisation of PCR reaction with Taq polymerase

The gel below represents the results obtained with varying amounts of template, Taq polymerase, and combinations of the primers 5', 3' and 5'M. Lane 1 contains molecular weight markers as shown on the left hand side (base pairs). The PCR reaction in lanes 2-4 used the primers 5' and 3' and 2µl, 0.5µl and 0.2µl of NSF template respectively. The PCR reaction in lanes 5-7 used the primers 5'M and 3' and 2µl, 0.5µl and 0.2µl of NSF template respectively. All PCR reactions were done with Taq-polymerase and 15µl samples were run per lane of the gel.

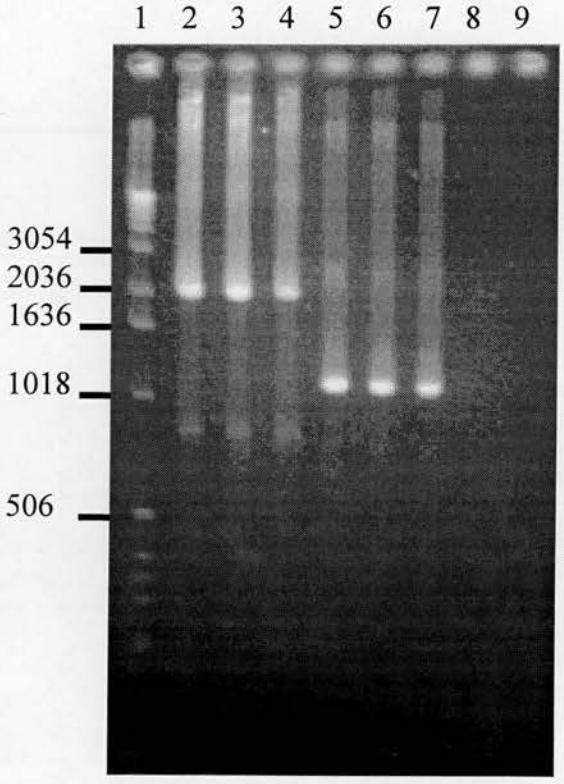

Figure 6.10 Optimisation of PCR reaction with VENT polymerase

The gel below shows the results obtained using VENT or Taq polymerase, and combinations of the primers 5' and 3' or 3' and 5'M. Lane 1 and lane 6 contain a 1kb DNA ladder (shown in base pairs). Lane 2 used primers 5' and 3' with Taq-polymerase, whilst lane 3 used the same primers but with VENT polymerase. Lane 4 used primers 5'M and 3' with Taq-polymerase, whilst lane 5 used the same primers with VENT-polymerase. All VENT-polymerase reactions used 2mM $MgSO_4$.

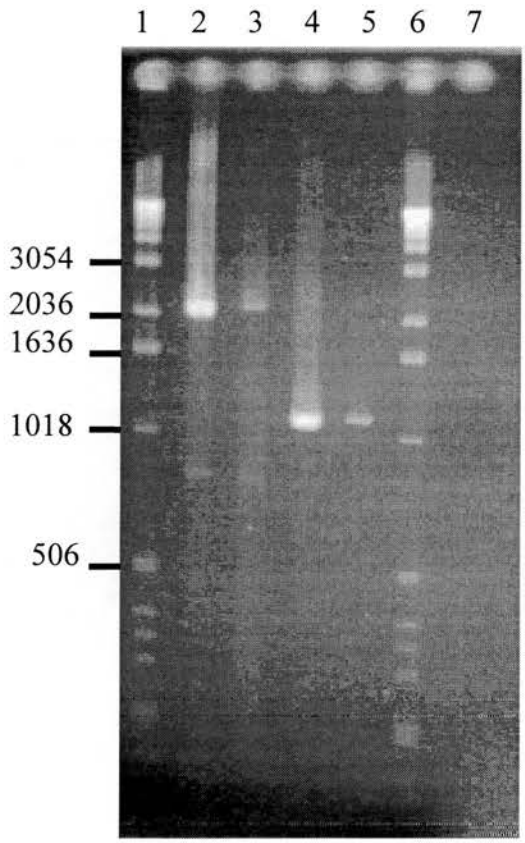

Figure 6.11 Production of both mutant fragments

The gel below shows the results obtained using both mutagenic primers and the appropriate flanking primer. Lanes 1 and 2, 5'M and 3' primers or 3'M and 5' primers respectively and VENT polymerase with 2mM $MgSO_4$. A 1kb DNA ladder is shown in base pairs.

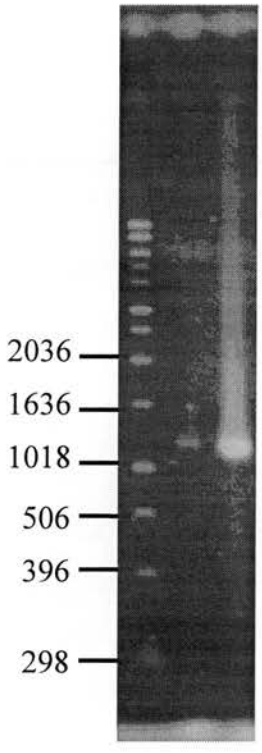

6.12 Purification and concentration of mutated fragments

The gel below represents the results obtained on purification of the fragments obtained in figure 6.10. Lanes 1 and 2, purified bands obtained using the 3'M and 5' primers or 5'M and 3' primers respectively. 15µl samples were run in each lane of the gel. Arrows denote bands of 1100bp.

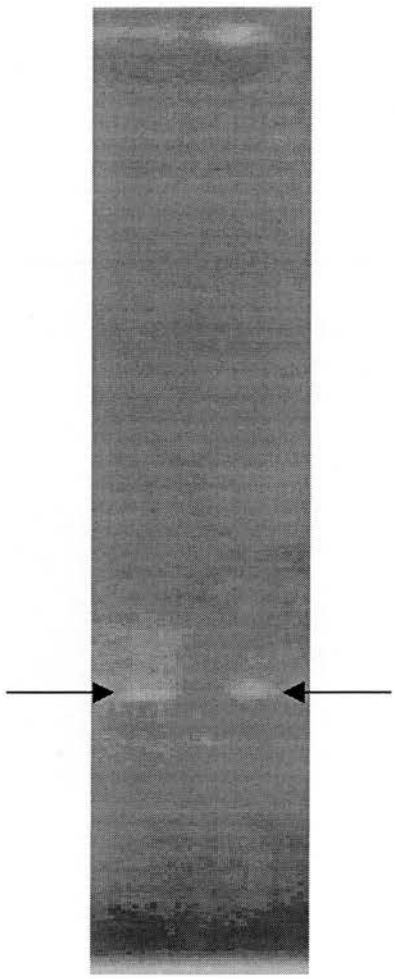

Figure 6.13 Joining of mutant fragments

Lane 1, 1kb DNA ladder shown in base pairs. Lanes 2 and 3 show the results obtained when the PCR reaction mixture contained the 5'M fragment and the 3'M fragment, along with 2mM and 4mM $MgSO_4$ respectively and VENT polymerase. Lanes 4 and 5 were controls with the 5'M fragment only and 2mM or 4mM $MgSO_4$ respectively. Lanes 6 and 7 were controls with the 3'M fragment only and 2mM or 4mM $MgSO_4$ respectively. Lanes 8 and 9 represents both the 5'M and 3'M fragments in a PCR reaction containing 2mM and 4mM $MgSO_4$ respectively, however the mutated fragments were unpurified and taken straight from the PCR reaction mixture. Lanes 2-8 all used VENT polymerase and the reaction mixture contained 5' and 3' primers.

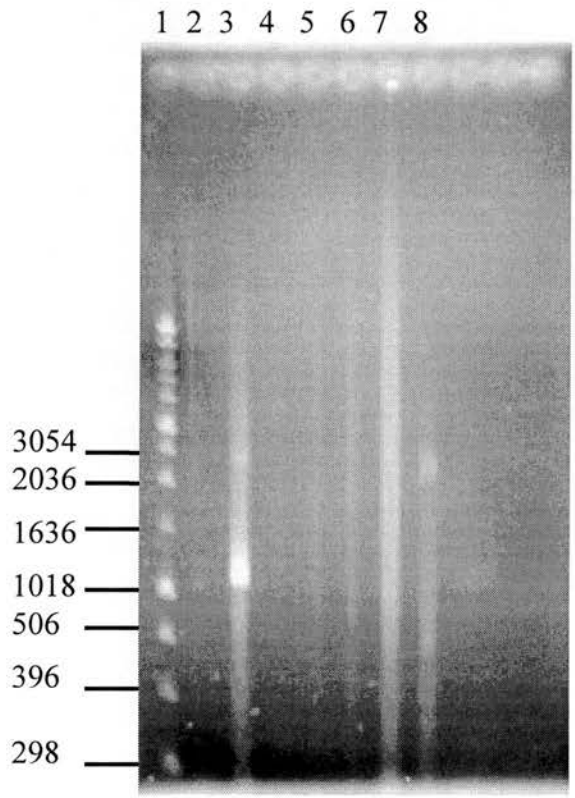

Chapter 7

Conclusions

Conclusions

Ca^{2+}-regulated exocytosis has been investigated in various cell types, and this particular study uses the AtT-20 mouse anterior pituitary cell line. The most commonly studied models have been neuroendocrine cells, such as chromaffin cells, and neuronal cells, and these differ considerably from AtT-20 cells in terms of their physiological functions. This project aimed to compare Ca^{2+}-regulated exocytosis in AtT-20 cells with that in neuronal and chromaffin cells, in order to assess whether similar mechanisms were involved. The first aim was to characterise process in molecular terms by elucidating which of the proteins currently believed to be involved in exocytosis were present in AtT-20 cells, and to which part of the cell they were localised. Having completed this section of the work some experiments on the actual mechanism of Ca^{2+}-regulated exocytosis in AtT-20 cells were performed. The final section of this project investigated an alternative method for measuring regulated secretion from AtT-20 cells.

Immunoblotting revealed the presence of synaptotagmin, αSNAP, SNAP-25, NSF, synaptobrevin 2, syntaxin I, rab3A, cofilin, ADF and CAPS, for all of which there is already strong evidence for an involvement in exocytosis in neuronal and chromaffin cells. This localised synaptobrevin, syntaxin and synaptobrevin in membrane fractions, CAPS, ADF and cofilin to cytosolic fractions and SNAP-25, αSNAP, NSF and rab3A to both. The most interesting result here was the presence of αSNAP and NSF in the membrane fraction, as they are soluble proteins with no method of membrane attachment other than via other SNARE proteins.

Immunofluorescence microscopy revealed different staining patterns for each of these proteins, αSNAP showing punctate, vesicular staining (very similar to that of ACTH) and NSF showing plasma membrane staining, similar to that obtained for SNAP-25. Cofilin displayed a distinct and very unusual staining pattern which was punctate and vesicular, but different in nature from that of ACTH or αSNAP. These cofilin rich bodies (CRBs) were larger and less abundant than secretory vesicles, and were associated with the cortical actin of the cell. The ACTH vesicles did not co-localise with the cortical actin structure nor with the CRBs, and existed within a general network of actin at the plasma membrane of AtT-20 cells. In this respect they

differed from chromaffin cells, where the vast majority of vesicles lie below the cortical actin layer. This forms two distinct phases of release on stimulation of exocytosis: fast ATP-independent fusion of a minority of pre-docked vesicles and the slower ATP-dependent release from undocked vesicles below the cortical actin (ATP-dependent). This particular study did not permit the measurement of these different time phases in AtT-20 cells, but if it were found to be true, the morphological evidence would not suggest an actin barrier to be the cause. AtT-20 cells stimulated with Ba^{2+} displayed no great change in ACTH-containing vesicles or actin distribution. When the total content of ACTH was measured, however, Ba^{2+} appeared to release about 70% of the total ACTH content, so it is surprising that no granule depletion was noted. It is unlikely that this is due to dynamic replacement of the granule pool as protein processing and membrane flow would not function on this time scale. It is more likely that the ACTH, which is unstable and easily degraded, was substantially lost during the lysis treatment, and total lysis values should be treated with caution. The lack of actin re-distribution suggests that it does not play a large part in Ca^{2+}-regulated exocytosis in AtT-20 cells, or that the changes were not detectable under these conditions.

Permeabilised AtT-20 cells, stimulated to secrete with 10μM Ca^{2+}, and an ACTH derection by RIA, were used to investigate the mechanism of exocytosis in AtT-20 cells. Antibodies, directed against various proteins thought to be involved in exocytosis, and introduced into permeabilised AtT-20 cells, had no effect on ACTH release. The same result was obtained with recombinant cytoplasimc synaptotagmin I (cytoplasmic domain), recombinant cofilin, phalloidin, cytochalasin and αSNAP. These negative results can be interpreted in a number of ways, but the most general explanation would be that the ACTH-containing vesicles exist in a pre-docked state in the cells, with αSNAP already bound to the SNARE complex. This would prevent antibodies or added recombinant proteins from having any effect on exocytosis, as the fusion complex would already be formed. The role of NSF is more difficult to understand as it appears to bind generally to the plasma membrane, with or without the presence of vesicles (hence its non-punctate staining pattern). Cytosolic rundown experiments in permeabilised chromaffin cells showed a decrease in Ca^{2+}-stimulated exocytosis, corresponding to the leakage of cytosolic components from the cells.

This could be prevented on addition of cytosol or αSNAP, but the same results was not found in AtT-20 cells. Rundown of Ca^{2+}-stimulated exocytosis was difficult to obtain and although the introduction of cytosol reversed it to some extent, the introduction of αSNAP had no effect, in support of this explanation. The lack of effect on exocytosis in AtT-20 cells, seen on the introduction of phalloidin and cytochalasin, again suggested that actin does not act as a major barrier to regulated secretion in these cells. These negative results were validated by the use of immunofluorescence microscopy to prove that proteins were able to enter and bind to intracellular components, under these conditions. However although presumptions could be made as yet there was no direct or functional evidence for the involvement of the proteins tested in AtT-20 cell exocytosis. The introduction of botulinum neurotoxin D and tetanus toxin light chains caused a major decrease in Ca^{2+}-stimulated exocytosis in AtT-20 cells and proved that the mechanism of regulated secretion in AtT-20 cells was similar to that seen in other cell types, in that synaptobrevin had a major role. The addition of α-latrotoxin to intact AtT-20 cells had an effect opposite to that seen in neuronal cells, in that a decrease in basal levels of secretion were seen, again suggesting definite differences between cell types.

These results suggest that the mechanisms involved in the secretion of ACTH from AtT-20 cells, are similar to those of exocytosis from neuronal and chromaffin cells. They show the definite involvement of synaptobrevin, and thus the probable involvement of αSNAP, NSF, synaptotagmin, syntaxin, SNAP-25, rab3A and CAPS. They do not however offer any evidence of a rate-determining role for actin, ADF or cofilin in exocytosis, although it would be interesting to elucidate the function of cofilin, due to its very distinct staining pattern.

Because of time limitations this project failed to produce a mutant NSF, however an alternative method for studying regulated secretion in AtT-20 cells was tested. AtT-20 cells were stably transfected with a construct expressing a fusion protein containing the SEAP reporter gene fused to the HGH gene. Basal secretion of the fusion protein over 24-72 hours could be detected using a spectrophotometric assay, however this assay was unable to detect the extra ACTH secreted during cell stimulation with Ba^{2+}.

Future work could involve further investigation of the effects of the other botulinum neurotoxins (directed against SNAP-25 and syntaxin) to show a role for these proteins in Ca^{2+}-regulated exocytosis in AtT-20 cells. Immunofluorescence microscopy could be used for co-localisation studies of SNAP-25, NSF, ACTH and αSNAP, as well as using new antibodies against other proteins thought to be involved in exocytosis. The production of a mutant NSF expression construct would be a major area of future work, as this should overcome the inability of proteins to interfere with the exocytotic machinery. The final aim would be to develop the SEAP-HGH assay for the detection of regulated secretion in AtT-20 cells, to avoid having to use the laborious ACTH RIA. This would initially centre on transient transfections of AtT-20 cells with the SEAP-HGH vector followed by the identification of an assay method sensitive enough to accurately measure regulated release of SEAP. Stable transfectants would then be selected and studied to ensure that normal regulated secretion was occurring.

Bibliography

Antoni, F. A. (1996) Calcium checks cyclic-AMP-corticosteroid feedback in adenohypophyseal corticotrophs. *J. Neuroendocrinology* 8:659-672

Araki, E., Shimada, F., Shichiri, M., Mori, M., and Ebina, Y. (1988) Psv00cat - low background CAT plasmid. *Nuc. Ac. Res.* 16:1627

Araki, S., Kikuchi, A., Hata, Y., Isomura, M., and Takai, Y. (1990) Regulation of reversible binding of smg p25a, a ras p21-like GTP-binding protein, to synaptic plasma-membranes and vesicles by its specific regulatory protein, GDP dissociation inhibitor. *J. Biol. Chem.* 265:13007-13015

Augustine, G. J. and Eckert, R. (1984) Divalent-cations differentially support transmitter release at the squid giant synapse. *J. Physiol. London* 346:257-271

Axelrod, J. and Reisine, T. D. (1984) Stress hormones - their interaction and regulation. *Science* 224:452-459

Bahler, M. and Greengard, P. (1987) Synapsin-I bundles F-actin in a phosphorylation-dependent manner. *Nature* 326:704-707

Banerjee, A., Barry, V. A., Dasgupta, B. R., and Martin, T. F. J. (1996) N-ethylmaleimide-sensitive factor acts at a prefusion ATP-dependent step in Ca^{2+}-activated exocytosis. *J. Biol. Chem.* 271:20223-20226

Barnard, R. J. O., Morgan, A., and Burgoyne, R. D. (1996) Domains of α-snap required for the stimulation of exocytosis and for N-ethylmalemide-sensitive fusion protein (NSF) binding and activation. *Mol. Biol. Cell.* 7:693-701

Bartels, F., Bergel, H., Bigalke, H., Frevert, J., Halpern, J., and Middlebrook, J. (1994) Specific antibodies against the Zn^{2+}-binding domain of clostridial neurotoxins

restore exocytosis in chromaffin cells treated with tetanus or botulinum A neurotoxin. *J. Biol. Chem.* 269:8122-8127

Bennet, M. K., Calakos, N., Kreiner, T., and Scheller, R. H. (1992) Synaptic vesicle membrane proteins interact to form a multimeric complex. *J. Cell. Biol.* 116:761-775

Berger, J., Hauber, J., Hauber, R., Geiger, R., and Cullen, B. R. (1988) Secreted placental alkaline-phosphatase - a powerful new quantitative indicator of gene-expression in eukaryotic cells. *Gene* 66:1-10

Binz, T., Kurazono, H., Popoff, M. R., Eklund, M. W., Sakaguchi, G., Kozaki, S., Krieglstein, K., Henschen, A., Gill, D. M., and Niemann, H. (1990) Nucleotide-sequence of the gene encoding clostridium-botulinum neurotoxin type-D. *Nuc.Ac. Res.* 18:5556

Blasi, J., Chapman, E. R., Link, E., Binz, T., Yamasaki, S., Decamilli, P., Sudhof, T. C., Niemann, H., and Jahn, R. (1993a) Botulinum neurotoxin-A selectively cleaves the synaptic protein SNAP- 25. *Nature* 365:160-163

Blasi, J., Chapman, E. R., Yamasaki, S., Binz, T., Niemann, H., and Jahn, R. (1993b) Botulinum neurotoxin-C1 blocks neurotransmitter release by means of cleaving HPC-1/syntaxin. *EMBO J.* 12:4821-4828

Bordier, C. (1981) Phase separation of integral membrane proteins in Triton X-114 solution. *J. Biol. Chem.* 256:1604-1607

Bourne, H. R., Sanders, D. A., and Mccormick, F. (1991) The GTPase superfamily - conserved structure and molecular mechanism. *Nature* 349:117-127

Boyd, R. S., Duggan, M. J., Shone, C. C., and Foster, K. A. (1995) The effect of botulinum neurotoxins on the release of insulin from the insulinoma cell-lines HIT-15 and RINM5F. *J. Biol. Chem.* 270:18216-18218

Bradford, M. M. (1976) A rapid and sensitive method for the quantitation of microgram quantities of protein utilizing the principle of protein-dye binding. *Anal. Biochem.* 72:248-254

Brakch, N., Cohen, P., and Boileau, G. (1994) Processing of human prosomatostatin in AtT-20 cells - S-28 and S-14 are generated in different secretory pathways. *Biochem. Biophys. Acta.* 205:221-229

Braun, J. E. A. and Scheller, R. H. (1995) Cysteine string protein, a DNAj family member, is present on diverse secretory vesicles. *Neuropharmacol.*34:1361-1369

Bretz, R. and Staubli, W. (1977) Detergent influence on rat-liver galactosyltransferase activities towards different acceptors. *Eur. J. Biochem.* 77:181-192

Brose, N., Petrenko, A. G., Sudhof, T. C., and Jahn, R. (1992) Synaptotagmin - a calcium sensor on the synaptic vesicle surface. *Science* 256:1021-1025

Browning, M. D., Huganir, R., and Greengard, P. (1985) Protein-phosphorylation and neuronal function. *J. Neurochem.* 45:11-23

Burgess, T. L. and Kelly, R. B. (1987) Constitutive and regulated secretion of proteins. *Ann. Rev. Cell Biol.* 3:243-293

Campbell, K. D., Collins, M. D., and East, A. K. (1993) Gene probes for identification of the botulinal neurotoxin gene and specific identification of neurotoxin type-B, type-E, and type-F. *J. Clin. Microbiol.* 31:2255-2262

Castellino, F., Heuser, J., Marchetti, S., Bruno, B., and Luini, A. (1992) Glucocorticoid stabilization of actin-filaments - a possible mechanism for inhibition of corticotropin release. *Proc. Nat. Acad. Sci. USA* 89:3775-3779

Castle, A. M., Huang, A., and Castle, J. D. (1995) Sorting of the exocrine proteins, proline-rich protein and amylase, from maturing storage granules in AtT-20 cells. *Mol. Biol. Cell* 6:405

Ceccarelli, B., Grohovaz, F., and Hurlbut, W. P. (1979) Freeze fracture studies of frog neuromuscular junctions during intense release of neurotransmitter. *J. Cell Biol.* 81:163-177

Chamberlain, L. H., Roth, D., Morgan, A., and Burgoyne, R. D. (1995) Distinct effects of α-snap, 14-3-3-proteins, and calmodulin on priming and triggering of regulated exocytosis. *J. cell Biol.* 130:1063-1070

Chavez, R. A. and Moore, H. P. H. (1997) Targeting of leptin to the regulated secretory pathway in pituitary AtT-20 cells. *Curr. Biol.* 7:349-352

Cheek, T. R. and Burgoyne, R. D. (1986) Nicotine-evoked disassembly of cortical actin-filaments in adrenal chromaffin cells. *FEBS Lett.* 207:110-114

Cheek, T. R. and Burgoyne, R. D. (1987) Cyclic-AMP inhibits both nicotine-induced actin disassembly and catecholamine secretion from bovine adrenal chromaffin cells. *J. Biol. Chem.* 262:11663-11666

Chen, C. A. and Okayama, H. (1988) Calcium phosphate-mediated gene-transfer - a highly efficient transfection system for stably transforming cells with plasmid DNA. *Biotechniques* 6:632

Chung, S. H., Takai, Y., and Holz, R. W. (1995) Evidence that the rab3A-binding protein, rabphilin3A, enhances regulated secretion - studies in adrenal chromaffin cells. *J. Biol. Chem.* 270:16714-16718

Clark, D. V., Rogalski, T. M., Donati, L. M., and Baillie, D. L. (1988) The unc-22(IV) region of *caenorhabditis-elegans* - genetic-analysis of lethal mutations. *Genetics* 119:345-353

Clark, T. P. and Kemppainen, R. J. (1994) Glucocorticoids do not affect intracellular calcium transients in corticotrophs - evidence supporting an effect distal to calcium influx. *Neuroendocrinol.* 60:273-282

Cool, D. R. and Loh, Y. P. (1994) Identification of a sorting signal for the regulated secretory pathway at the N-terminus of pro-opiomelanocortin. *Biochimie* 76:265-270

Cullen and Malim (1992) Secreted placental alkaline phosphatase as a eukaryotic reporter gene. *Meth. Enzymol.* 216: 362-368

Darnell, J., Lodish, H., and Baltimore, D. (1990) Molecular Biology of the Cell, 2nd Edition. Scientific American Books, New York.

Davletov, B. A., Shamotienko, O. G., Lelianova, V. G., Grishin, E. V., and Ushkaryov, Y. A. (1996) Isolation and biochemical-characterization of a Ca^{2+}-independent α-latrotoxin-binding protein. *J. Biol. Chem.* 271:23239-23245

Diantonio, A., Parfitt, K. D., and Schwarz, T. L. (1993) Synaptic transmission persists in synaptotagmin mutants of *drosophila. Cell* 73:1281-1290

Douglas, W. W. (1968) *Brit. J. Pharmacol.*. 34:451-474

East, A. K., Richardson, P. T., Allaway, D., Collins, M. D., Roberts, T. A., and Thompson, D. E. (1992) Sequence of the gene encoding type-F neurotoxin of clostridium-botulinum. *FEMS Microbiol. Lett.* 96:225-230

Edelmann, L., Hanson, P. I., Chapman, E. R., and Jahn, R. (1995) Synaptobrevin binding to synaptophysin - a potential mechanism for controlling the exocytotic fusion machine. *EMBO J.* 14:224-231

Eipper, B. A. and Mains, R. E. (1982) Phosphorylation of pro-adrenocorticotropin endorphin-derived peptides. *J. Biol. Chem.* 257:4907-4915

Eisel, U., Reynolds, K., Riddick, M., Zimmer, A., and Niemann, H. (1993) Tetanus toxin light-chain expression in sertoli cells of transgenic mice causes alterations of the actin cytoskeleton and disrupts spermatogenesis. *EMBO J.* 12:3365-3372

Elferink, L. A., Peterson, M. R., and Scheller, R. H. (1993) A role for synaptotagmin (p65) in regulated exocytosis. *Cell* 72:153-159

Eskeland, N. L., Zhou, A., Dinh, T. Q., Wu, H. J., Parmer, R. J., Mains, R. E., and Oconnor, D. T. (1996) Chromogranin-a processing and secretion - specific role of endogenous and exogenous prohormone convertases in the regulated secretory pathway. *J. Clin. Investigation* 98:148-156

Fischer von Mollard, G., Mignery, G. A., Baumert, M., Perrin, M. S., Hanson, T. J., Burger, P. M., Jahn, R., and Sudhof, T. C. (1990) Rab3 is a small GTP-binding protein exclusively localized to synaptic vesicles. *Proc. Natl. Acad. Sci. USA* 87:1988-1992

Fischercolbrie, R., Schachinger, M., Zangerle, R., and Winkler, H. (1982) Dopamine β-hydroxylase and other glycoproteins from the soluble content and the membranes of adrenal chromaffin granules -isolation and carbohydrate analysis. *J. Neurochem.* 38:725-732

Fleischer, B. and Fleming, A. M. (1970) Preparation and characterisation of Golgi membranes from rat liver. *Biochim. Biophys. Acta* 219:301-319

Fox, S. I. (1990) Human Physiology, 3rd edition. Wm. C. Brown Publishers, USA.

Fujita, Y., Sasaki, T., Fukui, K., Kotani, H., Kimura, T., Hata, Y., Sudhof, T. C., Scheller, R. H., and Takai, Y. (1996) Phosphorylation of munc-18/n-sec1/rbsec1 by protein-kinase-C -its implication in regulating the interaction of munc-18/n-sec1/rbsec1 with syntaxin. *J. Biol. Chem.* 271:7265-7268

Geppert, M., Bolshakov, V. Y., Siegelbaum, S. A., Takei, K., Decamilli, P., Hammer, R. E., and Sudhof, T. C. (1994a) The role of rab3A in neurotransmitter release. *Nature* 369:493-497

Geppert, M., Goda, Y., Hammer, R. E., Li, C., Rosahl, T. W., Stevens, C. F., and Sudhof, T. C. (1994b) Synaptotagmin-i - a major Ca^{2+} sensor for transmitter release at a central synapse. *Cell* 79:717-727

Gilman, A. G. (1987) G-proteins - transducers of receptor-generated signals. *Ann. Rev. Biochem.* 56:615-649

Glenn, D. E. and Burgoyne, R. D. (1996) Botulinum neurotoxin light-chains inhibit both Ca^{2+}-induced and CTP analog-induced catecholamine release from permeabilized adrenal chromaffin cells. *FEBS Lett.* 386:137-140

Goda, Y. (1997) SNAREs and regulated vesicle exocytosis. *Proc. Nat. Acad. Sci. USA* 94:769-772

Gomperts, B. D. (1990) Exocytosis - the role of Ca^{2+}, GTP and ATP as regulators and modulators in the rat mast-cell model. *J. Exp. Pathol.* 71:423-431

Guild, S. (1991) Effects of adenosine 3'-5'-cyclic monophosphate and guanine-nucleotides on calcium-evoked ACTH release from electrically permeabilized AtT-20 cells. *Brit. J. Pharmacol.* 104:117-122

Guild, S. and Reisine, T. (1987) Molecular mechanisms of corticotropin-releasing factor stimulation of calcium mobilization and adrenocorticotropin release from anterior- pituitary tumor-cells. *J. Pharmacol. Exp. Ther.* 241:125-130

Hall, A. (1990) The cellular functions of small GTP-binding proteins. *Science* 249:635-640

Halpern, J. L., Habig, W. H., Trenchard, H., and Russell, J. T. (1990) Effect of tetanus toxin on oxytocin and vasopressin release from nerve-endings of the neurohypophysis. *J. Neurochem.* 55:2072-2078

Harley, C. (1994) Analysis of the Sec18 protein from Saccharomyces cerevisiae. *Ph. D. Biochemistry Department, Edinburgh University.*

Hata, Y., Davletov, B., Petrenko, A. G., Jahn, R., and Sudhof, T. C. (1993) Interaction of synaptotagmin with the cytoplasmic domains of neurexins. *Neuron* 10:307-315

Hauser, D., Eklund, M. W., Kurazono, H., Binz, T., Niemann, H., Gill, D. M., Boquet, P., and Popoff, M. R. (1990) Nucleotide-sequence of clostridium-botulinum C1 neurotoxin. *Nuc. Ac. Res.* 18:4924

Hawkins, M., Pope, B., Maciver, S. K., and Weeds, A. G. (1987) Human actin depolymerising factor mediates pH-sensitive destruction of actin filaments. *J. Cell. Biol.* 105:2817-2825

Hay, J. C., Fisette, P. L., Jenkins, G. H., Fukami, K., Takenawa, T., Anderson, R. A., and Martin, T. F. J. (1995) ATP-dependent inositide phosphorylation required for Ca^{2+}-activated secretion. *Nature* 374:173-177

Hayashi, T., Mcmahon, H., Yamasaki, S., Binz, T., Hata, Y., Sudhof, T. C., and Niemann, H. (1994) Synaptic vesicle membrane-fusion complex - action of clostridial neurotoxins on assembly. *EMBO J.* 13:5051-5061

Heisler, S. and Reisine, T. (1984) Forskolin stimulates adenylate-cyclase activity, cyclic-amp accumulation, and adrenocorticotropin secretion from mouse anterior-pituitary tumor-cells. *J. Neurochem.* 42:1659-1666

Higashijima, T., Uzu, S., Nakajima, T., and Ross, E. M. (1988) Mastoparan, a peptide toxin from wasp venom, mimics receptors by activating GTP-binding regulatory proteins (G-proteins). *J. Biol. Chem.* 263:6491-6494

Ho, S. N., Hunt, H. D., Horton, R. M., Pullen, J. K., and Pease, L. R. (1989) Site-directed mutagenesis by overlap extension using the polymerase chain-reaction. *Gene* 77:51-59

Holm-Nielson, E., Braun, K., and Johansen, T. (1989) Reorganisation of the subplasmalemmal cytoskeleton in association with exocytosis in rat mast cells. *Histol. Histopath.* 4:473-477

Holz, R. W., Bittner, M. A., Peppers, S. C., Senter, R. A., and Eberhard, D. A. (1989) MgATP-independent and MgATP-dependent exocytosis - evidence that MgATP primes adrenal chromaffin cells to undergo exocytosis. *J. Biol. Chem.* 264:5412-5419

Holz, R. W., Brondyk, W. H., Senter, R. A., Kuizon, L., and Macara, I. G. (1994) Evidence for the involvement of Rab3A in Ca^{2+} dependent exocytosis from adrenal chromaffin cells. *J. Biol. Chem.* 269:10229-10234

Hong, R. M., Mori, H., Fukui, T., Moriyama, Y., Futai, M., Yamamoto, A., Tashiro, Y., and Tagaya, M. (1994) Association of N-ethylmaleimide-sensitive factor with synaptic vesicles. *FEBS Lett.*350:253-257

Hook, V. Y. H., Heisler, S., Sabol, S., and Axelrod, J. (1982) Corticotrophin releasing factor stimulates adrenocorticotrophin and β-endorphin release form AtT-20 mouse pituitary tumour cells. *Biochem. Biophys. Res.Comm.* 106:1364-1371

Huang, Z. J., Olson, N. A., You, W. M., and Haugland, R. P. (1992) A sensitive competitive ELISA for 2,4-dinitrophenol using 3,6-fluorescein diphosphate as a fluorogenic substrate. *J. Immunol. Meth.* 149:261-266

Hug, H. and Sarre, T. F. (1993) Protein-kinase-C isoenzymes - divergence in signal transduction. *Biochem. J.* 291:329-343

Hurtley, S. M. (1993) Recycling of a secretory granule membrane-protein after stimulated secretion. *J. Cell Sci.* 106:649-656

Huttner, W. B. (1988) Tyrosine sulfation and the secretory pathway. *Ann. Rev. Physiol.* 50:363-376

Inui, M., Watanabe, T., and Sobue, K. (1994) Annexin VI binds to a synaptic vesicle protein, synapsin-I. *J. Neurochem.* 63:1917-1923

Jahn, R. and Sudhof, T. C. (1994) Synaptic vesicles and exocytosis. *Ann. Rev. Neurosci.* 17:219-246

Jessell, T. M. and Kandel, E. R. (1993) Synaptic transmission - a bidirectional and self-modifiable form of cell-cell communication. *Cell* 72:1-30

Jung, L. J., Kreiner, T., and Scheller, R. H. (1993) Expression of mutant ELH prohormones in AtT-20 cells - the relationship between prohormone processing and sorting. *J. Cell. Biol.* 121:11-21

Keller-Wood, M., Leeman, E., Shinsako, J., and Dallman, M. F. (1988) Steroid inhibition of canine ACTH: in-vivo evidence for feedback at the corticotrope. *Am. J. Physiol.* 255:E241-E246

Kikkawa, S., Takahashi, K., Shimada, N., Ui, M., Kimura, N., and Katada, T. (1992) Activation of nucleoside diphosphate kinase by mastoparan, a peptide isolated from wasp venom. *FEBS Lett.* 305:237-240

Kishida, S., Shirataki, H., Sasaki, T., Kato, M., Kaibuchi, K., and Takai, Y. (1993) Rab3A GTPase-activating protein-inhibiting activity of rabphilin-3A, a putative rab3A target protein. *J. Biol. Chem.* 268:22259-22261

Koffer, A., Tatham, P. E. R., and Gomperts, B. D. (1990) Changes in the state of actin during the exocytotic reaction of permeabilized rat mast-cells. *J. Cell. Biol.* 111:919-927

Krasnoperov, V. G., Bittner, M. A., Beavis, R., Kuang, Y. N., Salnikow, K. V., Chepurny, O. G., Little, A. R., Plotnikov, A. N., Wu, D. Q., Holz, R. W., and Petrenko, A. G. (1997) α-latrotoxin stimulates exocytosis by the interaction with a neuronal G-protein-coupled receptor. *Neuron* 18:925-937

Kretzschmar, S., Volknandt, W., and Zimmermann, H. (1996) Colocalization on the same synaptic vesicles of syntaxin and SNAP-25 with synaptic vesicle proteins - a re-evaluation of functional models required. *Neurosci. Res.* 26:141-148

Kumakura, K., Sasaki, K., Ohara-Imaizumi, M., Misonou, H., Nakamura., s., Matsuda, Y., and Nonomura, Y. (1994) Essential role of myosin light chain kinase in the mechanism for Mg-ATP-dependent priming of exocytosis in adrenal chromaffin cells. *J. Neurosci.* 14: 7695-7703

Laeimmli, U. K. (1970) Cleavage of structural proteins during the assembly of the head of a bacteriophage T4. *Nature* 227:680-685

Lelkes, P. I., Friedman, J. E., Rosenheck, K., and Oplatka, A. (1986) Destabilization of actin-filaments as a requirement for the secretion of catecholamines from permeabilized chromaffin cells. *FEBS Lett.* 208:357-363

Leveque, C., Hoshino, T., David, P., Shojikasai, Y., Leys, K., Omori, A., Lang, B., Elfar, O., Sato, K., Martinmoutot, N., Newsomdavis, J., Takahashi, M., and Seagar, M. J. (1992) The synaptic vesicle protein synaptotagmin associates with calcium channels and is a putative lambert-eaton myasthenic syndrome antigen. *Proc. Natl. Acad. Sci. USA* 89:3625-3629

Loechner, K. J., Kream, R. M., and Dunlap, K. (1996) Calcium currents in a pituitary cell line (AtT-20): Differential roles in stimulus-secretion coupling. *Endocrinol.* 137:1429-1436

Link, H., Dayanithi, G., and Gratzl, M. (1993) Glucocorticoids rapidly inhibit oxytocin-stimulated adrenocorticotropin release from rat anterior-pituitary-cells, without modifying intracellular calcium transients. *Endocrinol.* 132:873-878

Littleton, J. T., Stern, M., Schulze, K., Perin, M., and Bellen, H. J. (1993) Mutational analysis of drosophila synaptotagmin demonstrates its essential role in Ca^{2+}-activated neurotransmitter release. *Cell* 74:1125-1134

Litvin, Y., Pasmantier, R., Fleischer, N., and Erlichman, J. (1984) Hormonal activation of the camp-dependent protein-kinases in AtT-20 cells - preferential activation of protein kinase-I by corticotropin releasing-factor, isoproterenol, and forskolin. *J. Biol. Chem.* 259:296-302

Loechner, K. J., Kream, R. M., and Dunlap, K. (1996) Calcium currents in a pituitary cell-line (AtT-20) -differential roles in stimulus-secretion coupling. *Endocrinol.* 137:1429-1437

Lovett, K. M. and Martin, T. F. J. (1997) Phosphatidylinositol 4,5-bisphosphate (PIP2) synthesis occurs on secretory granules during the ATP-dependent priming step of regulated secretion. *9th International Symposium on Chromaffin Cell Biology, Japan* PVI-1:143

Lowry, O. H., Roseburgh, N. J., Farr, A. L., and Randall, R. J. (1951) Protein measurement with the folin phenol reagant. *J. Biol. Chem.* 193:265-275

Luini, A. and Dematteis, M. A. (1988) Dual regulation of ACTH-secretion by guanine-nucleotides in permeabilized AtT-20 cells. *Cell. Mol. Neurobiol.* 8:129-138

Luini, A., Lewis, D., Guild, S., Corda, D., and Axelrod, J. (1985) Hormone secretagogues increase cytosolic calcium by increasing camp in corticotropin-secreting cells. *Proc. Nat. Acad. Sci. USA* 82:8034-8038

Lundbald, J. R. and Roberts, J. L. (1988) Regulation of proopiomelanocortin gene expression in pituitary. *Endocrinol. Rev.* 9:135-157

Malenick, D. A. and Anderson, S. R. (1983) High-affinity binding of the mastoparans by calmodulin. *Biochem. Biophys. Res. Comm.* 114:50-56

Martelli, A. M., Bareggi, R., Baldini, G., Scherer, P. E., and Lodish, H. F. (1995) Diffuse vesicular distribution of rab3D in the polarized neuroendocrine cell-line AtT-20. *FEBS Lett.* 368:271-275

Martin, T. F. J. (1997) Stages of regulated exocytosis. *Trends Cell Biol.* 7:271-276

Matsuuchi, L., Buckley, K. M., Lowe, A. W., and Kelly, R. B. (1988) Targeting of secretory vesicles to cytoplasmic domains in AtT-20 and PC-12 cells. *J. Cell Biol.* 106:239-251

Matsuuchi, L. and Kelly, R. B. (1991) Constitutive and basal secretion from the endocrine cell-line, AtT-20. *J. Cell Biol.* 112:843-852

Mcferran, B. W. and Guild, S. B. (1994) Effects of protein-kinase-C activators upon the late stages of the ACTH secretory pathway of AtT-20 cells. *Brit. J. Pharmacol.* 113:171-178

Mcferran, B. W. and Guild, S. B. (1995) Effects of mastoparan upon the late stages of the adrenocorticotropin (ACTH) secretory pathway of AtT-20 cells. *Brit. J. Pharmacol.* 114:P 66

Mcferran, B. W., Macewan, D. J., and Guild, S. B. (1995) Involvement of multiple protein-kinase-C isozymes in the ACTH secretory pathway of AtT-20 cells. *Brit. J. Pharmacol.* 115:307-315

Mcmahon, H. T., Foran, P., Dolly, J. O., Verhage, M., Wiegant, V. M., and Nicholls, D. G. (1992) Tetanus toxin and botulinum toxins type-A and type-B inhibit glutamate, gamma-aminobutyric-acid, aspartate, and met-enkephalin release from synaptosomes - clues to the locus of action. *J. Biol. Chem.* 267:21338-21343

Mcmahon, H. T., Missler, M., Li, C., and Sudhof, T. C. (1995) Complexins - cytosolic proteins that regulate SNAP receptor function. *Cell* 83:111-119

Mcmahon, H. T. and Sudhof, T. C. (1995) Synaptic core complex of synaptobrevin, syntaxin, and SNAP-25 forms high-affinity α-snap finding site. *J. Biol. Chem.* 270:2213-2217

Miyazaki, K., Reisine, T., and Kebabian, J. W. (1997) Cyclic AMP-dependent protein kinase activity in rodent pituitary tissue: possible role in cAMP-dependent hormone secretion. *Endocrinol.* 115:1933-1945

Morgan, A. (1995) Exocytosis. *Essays Biochem.* 30:77-95

Morgan, A. and Burgoyne, R. D. (1995a) A role for soluble NSF attachment proteins (SNAPs) in regulated exocytosis in adrenal chromaffin cells. *EMBO J.* 14:232-239

Morgan, A. and Burgoyne, R. D. (1995b) Is NSF a fusion protein?. *Trends Cell Biol.* 5:335-339

Muhlrad, D., Hunter, R., and Parker, R. (1992) A rapid method for localized mutagenesis of yeast genes. *Yeast* 8:79-82

Newsholme, E. A. and Leech, A. R. (1992) Biochemistry for the medical sciences. John Wiley & Sons, UK.

Nakanishi, S., Inoue, A., Kita, T. (1979) Nucleotide sequence of cloned cDNA for bovine corticotrophin-lipotropin precursor. *Nature* 278: 423-427

Ngsee, J. K., Fleming, A. M., and Scheller, R. H. (1993) A rab protein regulates the localization of secretory granules in AtT-20 cells. *Mol. Biol. Cell* 4:747-756

Ngsee, J. K., Miller, K., Wendland, B., and Scheller, R. H. (1990) Multiple GTP-binding proteins from cholinergic synaptic vesicles. *J. Neurosci.* 10:317-322

Nicholls, D. G. (1994) Proteins, Transmitters and Synapses. Blackwell Scientific Publications.

Niemann, H., Blasi, J., and Jahn, R. (1994) Clostridial Neurotoxins: new tools for dissecting exocytosis. *Trends Cell Biol.* 4:179-185

Nonet, M. L., Grundahl, K., Meyer, B. J., and Rand, J. B. (1993) Synaptic function is impaired but not eliminated in *C. elegans* mutants lacking synaptotagmin. *Cell* 73:1291-1305

Ohara-Imaizumi, M., Fukuda, M., Niinobe, M., Misonou, H., Ikeda, K., Murakami, T., Kawasaki, M., Mikoshiba, K., and Kumakura, K. (1997) Distinct roles of C2A and C2B domains of synaptotagmin in the regulation of exocytosis in adrenal chromaffin cells. *Proc. Nat. Acad. Sci. USA* 94:287-291

Orci, L., Gabbay, K. H., and Malaisse, W. J. (1972) Pancreatic β-cell web: its possible role in insulin secretion. *Science* 175:1128-1130

Orita, S., Sasaki, T., Naito, A., Komuro, R., Ohtsuka, T., Maeda, M., Suzuki, H., Igarashi, H., and Takai, Y. (1995) Doc2 - a novel brain protein having 2 repeated C2-like domains. *Biochem. Biophys. Res. Comm* 206:439-448

Papini, E., Rossetto, O., and Cutler, D. F. (1995) Vesicle-associated membrane-protein (VAMP) synaptobrevin-2 is associated with dense core secretory granules in PC12 neuroendocrine cells. *J. Biol. Chem.* 270:1332-1336

Perin, M. S., Fried, V. A., Mignery, G. A., Jahn, R., and Sudhof, T. C. (1990) Phospholipid binding by a synaptic vesicle protein homologous to the regulatory region of protein kinase-C. *Nature* 345:260-263

Petrenko, A. G., Perin, M. S., Davletov, B. A., Ushkaryov, Y. A., Geppert, M., and Sudhof, T. C. (1991) Binding of synaptotagmin to the α-latrotoxin receptor implicates both in synaptic vesicle exocytosis. *Nature* 353:65-68

Pevsner, J., Hsu, S. C., Braun, J. E. A., Calakos, N., Ting, A. E., Bennett, M. K., and Scheller, R. H. (1994) Specificity and regulation of a synaptic vesicle docking complex. *Neuron* 13:353-361

Pfeffer, S. R. (1992) GTP-binding proteins in intracellular transport. *Trends Biochem. Sci.* 2:41-46

Phillips, M. and Tashjian, A. H. (1982) Characterization of an early inhibitory effect of glucocorticoids on stimulated adrenocorticotropin and endorphin release from a clonal strain of mouse pituitary-cells. *Endocrinol.* 110:892-900

Poulet, S., Hauser, D., Quanz, M., Niemann, H., and Popoff, M. R. (1992) Sequences of the botulinal neurotoxin-E derived from clostridium-botulinum type-E (strain-beluga) and clostridium-butyricum (strains ATCC-43181 and ATCC-43755). *Biocehm. Biophys. Res. Comm.* 183:107-113

Pozzoli, G., Bilezikjian, L. M., Perrin, M. H., Blount, A. L., and Vitale, W. W. (1996) Corticotrophin releasing factor (CRF) and glucocorticoids modulate the expression of type I CRF receptor messenger ribonucleic acid in rat anterior pituitary cell cultures. *Endocrinol.* 137:65-71

Pryde, J. G. (1986) Triton X-114 - a detergent that has come in from the cold. *Trends Biochem. Sci.* 11:160-163

Pryde, J. G. and Phillips, J. H. (1986) Fractionation of membrane-proteins by temperature-induced phase-separation in triton X-114 - application to subcellular-fractions of the adrenal-medulla. *Biochem. J.* 233:525-533

Pryer, N. K., Wuestehube, L. J., and Schekman, R. (1992) Vesicle-mediated protein sorting. *Ann. Rev. Biochem.* 61:471-516

Rane, S. and Dunlap, K. (1986) Kinase C activator 1,2-oleoylacetylglycerol attenuates voltage-dependent calcium currents in sensory neurons. *Proc. Natl. Acad. Sci. USA* 83:184-188

Reetz et al. (1991) GABA and pancreatic β-cells: colocalisation of glutamic acid decarboxylase (GAD) and GABA with synaptic-like microvesicles suggests their role in GABA storage and secretion. *The EMBO J.* 10 no.5 1275-1284

Reisine, T. and Guild, S. (1987) Activators of protein kinase-C and cyclic amp-dependent protein-kinase regulate intracellular calcium levels through distinct mechanisms in mouse anterior-pituitary tumor-cells. *Mol.Pharmacol.* 32:488-496

Reisine, T., Rougon, G., and Barbet, J. (1986) Liposome delivery of cyclic amp-dependent protein-kinase inhibitor into intact-cells - specific blockade of cyclic amp-mediated adrenocorticotropin release from mouse anterior-pituitary tumor-cells. *J. Cell Biol.* 102:1630-1637

Reisine, T., Rougon, G., Barbet, J., and Affolter, H. U. (1985) Corticotropin-releasing factor-induced adrenocorticotropin hormone- release and synthesis is blocked by incorporation of the inhibitor of cyclic amp-dependent protein-kinase into anterior-pituitary tumor- cells by liposomes. *Proc. Nat. Acad. Sci. USA* 82:8261-8265

Rosenthal, L. and Meldolesi, J. (1989) α-latrotoxin and related toxins. *Pharmacol. & Ther.* 42:115-134

Roth, D. and Burgoyne, R. D. (1994) SNAP-25 is present in a SNARE complex in adrenal chromaffin cells. *FEBS Lett.* 351:207-210

Roth, D. and Burgoyne, R. D. (1995) Stimulation of catecholamine secretion from adrenal chromaffin cells by 14-3-3-proteins is due to reorganization of the cortical actin network. *FEBS Lett.* 374:77-81

Rothman, J. E. (1994) Mechanism of intracellular protein-transport. *Nature* 372:55-63

Sabol, S. (1980) Storage and secretion of β-endorphin and related peptides by mouse pituitary tumour cells: regulation by glucocorticoids. *Arch. Biochem. Biophys.* 203:37-48

Sakurai, T., Ohara-Imaizumi, M., Murakami, T., Kumakura, K. (1997) Possible roles of actin filaments in the regulation of catecholamine release. *9th International Symposium on Chromaffin Cell Biology* PVI-12: 154

Sambrook, J., Fritsch, E. F., and Maniatis, T. (1989) Molecular Cloning: A Laboratory Manual, 2nd Edition. Cold Spring Harbour Laboratory Press. Cold Spring Harbour, New York.

Schagger, H., and Jagow, G. (1987) Tricine-sodium dodecyl sulphate-polyacrylamide gel electrophoresis for the separation of proteins in the range from 1 to 100kDa. *Anal. Biochem.* 166: 368379

Schiavo, G., Benfenati, F., Poulain, B., Rossetto, O., Delaureto, P. P., Dasgupta, B. R., and Montecucco, C. (1992) Tetanus and botulinum-B neurotoxins block neurotransmitter release by proteolytic cleavage of synaptobrevin. *Nature* 359:832-835

Schiavo, G., Gu, Q. M., Prestwich, G. D., Sollner, T. H., and Rothman, J. E. (1996) Calcium-dependent switching of the specificity of phosphoinositide binding to synaptotagmin. *Proc. Nat. Acad. Sci. USA* 93:13327-13332

Schiavo, G., Stenbeck, G., Rothman, J. E., and Sollner, T. H. (1997) Binding of the synaptic vesicle v-SNARE, synaptotagmin, to the plasma membrane t-SNARE, SNAP-25, can explain docked vesicles at neurotoxin- treated synapses. *Proc. Nat. Acad. Sci. USA* 94:997-1001

Seidah, N. G., Marcinkiewicz, M., Benjannet, S., Gaspar, L., Beaubien, G., Mattei, M. G., Lazure, C., Mbikay, M., and Chretien, M. (1991) Cloning and primary sequence of a mouse candidate prohormone convertase PC1 homologous to PC2, furin, and kex2 - distinct chromosomal localization and messenger-rna distribution in brain and pituitary compared to PC2. *Mol. Endocrinol.* 5:111-122

Shipston, M. J. (1995) Mechanisms(s) of early glucocorticoid inhibition of adrenocorticotropin secretion from anterior-pituitary corticotropes. *Trends Endocrinol. Metabl.* 6:261-266

Shipston, M. J., Kelly, J. S., and Antoni, F. A. (1996) Glucocorticoids block protein-kinase a inhibition of calcium-activated potassium channels. *J. Biol. Chem.* 271:9197-9200

Sollner, T. (1995) SNAREs and targeted membrane-fusion. *FEBS Lett.* 369:80-83

Sollner, T., Whitehart, S. W., Brunner, M., Erdjumentbromage, H., Geromanos, S., Tempst, P., and Rothman, J. E. (1993) SNAP receptors implicated in vesicle targeting and fusion. *Nature* 362:318-324

Stahl, L. E., Wright, R. L., Castle, J. D., and Castle, A. M. (1996) The unique proline-rich domain of parotid proline-rich proteins functions in secretory sorting. *J. Cell Sci.* 109:1637-1645

Stella (1995) Glutamate-evoked release of arachidonic-acid from mouse brain astrocytes. *J. Neurosci.* 15:3307-3317

Stevens, C. F. and Tsujimoto, T. (1995) Estimates for the pool size of releasable quanta at a single central synapse and for the time required to refill the pool. *Proc. Nat. Acad. Sci. USA* 92:846-849

Strous, G. J., Vankerkhof, P., Willemsen, R., Geuze, H. J., and Berger, E. G. (1983) Transport and topology of galactosyltransferase in endomembranes of hela-cells. *J. Cell Biol.* 97:723-727

Stryer, L. (1988) Biochemistry, 3rd edition. W.H. Freeman and Company, New York.

Sudhof, T. C., Lottspeich, F., Greengard, P., Mehl, E., and Jahn, R. (1987) A synaptic vesicle protein with a novel cytoplasmic domain and 4 transmembrane regions. *Science* 238:1142-1144

Surprenant, A. (1982) Correlation between electrical-activity and ACTH/β-endorphin secretion in mouse pituitary-tumor cells. *J. Cell Biol.* 95:559-566

Sweeney, S. T., Broadie, K., Keane, J., Niemann, H., and Okane, C. J. (1995) Targeted expression of tetanus toxin light-chain in drosophila specifically eliminates synaptic transmission and causes behavioral defects. *Neuron* 14:341-351

Tagaya, M., Genma, T., Yamamoto, A., Kozaki, S., and Mizushima, S. (1996) SNAP-25 is present on chromaffin granules and acts as a SNAP receptor. *FEBS Lett.* 394:83-86

Tagaya, M., Toyonaga, S., Takahashi, M., Yamamoto, A., Fujiwara, T., Akagawa, K., Moriyama, Y., and Mizushima, S. (1995) Syntaxin-1 (HPC-1) is associated with chromaffin granules. *J. Biol. Chem.* 270:15930-15933

Tanaka, S., Kurabuchi, S., Mochida, H., Kato, T., Takahashi, S., Watanabe, T., and Nakayama, K. (1996) Immunocytochemical localization of prohormone convertases PC1/PC3 and pc2 in rat pancreatic-islets. *Arch. Histol. Cytol.* 59:261-271

Tanaka, S. and Kurosumi, K. (1992) A certain step of proteolytic processing of proopiomelanocortin occurs during the transition between 2 distinct stages of secretory granule maturation in rat anterior-pituitary corticotrophs. *Endocrinol.* 131:779-786

Tanaka, S., Nomizu, M., and Kurosumi, K. (1991) Intracellular sites of proteolytic processing of proopiomelanocortin in melanotrophs and corticotrophs in rat pituitary. *J. Histochem. Cytochem.* 39:809-821

Tanford, C. and Reynolds, J. (1976) Characterisation of membrane protein in detergent solutions. *Biochem. Biophys. Acta.* 457:133-170

Taylor, C. W. (1990) The role of G-proteins in transmembrane signaling. *Biochem. J.* 272:1-13

Tooze, J., Hollinshead, M., Frank, R., and Burke, B. (1987) An antibody specific for an endoproteolytic cleavage site provides evidence that pro-opiomelanocortin is packaged into secretory granules in AtT-20 cells before its cleavage. *J. Cell Biol.* 105:155-162

Trimble, W. S., Cowan, D. M., and Scheller, R. H. (1988) VAMP-1 - a synaptic vesicle-associated integral membrane-protein. *Proc. Nat. Acad. Sci. USA* 85:4538-4542

Ushkaryov, Y. A., Petrenko, A. G., Geppert, M., and Sudhof, T. C. (1992) Neurexins - synaptic cell-surface proteins related to the α-latrotoxin receptor and laminin. *Science* 257:50-56

Verhage, M., Hens, J. J. H., De Graan, P. N. E., Boomsma, F., Wiegant, V. M., Lopes da Silva, F. H., Gispen, W. H., and Ghijsen, W. E. J. M. (1995) Ba^{2+} replaces Ca^{2+}/calmodulin in the activation of protein phosphatases and in the exocytosis of all major transmitters. *Eur. J. Pharmacol.* 291:387-398

Vitale, M. L., Delcastillo, A. R., Tchakarov, L., and Trifaro, J. M. (1991) Cortical filamentous actin disassembly and scinderin redistribution during chromaffin cell stimulation precede exocytosis, a phenomenon not exhibited by gelsolin. *J. Cell Biol.* 113:1057-1067

Vitale, M. L., Seward, E. P., and Trifaro, J. M. (1995a) Chromaffin cell cortical actin network dynamics control the size of the release-ready vesicle pool and the initial rate of exocytosis. *Neuron* 14:353-363

Vitale, N., Aunis, D., and Bader, M. F. (1995b) GAP-43 controls the recruitment of secretory granules for exocytosis by stimulating the granule associated G_o. *8th International Symposium on Chromaffin Cell Biology, Edinburgh.* P-56:

Walent, J. H., Porter, B. W., and Martin, T. F. J. (1992) A novel 145-kd brain cytosolic protein reconstitutes Ca^{2+}-regulated secretion in permeable neuroendocrine cells. *Cell* 70:765-775

Walter, P., Gilmore, R., and Blobel, G. (1984) Protein translocation across the endoplasmic-reticulum. *Cell* 38:5-8

Weingarten, R., Ransnas, L., Mueller, H., Sklar, L. A., and Bokoch, G. M. (1990) Mastoparan interacts with the carboxyl terminus of the α-subunit of G_i. *J. Biol. Chem.* 265:11044-11049

Wendland, B. and Scheller, R. H. (1994) Secretion in AtT-20 cells stably transfected with soluble synaptotagmins. *Mol. Endocrinol.* 8:1070-1082

Whelan, S. M., Elmore, M. J., Bodsworth, N. J., Brehm, J. K., Atkinson, T., and Minton, N. P. (1992) Molecular-cloning of the Clostridium botulinum structural gene encoding the type-B neurotoxin and determination of its entire nucleotide-sequence. *App. Env. Microbiol.* 58:2345-2354

Whiteheart, S. W., Griff, I. C., Brunner, M., Clary, D. O., Mayer, T., Buhrow, S. A., and Rothman, J. E. (1993) SNAP family of NSF attachment proteins includes a brain-specific isoform. *Nature* 362:353-355

Wiedemann, C., Schafer, T., and Burger, M. M. (1996) Chromaffin granule-associated phosphatidylinositol 4-kinase activity is required for stimulated secretion. *EMBO J.* 15:2094-2101

Wilson, D. W., Wilcox, C. A., Flynn, G. C., Chen E Kuang, W-J., Henzel, W. J., Block, M. R., Ullrich, A., and Rothman, J. E. (1989) A fusion protein required for vesicle-mediated transport in both mammalian cells and yeast. *Nature* 339:355-359

Wilson, D. W., Whiteheart, S. W., Wiedmann, M., Brunner, M., and Rothman, J. E. (1992) A multisubunit particle implicated in membrane-fusion. *J. Cell Biol.* 117:531-538

Woods, M. D., Shipston, M. J., Mullens, E. L., and Antoni, F. A. (1992) Pituitary corticotrope tumor (AtT-20) cells as a model system for the study of early inhibition by glucocorticoids. *Endocrinol.* 131:2873-2880

Yamaguchi, T., Shirataki, H., Kishida, S., Miyazaki, M., Nishikawa, J., Wada, K., Numata, S., Kaibuchi, K., and Takai, Y. (1993) 2 functionally different domains of rabphilin-3A, rab3A p25/smg p25A- binding and phospholipid-binding and ca^{2+}-binding domains. *J. Biol. Chem.* 268:27164-27170

Zhang, L., Marcu, M. G., NauStaudt, K., and Trifaro, J. M. (1996) Recombinant scinderin, a Ca^{2+} dependent F-actin severing protein, enhances Ca^{2+}-evoked exocytosis in permeabilized chromaffin cells, an effect blocked by two scinderin-derived actin-binding peptides and phosphatidylinositol 4,5-bisphosphate. *Mol. Biol. Cell* 7:3163

Zhou, A. and Mains, R. E. (1994) Endoproteolytic processing of proopiomelanocortin and prohormone convertase-1 and convertase-2 in neuroendocrine cells overexpressing prohormone convertase-1 or convertase-2. *J. Biol. Chem.* 269:17440-17447